The background of the cover features a stylized illustration of yellow, rod-shaped bacteria with flagella, scattered across the page. Interspersed among these are several irregular black ink splatters of varying sizes, creating a dynamic and somewhat abstract composition.

# Microbiological and process technological aspects of nanofiltration and reverse osmosis membrane biofouling

Florian Beyer

Microbiological and process technological aspects of nanofiltration and reverse osmosis membrane biofouling | Florian Beyer

## PROPOSITIONS

1. Spingomonads are more relevant in industrial membrane biofouling than the currently used model organisms in biofouling studies.

(this thesis)

2. Research on glycosphingolipid-producing microorganisms in the process of biofouling should be extended beyond their role as primary colonizers.

(this thesis)

3. “Perfect is the enemy of good” is an attitude that is celebrated in industry and frowned upon at universities.

4. The quick evolution of science from “understanding the world” to “manipulating the world” has left many fundamental questions unanswered.

5. The tax payer should have free access to scientific publications.

6. The denial of global climate change is just one example that indicates the rapidly growing gap between knowledge and consequent actions.

Propositions belonging to the thesis

**“Microbiological and process technological aspects of nanofiltration and reverse osmosis membrane biofouling”**

Florian Beyer

Wageningen, 22 February 2019

**Microbiological and process technological  
aspects of nanofiltration and reverse osmosis  
membrane biofouling**

Florian Beyer

## **Thesis committee**

### **Promotor**

Prof. Dr Alfons J.M. Stams

Personal chair at the Laboratory of Microbiology  
Wageningen University & Research

### **Co-promotor**

Dr Caroline M. Plugge

Associate professor, Laboratory of Microbiology  
Wageningen University & Research

### **Other members**

Prof. Dr Albert van der Wal, Wageningen University & Research

Prof. Dr Gert-Jan W. Euverink, University of Groningen

Prof. Dr Maria D. Kennedy, IHE Delft Institute for Water Education, Delft

Dr Emmanuelle I.E.D. Prest, PWN Technologies, Andijk

This research was conducted under the auspices of the Graduate School for Socio-Economic and Natural Sciences of the Environment (SENSE).



**Microbiological and process technological  
aspects of nanofiltration and reverse osmosis  
membrane biofouling**

Florian Beyer

**Thesis**

submitted in fulfilment of the requirements for the degree of doctor  
at Wageningen University

by the authority of the Rector Magnificus,

Prof. Dr A.P.J. Mol,

in presence of the

Thesis Committee appointed by the Academic Board

to be defended in public

on Friday 22 February 2019

at 1:30 p.m. in the Aula.

Florian Beyer

Microbiological and process technological aspects of nanofiltration and reverse osmosis membrane biofouling,

214 pages.

PhD thesis, Wageningen University, Wageningen, the Netherlands (2019)

With references, with summary in English

ISBN: 978-94-6343-407-2

DOI: <https://doi.org/10.18174/468283>

## Table of contents

<b>Chapter 1</b>	General introduction	7
<b>Chapter 2</b>	Long-term performance and fouling analysis of full-scale direct nanofiltration (NF) installations treating anoxic groundwater	39
<b>Chapter 3</b>	Bacterial communities in nanofiltration membranes used for drinking water production from anoxic groundwater	75
<b>Chapter 4</b>	Membrane fouling and chemical cleaning in three full-scale reverse osmosis plants producing demineralized water	99
<b>Chapter 5</b>	Isolation and characterization of <i>Sphingomonadaceae</i> from fouled membranes	131
<b>Chapter 6</b>	General discussion and outlook	173
<b>Appendixes:</b>	Summary	202
	Co-authors' affiliations	204
	List of publications	205
	Acknowledgments	206
	About the author	211
	Overview of completed training activities (SENSE certificate)	212





# Chapter **1**

**General Introduction**

## **1.1. Biofilms – The preferred and predominant form of microbial life on earth**

Biofilms have been recognized as the preferred and predominant phenotype of microorganisms on earth (*Costerton 1999, Flemming 2002, Flemming 2008, Costerton 2007, Donlan and Costerton 2002, Xavier and Foster, 2007, Petrova and Sauer, 2012*). Donlan and Costerton (2002) defined a biofilm as “a microbially derived sessile community characterized by cells that are irreversibly attached to a substratum or interface or to each other and that are embedded in a matrix of extracellular polymeric substances that they themselves have produced. The cells in the biofilm may also exhibit an altered phenotype with respect to growth rate and gene transcription”. Besides the typical image of solid/liquid interface attached microorganisms (films), which will be the focus of this thesis, the biofilm definition also applies aggregates such as mats, sludge, flocs or granules in suspension and biofilms formed at e.g. solid-air or liquid-air interfaces (*Wingender et al., 1995, Flemming 2002, Flemming 2008*). Biofilms are highly complex and dynamic (*Franklin et al., 2015*) and proliferate in a wide range of habitats and consequently have been reported in virtually every natural environment (*Stoodley et al., 2002, Costerton 2007, Carvalho 2018*). The proliferation under extreme environmental conditions such as in hydrothermal vents, frozen glaciers, the bottom of the ocean or hypersaline environments (e.g. salt lakes, salterns or hypersaline lagoons (*Flemming 2008, Decho and Guitierrez 2017*) is remarkable and a sign for their success and persistence in nature. Biofilms support self-purification processes in nature by carrying out an extensive range of biological processes involved in the biogeochemical cycles of carbon, nitrogen, phosphorus, sulfur and many metals (*Davey and O’Toole 2000, Flemming 2002, Dang and Lovell 2016*). Although biofilm research has much focused on bacterial biofilms, natural and industrial biofilms contain a diverse range of microorganisms such as bacteria, archaea, protozoa, fungi and algae (*Wingender et al., 1995, Flemming 2008, Dobretsov 2010*).

### 1.1.1. Biofilms – Structure and Development

Biofilm formation is a well-regulated sequential process. Within seconds after first contact of a clean surface with a liquid, a conditioning layer of macromolecules such as humic substances, proteins and polysaccharides will form (Flemming 2002). Subsequent biofilm formation on conditioned surfaces may be succeeded by the following distinct phases of microbial biofilms (Figure 1.1.).

**The five stages of biofilm development** (Sauer et al., 2002, Stoodley et al., 2002)

1. **Reversible attachment** to a surface (within minutes after first microbial contact with a surface).
2. **Irreversible attachment** and development of cell clusters
3. **Biofilm maturation I** (cell clusters get progressively layered)
4. **Biofilm maturation II** (cell clusters reach maximum thickness)
5. **Microbial dispersal** (completes the biofilm lifecycle, as detached microorganisms may re-enter planktonic lifestyle)

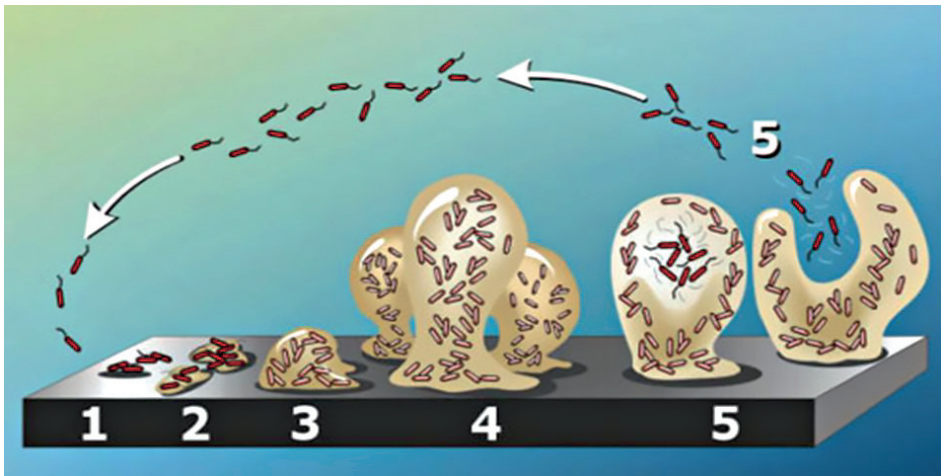


Figure 1.1. Diagram showing the development of a biofilm as a five-stage process 1. Reversible attachment, 2. Irreversible attachment, 3. Biofilm maturation I, 4. Biofilm maturation II and 5. Dispersal (adapted from Stoodley et al., 2002).



Although mature biofilms may be highly heterogeneous and diverse in space and time (Flemming 2008, Franklin et al., 2015), the defining component of the mature biofilm is unique: microcolonies embedded in self-produced (during growth or cell lysis) layers of extracellular polymeric substances (EPS) (Wingender et al., 1995). The EPS may consist of water, polysaccharides, proteins, nucleic acids (e.g. extracellular deoxyribonucleic acids, lipids, other biopolymers and inorganic colloids (Wingender et al., 1995, Flemming and Wingender, 2010, Decho and Gutierrez 2017). The sticky nature of the EPS produced, enables the attachment of microorganisms to surfaces and to each other. The EPS furthermore gives the biofilm its structure and retains water (Flemming 2008, Flemming and Wingender, 2010). The EPS is not merely a structural component of the biofilm, but also contributes to the biofilms metabolic activity, persistence and ecological success (Wingender et al., 1995). The combination of physical factors (e.g. temperature, flow rate, hydrodynamic forces, substrate properties, and viscosity), chemical factors (e.g. nutrient availability and composition, dissolved oxygen content, pH, EPS production) and biological factors (e.g. diversity, competition, predation, grazing, and cooperation) will ultimately define the structural and metabolic properties of a mature biofilm (Flemming et al., 1997, Sriyutha Murthy and Venkatesan 2009, Dobretsov, 2010, Maddah and Chogle 2017, Nguyen 2012). The biofilms EPS may be produced by bacteria, fungi (yeasts and molds), algae and archaea (Wingender et al., 1995, Flemming 2008, Flemming and Wingender, 2010).

### **1.1.2. Advantages of a biofilm lifestyle**

Biofilm formation comes with some undeniable investments. The high cell densities in biofilms create a strong exploitative competition for resources (Stoodley et al., 2002, Cornforth and Foster, 2013, Franklin et al., 2015, Rendueles and Ghigo 2015, Dang and Lovell, 2016). Competition for resources rather than cooperation seems to be the dominating factor in microbial interactions (Foster and Bell, 2012, Hibbing et al., 2010). Microorganisms in biofilms may employ a diverse range of strategies in the competition with other cells, such as predation (phagocytosis, cell invasion), production of antimicrobials (e.g. colicins, microcins, pesticins), contact dependent growth inhibition, cell-to-cell communication inhibition, EPS matrix degradation,



induced dispersal or motility techniques (e.g. surface-blanketing, induction of motility) (Dobretsov 2010, Hibbing et al., 2010, Cornforth and Foster, 2012, Rendueles and Ghigo 2015). An additional challenge of the biofilm phenotype is the accumulation of poorly degradable metabolic products and other toxic substances (Foster and Bell, 2012, Flemming et al., 2016). Furthermore, the production of EPS is very nutrient and energy demanding. In biofilms the vast majority of the dry weight originates from EPS, while the embedded cells only provide a minor fraction of the dry weight (Costerton 1999, Donlan and Costerton 2002, Flemming and Wingender, 2010). Yet, the microorganisms must still largely benefit from biofilm formation in order to justify the nutrient and energy investments made. Some of the core advantages of biofilm formation include:

### **Nutrient availability**

Biofilms on solid-liquid interfaces, in an environment with liquid flow, have constant supply of fresh nutrients (Steenackers et al., 2016). In addition, the EPS matrix contains extracellular enzymes and binding sites for nutrients, allowing further increasing the availability of nutrients in biofilms (Flemming et al., 2016, Dang and Lovell, 2016). Those advantages in combination with retention and efficient recycling of molecules from dead cells may explain the reported formation of biofilms under very oligotrophic (low nutrient) and starvation conditions (Petrova and Sauer, 2012, Flemming et al., 2016). However, it is unclear whether all cells in a biofilm benefit from the described advantages (Flemming and Wingender, 2010).

### **Formation of stable microconsortia**

Besides strong competition exerted on microorganisms living in dense biofilms, the biofilm-immobilized cells may also develop intensive interactions, forming synergistic microconsortia (Flemming 2008). Examples of such synergistic interactions are cross-feeding and degradation of toxic compounds (Rendueles and Ghigo 2015). One well-studied example of biofilm associated synergistic interactions is the two-step nitrification process. In the first step ammonia oxidizers, produce nitrite. The nitrite, that is an inhibitory end product for the ammonia oxidizers, is readily oxidized to nitrate by the nitrite oxidizers in the second step of the nitrification process (Flemming 2008).

### Heterogeneity: gradients create diverse habitats

Diffusion limitation, sorption, consumption or degradation of high energy yielding electron acceptors and nutrients will create steep gradients in physicochemical conditions within a biofilm (*Dang and Lovell 2016*). The diverse gradients in biofilms (e.g. organic carbon, oxygen, carbon dioxide, hydrogen sulfide, methane, nitrate, nitrite, ammonium, pH, ion strength or redox) create a large number of niches that are different from the surrounding water phase (*Flemming 2008, Stewart and Franklin, 2008, Dang and Lovell 2016, Steenackers et al., 2016*).

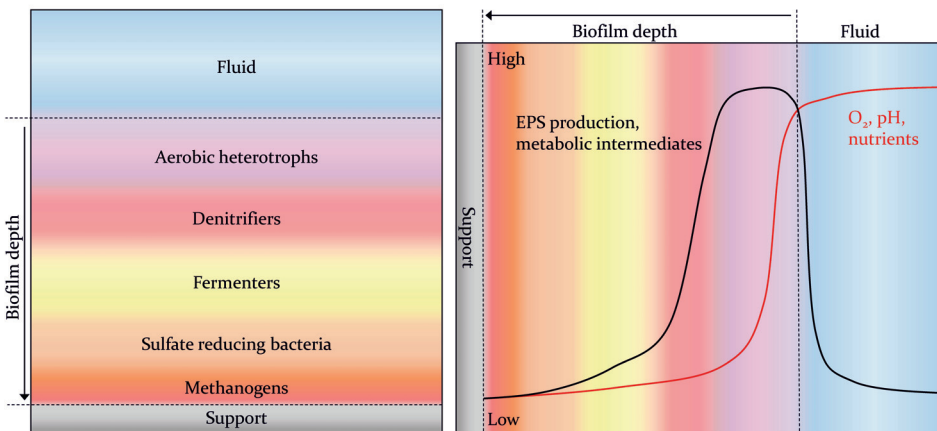


Figure 1.2. Simplified illustration of potential physiological (left) and chemical (right) heterogeneity in biofilms.

For example, oxygen and easily biodegradable organic carbon will be readily consumed in the upper layers of the biofilm, while slower growing anaerobic microorganisms may dominate life in the bottom layers of the biofilm (*Flemming 2008, Stewart and Franklin, 2008, Rendueles and Ghigo 2015, Dang and Lovell 2016, Figure 1.2.*). Sulfate-reducing and acid producing fermentative microorganisms may manifest in anoxic zones at the base of the biofilm (*Davis and McDonald 2005*). If the acids produced by those microorganisms are not readily converted by other microorganisms or abiotic processes, pH gradients in the biofilm may evolve (*Geesey 1991*).

In addition to this rather global gradients (stratification), additional metabolic and chemical gradients (microdomains) may be found within individual microcolonies (*Lawrence et al., 2016*).

The large number of niches and increased nutrient availability results in more diverse microbial communities with increased metabolic and biochemical activities in biofilms, when compared to the planktonic lifestyle (*Franklin et al., 2015, Dang and Lovell 2016*).

### **High genetic diversity: Horizontal gene transfer and increased recombination rates**

To adapt to changing environmental conditions and to survive attacks, biofilms sustain great genetic diversity. Some of the mechanisms to maintain greater genetic diversity are drastically increased recombination rates and horizontal gene transfer (of e.g. antibiotic resistance or virulence genes). Although cells growing in a suspension may be more likely to randomly meet, the spatial stability of EPS embedded cells favors horizontal gene transfer in biofilms (*Hausner und Wuertz, 1999, Decho and Gutierrez 2017*). For example, conjugation frequencies in laboratory grown biofilms were shown to be up to ~7,000-fold increased compared to those seen with planktonic cultures (*Savage et al., 2013*).

### **Protection against environmental stress**

The EPS produced by biofilms protects the embedded microorganisms against environmental stress, including predation, desiccation, UV exposure and fluctuating environmental conditions (e.g. temperature and pH) (*Flemming and Wingender 2010, Carvalho 2018*).

### **Protection against antimicrobials**

Microorganisms in biofilms exhibit a much higher tolerance to antimicrobials such as antibiotics and biocides (e.g. disinfectants or preservatives) when compared to their planktonic living counterparts (*Costerton 1999, Foley and Gilbert, 1996, Donlan and Costerton 2002*). The increased tolerance and resistance of biofilm microorganisms cannot be solely explained by diffusion limitation (*Foley and Gilbert, 1996, Cochran et al., 2000, Flemming 2002*). Tolerance and resistance of biofilms towards antimicrobials is modulated by a multitude of factors such as reduced access of biocide to microbial cells, sorption and degradation of the antimicrobials, starvation and presence of persisters, genetic exchange between cells, adaptation

and mutation of the microbial cells and biocide efflux (Russell, 2003, Zhou et al., 2015).

## **1.2. Biofilms in engineered systems**

Biofilms are successfully utilized in biotechnological processes including the biological filtration of water, the degradation of wastewater and solid waste, and biocatalysis in biotechnological processes such as the production of bulk and fine chemicals, as well as biofuels (Qurechi 2009, Halan et al., 2012).

However, biofilms in engineered systems are frequently associated with strong negative economic and/or health effects impacts when proliferating in unwanted places. Similar to nature, biofilms in engineered systems may proliferate even under extreme conditions as for example found in ultrapure water systems (Kulakov et al., 2002), potable water from space stations (Koenig and Pierson 1997), highly acidic waters from mines (Edwards et al., 1999), concentrated disinfectants or nuclear power plants (Flemming 2009).

The industries affected by the detrimental economic and/or health effects of biofilm formation are numerous and include: food and beverage (Galié et al., 2018), oil and gas (Passman 2013, Vigneron et al., 2018), metal (Trafny et al., 2015), semiconductor (Kulakov et al., 2002), pulp, paper and board (Bajpai 2015a and 2015b), marine transportation and marine aquacultures (Carvalho, 2018), water and wastewater treatment (Nguyen et al., 2012), desalination (Carvalho 2018, Nagaraj et al., 2018), power (Satpathy et al., 2010, Sriyutha Murthy and Venkatesan, 2009, Frota et al., 2014), chemical, health/medical (Donlan and Costerton 2002, Licker et al., 2017), pharmaceuticals, automobile, paint (Flemming 2011) and virtually any other type of water intensive industries.

### **1.2.1. Biofouling - Troublesome biofilms in engineered systems**

When biofilms in engineered systems become troublesome, they are usually referred to as biofouling (Characklis 1991, Flemming 1997, Flemming 2002, Sriyutha Murthy and Venkatesan 2009). There are some differences in the definition of biofouling amongst different industries, but the definitions typically describe an impediment to efficient operation (in respect of energy usage such as pumping energy, heat

transfer, and engine energy), material degradation, or biofilm associated health risks (Characklis 1991, Flemming 1997, Sriyutha Murthy and Venkatesan 2009, Bott 2011a). Biofouling thus always describes negative consequences of biofilm formation in an application context. Although the affected industries are very diverse in terms of products or applications, the operational problems, risks and consequences related to biofilm formation are quite similar.

The general consequences of biofouling can be categorized into (Edyvean 1990, Characklis 1991, Morton *et al.*, 1998, Dobretsov 2010, Bott 2011a, Khweek *et al.*, 2013, Bajpai 2015a, Gallié *et al.*, 2018):

1. Decrease in product quality
  - Degradation of product or damaged products
  - Product contamination
  - Spoilage of product
2. Loss in performance
  - Reduced heat transfer in heat exchangers
  - Increased differential pressure drop in-, or clogging of liquid-carrying systems such as pipes or filters
  - Biofilm increases frictional resistance
  - Interference with the function of chemical additives (e.g. corrosion inhibitors)
  - Blockage of filters and screens
3. Increase in cleaning expenses and down time
  - Lengthy shut-downs for repairs, cleanings, filter change-outs, etc.
4. Damage and shorter life of plant components
  - Microbial induced corrosion including mechanisms such as cathodic and anodic depolarization, hydrogen production, metal reduction, deposition, production of corrosive metabolites (e.g. organic acids and exopolymers) or ennoblement
  - Direct attack or degradation (e.g. cellulose acetate membranes, fuels, cooling tower timber)

## 5. Security and health problems for personnel, public and environment

- Makes surfaces slippery
- Proliferation and release of pathogenic microorganisms (e.g. *Legionella pneumophila*, *Pseudomonas* spp., *Staphylococcus* spp., *Mycobacterium* spp., *Bacillus cereus*, *Salmonella enterica*)
- Increased virulence of pathogens through biofilm passage

Altogether, biofouling is a common and costly problem. The increased energy usage (largely originating from fossil fuels) of the pumps and engines, to overcome the performance losses caused by biofouling, contributes to global warming and displays a strong economic risk to the operators (Bott 2011a). Operational downtime related to biofouling problems further adds up to the negative economic effects (Bott 2011b). However, it is difficult to estimate the real costs of biofouling across the diverse types of industries, as quantitative data in literature is very limited. Some examples: Flemming (1997) reported costs of biofouling prevention and control for a Reversed Osmosis (RO) plant in California of ~ \$700,000 per year, which equals to 30% of total operating costs. Flemming *et al.* (2013) reported that one to two out of five paper breaks at the paper machine, which can occur multiple times per day, are due to microbial biomass. A single paper break at the paper machine costs between \$2,000 to \$10,000, depending on the size of the plant, the process and the quality of the paper (Flemming *et al.*, 2013). A single day of downtime may easily result in a commercial loss of \$180,000 in a power plant (Frota *et al* 2014), \$1,000,000 in a refinery or \$10,000,000 in oil production (Characklis 1991). It was estimated that biofouling control costs the aquaculture industry about 1.5 to 3 billion US dollar per year (Fitridge *et al.*, 2012)

### 1.2.2. Biofouling prevention and control

There is a multitude of established biofilm prevention and control techniques that can be roughly divided into chemical and physical methods. In addition, there are a number of microbiological methods, which are not yet commonly applied in industrial water systems. The methods to prevent and control biofilm formation can be applied to the fresh process liquid during pretreatment or to the recirculating or once-through process liquid directly during normal operation. The core biofouling

prevention and control applied in engineered systems can be divided into different strategies.

#### 1.2.2.1. Prevention of biofilm formation

**Removal of biodegradable compounds** can be achieved by various techniques such as adsorption, coagulation, low-pressure and high-pressure membrane filtration or media filtration (e.g. sand, anthracite or diatomaceous earth) (*Sriyutha Murthy and Venkatesan 2009, Jiang et al., 2017*). The filtration techniques mentioned above will also remove a substantial part (efficiency is dependent for each method) of the microorganisms in the liquid stream (*Jiang et al., 2017*). The nutrient removal is typically aimed at easily biodegradable organic carbon, but can also be applied for other nutrients such as phosphate (*Vrouwenvelder et al., 2010*). Nutrient limitation has been termed the most elegant way to prevent biofouling (*Sriyutha Murthy and Venkatesan 2009*).

**Reduction of microbial biomass** can be achieved by, amongst others, sand filters, granular filters (*Flemming 2002*) and membrane filtration. Reduction of biomass is typically employed during pretreatment, but also frequently used during side stream-, and full stream filtration.

**Inactivation of microorganisms** can be achieved by a variety of physical and chemical methods. Chemical inactivation typically involves the continuous, intermittent or shock treatment with oxidizing and non-oxidizing biocides (*Bott 2011b, Pippo et al., 2018*). Physical disinfection may be achieved by applying techniques such as high temperature, ultraviolet light, ultrasound, osmotic shocks, electricity or gamma radiation (*Maddah and Chogle 2017, Bott 2011b*). As an alternative to commonly used industrial biocides, free-radical generating compounds such as nitric oxide precursors, such as sodium nitroprusside, are currently being explored (*Nagaraj et al., 2018*). A number of biological methods may be promising alternatives or additions to the currently applied chemical and physical methods such as the use of bacteriophages and competing microorganisms (*Simões et al. 2010, Bajpai 2015c*) or introduction grazing amoeba (*Plasson and Bodennec 2016*).

**Surface modifications** aim to prevent biofilm formation on surfaces that are in contact with liquids. There is a multitude of different methods that can be roughly divided into surface modification that prevents attachment of microorganisms (by e.g. increased hydrophilicity, decreased surface roughness, electrostatic repulsion (Jiang *et al.*, 2017, Maddah and Chogle 2017) and surface modification that releases antimicrobials to prevent biofilm formation (Simões *et al.* 2010). The approach of surface modification is somewhat controversially discussed, as often only a short term effect can be seen. Once the antimicrobials are consumed or the initial surface is masked by dead microorganisms or other deposits, biofilm formation may resume at normal rates.

#### **1.2.2.2. Control of biofilm formation**

**Biodispersants** are a range of chemicals (e.g. organic compounds, polymers or surface active agents) that are applied to penetrate and disperse biofilms, in order to regain systems cleanliness (Bajpai 2015c, Bott 2011b). Typically, biodispersants are applied together with biocides to enhance the effect of the treatment (Bajpai 2015c). Some biodispersants also act as biocides (Bott 2011b). Similar to biocides, biodispersant can be applied continuously, intermittent or as shock treatment (Bajpai 2015c).

**Chemical cleaning in place (CIP)** is applied when standard biodispersant and biocide additions are not successful anymore to prevent biofouling (or when biocides cannot be used). Commercially available cleaning agents include alkalis, acids, oxidizers, surfactants, metal chelating agents, enzymes, or combinations thereof (Flemming *et al.*, 1997, Jiang *et al.*, 2017, Maddah and Chogle 2017, Galié *et al.*, 2018).

**Mechanical/physical cleaning** is typically applied when all of the previously mentioned control strategies fail. Traditional mechanical/physical cleaning with sponges and brushes is typically highly effective (Simões *et al.* 2010), but it is also very labor intensive, increases downtime and often not all parts of the liquid carrying system can be accessed. To overcome accessibility limitations in some of the system parts, sponge rubber balls, ice crystals or other objects can be circulated with the liquid flow (Bott 2011b). In addition, there are several methods that aim at the



detachment of biomass by alterations of the hydrodynamic conditions such as backwashing, flow reversal, pulsed flow or injection of gases (rumbling) (*Bott 2011b*). An efficient biofouling prevention and control approach in industrial settings involves a combination of multiple elements of the above described techniques (*Nguyen et al., 2012, Passman 2013*).

When all of the above mentioned strategies fail, additional treatment steps and premature replacement of equipment may be inevitable for operational-, and/or hygienic sound operation of the affected systems (*Characklis 1991, Flemming 1997, Bajpai 2015b, Vrouwenvelder et al., 2008*).

### **1.2.3. High-pressure membrane filtration – Application and working principle**

Biofouling has long been acknowledged to be the “Achilles heel” of pressure driven membrane filtration processes (*Flemming et al., 1997*). Pressure driven membrane filtration is a process where a liquid stream is purified or concentrated with the help of a semi-permeable membrane (*Figure 1.3. A*). Those semi-permeable membranes are classified by their retention of solutes into four major categories microfiltration- (MF), ultrafiltration- (UF), nanofiltration- (NF), and reverse osmosis (RO) membranes (*Figure 1.3. B*). The membranes may also be categorized by the required driving force for filtration into low-pressure membranes (MF and UF) and high-pressure membranes (NF and RO) (*Frenkel 2015*). The high pressure membrane filtration processes using NF and RO will be the focus of this thesis. While NF has a high removal efficiency for multivalent ions, it will only remove monovalent ions partially (depending on the size cutoff of the membrane) (*Figure 1.3. B, Frenkel 2015*). RO in contrast has high removal efficiency for monovalent ions and therefore can be employed for brackish and seawater desalination (*Figure 1.3. B, Frenkel 2015*).

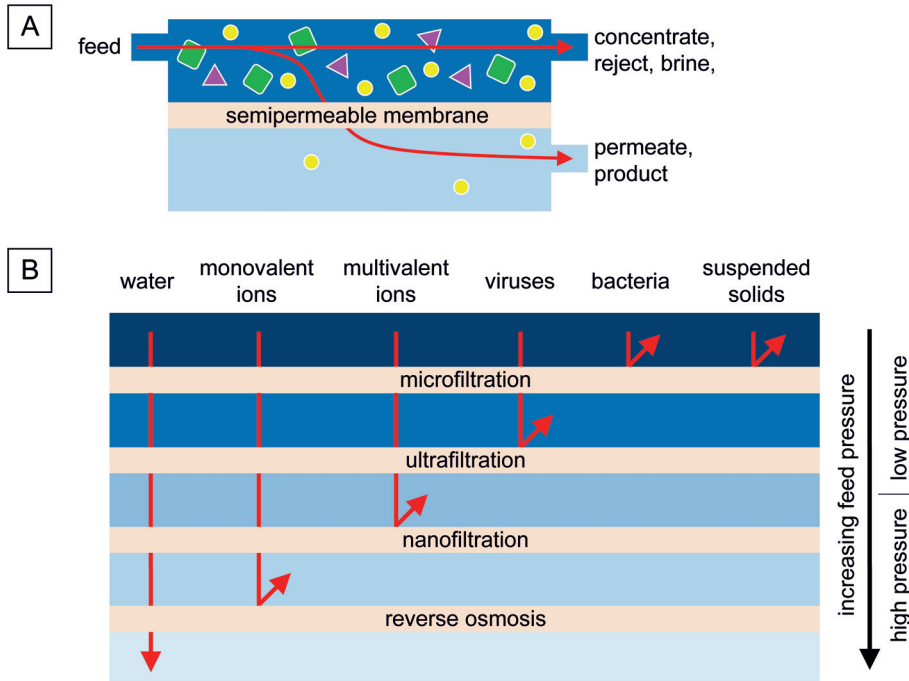


Figure 1.3. General working principle of pressure driven membrane filtration processes (A) and scheme of different membrane types and rejection capabilities (B)

Large amounts of high purity water for drinking water or industrial applications can be produced, at reasonable cost, by the application of high-pressure membrane filtration processes such as NF and RO (Frenkel 2015, Jiang et al., 2017). The widespread application and success of high-pressure membrane filtration can be associated with the ability to desalinate water and to remove a huge variety of compounds in a single purification step. During cross-flow high-pressure membrane filtration a water stream (namely feed) is divided, with the help of a semi-permeable membrane, into a highly concentrate waste stream (namely concentrate, reject or brine) and a high-purity product stream (namely permeate or product) (Mulder 1996, Frenkel 2015) (Figure 1.3. A).

The two basic membrane configurations are flat sheet and tubular. In order to increase productivity by maximizing the surface to volume ratio, the membranes are arranged into membrane elements (also called membrane modules) (Mulder 1996). Common membrane arrangements are spiral wound (flat sheet), plate and frame (flat sheet), hollow fiber (tubular) and capillary (tubular). (Mulder 1996, Frenkel

2015). The most widespread used nanofiltration and reverse osmosis membrane elements in water and wastewater treatment are configured as spiral wound elements (Nguyen *et al.*, 2012, Curcio *et al.*, 2015, Figure 1.4. and 1.5.).

In a spiral wound membrane element, membrane envelopes are glued to-, and wound around the perforated permeate collection tube (Figure 1.4. and 1.5.). A membrane envelope consist of two membranes sheets, separated by a thin permeate collection spacer, that are glued to each other on three of the sides. The open side is glued to, and rolled around, the perforated permeate collection tube. Individual membrane envelopes are then separated by a feed spacer (Mulder 1996, Curcio *et al.*, 2015, Figure 1.4. and 1.5.).

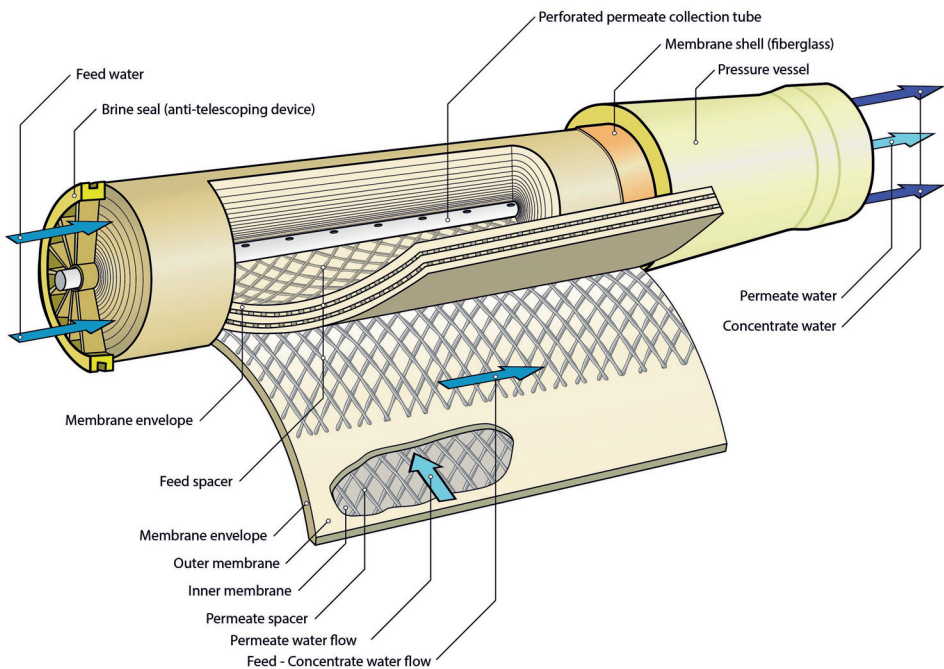


Figure 1.4. Schematic representation of a spiral wound membrane element and pressure vessel

During operation, feed water enters the membrane element and is distributed by the feed spacer. The feed spacer is not merely designed for distribution of the feed water, but also acts as a turbulence promoter (Mulder 1996). A portion of the feed water then eventually passes the membrane surfaces as permeate and flows along the permeate spacer towards the perforated permeate collection tube. The majority of

the feed water and its rejected solutes leaves the membrane as concentrate (Mulder 1996, Curcio et al., 2015, Figure 1.4. and 1.5.). The driving force for the filtration is the pressure difference between the feed – concentrate channel and the permeate channel, which is called transmembrane pressure.

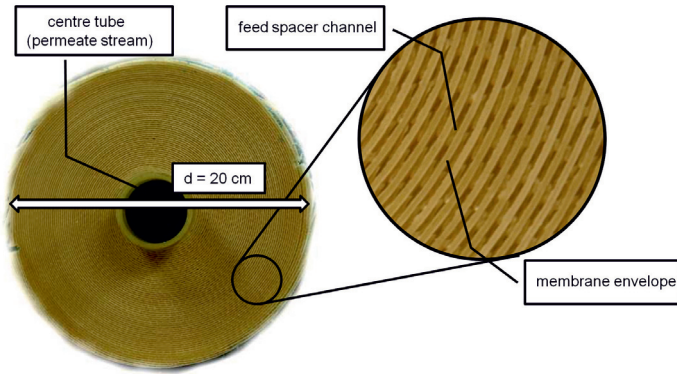


Figure 1.5. Side-view and close-up of a spiral wound membrane element

A number of individual membrane elements are then placed into pressure vessels, in order to maximize the water usage (Figure 1.6.). By placing several membrane elements in a series, the ratio of permeate to concentrate (recovery rate) can be increased. The pressure vessels are then group into stages to further increase recovery rate (Curcio et al., 2015). Most membrane filtration installation are arranged into two stages using pressure vessels that house 6 to 8 membrane elements (Curcio et al., 2015, Figure 1.6.). In addition, hydrodynamic optimized arrangements (pressure vessel housing 3 membrane elements arranged in 3 stages) can be found in industry (van der Meer et al., 2003, van Paassen et al., 2005). Usual recovery rates for industrial RO installations range from 40 – 60 % (for seawater) and 75 – 85 % (for brackish water) (Frenkel 2015).

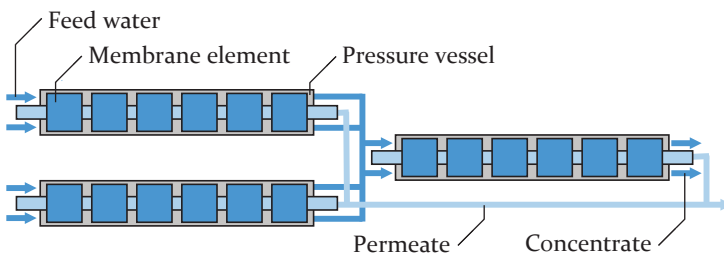


Figure 1.6. Arrangement of membrane elements into pressure vessels and stages

#### 1.2.4. Fouling during high pressure membrane filtration

A major drawback for the continuous and worry-free operation of membrane filtration installations is the development of fouling. Fouling is the unwanted accumulation of debris hindering the performance of industrial processes. Based on the nature of the debris, the most important fouling types in membrane technology can be divided into (Flemming 1997):

- Crystalline fouling (mineral scaling, deposition of minerals due to the excess of the solution product)
- Organic fouling (deposition of dissolved humic acids, oil, grease, etc.)
- Particle and colloid fouling (deposition of clay, silt, particulate humic substances, debris, silica)
- Microbiological fouling (biofouling, adhesion and accumulation of microorganisms, forming biofilms)

Biofouling in contrast remains the most common and tough type of membrane fouling which is also hardest to prevent and control (Flemming *et al.*, 1997, Nguyen *et al.*, 2012, Peña *et al.*, 2012, Bucs *et al.*, 2014, Jiang *et al.*, 2017, Maddah and Chogle 2017). Other types of fouling such as organic or crystalline fouling are less frequent and typically can be prevented or controlled by pretreatment, chemical addition, or chemical cleaning. Even the removal of 99.99% of the microorganisms by pretreatment will not guarantee the prevention of biofilm formation on the downstream membranes (Flemming *et al.*, 1997a, Flemming 2002).

#### 1.2.5. Membrane biofouling – A matter of definition

Biofilms, once developed in a membrane element, act as a secondary layer on the membrane surface. This secondary layer decreases the water flow rate (flux) through the membrane by an increase in the overall filtration resistance (Flemming *et al.*, 1997, Gutman *et al.*, 2012, Figure 1.7.). In addition to the increased filtration resistance, the biofilm increases the stagnant boundary layer thickness leading to enhanced concentration polarization and osmotic effects, further reducing the membrane flux (Gutman *et al.*, 2012). A key performance parameter that can be calculated from the membrane flux (by normalization of surface area, filtration pressure, osmotic differences in feed and permeate and temperature) is called

normalized membrane permeability ( $K_w$ ) (in some literature referred to as MTC) (van de Lisdonk *et al.*, 2001).

In addition to the “vertical” filtration barrier caused by biofilm enhanced concentration polarization and the biofilms filtration resistance, biofilms also act as a “vertical” barrier that increases the feed – concentrate channel pressure drop (FCP) (Gutman *et al.*, 2012, Figure 1.7.). The increase in FCP can be attributed to flow disturbances introduced by biofilm growth on the membrane and spacer surfaces of a membrane element (Vrouwenvelder *et al.*, 2009) and increased drag resistance to flow over the biofilm covered membrane surfaces. (Flemming 1997, Figure 1.7.). An increase in FCP leads to a decrease in the pressure available to drive downstream filtration consequently causing reduced membrane flux. Excessive FCP increase may also lead to displacement of the membrane and spacer surface causing membrane element damage by a process termed telescoping (Schneider *et al.*, 2005). The key performance parameter that is calculated from the FCP (by normalization of temperature and feed flowrate) is called normalized (feed-concentrate channel) pressure drop (NPD) (van den Broek *et al.*, 2010).

An increase in NPD and decrease in  $K_w$  both lead to an increase in feed pressure, as the majority of membrane filtration plants are operated at constant permeate production (Nguyen *et al.*, 2012).

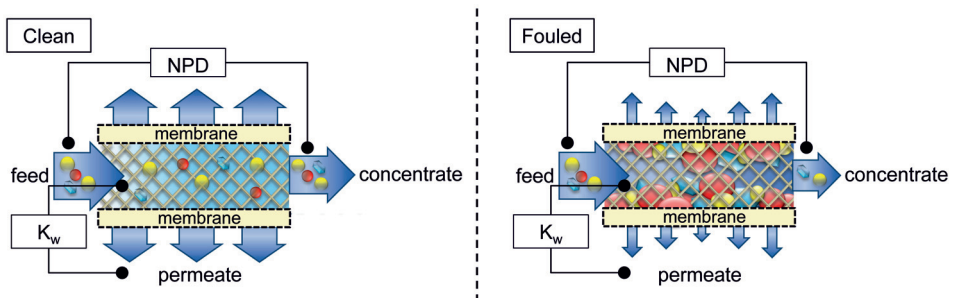


Figure 1.7. Schematic representation of spiral wound membrane flow channel in clean and fouled conditions.

Another detrimental effect of biofilm formation in membrane elements is reduced product (permeate) quality due to decreased solute rejection. Biofilms may have direct and indirect negative consequences on membrane integrity, lowering the

solute rejection. A direct consequence may be membrane degradation by microbial attack as known from cellulose acetate membranes or glue lines (Flemming 1997, Nguyen et al., 2012). An indirect consequence is membrane deterioration by repetitive and harsh cleanings to control the biofilms developed (Flemming 1997). Both the direct and indirect mechanisms will result in decreased rejection of solutes, lowering the purity of the permeate. In addition, reduced solute rejection may also be caused by biofilm enhanced concentration polarization (Flemming 1997, Gutman et al., 2012, Nguyen et al., 2012). The key performance parameter that is calculated from the overall solute rejection (by normalization of temperature, membrane properties, flow rates and recovery) is called normalized salt retention / rejection, or normalized salt passage (the inverse of salt retention / rejection) (van den Broek et al., 2010).

The operational defined term “biofouling” can then be determined from the negative effects of biofilm formation on one-, or combination of the three key performance indicators  $K_w$ , NPD and salt retention. In full-scale NF and RO operation, membrane fouling is typically defined as (Nederlof et al., 2000, Huiting et al., 2001, Vrouwenvelder et al., 2008):

- $K_w$  decrease  $\geq 15\%$  and/or,
- NPD increase  $\geq 15\%$  and/or,
- Salt retention decrease  $\geq 5\%$

Once biofouling is present within the installation, chemical cleaning of the membranes will be initiated as an attempt to restore original membrane performance (Nguyen et al., 2012). Chemical cleaning in place (CIP) comes with downtime of production marking another indirect detrimental effect of biofilm formation in membrane filtration plants (van den Broek et al., 2010).

In summary, the adverse effects of biofouling on the key performance indicators of nanofiltration and reverse osmosis membrane processes are (Flemming 1997, Gutman et al., 2012, Nguyen et al., 2012, Maddah and Chongle 2017):

1. Reduced membrane flux and membrane permeability ( $K_w$ )
  - Biofilms as secondary separation layer causes increased hydraulic filtration resistance
  - Biofilms increase stagnant boundary layer thickness leading to biofilm enhanced concentration polarization
  - Biofilms on spacer surfaces decrease the efficiency of spacers to reduce concentration polarization
  - Biofilm enhanced concentration polarization and metabolic processes increase inorganic precipitation (scaling)
2. Increased normalized pressure drop (NPD)
  - Reduced membrane flux due to decrease in pressure available for downstream filtration
  - Membrane element damage due to membrane and spacer displacement (telescoping)
3. Decrease in solute rejection (salt rejection)
  - Microbial acidic metabolites or exoenzymes cause damage to the membrane materials (e.g. cellulose acetate membranes and glue lines)
  - Frequent chemical cleaning damages membrane materials leading to decrease solute rejection consequently shortening membrane lifetime
  - Biofilm enhanced concentration polarization reduces solute rejection

### **1.2.6. Microbial diversity of membrane biofouling**

Typically, high-pressure membrane filtration biofilms are dominated by bacteria. Other types of microorganisms such as fungi or archaea may also be found, but usually in much smaller abundancies. Biofilms are highly dynamic structures and hence, the microbial diversity may change with biofilm maturation, biofouling control efforts or with seasonal variations in feed water quality parameters such as temperature or organic carbon availability. Furthermore, a wide range of feed water types may be employed for high-pressure membrane filtration (e.g. groundwater, surface water, seawater or wastewater effluent), further affecting the microbial diversity developing.



However, some general microbial diversity patterns can be revealed when reviewing literature data. Most studies found a strong predominance of the bacterial phylum Proteobacteria (especially the  $\alpha$ -,  $\beta$ -, and  $\gamma$ -Proteobacteria, while  $\delta$ -, and  $\epsilon$ -Proteobacteria are typically low in abundance) in 'biofouling biofilms' (Chen *et al.*, 2004, Pang and Liu 2007, Bereschenko *et al.*, 2008 and 2010, Ayache *et al.*, 2013, Al Ashhab *et al.*, 2014, Lee and Kim, 2011, Levi *et al.*, 2016, Nagaraj *et al.*, 2017). Bacteria producing glycosphingolipids (namely Sphingomonadales, Rhizobiales and Sphingobacteria) have recently gotten more into focus, as they appear to play a crucial role in membrane biofouling development (Al Ashhab *et al.*, 2014, Nagaraj *et al.*, 2017).

Special attention has been attributed to the *Sphingomonadaceae*, a family within the order Sphingomonadales, belonging to the class of  $\alpha$ -Proteobacteria (Balkwill *et al.*, 2006). Within the *Sphingomonadaceae* family, the group of Sphingomonads that consists of *Sphingomonas sensu stricto*, *Sphingobium*, *Novosphingobium* and *Sphingopyxis* (Takeuchi 2001) has been of particular interest. Members of the Sphingomonads, have been frequently associated with biofouling in RO but also in other membrane systems, regardless of the feed water source (e.g. surface water (Bereschenko *et al.*, 2008 and 2010), brackish water (Khambhaty and Plumb, 2010), wastewater (Ivnitsky *et al.*, 2007, Al Ashhab *et al.*, 2014) and seawater (Nagaraj *et al.*, 2017).

The overall contribution of Sphingomonads to the biofouling process has mainly been attributed to very successful primary colonization of fresh membranes. The very sticky EPS of glycosphingolipid producing bacteria appears to strongly aid primary colonization and contributing significantly to the cohesive strength of the biofouling layers (Bereschenko *et al.*, 2008, Bereschenko *et al.*, 2010, Lee and Kim 2011, van Loosdrecht *et al.*, 2012, Al Ashhab *et al.*, 2014, Haas *et al.*, 2015, Nagaraj *et al.* 2017). Furthermore, Sphingomonads possess twitching and swarming motilities, which facilitate the colonization of membrane and spacer surfaces (Pang *et al.* 2005; Bereschenko *et al.* 2010). For example, Pang *et al.* (2005) showed that *Sphingomonas* RO2, a swarming and twitching isolate from a potable water treating RO plant,

attached to different RO membrane materials regardless of membrane surface characteristics like microroughness, hydrophobicity and zeta potential.

Van Loosdrecht *et al.* (2012) proposed that members of *Sphingomonadaceae* rapidly colonize fresh membranes by forming a thin biofilm layer without performance loss and that further colonization by other microorganisms may be required to lead to subsequent biofouling development by forming a thicker and mature biofilm. The role of *Sphingomonadaceae* in biofilm maturation is not well understood yet. In another study *Sphingomonas* spp. did not only initiate biofilm development on RO membranes and spacers, but also dominated consequent biofouling development (Bereschenko *et al.*, 2010).

*Sphingomonadaceae* were also often detected after failed chemical cleaning attempts. In two RO membrane cleaning studies only *Sphingomonas* spp. survived the chemical treatments (Bereschenko *et al.*, 2010 and 2011). *Sphingopyxis* spp. and *Sphingomonas* spp. have also been shown to dominate 3 – 6 months old membranes that had been weekly cleaned (Berenschenko *et al.*, 2011). Similar observations were made for membrane-coupled anaerobic bioreactors, where *Sphingomonadaceae* were abundant in the biofouling layers and resistant to chemical cleaning and back flushing (Calderón *et al.*, 2011).

It was concluded that the development of novel antifouling strategies, specifically targeted towards glycosphingolipid producing bacteria in general, and *Sphingomonadaceae* in particular (Bereschenko *et al.*, 2011, Calderón *et al.*, 2011, van Loosdrecht *et al.*, 2012, Al Ashab *et al.* 2014, Nagaraj *et al.*, 2017) seems to be a promising approach for improving biofouling prevention and control.

Other phyla typically detected on biofouled membranes include Bacteroidetes, Planctomycetes, Firmicutes, Acidobacteria and Actinobacteria (Chen *et al.*, 2004, Pang and Liu 2007, Bereschenko *et al.*, 2008 and 2010, Ayache *et al.*, 2013; Al-Ashhab *et al.*, 2014, Lee and Kim, 2011, Levi *et al.*, 2016, Nagaraj *et al.*, 2017).

## **Aim and scope of this thesis**

Biofouling contributes significantly to operational costs, downtime and carbon emissions. Despite many research attempts, past and present strategies to prevent and control biofouling in membrane systems have not been successful under all circumstances.

A key to the development of novel biofouling prevention and control strategies is the study of relevant biofouling microorganisms (biofouling key-players) under representative hydrodynamic conditions as experienced under full-scale operation. Current commonly applied short-term static biofilm tests are not able to simulate the complex hydrodynamic conditions experienced in full-scale membrane elements and therefore lack important information on the effects of biofouling on the key-performance parameters  $K_w$ , NPD and rejection capacity. However, those key-performance parameters must be included in the ultimate validation of novel biofouling prevention and control strategies, in order to deliver representative results.

This study focuses on the comparison of installations that do not suffer from biofouling, with installations suffering from rapid biofouling problems. The study furthermore aims to display the limits of current biofouling control strategies such as chemical membrane cleaning. The study also aims at the isolation and physiological characterization of relevant biofouling key-players. The ultimate goal was to study the biofouling key-players under representative hydraulic conditions, as experienced during full-scale operation.

With the presented tools and clues, advanced biofouling prevention and control strategies may be developed.

## Research Objectives

The specific objectives of this thesis were the following:

1. Study membrane filtration installations that do not suffer from rapid biofouling development
2. Investigate the microbial diversity of installations without rapid biofouling problems
3. Demonstrate the limitations of chemical cleaning to control matured biofouling layers
4. Understanding the physiology of bacteria that play crucial role in membrane biofouling

## Outline of this thesis

This thesis is made up of 6 chapters, starting with the general introduction followed by

- Chapter 2, a study of direct nanofiltration installations that treat anoxic groundwater and do not suffer from rapid biofouling problems is presented
- In Chapter 3, the microbial diversity of anoxic groundwater treating direct nanofiltration installations that do not suffer from rapid fouling was investigated and compared to literature data from installations suffering from rapid biofouling development.
- In Chapter 4, experimental studies to demonstrate the limitations of chemical cleaning of aged and persistent biofouling layers are presented
- In Chapter 5, biofouling microorganisms are isolated and key-physiological properties are characterized
- And finally, Chapter 6 provides a summary of conclusions, an outlook and recommendations for further research including a preliminary experimental study to the development of a laboratory set-up to study relevant biofouling microorganisms under controlled conditions.

## References

- Al Ashhab, A., Herzberg, M., Gillor, O. Biofouling of reverse-osmosis membranes during tertiary wastewater desalination: Microbial community composition, *Water Res.* 50: 341-349 (2014).
- Ayache, C., Manes, C., Pidou, M., Croué, J.P., Gernjak, W. Microbial community analysis of fouled reverse osmosis membranes used in water recycling. *Water Res.* 47: 3291-3299 (2013).
- Balkwill, D.L., Fredrickson, J.K., Romine, M.F. Sphingomonas and related genera. In: Dworkin, M., Falkow, S., Rosenberg, E., Schleifer K.-H., Stackebrandt, E. (eds.) *The Prokaryotes: A handbook on the biology of bacteria, volume 5, Proteobacteria: alpha and beta subclasses.* Springer, Singapore. 605-629 (2006).
- Bereschenko, L.A., Heilig, G.H., Nederlof, M.M., van Loosdrecht, M.C.M., Stams, A.J.M., Euverink, G.-J.W. Molecular characterization of the bacterial communities in the different compartments of a full-scale reverse-osmosis water purification plant, *Appl. Environ. Microbiol.* 74(17): 5297-5304 (2008).
- Bereschenko, L.A., Stams, A.J.M., Euverink G.-J.W., van Loosdrecht, M.C.M. Biofilm formation on reverse osmosis membranes is initiated and dominated by Sphingomonas spp. *Appl. Environ. Microbiol.* 76(8): 2623-2632 (2010).
- Bereschenko, L.A., Prummel, H., Euverink, G.-J.W., Stams, A.J.M., van Loosdrecht, M.C.M. Effect of conventional chemical treatment on the microbial population in a biofouling layer of reverse osmosis systems. *Water Res.* 45(2): 405-416 (2011).
- Bott, T.R. Industrial biofouling. In: Bott, T.R. (ed.) *Industrial Biofouling.* Elsevier, Amsterdam. 1-6 (2011a).
- Bott, T.R. Biofouling control. In: Bott, T.R. (ed.) *Industrial Biofouling.* Elsevier, Amsterdam. 81-150 (2011b).
- Bucs, S.S., Valladares Linares, R., van Loosdrecht, M.C.M., Kruithof, J.C., Vrouwenvelder, J.S. Impact of organic nutrient load on biomass accumulation, feed channel pressure drop increase and permeate flux decline in membrane systems, *Water Res.*, 67: 227-242 (2014).
- Calderon, K., Rodelas, B., Cabirol, N., Gonzalez-Lopez, J., Noyola, A. Analysis of microbial communities developed on the fouling layers of a membrane-coupled anaerobic bioreactor applied to wastewater treatment. *Bioresour. Technol.* 102(7): 4618-4627 (2011).
- Characklis, W.G. Biofouling: Effects and Control. In: Flemming, H.-C., Geesey, G.G. (eds.) *Biofouling and Biocorrosion in Industrial Water Systems.* Springer, Berlin, Heidelberg. 7-27 (1991).
- Chen, C.L., Liu, W.-T., Chong, M.L., Wong, M.T., Ong, S.L., Seah, H., Ng, W.J. Community structure of microbial biofilms associated with membrane-based water purification processes as revealed using a polyphasic approach. *Appl. Microbiol. Biotechnol.* 63: 466-473 (2004).
- Cochran, W.L., McFeters, G.A., Stewart, P.S. Reduced susceptibility of thin *Pseudomonas aeruginosa* biofilms to hydrogen peroxide and monochloramine. *J. Appl. Microbiol.* 88: 22-30 (2000).
- Cornforth, D.M., Foster K.R. Competition sensing: the social side of bacterial stress responses. *Nat. Rev. Microbiol.* 11: 285-293 (2013).
- Costerton, J.W. Introduction to biofilm. *Int. J. Antimicrob. Agents.* 11: 217-221 (1999).
- Costerton, J.W. Direct Observations. In: Eckey, C. (ed.) *The Biofilm Primer.* Springer, Berlin, Heidelberg. 3-84. (2007).
- Curcio, E., Di Profio, G., Fontananova, E., Drioli, E. Membrane technologies for seawater desalination and brackish water treatment. In: Basile, A., Cassano, A., Rastogi, N. (eds.) *Advances in Membrane Technologies for Water Treatment.* Elsevier/Woodhead Publishing, Amsterdam, Boston. 411-441 (2015).

- Dang, H., Lovell, C.R. Microbial surface colonization and biofilm development in marine environments. *Microbiol. Mol. Biol. Rev.* 80(1): 91-138 (2016).
- Davey, M.E., O'Toole, G.A. Microbial biofilms: from ecology to molecular genetics. *Microbiol. Mol. Biol. Rev.* 64(4): 847-867 (2000).
- Davis, K.E., McDonald, L.K. Potential corrosion and microbiological mechanisms and detection techniques in solution mining and hydrocarbon storage wells. In: Tsang, C.-F., Apps, J.A. (eds.) *Underground Injection Science and Technology*. Elsevier, Amsterdam. 177-192 (2005).
- de Carvalho, C.C.C.R. Marine biofilms: A successful microbial strategy with economic implications. *Front. Mar. Sci.* 5(126): 1-11 (2018).
- Decho, A.W., Gutierrez, T. Microbial extracellular polymeric substances (EPSs) in ocean systems. *Front. Microbiol.* 8(922): 1-28 (2017).
- Di Pippo, F., Gregorio Di, L. Congestri, R., Tandoi, V., Rossetti, S. Biofilm growth and control in cooling water industrial systems. *FEMS Microbiol Ecol.* 94(5): 1-13 (2018).
- Dobretsov, S. Marine Biofilms. In: Dürr, S., Jeremy, Thomason, J.C. (eds.) *Biofouling*. John Wiley & Sons, Ltd, Chichester. 123-136 (2010).
- Donlan, R., Costerton, J.W., Biofilms: survival mechanisms of clinically relevant microorganisms. *Clin. Microbiol. Rev.* 15(2): 167-193 (2002).
- Edwards, K.J., Gihring, T.M., Banfield, J.F. Seasonal variations in microbial populations and environmental conditions in an extreme acid mine drainage environment. *Appl. Environ. Microbiol.* 65(8): 3627-3632 (1999).
- Edyvean, R.G.J. Fouling and corrosion in water filtration and transportation systems. In: Howsam, P. (ed.) *Microbiology in civil engineering*. Chapman and Hall, London. 62-74 (1990).
- Fitridge, I., Dempster, T., Guenther, J., de Nys, R. The impact and control of biofouling in marine aquaculture: a review. *Biofouling.* 28(7): 649-669 (2012).
- Flemming, H.-C., Schaule, G., Griebe, T., Schmitt, J., Tamachkiarowa, A. Biofouling - the Achilles heel of membrane processes. *Desalination.* 113: 215-225 (1997).
- Flemming, H.-C. Reverse osmosis membrane biofouling. *Exp. Thermal Fluid. Sci.*, 14: 382-391 (1997).
- Flemming, H.-C. Biofouling in water systems – Cases, causes and countermeasures. *Appl. Microbiol. Biotechnol.* 59: 629-640 (2002).
- Flemming, H.-C. Biofilms. In: *Encyclopedia of Life Sciences (ELS)*. John Wiley & Sons, Ltd, Chichester. 1-10 (2008).
- Flemming, H.-C. Why microorganisms live in biofilms and the problem of biofouling. In: Flemming, H.-C., Sriyutha Murthy, P., Venkatesan, R., Cooksey, K.E. (eds) *Marine and industrial biofouling*. Springer, Berlin, Heidelberg. 3-12 (2009).
- Flemming, H.-C., Wingender, J. The biofilm matrix. *Nat. Rev. Microbiol.* 8(9): 623-633 (2010).
- Flemming, H.-C. Microbial biofouling: Unsolved problems, insufficient approaches, and possible solutions. In: Flemming, H.-C., Wingender, J., Szewzyk, U. (eds.) *Biofilm Highlights*. Springer, Berlin, Heidelberg. 81-109 (2011).
- Flemming, H.-C., Meier, M., Schild, T. Mini-review: microbial problems in paper production. *Biofouling.* 29(6): 683-696 (2013).
- Flemming, H.-C., Wingender, J., Kjelleberg, S., Steinberg, P., Rice, S., Szewzyk, U. Biofilms: an emergent form of microbial life. *Nat. Rev. Microbiol.* 14: 563-575 (2016).
- Foley, I., Gilbert, P. Antibiotic resistance of biofilms. *Biofouling.* 10: 331-346 (1996).

- Foster, K.R., Bell, T. Competition, not cooperation, dominates interactions among culturable microbial species. *Curr. Biol.* 22(19): 1845-1850 (2012).
- Franklin, M.J., Chang, C., Akiyama, T., Bothner, B. New technologies for studying biofilms. *Microbiol. Spectr.* 3(4): (2015).
- Frenkel, V.S. Planning and design of membrane systems for water treatment. In: Basile, A., Cassano, A., Rastogi, N. (eds.) *Advances in membrane technologies for water treatment*. Elsevier/Woodhead Publishing, Amsterdam, Boston. 329-347 (2015).
- Frota, M.N., Ticona, E.M., Neves, A.V., Marques, R.P., Braga, S.L., Valente, G. On-line cleaning technique for mitigation of biofouling in heat exchangers: A case study of a hydroelectric power plant in Brazil. *Exp. Thermal Fluid. Sci.*, 53: 197-206 (2014).
- Galié, S., García-Gutiérrez, C., Miguélez, E.M., Villar, C.J., Lombó, F. Biofilms in the food industry: Health aspects and control methods. *Front. Microbiol.* 9(898): 1-18 (2018).
- Geesey, G.G. What is biocorrosion? In: Flemming, H.-C., Geesey, G.G. (eds.) *Biofouling and biocorrosion in industrial water systems*. Springer, Berlin, Heidelberg. 7-27 (1991).
- Gutman, J., Fox, S., Gilron, J. Interactions between biofilms and NF/RO flux and their implications for control - A review of recent developments. *J. Memb. Sci.* 421-422: 1-7 (2012).
- Haas, R., Gutman, J., Wardrip, N.C., Kawahara, K., Uhl, W., Herzberg, M., Arnusch, C.J. Glycosphingolipids enhance bacterial attachment and fouling of nanofiltration membranes. *Environ. Sci. Technol. Lett.* 2: 43-47 (2015).
- Halan, B., Bühler, K., Schmid, A. Biofilms as living catalysts in continuous chemical syntheses. *Trends Biotechnol.* 30: 453-465 (2012).
- Hausner M., Wuertz S. High rates of conjugation in bacterial biofilms as determined by quantitative in situ analysis. *Appl. Environ. Microbiol.* 65: 3710-3713 (1999).
- Hibbing, M.E., Fuqua, C., Parsek, M.R., Peterson, S.B. Bacterial competition: surviving and thriving in the microbial jungle. *Nat. Rev. Microbiol.* 8: 15-25 (2010).
- Huiting, H., Kappelhof, J.W.N.M., Bosklopper, T.G.J. Operation of NF/RO plants: from reactive to proactive, *Desalination* 139: 183-189 (2001).
- Ivnitsky, H., Katz, I., Minz, D., Volvovic, G., Shimoni, E., Kesselman, E., Semiat, R., Dosoretz, C.G. Bacterial community composition and structure of biofilms developing on nanofiltration membranes applied to wastewater treatment, *Water Res.* 41(17): 3924-3935 (2007).
- Jiang, S., Li, Y., Ladewig, B.P. A review of reverse osmosis membrane fouling and control strategies. *Sci. Total Environ.* 595: 567-583 (2017).
- Khambhaty, Y., Plumb, J. Characterization of bacterial population associated with a brackish water desalination membrane. *Desalination.* 269(1-3): 35-40 (2011).
- Khweek A.A., Fernandez Davila, N.S., Caution, K., Akhter, A., Abdulrahman, B.A., Tazi, M., Hassan, H., Novotny, L.A., Bakaletz, L.O., Amer, A.O. Biofilm-derived *Legionella pneumophila* evades the innate immune response in macrophages. *Front. Cell Infect. Microbiol.* 3(18): 1-8 (2013).
- Koenig, D.W., Pierson, D.L. Microbiology of the space shuttle water system. *Water Sci. Technol.* 35(II-12): 59-64 (1997).
- Kulakov, L.A., McAlister, M.B., Ogden, K.L., Larkin, M.J., O'Hanlon, J.F. Analysis of bacteria contaminating ultrapure water in industrial systems. *Appl. Environ. Microbiol.* 68: 1548-1555 (2002).
- Lawrence, J.R., Swerhone, G.D.W., Kuhlicke, U., Neu, T. R. In situ evidence for metabolic and chemical microdomains in the structured polymer matrix of bacterial microcolonies. *FEMS Microbiol. Ecol.* 92(11): 1-12 (2016).

- Lee, J., Kim, I.S. Microbial community in seawater reverse osmosis and rapid diagnosis of membrane biofouling. *Desalination*. 273: 118-126 (2011).
- Levi, A., Bar-Zeev, E., Elifantz, H., Berman, T., Berman-Frank, I. Characterization of microbial communities in water and biofilms along a large scale SWRO desalination facility: Site-specific prerequisite for biofouling treatments, *Desalination*, 378: 44-52 (2016).
- Licker, M., Moldovan, R., Hoge, E., Muntean, D., Horhat, F., Baditoiu, L., Rogobete, A.F., Tîrziu, E., Zambori, C. Microbial biofilm in human health - an updated theoretical and practical insight. *Rev. Romana Med. Lab.* 25(9): (2017).
- Maddah, H. Chogle, A. Biofouling in reverse osmosis: phenomena, monitoring, controlling and remediation. *Appl. Water Sci.* 7: 2637-26517 (2017).
- Morton, L.H.G., Greenway, D.L.A., Gaylarde, C.C., Surman, S.B. Consideration of some implications of the resistance of biofilms to biocides. *Int. Biodeterior. Biodegrad.* 41: 247-259 (1998).
- Mulder, M. Module and process design. In: Mulder, M. (ed.) *Basic principles of membrane technology*. Kluwer Academic Publishers, Dordrecht. 465-521 (1996).
- Nagaraj, V., Skillman, L., Li, D., Gofton, A. Characterisation and comparison of bacterial communities on reverse osmosis membranes of a full-scale desalination plant by bacterial 16S rRNA gene metabarcoding. *NPJ Biofilms Microbi.* 3(13): 1-14 (2017).
- Nagaraj, V, Skillman, L., Li, D. Ho, G. Review – Bacteria and their extracellular polymeric substances causing biofouling on seawater reverse osmosis desalination membranes. *J. Environ. Manage.* 223: 586-599 (2018).
- Nederlof, M.M., Kruithof, J.C., Taylor, J.S., van der Kooij, D., Schippers, J.C. Comparison of NF/RO membrane performance in integrated membrane systems, *Desalination* 131: 257–269 (2000).
- Nguyen, T., Roddick, F.A., Fan, L. Biofouling of water treatment membranes: a review of the underlying causes, monitoring techniques and control measures, *Membranes*. 2: 804-840 (2012).
- Pang, C.M., Hong, P., Guo, H., Liu, W.-T. Biofilm formation characteristics of bacterial isolates retrieved from a reverse osmosis membrane. *Environ. Sci. Technol.* 39(19): 7541-7550 (2005).
- Pang, C.M, Liu, W.-T. Community structure analysis of reverse osmosis membrane biofilms and the significance of Rhizobiales bacteria in biofouling. *Environ. Sci. Technol.* 41: 4728-4734 (2007).
- Passman, F.J. Microbial contamination and its control in fuels and fuel systems since 1980 – a review, *Int. Biodeterior. Biodegradation*. 81: 88-107 (2013).
- Peña, N., Gallego, S., del Vigo, F., Chesters, S.P. Evaluating impact of fouling on reverse osmosis membranes performance. *Desalin. Water Treat.* 51(4-6): 958-968 (2012).
- Petrova, O.E., Sauer, K. Sticky situations: key components that control bacterial surface attachment. *J Bacteriol* 194: 2413-2425 (2012).
- Plasson, F., Bodennec S. European Patent No. EP2809161B1. Process for the biocontrol of *Pseudomonas*. Munich, Germany: European patent office (2016).
- Qureshi, N. Beneficial biofilms: wastewater and other industrial applications. In: Fratamico, P.M., Annous, B.A., Gunther, N.W. (eds.) *Biofilms in the food and beverage industries*. Woodhead Publishing Ltd., Oxford. 474-498 (2009)
- Rendueles, O., Ghigo, J.-M. Mechanisms of competition in biofilm communities. *Microbiol. Spectr.* 3(3): 1-18 (2015).
- Russell, A.D. Similarities and differences in the responses of microorganisms to biocides. *J. Antimicrob. Chemother.* 52(5): 750-763 (2003).



- Satpathy, K.K., Mohanty, A., Sahu, G., Biswas, S., Selvanayagam, M. *Biofouling and its control in seawater cooled power plant cooling water system - a review*. In: Tsvetkov, P. (ed.) *Nuclear Power*. IntechOpen. 191-242 (2010).
- Sauer, K., Camper, A.K., Ehrlich, G.D., Costerton, J.W., Davies, D.G. *Pseudomonas aeruginosa displays multiple phenotypes as a biofilm*. *J. Bacteriol.* 184: 1140-1154 (2002).
- Savage, V.J., Chopra, I., O'Neill, A.J. *Staphylococcus aureus biofilms promote horizontal transfer of antibiotic resistance*. *Antimicrob. Agents Chemother.* 57(4): 1968-1970 (2013).
- Schneider, R.P., Ferreira, L.M., Binder, P., Bejarano, E.M., Góes, K.P., Slongo, E., Machado, C.R., Rosa, G.M.Z. *Dynamics of organic carbon and of bacterial populations in a conventional pretreatment train of a reverse osmosis unit experiencing severe biofouling*. *J. Membr. Sci.* 266: 18-29 (2005).
- Simões, M., Simões, L.C., Vieira, M.J. *A review of current and emergent biofilm control strategies*. *LWT-Food Sci. Technol.* 43(4): 573-583 (2010).
- Sriyutha Murthy P., Venkatesan R. *Industrial biofilms and their control*. In: Flemming, H.-C., Sriyutha Murthy, P., Venkatesan, R., Cooksey, K.E. (eds.) *Marine and industrial biofouling*. Springer, Berlin, Heidelberg 65-02. (2009).
- Stewart, P.S., Franklin, M.J. *Physiological heterogeneity in biofilms*. *Nat. Rev. Microbiol.* 6(3): 199-210 (2008).
- Stoodley, P., Sauer, K., Davies, D.G., Costerton, J.W. *Biofilms as complex differentiated communities*. *Annu. Rev. Microbiol.* 56: 187-209 (2002).
- Takeuchi, M., Hamana, K., Hiraishi, A. *Proposal of the genus Sphingomonas sensu stricto and three new genera, Sphingobium, Novosphingobium and Sphingopyxis, on the basis of phylogenetic and chemotaxonomic analyses*. *Int. J. Syst. Evol. Microbiol.* 51(4): 1405-1417 (2001).
- Trafny, E.A., Lewandowski, R., Kozłowska, K., Zawistowska-Marciniak, I., Stępińska, M. *Microbial contamination and biofilms on machines of metal industry using metalworking fluids with or without biocides*, *Int. Biodeterior. Biodegradation.* 99: 31-38 (2015).
- van Loosdrecht, M.C.M., Bereschenko, L., Radu, A., Kruihof, J.C., Picioreanu, C., Johns, M.L., Vrouwenvelder, J.S. *New approaches to characterizing and understanding biofouling of spiral wound membrane systems*. *Water Sci. Technol.* 66(1): 88-94 (2012).
- van Paassen, J.A.M., van der Meer, W.G.J., Post, J. *Optiflux®: from innovation to realisation*, *Desalination* 178(1-3) 325-331 (2005).
- van de Lisdonk, C.A.C., Rietman, B.M., Heijman, S.G.J., Sterk, G.R., Schippers, J.C. *Prediction of supersaturation and monitoring of scaling in reverse osmosis and nanofiltration membrane systems*, *Desalination* 138(1-3): 259-270 (2001).
- van den Broek, W.B.P., Boorsma, M.J., Huiting, H., Dusamos, M.G., van Agtmaal S. *Prevention of biofouling in industrial RO systems: Experiences with peracetic acid*, *Water Sci. Technol.* 5(2): 1-II (2010).
- van der Meer, W.G.J., van Paassen, J.A.M., Riemersma, M.C., van Ekkendonk, F.H.J. *Optiflux®: from innovation to realisation*, *Desalination* 157(1-3): 159-165 (2003).
- Vigneron, A., Head, I.M., Tsesmetzis, N. *Damage to offshore production facilities by corrosive microbial biofilms*. *Appl. Microbiol. Biotechnol.* 102(6): 2525-2533 (2018).
- Vrouwenvelder, J.S., Manolarakis, S.A., van der Hoek, J.P., van Paassen, J.A.M., van der Meer, W.G.J., van Agtmaal, J.M.C., Prummel, H.D.M., Kruihof, J.C., van Loosdrecht, M.C.M. *Quantitative biofouling diagnosis in full scale nanofiltration and reverse osmosis installations*, *Water Res.* 42(19): 4856-4868 (2008).

Vrouwenvelder, J.S., van Paassen, J.A.M., Kruithof, J.C., van Loosdrecht, M.C.M. Sensitive pressure drop measurements of individual lead membrane elements for accurate early biofouling detection. *J. Memb. Sci.* 338(1-2): 92-99 (2009).

Vrouwenvelder, J.S., Beyer, F., Dahmani, K., Hasan, N., Galjaard, G., Kruithof, J.C., van Loosdrecht, M.C.M. Phosphate limitation to control biofouling. *Water Res.* 44(11): 3454-3466 (2010).

Wingender, J., Neu, T., Flemming, H.-C. What are bacterial extracellular polymer substance? In: Wingender, J. and Flemming, H.-C. (eds.). *Bacterial extracellular polymer substances*. Springer, Berlin, Heidelberg, New York. 1-19 (1995)

Xavier, J.B., Foster, K.R. Cooperation and conflict in microbial biofilms. *Proc. Natl. Acad. Sci. USA.* 104: 876-881 (2007).

Zhou, G., Shi, Q.-S., Huang, X.-M., Xie, X.-B. The three bacterial lines of defense against antimicrobial agents. *Int. J. Mol. Sci.* 16: 21711-21733 (2015).





# Chapter 2

## **Long-term performance and fouling analysis of full-scale direct nanofiltration (NF) installations treating anoxic groundwater**

Florian Beyer, Bas M. Rietman, Arie Zwijnenburg,  
Paula van den Brink, Johannes S. Vrouwenvelder,  
Monika Jarzembowska, Judita Laurinonyte,  
Alfons J.M. Stams, Caroline M. Plugge

This chapter is adapted from:  
Beyer, F., Rietman, B.M., Zwijnenburg, A., van den Brink, P.,  
Vrouwenvelder, J.S., Jarzembowska, M., Laurinonyte, J., Stams, A.J.M.,  
Plugge, C.M. Long-term performance and fouling analysis of full-scale  
direct nanofiltration (NF) installations treating anoxic groundwater.  
J. Membr. Sci. 468: 339-348 (2014).

## Abstract

Long-term performance and fouling behavior of four full-scale nanofiltration (NF) plants, treating anoxic groundwater at 80 % recovery for drinking water production, were characterized and compared with oxic NF and reverse osmosis systems. Plant operating times varied between 6 and 10 years and pretreatment was limited to 10  $\mu\text{m}$  pore size cartridge filtration and antiscalant dosage (2 - 2.5  $\text{mg L}^{-1}$ ) only. Membrane performance parameters normalized pressure drop (NPD), normalized specific water permeability ( $K_w$ ) and salt retention generally were found stable over extended periods of operation (> 6 months). Standard acid–base cleanings (once per year or less) were found to be sufficient to maintain satisfying operation during direct NF of the described iron rich ( $\leq 8.4 \text{ mg L}^{-1}$ ) anoxic groundwaters.

Extensive autopsies of eight NF membrane elements, which had been in service since the plant startup (6 - 10 years), were performed to characterize and quantify the material accumulated in the membrane elements. Investigations using scanning electron microscopy (SEM), energy dispersive X-ray spectroscopy (EDS), total organic carbon (TOC) and adenosine triphosphate (ATP) measurements revealed a complex mixture of organic, biological and inorganic materials. The fouling layers that developed during half to one year of operation without chemical cleaning were very thin (< 2  $\mu\text{m}$ ). Most bio(organic) accumulates were found in the lead elements of the installations while inorganic precipitates/deposits (aluminosilicates and iron(II)sulfides) were found in all autopsied membrane elements.

The high solubility of reduced metal ions and the very slow biofilm development under anoxic conditions prevented rapid fouling during direct NF of the studied groundwaters. When compared to oxic NF and RO systems in general (e.g. aerated ground waters or surface waters), the operation and performance of the described anoxic installations (with minimal pretreatment) can be described as very stable.



## 2.1. Introduction

High pressure driven membrane filtration processes, such as nanofiltration (NF) and reverse osmosis (RO) are capable of generating large amounts of high quality drinking water. The excellent removal capacity of contaminants, decreasing prices for the membranes and enhanced membrane lifetimes led to the wide acceptance and popularity of NF and RO. NF is applied for the treatment of surface waters (*Speth et al., 1998, Reiss et al., 1999*), as pretreatment in desalination (*Al-Amoudi and Farooque 2005*), during wastewater reclamation (*Rautenbach et al., 2000*) and for the treatment of oxic groundwater (*Gwon et al., 2003*).

Vitens Water Supply Company (The Netherlands) uses direct NF, with minimal pretreatment, for drinking water production from anoxic groundwater (*van der Meer and van Winkelen 2001*), in nine of its installations. Four of these installations were investigated in the present study (*Table 2.1.*) and compared to literature data of oxic NF and RO systems.

*Table 2.1.* Design and operational characteristics of the 4 described installations.

Installation name	Weerseloeweg	Rodenmors	Diepenveen	Witharen
Abbreviation	WW	RM	DV	WH
Years of operation*	10	9	8.8	5.7
Cleaning frequency [CIPs year <sup>-1</sup> ]	0.7	0.6	0.6	0.7
Production capacity [m <sup>3</sup> day <sup>-1</sup> ]	2,880	1,785	4,608	2,880
Membrane area [m <sup>2</sup> ]	2,412	1,809	4,221	2,412
Number of stages	2	2	2	3
Recovery	80%	80%	78%	80%
Well depth [m]	80 - 150	23 - 45	33 - 35	60 - 90
Antiscalant dosage [mg L <sup>-1</sup> ]	2 - 2.5	2 - 2.5	2 - 2.5	2 - 2.5

\* = at day of autopsies for fouling analysis

At present, approximately 55 % of the water volume produced by the Dutch drinking water companies originates from deep groundwater layers, corresponding to a total volume of 675 million m<sup>3</sup> year<sup>-1</sup> in 2010. The composition of the untreated deep groundwater does not meet the Dutch drinking water standards or the standards of Vitens in terms of hardness, color, total organic carbon (TOC), sulfate, ammonium, iron, manganese, barium and/or organic micro pollutants (*Table 2.2.*). Therefore, the groundwater needs to be treated. Conventional groundwater treatment (aeration and filtration) does not remove, e.g., color, hardness and pollutants such as pesticides (*Hiemstra et al., 1999*). NF is used by Vitens when two or more of the

water standards (that cannot be removed with conventional treatment, aeration and sand filtration) are not met, as the simultaneous removal of these compounds by NF is cheaper compared to the combination of other treatments, such as softening and carbon filtration (*Hiemstra et al., 1999, van der Meer and van Winkelen 2001*).

*Table 2.2.* Overview of the physical, chemical and biological parameters (average concentration and standard deviation) of the feed waters of the 4 NF installations, as well as the Dutch drinking water standards and the desired drinking water qualities by Vitens. Red color indicates that either Dutch or Vitens standards for drinking water are not met.

Measurement	Units	Dutch Norm*	Vitens Norm**	Diepenveen	Rodenmors	Weerseloseweg	Witharen
temp <sub>min,max</sub>	°C	≤ 25	≤ 25	9.5 - 13.1	10.6 - 13.2	9.5 - 14.2	11.6 - 13.2
pH	pH	7.0 - 9.5	7.8 - 8.3	7.22 ± 0.03	6.99 ± 0.03	7.22 ± 0.05	6.81 ± 0.03
conductivity	mS m <sup>-1</sup>	≤ 125	≤ 80	63 ± 1	56 ± 4	67 ± 1	53 ± 1
oxygen	mg L <sup>-1</sup>	≥ 2	≥ 4	< 0.01	< 0.01	< 0.01	< 0.01
colour	mg Pt/Co L <sup>-1</sup>	≤ 20	≤ 10	≥ 20	≥ 20	≤ 10	≥ 20
total hardness (TH)	mmol (Ca <sup>2+</sup> + Mg <sup>2+</sup> ) L <sup>-1</sup>	≥ 1.0	1.0 - 1.2	3.25 ± 0.1	2.74 ± 0.2	3.48 ± 0.1	2.66 ± 0.1
TOC	mg L <sup>-1</sup>		≤ 3	7.3 ± 0.3	7.9 ± 0.5	3.1 ± 0.3	9.2 ± 0.2
DOC	mg L <sup>-1</sup>			6.6 ± 0.3	6.8 ± 0.6	2.9 ± 0.2	8.6 ± 0.4
ATP	ng L <sup>-1</sup>			2.4 ± 1.8	2.3 ± 3.1	1.9 ± 1.4	< 1
sulfate	mg SO <sub>4</sub> <sup>2-</sup> L <sup>-1</sup>	≤ 150	≤ 120	65.3 ± 1.2	9.5 ± 2.7	123.8 ± 4.1	< 2
sulfide	mg S <sup>2-</sup> L <sup>-1</sup>			n.d.	< 2	< 2	n.d.
nitrate	mg NO <sub>3</sub> <sup>-</sup> L <sup>-1</sup>	≤ 50	≤ 25	< 1	< 1	< 1	< 1
ammonium	mg NH <sub>4</sub> <sup>+</sup> L <sup>-1</sup>	≤ 0.2	≤ 0.05	1.1 ± 0.0	1.5 ± 0.1	0.3 ± 0.0	1.4 ± 0.0
ortho-phosphate	mg PO <sub>4</sub> <sup>3-</sup> L <sup>-1</sup>			0.5 ± 0.0	0.8 ± 0.4	0.5 ± 0.3	0.6 ± 0.2
hydrogen carbonate	mg HCO <sub>3</sub> <sup>-</sup> L <sup>-1</sup>	≥ 60	≥ 90	319 ± 2	329 ± 15	286 ± 3	337 ± 2
methane <sub>(headspace)</sub>	µg L <sup>-1</sup>			313 ± 8	14,857 ± 63	145 ± 20	15,143 ± 639
calcium	mg L <sup>-1</sup>			116 ± 3	99 ± 6	121 ± 4	96 ± 3
chloride	mg L <sup>-1</sup>	≤ 150	≤ 100	37.3 ± 0.9	38.0 ± 12.0	30.8 ± 1.1	30.4 ± 1.9
sodium	mg L <sup>-1</sup>	≤ 150	≤ 100	22.1 ± 0.8	21.0 ± 4.8	22.6 ± 0.8	19.4 ± 0.9
magnesium	mg L <sup>-1</sup>			8.5 ± 0.2	6.8 ± 0.6	11.3 ± 0.6	6.6 ± 0.1
iron	mg L <sup>-1</sup>	≤ 0.2	≤ 0.05	4.2 ± 0.0	7.1 ± 0.2	2.0 ± 1.2	8.4 ± 0.2
potassium	mg L <sup>-1</sup>			3.7 ± 0.1	2.2 ± 0.2	3.3 ± 0.1	2.2 ± 0.0
manganese	mg L <sup>-1</sup>	≤ 0.05	≤ 0.01	0.3 ± 0.0	0.3 ± 0.0	0.2 ± 0.1	0.3 ± 0.0
silicon	mg L <sup>-1</sup>			6.7 ± 0.2	9.6 ± 0.3	11.6 ± 0.2	10.7 ± 0.3
strontium	µg L <sup>-1</sup>			409 ± 11	396 ± 30	772 ± 35	400 ± 6
barium	µg L <sup>-1</sup>	≤ 500	≤ 100	197 ± 6	78 ± 7	101 ± 5	14 ± 0
aluminum	µg L <sup>-1</sup>	≤ 200	≤ 30	4.1 ± 2.1	2.4 ± 0.3	< 2	2.8 ± 1.0

n.d. = not determined

\* = Dutch drinking water standards (Drinkwaterbesluit 2011)

\*\* = Desired drinking water quality (Vitens)

Similar to other membrane filtration processes and feed water sources, the major concern is reduced membrane performance caused by fouling. An increase of the normalized feed channel pressure drop (NPD), a decrease in the normalized specific membrane permeability ( $K_w$ ) or changes in salt retention (or combinations thereof) are common operational signs indicating fouling development in full-scale applications (*Nederlof et al., 2000, Huiting et al., 2001*).



To overcome the fouling problems, the membranes have to be cleaned with chemicals. The physical–chemical treatments, applied to restore membrane performance, are not successful under all circumstances (*Flemming et al., 1997, Flemming et al., 2002, Al-Amoudi and Lovitt 2007, Bereschenko et al., 2011*). The most important causes of membrane fouling include (*Flemming 1997*) the following:

- Scaling (crystallization of solid minerals from solution)
- Organic fouling (deposition of dissolved humic acids, oil, grease, etc.)
- Particle and colloid fouling (deposition of clay, silt, iron oxides etc.)
- Biofouling (adhesion and accumulation of microorganisms, forming biofilms)

In practice, several types of fouling may occur simultaneously within the same installation or even within one single membrane element. So far, destructive membrane autopsies are needed to identify and quantify the fouling types that had developed within the system.

Only in 3 studies, anoxic treatment of groundwater by NF was described in terms of fouling development (*van Paassen et al., 1998, Hiemstra et al., 1999, Nederlof et al., 2000*). These studies showed that the plant performance was more stable with anoxic groundwater compared to oxic feed waters. In anoxic groundwater, metal ions such as iron and manganese exist in their soluble forms, iron (II) and manganese (II). When brought into contact with oxygen, iron (II) will readily be oxidized with dissolved oxygen and subsequently iron (III) (hydr)oxides, with very low solubility, are formed (*Tuhela et al., 1993*). The high solubility of reduced metal ions under anoxic conditions results in a much lower modified fouling index (*Schippers and Verdouw 1980*) ( $\text{MFI} < 1 \text{ s L}^{-2}$ ) of the feed water, compared to aerated ground-water (*van Paassen et al., 1998, Hiemstra et al., 1999*). This means, as long as oxygen introduction to the system can be avoided, rapid iron fouling is not expected (*van Paassen et al., 1998, Hiemstra et al., 1999*). Furthermore, biofilms might develop much more slowly under anoxic conditions (*Hiemstra et al., 1999*). In the absence of oxygen, microorganisms have to gain their energy from anaerobic respiration and fermentation, leading to substantially less adenosine triphosphate (ATP) production

and therefore less biomass, compared to aerobic respiration with the same biodegradable substrate concentration.

Only little information on full-scale long term NF operation under anoxic conditions is available in literature. This research focuses on the fouling assessment of 4 full-scale direct NF installations, treating anoxic groundwater. From each of the installations, two membrane elements from different positions (*Table 2.3.*) were taken and opened for fouling analysis. The operational lifetime of the membrane elements varied between six and ten years (*Table 2.3.*).

*Table 2.3.* Operational history of the membrane elements autopsied.

Installation	Membrane code	Stage/position	Years of operation	Last CIP [days]
Weerseloseweg	WW lead	1/1	10.0	340
Weerseloseweg	WW last	2/6	10.0	340
Rodenmors	RM lead	1/1	9.0	164
Rodenmors	RM middle	2/1	9.0	164
Diepenveen	DV lead	1/1	8.8	303
Diepenveen	DV last	2/6	8.8	303
Witharen	WH lead	1/1*	5.7	208
Witharen	WH last	3/3*	5.7	208

\* = Installation uses hydrodynamic optimized pressure vessels housing three membranes in series per stage

The main objectives of this study are the following:

- to describe the particular characteristics of anoxic groundwater treatment by NF
- to study the long-term performance and fouling behavior of four full-scale NF plants treating anoxic groundwater for drinking water production; and
- to characterize and quantify the fouling in the NF membrane elements.

## 2.2. Materials and methods

### 2.2.1. Plant description, operation and performance

The full-scale installations described were operated with anoxic groundwater from different wells (*Tables 2.1* and *2.2*) using 8040-TS82 (Trisep Corporation, USA) NF membrane elements. At the time of membrane sampling for autopsies, the installations were still running with the original set of membrane elements. The minimal pretreatment consisted of 10  $\mu\text{m}$  pore size cartridge filtration and the addition of a phosphonate based antiscalant (4Aqua OSM 92, AquaCare Europe BV, The Netherlands) only. Cartridge filters are installed in the vast majority of NF and RO plants worldwide to prevent physical damage of the membrane elements and

high pressure pumps due to bigger particles. As the minimal pretreatment did not significantly contribute to the removal efficiency of the described installations, the process can be referred to as direct NF.

All installations were operated at a constant flux by adjusting the feed pressure. The applied feed pressures of the installations, at day zero with new membrane elements, ranged from 640 to 830 kPa. The installations Diepenveen (DV), Weerseloseweg (WW) and Rodenmors (RM) were designed in typical two stage design, housing six membrane elements per pressure vessel. In contrast, Witharen (WH) is a three stage installation, housing three membrane elements in a pressure vessel. This hydrodynamic optimized design is called Optiflux® (*van der Meer et al., 2003, van Paassen et al., 2005*). In this design the number of lead elements is doubled, compared to the conventional design, resulting in a lower linear flow velocity in the lead elements (*Huiting et al., 2001, van der Meer et al., 2003, van Paassen et al., 2005*). An overview of the main characteristics of the individual installations can be found in *Table 2.1*.

### 2.2.2. Feed water quality parameters

Key physical, chemical and biological parameters of the anoxic groundwaters treated in the full-scale installations are summarized in *Table 2.2*. The reported average concentrations and respective standard deviations are based on at least three independent measurements.

Feed water parameters were measured according to Dutch (NEN), European (EN) or international (ISO) norms. Conductivity was measured according to NEN-ISO 7888, nitrate and sulfate according to NEN-ISO 10304-1, dissolved organic carbon (DOC) and TOC according to NEN-EN-1484 and aluminum, barium, strontium, calcium, potassium, magnesium, manganese and sodium according to NEN-ISO 17294-2. Oxygen was constantly monitored using a digital optical sensor (Oxymax COS6ID, Endress+Hauser, Naarden, The Netherlands). Vitens Laboratorium (Leeuwarden, The Netherlands) in-house methods (accredited laboratory based on NEN-EN-ISO/IEC17025) were used to determine the pH and the concentrations of hydrogen carbonate, ammonium, chloride, ortho-phosphate and silicon, iron and methane. Sulfide was captured with zinc acetate (0.2 M) to avoid rapid oxidation after

sampling. The sulfide concentrations were then determined with the Hach Lange (Düsseldorf, Germany) sulfide kit LCK-653, after filtration through a 0.45 µm pore size filter. ATP concentrations were determined with the Biomass Kit HS (BioThema, Dalarö, Sweden) and a Centro XS3 Microplate Luminometer (Berthold, Wildbad, Germany).

### 2.2.3. Fouling diagnosis based on plant performance data

To allow a fair comparison between different plant designs and operational conditions, the feed channel pressure drop and membrane flux measurements were normalized to standard conditions as described in detail in *Supplementary data S2.1*. The normalizations described are generally used by the Dutch drinking water companies. The normalized specific water permeability of the membranes ( $K_w$ ) represents the actual membrane flux corrected for surface area, the net driving pressure (subtraction of osmotic pressure differences between feed and permeate from transmembrane pressure) and temperature (reference temperature 10°C) (*van de Lisdonk et al., 2001*).

The normalized pressure drop (NPD) represents the actual feed channel pressure drop per membrane element corrected for temperature (reference temperature 10 °C) and feed volume flow rate (reference feed volume flow rate 10 m<sup>3</sup> h<sup>-1</sup>) (*van den Broek et al., 2010*). The performance data presented in this manuscript represent the overall plant performance and were derived from the normalized data of the individual stages, taking the number of elements per stage into account. The reference temperature of 10 °C was chosen, as it represents the yearly average temperature of the Dutch ground and surface waters.

The normalized specific water permeability was calculated using the following equation (*van de Lisdonk et al., 2001*):

$$K_w = \frac{Q_p * TCF_{K_w}}{\left(\left(\frac{P_f + P_c}{2} - P_p\right) - \left(\frac{\Pi_f + \Pi_c}{2} - \Pi_p\right)\right) * A * 3600} \quad [m s^{-1} kPa^{-1} \text{ at } 10^\circ C] \quad (1)$$

where  $Q_p$  is the permeate volume flow rate [m<sup>3</sup> h<sup>-1</sup>],  $P_f$  is the feed pressure [kPa],  $P_c$  is the concentrate pressure [kPa],  $P_p$  is the permeate pressure [kPa],  $\Pi_f$  is the osmotic feed pressure [kPa],  $\Pi_c$  is the osmotic concentrate pressure [kPa],  $\Pi_p$  is the osmotic

permeate pressure [kPa], A is the surface area [m<sup>2</sup>], and  $TCF_{K_w}$  (=  $e^x$ ) is the temperature correction factor  $K_w$ .

$$x = U * \left( \frac{1}{T_{act} + 273} - \frac{1}{T_{ref} + 273} \right)$$

where U is the membrane constant (membrane type dependent, supplied by manufacturer),  $T_{act}$  is the actual feed water temperature [= 10 °C], and  $T_{ref}$  is the reference water temperature [= 10 °C].

The normalized feed channel pressure drop (NPD) was calculated using the following equation (*van den Broek et al., 2010*):

$$NPD = FCP * \frac{Q_{ref}^{1.6}}{\left(\frac{Q_f + Q_c}{2}\right)^{1.6}} * (1.03^{T_{act} - T_{ref}})^{0.4} \quad [kPa] \quad (2)$$

FCP is the feed channel pressure drop (= feed-concentrate pressure) [kPa],  $Q_f$  is the feed volume flow rate [m<sup>3</sup> h<sup>-1</sup>],  $Q_c$  is the concentrate volume flow rate [m<sup>3</sup> h<sup>-1</sup>],  $Q_{ref}$  is the reference feed volume flow rate [= 10 m<sup>3</sup> h<sup>-1</sup>],  $T_{act}$  is the actual feed water temperature [°C], and  $T_{ref}$  is the reference water temperature [= 10 °C].

The salt retention was calculated based on conductivity measurements using the following equation:

$$Salt\ retention = 1 - \left( \frac{EC_p}{((EC_f + EC_c) / 2)} \right) \quad [dimensionless] \quad (3)$$

where salt retention is dimensionless,  $EC_p$  is the electrical conductivity permeate water [mS m<sup>-1</sup>],  $EC_f$  is the electrical conductivity feed water [mS m<sup>-1</sup>], and  $EC_c$  is the electrical conductivity concentrate water [mS m<sup>-1</sup>].

Based on literature references (*Nederlof et al., 2000, Huiting et al., 2001*) and cleaning recommendations given by the membrane manufacturers, fouling in this manuscript is defined as NPD increase of > 15% and / or a  $K_w$  decline of > 15% and/or a change in rejection capacity of more than 5 %, relative to start values of the installation with new membranes (t = 0). As membrane compaction effects might occur during the first days of operation, causing unstable  $K_w$  measurements (*Huiting et al., 2001*), start values were defined four days after the start of an installation with new membranes.

### 2.2.4. Chemical cleaning of the membranes

Chemical cleaning in place (CIP) was performed preventively once every two years or when the feed pressure of an installation increased by 25 – 40 %. The chemical CIP protocol was identical for all installations. The membranes were cleaned for 3 h with a 2 % (w/w) citric acid solution at 35 °C, followed by three hours of cleaning with caustic soda (pH = 11 – 12) at 35 °C. During both acid and base cleaning, the flow velocity was changed every 30 min. One cycle started with 30 min at high flow (5 – 10 m<sup>3</sup> h<sup>-1</sup> per element), followed by a very low flow (soaking) for 30 min. The cycle was repeated three times for both acid and base cleaning. The maximum feed pressure applied during CIP operations was 400 kPa. After CIP the installations were flushed (from the feed side) with permeate water, before being taken back into operation.

### 2.2.5. Fouling identification by membrane autopsies

From the four full-scale installations, in total eight membrane elements were taken for autopsies. From all installations, the lead element of the first stage has been autopsied. In addition, a lead element of the second stage of RM and the last element of the last stage of the installations in DV, WW and WH were autopsied. An overview of the operational history of the autopsied membrane elements can be found in *Table 2.3*. Membrane elements were transported, inspected and autopsied at Wetsus (Leeuwarden, The Netherlands). For ATP and TOC analyses, five samples were taken over the membrane length, whereas scanning electron microscopy (SEM) and energy dispersive X-ray spectroscopy (EDS) samples were taken only from the inlet and outlet side of each membrane element (*Figure 2.1*).

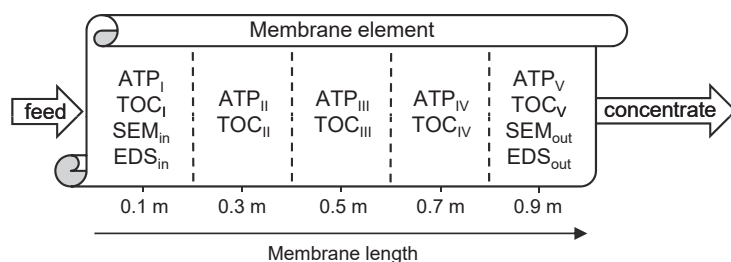


*Figure 2.1.* General sampling scheme for the chemical and morphological membrane fouling characterization.

Sample preparation and ATP analyses were performed as described previously (Vrouwenvelder *et al.*, 2008). TOC samples were prepared in a similar way, but Milli-Q water was used instead of autoclaved tap water. TOC was measured indirectly, based on the fractions of total carbon and inorganic carbon, using a Shimadzu TOC-VCPH analyzer (Shimadzu, Japan). For SEM and EDS analysis, samples were fixed in a solution of 3 % (w/v) glutaraldehyde in phosphate buffered saline (24 hours at 4 °C), washed twice with phosphate buffered saline, dehydrated in increasing concentrations of ethanol (30 %, 50 %, 70 %, 90 % for 20 min, twice 96 % for 30 min at room temperature), air dried (1 hours at 45 °C) and kept in a desiccator overnight. Samples were then coated with a thin layer of gold particles and analyzed using a Noran System SIX model 300 X-ray microanalysis system (Thermo Fisher Scientific, USA) attached to a JEOL JSM-6480LV microscope (JEOL Technics LTD., Japan). SEM pictures were taken in high vacuum mode at 6 kV, EDS was performed at 10 kV. Dried inorganic crystals from the permeate spacer of the last element of the WW installation were characterized by Raman spectroscopy using a LabRAM HR (HORIBA Jobin-Yvon Inc, USA).

## 2.3. Results and discussion

### 2.3.1. Operational parameters ( $K_w$ , NPD, salt retention and cleaning frequency)

Figure 2.2. summarizes the  $K_w$  and NPD development over time of the two “most problematic” installations: WW (strongest NPD increase) and RM (strongest  $K_w$  decline and highest CIP frequency during the last four years of operation). The  $K_w$  and NPD development over time for the installations DV and WH is shown in *Supplementary data S2.2*. The salt retention graphs for the installations WW, RM and WH are shown in *Supplementary data S2.3*. The installation of DV was operated temporarily with water from wells with a difference in sodium and chloride concentrations and therefore the retention graph of DV is not fully conclusive and is not presented in this manuscript.

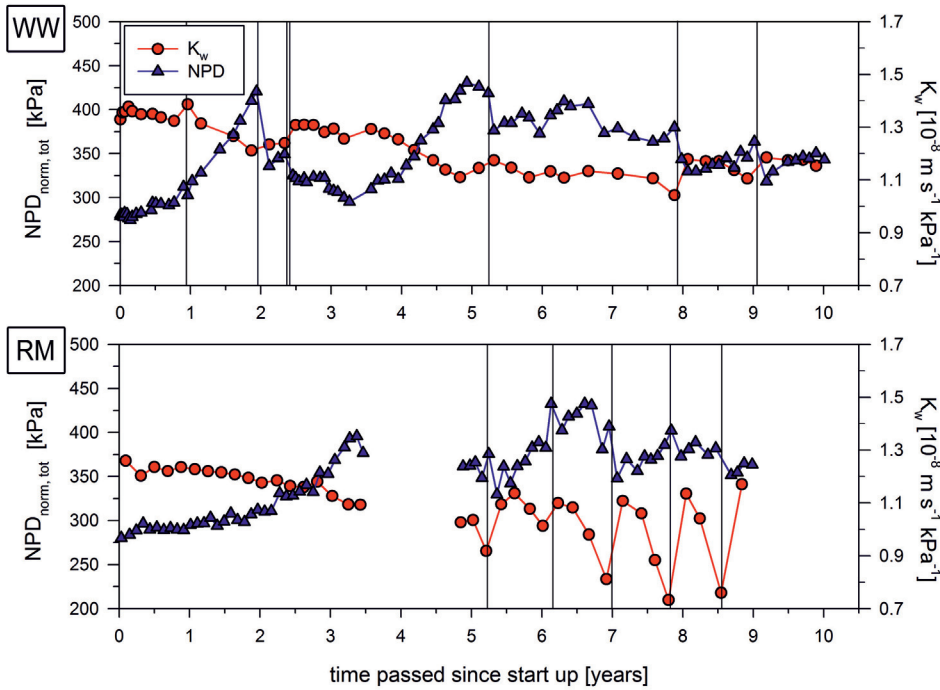


Figure 2.2. Development of performance parameters  $K_w$  (circles) and NPD (triangles) for the installations Weerseloseweg (WW) and Rodenmors (RM). The vertical lines indicate events of chemical cleanings in place (CIP). The data of the installation RM between 3.5 and 5 years are not fully conclusive due to a fouled flow meter in the installation and are not presented. Directly after the last data point the membrane elements were autopsied and analyzed.

“Stable operation” is here defined as NPD increase  $\leq 15\%$  per half year,  $K_w$  decrease  $\leq 15\%$  per half year and salt retention change  $\leq 5\%$  per half year. The definition is based on two membrane cleanings per year (average low cleaning frequency of pretreated oxic groundwaters (van Paassen et al., 1998) and the fouling criteria are defined in Section 2.2.3.

Installation WW shows slightly increasing NPD values (8%) during the first year of operation. CIP after 0.9 years had no effect on the NPD. After this CIP the NPD increased more prominently (~60% within the first two years). The chemical cleanings applied were not efficient to restore the  $K_w$  close to start values. The  $K_w$  decreases slightly, but gradually, during the first five years of operation. After five years the  $K_w$  stabilized at a level of about -20% of the start value. The CIP's at 0.9 years and 2.5 years of operation had a negative impact on the salt retention (-3.6%



and -2.5 %) of the membranes (*Supplementary data S2.3.*). Both these CIP's were performed with a commercially available cleaning agent (Genesol 34) because of rapid sulfate scaling (*data not shown*). As this installation was temporarily operated with groundwater from different wells, a wrong combination of those wells resulted in an increased sulfate concentration ( $\leq 150 \text{ mg L}^{-1}$ ) in the feed water, causing rapid sulfate scaling (*data not shown*). Other than that, salt retention values remained stable ( $\pm 2 \%$  per year) over the whole period of the operation.

At RM the NPD and  $K_w$  were slightly affected during the first two years of operation. The NPD increased by 10 % and the  $K_w$  decreased by 5.1 %. After two years the recovery was optimized with the use of a ScaleGuard® (*van de Lisdonk et al., 2001*). The ScaleGuard® tests indicated that the recovery could be increased to 83 %. However, the recovery was not increased, but it was concluded that the antiscalant dosage could be stopped when recovery remained at 80 %. Because of a fouled flow meter, this conclusion was not correct. In fact, the recovery was lower than the 80 % as it was set. After the flow meter was cleaned, the installation was cleaned for the first time after more than five years of operation. The NPD and  $K_w$  could only partially be restored by this CIP. Since then, the CIP frequency was increased to about once every year. The CIP's are efficient in restoring the  $K_w$  temporarily, but NPD values increased steadily till about 33 % of the start value at 6.7 years of operation. During the last two years the NPD stabilized at a level of about 20 % above the start value. Retention generally remained stable (72 % per year) over the whole period of operation of nine years (*Supplementary data S2.3.*), although the CIP at 7.9 years of the operation seemed to have a negative effect of -2.5 % on the retention.

At DV infrequent CIP's were sufficient to restore the decreased  $K_w$  values (*Supplementary data S2.2.*). NPD values, in contrast, could not be completely restored by the CIP's leading to a permanent slightly increased NPD during operation of about 30 % till six years of operation. After these six years the NPD more or less stabilized at that level. Retention values stayed stable over the whole period when treating the same feed water quality (*data not shown*). At WH the NPD values were more affected than the  $K_w$  (*Supplementary data S2.2.*). The  $K_w$  decreased

with 10 – 15 % between the chemical cleanings and could be restored to the start values and the NPD increased with 20 – 40 % between the chemical cleanings. After the chemical cleaning about 10% of the increased NPD remained. The CIP's at WH caused an average permanent decline in salt retention of 1.8 % for each chemical cleaning (*Supplementary data S2.3.*).

Not all CIP's were successful in restoring the membrane performance close to day zero values. This is a general problem in high pressure membrane filtration (*Flemming et al., 1997, Flemming et al., 2002, Al-Amoudi and Lovitt 2007, Bereschenko et al., 2011*) and it is likely due to the membranes spiral wound element design, where all membrane sheets are tightly packed and removal of accumulated material is difficult. Some of the CIP's furthermore had a negative effect on the salt retention of the membranes. At WH each CIP caused a permanent loss in salt retention of 1.8% (*Supplementary data S2.3.*). As a consequence, at WH the membrane elements had to be replaced prematurely after six years of operation. In the other installations some of the CIP's had a negative effect on salt retention, suggesting that membrane degradation did not exclusively occur at WH. Installations DV and WH show increased  $K_w$  values (relative to day zero), which is another indicator for possible membrane degradation. It is generally known that any kind of chemical cleaning agent changes the membrane elements performance adversely (*Carnahan et al., 1995, van der Bruggen et al., 2008*). All CIP operations were performed with a mobile CIP unit, thus the chemicals and cleaning solutions were identical at all installations. Only at WW the first and third CIPs were performed with a specific cleaning agent (Genesol 34) in order to remove (sulfate) scaling. Those two cleanings had a negative effect on the salt retention of the installation as well (-3.6 % and -2.5 %). An explanation as to why the chemical membrane degradation/aging was most problematic at WH is missing, as the other installations used identical membrane elements, were cleaned more often and still performed satisfactorily with the original membrane elements on the day of membrane autopsies. The membrane elements of the installations DV, RM and WW were under operation for 8.8 – 10 years which can be considered as excellent, compared to their projected lifetime of five years.

Overall, the performance of the four installations can be described as stable and unproblematic. On average, less than one CIP per year is needed to maintain the NPD and the  $K_w$  at stabilized levels during production, although this level can be up to 20 % increased (NPD) or up to 10% decreased ( $K_w$ ) relative to day zero of operation. For pretreated surface waters the CIP frequency is usually in the range of once per week to once every two months and the average CIP frequency of pretreated oxic groundwater is once every six months (*van Paassen et al., 1998*). The NF treatment of the described groundwaters, with minimal pretreatment and an average CIP frequency of less than once per year, is remarkably good.

### 2.3.2. Membrane autopsies for fouling analysis

#### 2.3.2.1. Inspection of the elements and visual observations during autopsy

All membrane elements autopsied appeared visually in good physical shape. The membrane elements of the installations DV, WW and RM were brown/black discolored. The lead elements usually were only partially discolored whereas the elements from the second stage showed stronger discolorations (*Figure 2.3*).

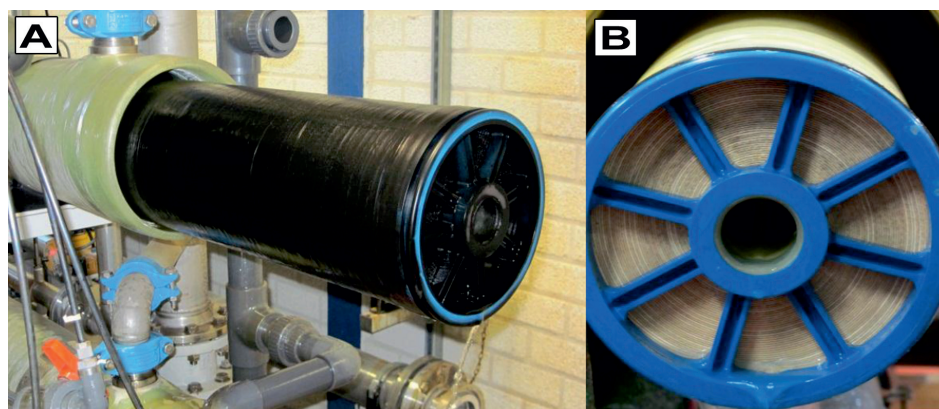


*Figure 2.3.* Representative pictures of the membrane elements taken for autopsies. (A) Membrane element from the installation Rodenmors (first element of second stage) strongly stained black by precipitated/accumulated material similar to installation WW and DV. (B) Membrane element (unstained and original color) from the installation Witharen (all stages).

The fouling layers within the elements were equally distributed, except for the lead element of the WW installation, where more fouling was found on the first third of the membrane element. The accumulated material was easily removable by soft mechanical scraping, but the discolorations of the membrane elements of DV, WW

and RM remained after scraping. During autopsy the black color faded to orange in all discolored elements, indicating a chemical oxidation of iron containing foulants of the anoxic elements. Autopsy of the elements from the second and third stages revealed brown-black gel-like fouling layers as found in the lead elements. Except for the installation in DV, the (bio)organic fouling layers in the lead elements appeared to be thicker and less dense, compared to the elements from later stages. Furthermore, the last element of the installations in DV and WW showed the presence of inorganic precipitates, which could not be removed by mechanical force (e.g. mechanical scraping or ultrasonic treatment). The permeate spacer channel of the last element of the WW installation showed strong white scale formation (*Supplementary data S2.5.*).

The fouling layer morphology and composition were further examined by TOC, ATP, SEM and EDS analyses (*Sections 2.3.2.2. and 2.3.2.3.*).

### **2.3.2.2. Organic and biological fouling**

The extent of organic accumulation and biofilm formation was determined by ATP and TOC measurements along the membrane lengths (*Figure 2.4.*). Higher concentrations of ATP and TOC were found in lead elements compared to the mid/last elements of the same installation (*Figure 2.4.*), except for the installation RM where ATP values were low in both autopsied membrane elements. These findings match the visual observations made during autopsy, showing that (bio)organic accumulation was more prominent within the lead elements. This is not surprising, as the accumulation of (bio)organic matter is generally observed to be strongest at the feed side of an installation (*Al-Amoudi 2010*). Vrouwenvelder and van der Kooij (*2003*) related a 15 % NPD increase to 3,000 pg ATP cm<sup>-2</sup>, while ATP values below 1000 pg ATP cm<sup>-2</sup> indicated plants without biofouling problems. When ranked among ATP measurements found in literature for autopsied membrane elements from oxic NF and RO installations (4 - 102,000 pg ATP cm<sup>-2</sup>, *Table 2.4.*), the ATP concentrations measured in this study (membrane element average = 268 - 1,413 pg ATP cm<sup>-2</sup>) are in the low range. TOC concentrations reported here (*Table 2.4.*) ranged from 9.7 to 43.2 µg TOC cm<sup>-2</sup> (membrane element average). In the framework of a large autopsy study of 25 different NF and RO membrane elements

treating (an)oxic feed waters we found TOC concentrations ranging from 5 to 150  $\mu\text{g TOC cm}^{-2}$  (*unpublished data*). The anoxic elements autopsied in this study have low TOC concentrations, compared to other oxidic installations investigated earlier.

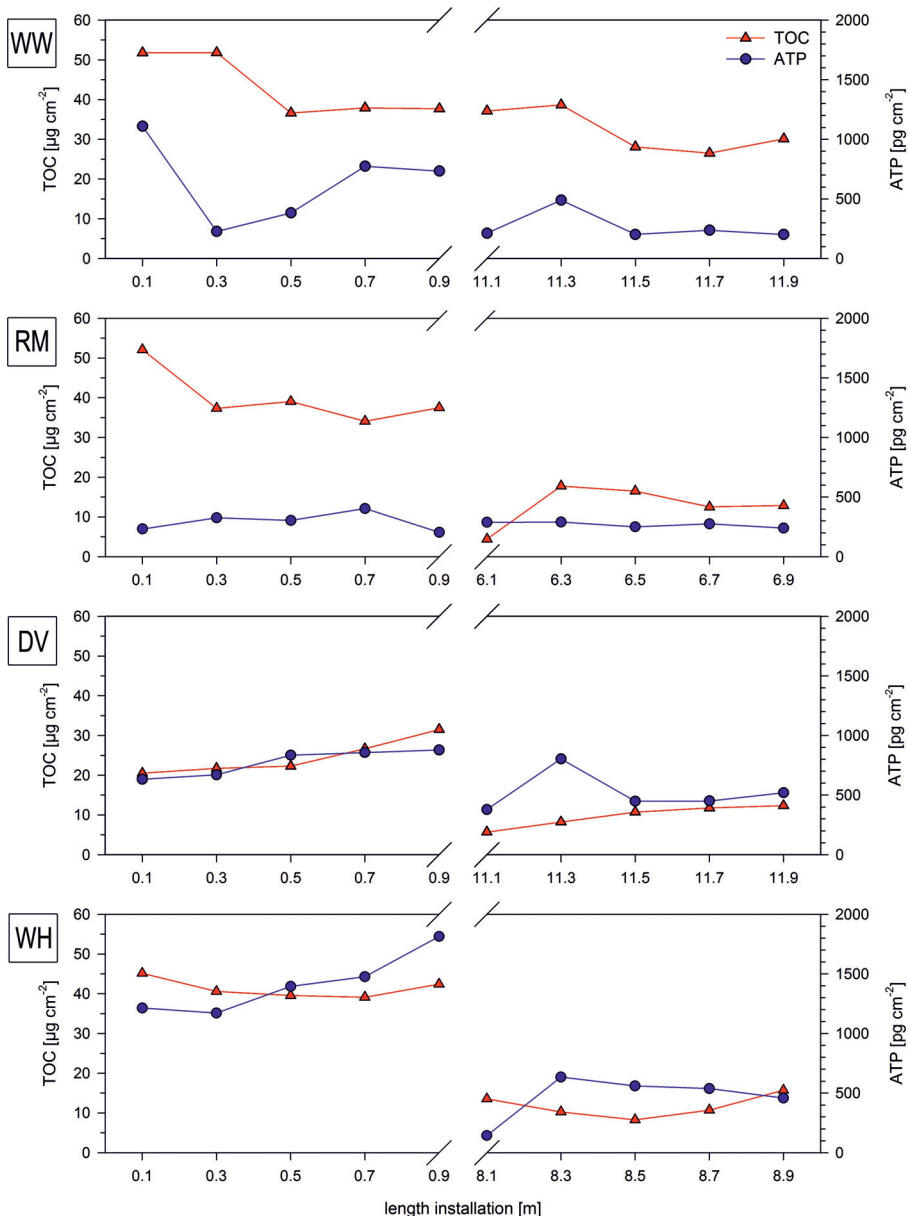


Figure 2.4. Concentrations of the active biomass parameters, TOC (triangles) and ATP (circles), over the length of the installation of the autopsied membrane elements (Table 2.3.). (WW) Weerseloseweg, (RM) Rodenmors, (DV) Diepenveen and (WH) Witharen.

The generally very low ATP concentrations (membrane element average  $\leq 1500$  pg ATP  $\text{cm}^{-2}$ ) suggest that part of the organic fouling by TOC is related to the deposition of natural organic matter (NOM), as opposed to biofilm formation. NOM is a typical membrane foulant in groundwater NF (*Al-Amoudi 2010*). Pilot research was performed to select membrane elements that are insensitive to fouling by NOM (*Hiemstra et al., 1999*). The Trisep 8040-TS82 membrane elements showed only minor fouling by NOM and were selected for all four installations.

*Table 2.4.* Design and operational characteristics of the 4 described installations.

	Oxic	Ref.	Anoxic (this study)
CIP frequencies	twice a week - once every 3 months (for surface water NF & RO)	1, 2, *	once per year or less
	average 6 months (for pretreated groundwater NF)	1	
CIP frequency < 1 year	intensive pre-treatment	2, *	10 $\mu\text{m}$ cartridge prefiltration and antiscalant dosage only
	(dis)continuous dosage of biocides	2, *	no biocides
Iron (feed water)	0.3 mg L <sup>-1</sup> iron (III) may lead to iron fouling	1	8.4 mg L <sup>-1</sup> iron (II) unproblematic
TOC (autopsy)	5 - 150 $\mu\text{g cm}^{-2}$	**	4,5 - 52 $\mu\text{g cm}^{-2}$
ATP (autopsy)	5 - 150 $\mu\text{g cm}^{-2}$	3, 4	150 - 1,800 pg $\text{cm}^{-2}$
Fouling layer thickness	3 - 100 $\mu\text{m}$	3, 5, 6	1 - 2 $\mu\text{m}$
Biofouling	general problem in most plants	7, 8, 9	only thin biofilm or patches

\* = personal communication with Dutch drinking water companies

\*\* = Autopsy study of 25 NF and RO membrane elements treating diverse (an)oxic feed waters (unpublished data)

1 (*van Paassen et al., 1998*), 2 (*van den Broek et al., 2010*), 3 (*Vrouwenvelder et al., 2008*), 4 (*Vrouwenvelder and van der Kooij 2003*), 5 (*Speth et al., 1998*), 6 (*Geesey and Bryers 2000*), 7 (*Flemming et al., 1997*), 8 (*Peña et al., 2012*), 9 (*Paul 1991*)

In general it must be considered that ATP is a cell activity parameter and reveals limited information about the actual effect of biofilm formation on plant performance, as reduced performance due to biofouling is mainly caused by the excreted EPS and not by the cells and their ATP (*Flemming 1997, Dreszer et al., 2013*). SEM pictures showed the presence of microorganisms on all membrane surfaces (*Figures 2.5. and 2.6.*). Furthermore, microcolonies of microorganisms embedded in EPS were observed in all membrane elements (*Figures 2.5. A and 2.6. B*), showing that biofilm formation took place in each of the installations.



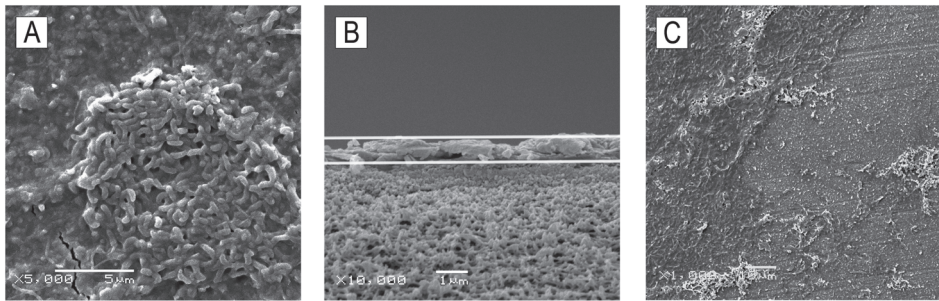


**Figure 2.5.** Representative SEM overview of the accumulated material on the membrane surfaces of the autopsied membrane elements. (A) Microcolonies of rod and vibrio-shaped microorganisms embedded in EPS of lead element RM. (B) Cross section of lead element of RM showing that average thickness of the accumulated material (area in-between two solid lines) is about 1 mm and (C) low magnification overview (1000 x) of the lead element of the WW installation showing that the fouling layers were not covering the whole membrane surface, but appearing in patches (upper right side of the picture shows original “ridge and valley” membrane surface).

The biofilms were not covering the whole membrane and spacer surface, but appeared as patches (*Figure 2.5. C*). Big parts of the membrane surfaces, in contrast, contained just single microorganisms embedded in a thin layer of amorphous deposits (*Figure 2.5. C*).

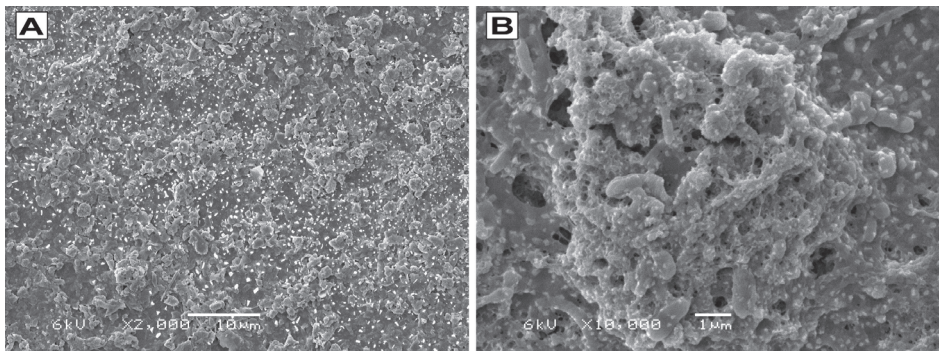


**Figure 2.6.** SEM observations of the fouling layer from the last element of the Weerseloseweg installation showing simultaneous inorganic precipitation and biofilm formation. (A) Aluminosilicate deposits. (B) Microcolonies of rod shaped bacteria embedded in EPS.

The slow biofilm formation could be explained by the absence of oxygen and nitrate in the feed water, where also metal ions mainly exist in their reduced form, iron (II) and manganese (II) (*Tuhela et al., 1993, Hiemstra et al., 1999*). Under those conditions sulfate reduction or methanogenesis occurs (*Muyzer and Stams 2008*).

These processes yield less energy for growth when compared to e.g. oxic respiration and nitrate reduction. As a consequence less biofilm could develop in the anoxic membrane elements.

In general, SEM cross section observations (dry state) revealed that the layers of accumulated material on the membrane surfaces are very thin (average 1 - 2  $\mu\text{m}$ ) (*Figure 2.5. B*). Calculations on the TOC deposition from the feed (*Supplementary data S2.4.*) indicated that in all the installations only a very small portion of the TOC in the feed (< 0.05 %) accumulated on the membrane surfaces, regardless of CIP frequency or feed water composition (*Table 2.2.*). In a mass balance of the feed, concentrate and permeate streams, such low deposition rates will not be detected, due to the fluctuations of the feed water quality (*Table 2.2.*) and the added up inaccuracy of, e.g., flow meters, pressure meters and measurements itself.

### **2.3.2.3. Inorganic precipitation and scaling**

The risk of inorganic precipitation can be calculated based on the saturation index of minerals from the feed water (*van de Lisdonk et al., 2001*). For the described installations, this was calculated with Troi, a software program supplied by Trisep. The results (*data not shown*) indicated that some of the waters are close to supersaturation with respect to calcium carbonate, calcium sulfate, barium sulfate and strontium sulfate (or combinations of them) when recoveries between 78 % and 80 % (*Table 2.1.*) were obtained. The feed waters were similar in calcium concentrations, alkalinity and pH (*Table 2.2.*) and to mainly avoid calcium carbonate scaling, 2 - 2.5  $\text{mg L}^{-1}$  of antiscalant were dosed to the feed waters. Acid was not used for scaling prevention, as it lowers the pH of the feed water and therefore increases the need of caustic soda to adjust the pH of the permeate. Furthermore, with acid still a minor antiscalant dosage of 0.5  $\text{mg L}^{-1}$  would be required to avoid other types of scaling than calcium carbonate. Dosing antiscalant alone turned out to be more cost effectively compared to the dosage of acid and antiscalant.

EDS measurements of the autopsied membrane elements rarely detected barium ( $\leq 0.5$  at% if detected) and did not detect strontium, thus barium sulfate and strontium sulfate scaling have probably not occurred. Calcium carbonate scaling was observed for the permeate spacer of the last element of the installation WW only



(*Supplementary data S2.5.*). Increased percentages of calcium (up to 14 at%) were observed on the membrane sheets of the same element, suggesting that calcium carbonate scaling did not exclusively occur in the permeate channel. In the other autopsied elements the calcium concentrations were generally below 2 at%, indicating that calcium carbonate and calcium sulfate scaling probably did not affect the performance of the installations DV, RM and WH. Sodium, calcium and phosphate were found in some of the spectra (generally below 2 at%) and magnesium, potassium, manganese, copper, chloride and zinc were rarely detected (< 1 at%, if detected at all). Some selected spectra and their related elemental analyses can be found in *Supplementary data S2.6*. The trends presented in this paragraph were inferred from multiple EDS spectra ( $\geq 5$ ) per membrane element. Due to the partially heterogeneous distribution of the foulants (*Sections 2.3.2.1 and 2.3.2.2*) and the small scanning area ( $0.012 \text{ mm}^2$  at 1000 x magnification), the representativeness of the EDS measurements might be improved by obtaining an increased amount of spectra (> 15 per element).

Aluminum and silicon were detected by EDS in all of the membrane samples with an average concentration of 1 - 5 at% (*Supplementary data S2.6*) and local maxima up to 17 at%, showing the presence of aluminosilicates (e.g. clay), a commonly found colloidal foulant in NF and RO membrane elements (*Peña et al., 2012*). The deposition and precipitation of aluminosilicates leads to an NPD increase,  $K_w$  decrease, gradually affects all membrane elements and it is one of the limiting factors of high-recovery reverse osmosis operations (*Peña et al., 2012, Cob et al., 2012*). An autopsy of a 10  $\mu\text{m}$  pore size cartridge prefilter showed that the aluminosilicates were already present as bigger particles in the feed water (data not shown), suggesting precipitation. On the membranes, in contrast, the aluminosilicates appeared to originate from colloidal (< 0.5  $\mu\text{m}$ ) aluminosilicate particles (*Figure 2.6. A*), which passed the 10  $\mu\text{m}$  pore size cartridge prefilter and then were subsequently deposited on the membrane surface.

The black discolorations of the membrane elements of DV, RM and WW (*Figure 2.3.*) commonly contained substantial amounts of iron (1 - 15 at%) and sulfur (1 - 19 at%) (*Supplementary data S2.6.*). The presence of both sulfur and iron during EDS

measurements and the absence of black precipitants in the WH installation, where sulfate concentrations were very low (*Table 2.2.*), suggested that the black precipitates are iron (II) sulfides (*Supplementary data S2.6.*). A possible explanation for iron (II) sulfide precipitation is the production of hydrogen sulfide by sulfate reducing bacteria (SRB). The hydrogen sulfide produced by SRB will rapidly form insoluble iron (II) sulfide with the high concentrations of iron (II) from the feed water (*Connel and Patrick 1968*). The abundance of SRB in the black stained membrane elements was confirmed with molecular analysis (*data not shown*). In the described installations this process likely occurred very slowly and therefore did not result in operational problems. Under changing environmental conditions (e.g. high concentrations of easily biodegradable nutrients), the activity of SRB could lead to rapid iron (II) sulfide fouling (*Connell and Patrick 1968*). Given the stable feed water composition of the groundwater, this rapid fouling will likely not occur in the studied installations.

## **2.4. Conclusions and recommendations**

In this study, plant performance analyses and membrane autopsies provided insight into the fouling development and specialties of anoxic groundwater treatment by NF. The performance of four anoxic groundwater treating NF installations, with minimal pretreatment, was shown to be stable for very long periods without chemical cleaning. Some results of this study, in comparison with literature data available from oxidic NF and RO, are summarized in *Table 2.4.*

The prevention of membrane biofouling, the most common foulant of NF and RO membranes (*Table 2.4.*), usually aims at the reduction of organic carbon (*Griebe and Flemming 1998, Schneider et al., 2005*) to reduce the formation of aerobic heterotrophic biofilms. Besides the great efforts to reduce biofouling by pretreatment, it is still the most common and problematic NF and RO fouling type (*Table 2.4.*), which is hard to clean and causes irreversible membrane damage (*Peña et al., 2012*). With this study we have shown that biofouling will likely not occur when the feed water is anoxic and will be low in potential electron acceptors for microbial growth. Specific removal of high energy yielding electron acceptors from the feed water, and also other innovative biofilm prevention approaches such as

phosphate limitation (*Vrouwenvelder et al., 2010*) deserve further investigations, in order to develop novel and effective pretreatment strategies for NF and RO.

Anoxic groundwater treatment by NF was also insensitive to metal fouling such as iron(hydr)oxide ( $\leq 8.4 \text{ mg L}^{-1}$  iron in the feed). The high solubility of reduced metal ions prevented rapid metal fouling and therewith enabled stable long-term operation ( $\geq 1$  year), without the need for CIP, in all installations. We have shown that each CIP potentially may harm the membrane elements. Interestingly, in a previous study with 500 membrane elements (*Peña et al., 2012*) it was concluded that one of the major impacts of fouling on performance is damage of the membranes polyamide top layer, leading to poor rejection capabilities and premature membrane replacement. We have shown the effect of CIP on NPD,  $K_w$  and rejection, but not directly on the membrane lifetime. This may be the case, but there is no cause effect.

Membrane fouling occurred very slowly and different types of fouling were detected simultaneously in the membrane elements. This was also found by Peña et al. (2012) in their elaborated study on membrane fouling. Specifically, we likely observed an event of microbial induced precipitation of inorganics by the activity of SRB's, which led to iron(II)sulfide precipitation and thus fouling of the elements. Laboratory fouling studies should in general focus on the complex interactions of the individual foulants within a composite fouling layer, rather than studying pure model foulants.

## Acknowledgments

This work was performed at Wetsus, Centre of Excellence for Sustainable Water Technology ([www.wetsus.nl](http://www.wetsus.nl)). Wetsus is funded by the Dutch Ministry of Economic Affairs, the European Union European Regional Development Fund, the Province of Fryslân, the city of Leeuwarden and by the EZ-KOMPAS Program of the “Samenwerkingsverband Noord-Nederland”. The authors would like to thank the participants of the research theme “Biofouling” for the fruitful discussions and their financial support and in particular the water company “Vitens”, for supply of the operational data and membrane elements and the possibility to perform the research presented in this manuscript.

## Supplementary data Chapter 2

Table S2.0. List of symbols and subscripts

Symbol	Description	Units
A	surface area	m <sup>2</sup>
EC	electrical conductivity	mS m <sup>-1</sup>
FCP	feed-concentrate pressure drop	kPa
J	membrane flux	m <sup>-3</sup> m <sup>-2</sup> h <sup>-1</sup>
K <sub>w</sub>	normalized specific water permeability	m s <sup>-1</sup> kPa <sup>-1</sup>
M	constant $QCF_{NPD}$	-
m	mass	mg
N	constant $TCF_{NPD}$	-
NDP	net driving pressure	kPa
NPD	normalized pressure drop	kPa
P	pressure	kPa
Q	volume flow	m <sup>3</sup> h <sup>-1</sup> or L since last cleaning
QCF	correction factor volume flow	-
T	temperature	°C
t	time	h
TCF	correction factor temperature	-
TDS	total dissolved solids	ppm
TOC	total organic carbon	mg or mg L <sup>-1</sup> or mg cm <sup>-2</sup>
SDP	solute deposition/precipitation	mg L <sup>-1</sup> or %
U	constant at $TCF_{K_w}$	kelvin
Π	osmotic pressure	kPa
η	dynamic viscosity	kPa s

Subscript	Description
accu	accumulated
act	actual
f	feed
c	concentrate
K <sub>w</sub>	normalized specific water permeability
mem	membrane
norm	normalized
NPD	normalized pressure drop
p	permeate
ref	reference
tot	total
w	water

## Supplementary data S2.1. - Operational data normalization ( $K_w$ , NPD and salt retention)

### S2.1.1. - Normalized membrane flux - the normalized specific water permeability ( $K_w$ )

The water flux ( $J_w$ ) through a membrane can be expressed by the amount of water ( $Q_p$ ) passing a certain membrane area ( $A_{mem}$ ).

$$\text{Equation S2.1.1} \quad J_w [m^3 m^{-2} h^{-1}] = \frac{Q_p [m^3 h^{-1}]}{A_{mem} [m^2]}$$

The normalized specific water permeability ( $K_w$ ) can be derived from the water flux ( $J_w$ ) by correcting for the net driving pressure ( $NDP$ ) and by introducing a correction factor for temperature ( $TCF_{K_w}$ ).

$$\text{Equation S2.1.2} \quad K_w [m s^{-1} kPa^{-1}] = \frac{Q_p [m^3 h^{-1}] * TCF_{K_w}}{A_{mem} [m^2] * NDP [kPa] * 3600}$$

The temperature correction factor ( $TCF_{K_w}$ ) allows to normalize the normalized specific water permeability ( $K_w$ ) for a defined reference temperature ( $T_{ref}$ ). The  $U$ -value expresses the temperature dependency of the membrane properties and was obtained from the membrane manufacturer.

$$\text{Equation S2.1.3} \quad TCF_{K_w} = e^{U [k] * \left( \frac{1}{T_{act} [^\circ C] + 273} - \frac{1}{T_{ref} [^\circ C] + 273} \right)}$$

$U = 2,900$  (provided by membrane manufacturer Trisep for Trisep 8040-TS82 membranes)

$T_{ref} = 10^\circ C$  (used by the Dutch drinking water companies)

The net driving pressure can ( $NDP$ ) be derived by subtracting the average osmotic pressure difference between feed and permeate from the average pressure difference between feed and permeate.

$$\text{Equation S2.1.4} \quad NDP [kPa] = \left( \frac{P_f + P_c}{2} - P_p \right) [kPa] - \left( \frac{\Pi_f + \Pi_c}{2} - \Pi_p \right) [kPa]$$

The osmotic pressure can be derived from electrical conductivity (EC,  $mS m^{-1}$ ) measurements. First EC is converted to the amount of total dissolved salts (TDS,

ppm), then further converted to the osmotic pressure ( $\Pi$ , kPa). The conversion factors were determined from experimental data.

$$\text{Equation S2.1.5} \quad \Pi = EC \times factor_{EC [mS m^{-1}] \rightarrow TDS [ppm]} * factor_{TDS [ppm] \rightarrow \Pi [kPa]}$$

$$factor_{EC \rightarrow TDS} = 0.5$$

$$factor_{TDS \rightarrow \Pi} = 0.699$$

### S2.1.2. - Normalized (feed - concentrate channel) pressure drop (NPD)

The feed-concentrate pressure drop ( $FCP$ ) of a membrane element can be expressed as the pressure difference between feed ( $P_f$ ) and concentrate ( $P_c$ ).

$$\text{Equation S2.1.8} \quad FCP [kPa] = (P_f - P_c)$$

The feed-concentrate pressure drop ( $FCP$ ) was then corrected for a temperature of 10°C ( $TCF_{NPD}$ ) and normalized to a volume flow of 10m<sup>3</sup> h<sup>-1</sup> ( $QCF_{NPD}$ ) in order to obtain the normalized pressure drop ( $NPD$ ).

$$\text{Equation S2.1.9} \quad NPD [kPa] = FCP [kPa] * QCF_{NPD} * TCF_{NPD}$$

For the normalization of the volume flow ( $QCF_{\Delta P}$ ) and the correction of the temperature dependent viscosity of the water ( $TCF_{\Delta P}$ ) Equation S1.8 and S1.9 were used.

$$\text{Equation S2.1.10} \quad QCF_{NPD} = \left( \frac{Q_{fc,ref} [m^3 h^{-1}]}{Q_{fc,act} [m^3 h^{-1}]} \right)^M = \left( \frac{Q_{fc,ref} [m^3 h^{-1}]}{(Q_{f,act} + Q_{c,act}) [m^3 h^{-1}] / 2} \right)^M$$

$$\text{Equation S2.1.11} \quad TCF_{NPD} = \left( \frac{\eta_{T,ref} [kPa s]}{\eta_{T,act} [kPa s]} \right)^N$$

$Q_{fc,ref}$  = Feed – concentrate reference volume flow of 10 m<sup>3</sup> h<sup>-1</sup> per membrane element.

$\eta_T$  = viscosity of the water

The factors  $M$  and  $N$  were experimental determined with new membrane elements and clean water in a test unit. The actual pressure drop ( $FCP [kPa]$ ) was measured

at different water temperatures ( $T_{act}$  [ $^{\circ}C$ ]) and volume flows ( $Q_{fc,act}$  [ $m^3 h^{-1}$ ]). The  $M$ -value and  $N$ -value were then derived from the best fit of the experimental data with *Equations S1.10* and *S.11*.

$M$ -value      experimental determined (= 1.6)

$N$ -value      experimental determined (= 0.4)

The normalized pressure drop ( $NPD$ ) was calculated separate for each individual stage of the installations. The overall normalized pressure drop per membrane element ( $NPD_{tot}$ ) over the whole installation was calculated by a weighted average of the pressure vessels per stage and the normalized pressure drop per membrane element per stage ( $NPD_{stage}$ ).

$$\text{Equation S2.1.12} \quad NPD_{tot} [kPa] = \frac{\left( \sum_{i=stage_1}^{i=stage_3} (NPD_{stage} * \text{number pressure vessels}) \right)}{\sum_{i=stage_1}^{i=stage_3} (\text{number pressure vessels})}$$

### S2.1.3. - Salt retention

$$\text{Equation S2.1.13} \quad \text{Salt retention} = 1 - \left( \frac{EC_p}{((EC_f + EC_c) / 2)} \right)$$

Supplementary data S2.2. -  $K_w$  and NPD graphs of installations DV and WH

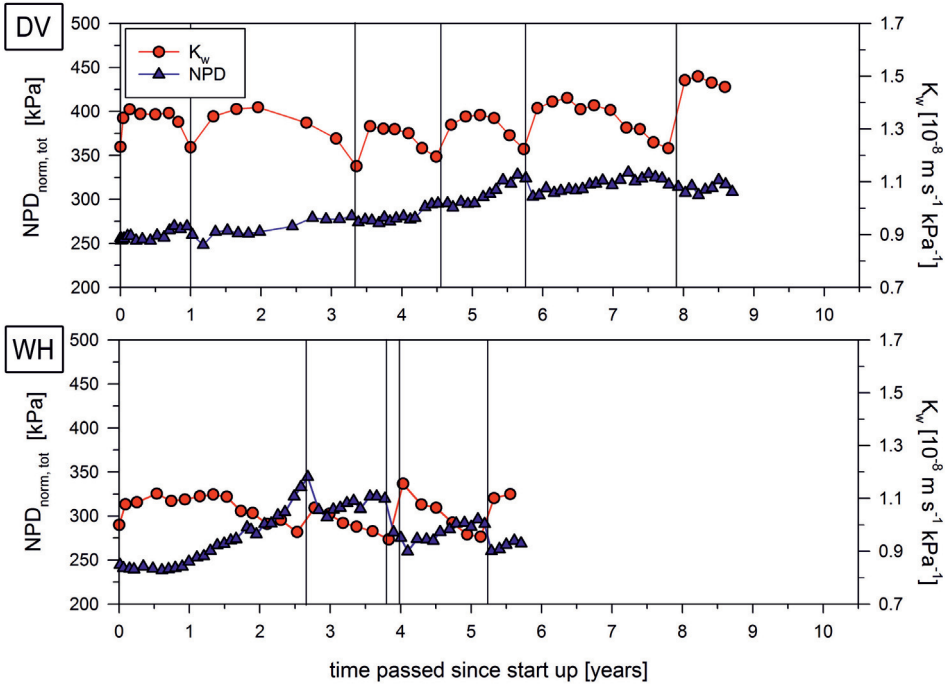


Figure S2.1. Development of performance parameters  $K_w$  (circles) and NPD (triangles) for the installations Diepenveen (DV) and Witharen (WH). The vertical lines indicate events of chemical cleanings in place (CIP). Directly after the last data point the membrane elements were autopsied and analyzed.



**Supplementary data S2.3. - Salt retention graphs of the installations WW, RM and WH**

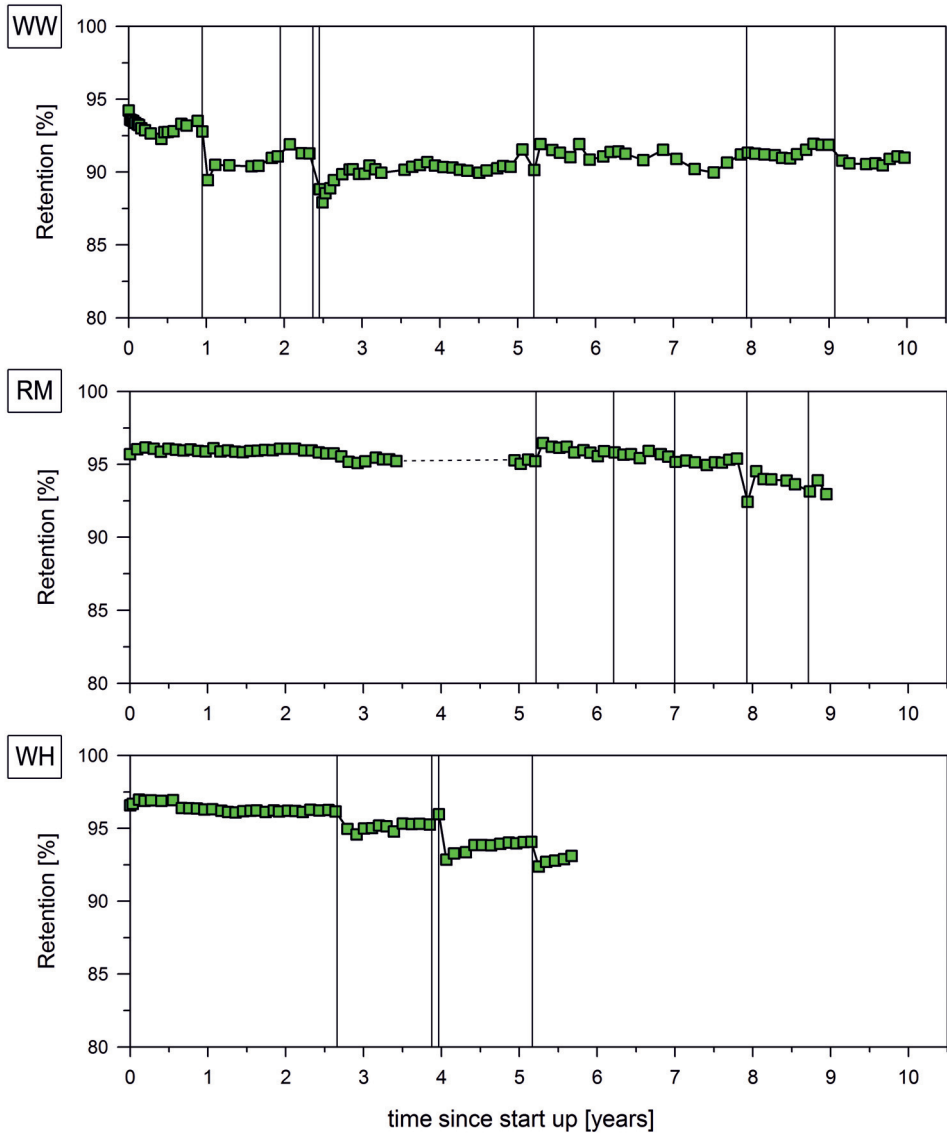


Figure S2.2. Development of the salt retention over time of the installations Weerseloseweg (WW), Rodenmors (RM) and Witharen (WH). The vertical lines indicate events of chemical cleanings in place (CIP). Directly after the last data point the membrane elements were autopsied and analyzed.

### Supplementary data S2.4. - Determining solute deposition / precipitation based on autopsy results

The solute deposition/precipitation in nanofiltration processes can be expressed as shown in *Equation S2.4.1*.

$$\text{Equation S2.4.1} \quad SDP = \frac{m_{accu}}{Q_f}$$

$SDP$  = deposition/precipitation of solutes from the feed [mg L<sup>-1</sup>]

$Q_f$  = volume flow of feed since last chemical cleaning [L since last cleaning]

$m_{accu}$  = accumulated material on membrane since last chemical cleaning [mg since last cleaning]

### Calculation example total organic carbon (TOC) for Rodenmors (RM), the most problematic installation in terms of cleaning frequency:

The total accumulated material in the membrane installation can be calculated under the assumption that the autopsied membrane elements are representative for the other membrane elements of their respective stage.

$$\text{Equation S2.4.2} \quad m_{accu} = \sum_{i=stage_1}^{i=stage_2} (TOC_{average} * A_{mem} * number_{elements\ per\ vessel} * number_{vessels})$$

$TOC_{average}$  = 400 mg TOC m<sup>-2</sup> for elements from first stage and  
128 mg TOC m<sup>-2</sup> for elements from second stage

$number\ elements\ per\ vessel$  = 6 elements per pressure vessel

$number\ of\ vessels$  = 6 vessels in the first stage and 3 vessels in the second stage

$A_{mem}$  = 33.5 m<sup>2</sup> for Trisep 8040-TS82 membrane elements

With the values above we calculate a  $m_{accu}$  of 559584 mg TOC accumulated since last chemical cleaning.

$$\text{Equation S2.4.3} \quad Q_f = Q_{f,vessel} * 1000 * number_{vessels,stage 1} * 24 * days_{last cleaning}$$

$$Q_f = 7.8 \text{ m}^3 \text{ h}^{-1}$$

$$days_{last cleaning} = 164 \text{ days}$$

By solving *equation S2.4.3* we get a  $Q_f$  of 184204800 liter. Solving *equation S4.1* with the obtained values for  $m_{accu}$  [mg since last cleaning] and  $Q_f$  [L since last cleaning] we calculated the TOC deposition = 0.003 mg TOC per liter of feed. With the known TOC concentration of the feed (7.9 mg L<sup>-1</sup>) the TOC deposition can be expressed as a percentage = 0.04 % of the TOC from the feed accumulates on the membranes.

#### Results for each of the installations:

Diepenveen = 0.01 % of the feed TOC accumulates on the membrane surfaces

Rodenmors = 0.04 % of the feed TOC accumulates on the membrane surfaces

Weerseloseweg = 0.05 % of the feed TOC accumulates on the membrane surfaces

Witharen = 0.05 % of the feed TOC accumulates on the membrane surfaces

#### Supplementary data S2.5. - Calcium carbonate scaling in last element of WW installation

The white scaling layer, that was found during autopsy in the permeate channel of the last element of the WW installation, was identified as calcium carbonate by EDS measurements and further analyses using Raman spectroscopy revealed the presence of pure calcite (*Figure S2.3A*). The obtained spectrum (*Figure S2.3B*) shows pure calcite (reference calcite peaks 156, 283, 711, 1085 (Raman shift, cm<sup>-1</sup>) formation (*Burke 2001*). High concentrations of calcium (up to 14%) have been also observed on the membrane sheets of the same installation, suggesting that calcium carbonate scaling did not exclusively occur in the permeate channel.

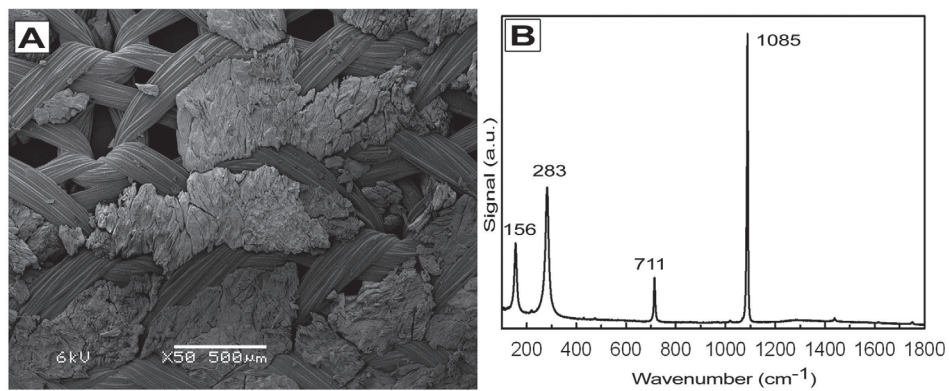


*Figure S2.3.* Fouling analysis showing the development of calcite scaling in the product (permeate) spacer channel of the last element of the Weerseloseweg installation. (A) SEM picture showing scale formation on the permeate spacer (50x) (B) Raman spectrum obtained from scaling layer.

**Supplementary data S2.6. - Energy dispersive X-Ray spectroscopy (EDS) spectra and related elemental analysis of WW, RM, DV and WH**

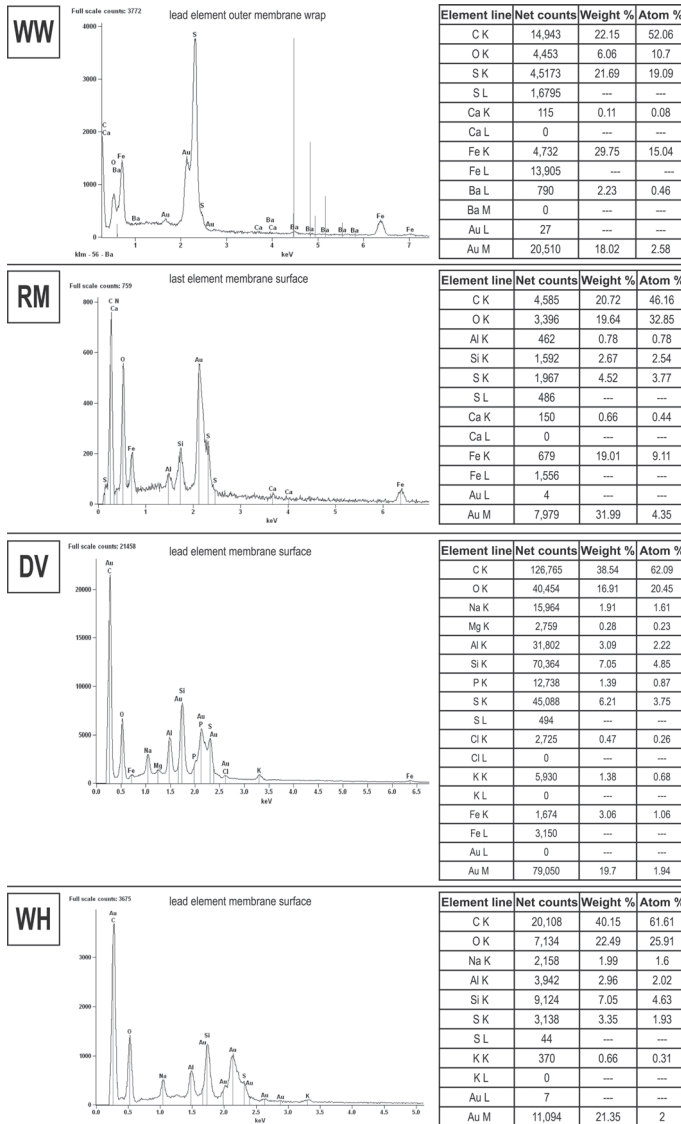
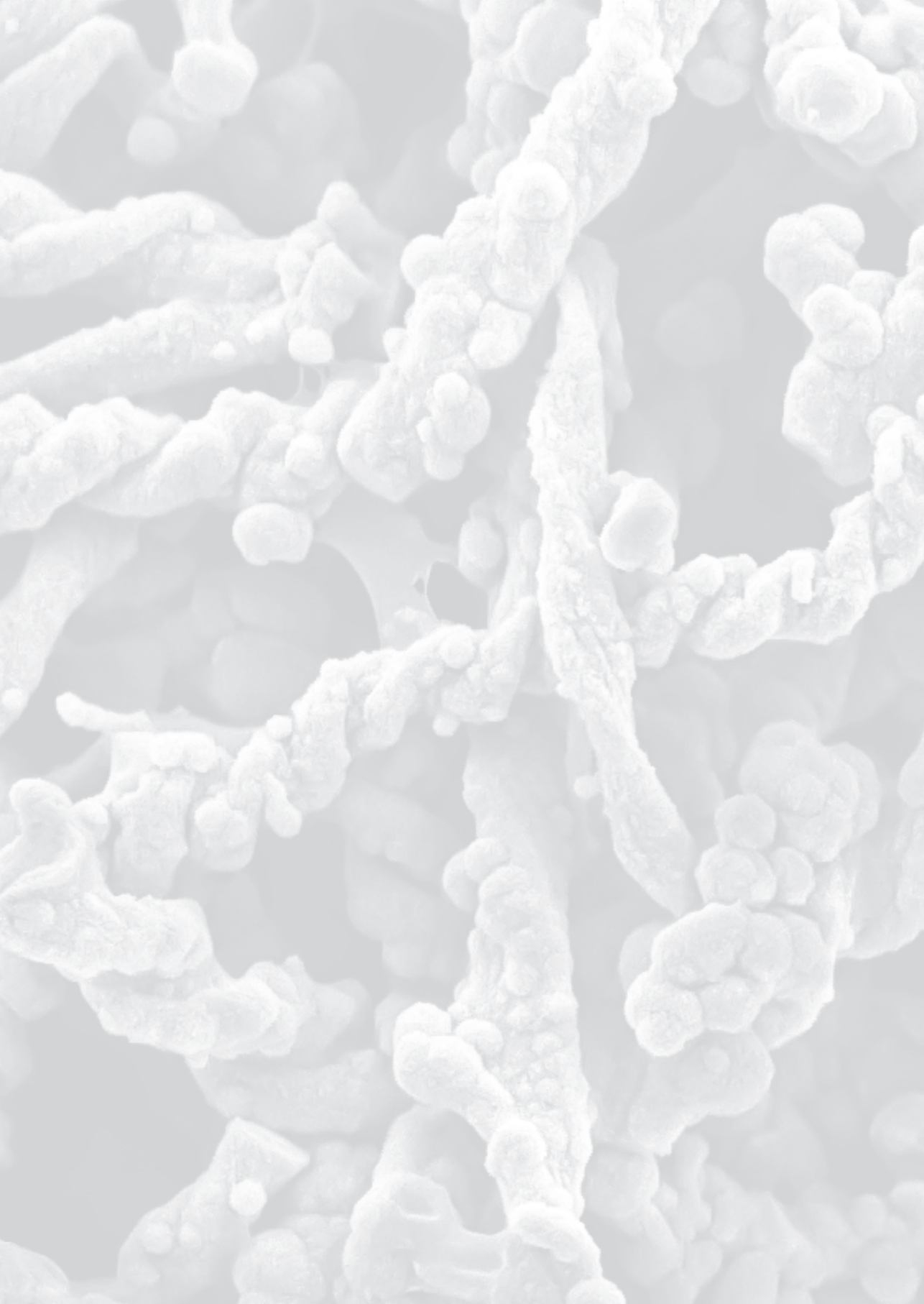


Figure S2.4. Selected EDS spectra and elemental analysis of the installations (WW) Weerseloseweg, (RM) Rodenmors, (DV) Diepenveen and (WH) Witharen. The spectra presented were selected from multiple spectra per element ( $\geq 5$ ). Due to the partially heterogeneous distribution of the foulants (section 3.1.1 and 3.1.2) and the small scanning area (0.012mm<sup>2</sup> at 1000x magnification), the representivness of the EDS measurements might be improved by obtaining an increased amount of spectra ( $>15$  per element). The trends observed during multiple measurements are discussed in the manuscript.

## References

- Al-Amoudi, A.S., Farooque, A.M. Performance restoration and autopsy of NF membranes used in seawater pretreatment. *Desalination*. 178(1-3): 261-271 (2005).
- Al-Amoudi, A., Lovitt, R.W. Fouling strategies and the cleaning system of NF membranes and factors affecting cleaning efficiency. *J. Membr. Sci.* 303(1-2): 4-28 (2007).
- Al-Amoudi, A.S. Factors affecting natural organic matter (NOM) and scaling fouling in NF membranes: A review. *Desalination*. 259(1-3): 1-10 (2010).
- Bereschenko, L.A., Prummel, H., Euverink, G.J.W., Stams, A.J.M., van Loosdrecht, M.C.M. Effect of conventional chemical treatment on the microbial population in a biofouling layer of reverse osmosis systems. *Water Res.* 45(2): 405-416 (2011).
- Burke, E.A.J. Raman microspectrometry of fluid inclusions. *Lithos*. 55(1-4): 139-158 (2001).
- Connell, W.E., Patrick Jr., W.H. Sulfate reduction in soil: Effects of redox potential and pH. *Science*. 159(3810): 86-87 (1968).
- Cob, S.S., Beaupin, C., Hofst, B., Nederlof, M.M., Harmsen, D.J.H., Cornelissen, E.R., Zwijnenburg, A., Genceli Güner, F.E., Witkamp, G.J. Silica and silicate precipitation as limiting factors in high-recovery reverse osmosis operations. *J. Membrane Sci.* 423-424: 1-10 (2012).
- Carnahan, R.P., Bolin, L., Suratt, W. Biofouling of PVD-1 reverse osmosis elements in the water treatment plant of the city of Dunedin, Florida. *Desalination* 102(1-3): 235-244 (1995).
- Dreszer, C., Vrouwenvelder, J.S., Paulitsch-Fuchs, A.H., Zwijnenburg, A., Kruithof, J.C., Flemming, H.-C. Hydraulic resistance of biofilms. *J. Membrane Sci.* 429: 436-447 (2013).
- Flemming, H.-C., Schaule, G., Griebe, T., Schmitt, J., Tamachkiarowa, A. Biofouling - the Achilles heel of membrane processes. *Desalination*. 113(2-3): 215-225 (1997).
- Flemming, H.-C. Reverse osmosis membrane biofouling. *Exp. Therm. Fluid Sci.* 14(4): 382-391 (1997).
- Flemming, H.-C. Biofouling in water systems - cases, causes and countermeasures. *Appl. Microbiol. Biotechnol.* 59(6): 629-640 (2002).
- Geesey, G., Bryers, J.D. Biofouling of engineered materials and systems. In: Bryers, J.D. (ed.) *Biofilms II Process analysis and applications*. Wiley-Liss, New York. 242-245 (2000).
- Griebe, T. and Flemming, H.C. Biocide-free antifouling strategy to protect RO membranes from biofouling. *Desalination*. 118(1-3): 53-156 (1998).
- Gwon, E.-M., Yu, M.J., Oh, H.-K., Ylee, J.-H. Fouling characteristics of NF and RO operated for removal of dissolved matter from groundwater. *Water Res.* 37(12): 2989-2997 (2003).
- Hiemstra, P., van Paassen, J., Rietman, B., Verdouw, J. Aerobic versus anaerobic nanofiltration: fouling of membranes. In: *Proceedings of AWWA Membrane Conference*, Long Beach, CA. (1999).
- Huiting, H., Kappelhof, J.W.N.M., Bosklopper, T.G.J. Operation of NF/RO plants: from reactive to proactive. *Desalination*. 139(1-3): 183-189 (2001).
- Muyzer, G., Stams, A.J.M. The ecology and biotechnology of sulphate-reducing bacteria. *Nat. Rev. Microbiol.* 6(6): 441-454 (2008).
- Nederlof, M.M., Kruithof, J.C., Taylor, J.S., van der Kooij, D., Schippers, J.C. Comparison of NF/RO membrane performance in integrated membrane systems. *Desalination*. 131: 257-269 (2000).
- Paul D.H. Reverse osmosis: scaling, fouling & chemical attack. *Desal. Water Reuse*. 1: 8-11 (1991).
- Peña, N., Gallego, S., del Vigo, F., Chesters, S.P. Evaluating impact of fouling on reverse osmosis membranes performance. *Desalin. Water Treat.* 51(4-6): 958-968 (2012).

- Rautenbach, R., Linn, T., Eilers, L. Treatment of severely contaminated waste water by a combination of RO, high-pressure RO and NF - potential and limits of the process. *J. Membr. Sci.* 174(2): 231-241 (2000).
- Reiss, C.R., Taylor, J.S., Robert, C. Surface water treatment using nanofiltration - pilot testing results and design considerations. *Desalination.* 125(1-3): 97-112 (1999).
- Schippers, J.C. and Verdouw, J. The modified fouling index, a method of determining the fouling characteristics of water. *Desalination.* 32: 137-148 (1980).
- Schneider, R.P., Ferreira, L.M., Binder, P., Bejarano, E.M., Góes, K.P., Slongo E., Machado, C.R., Rosa, G.M.Z. Dynamics of organic carbon and of bacterial populations in a conventional pretreatment train of a reverse osmosis unit experiencing severe biofouling. *J. Membrane Sci.* 266(1-2): 18-29 (2005).
- Speth, T.F., Summers, R.S., Gusses, A.M. Nanofiltration foulants from a treated surface water. *Environ. Sci. Technol.* 32(22): 3612-3617 (1998).
- Tuhela, L., Smith, S.A., Tuovinen, O.H. Microbiological analysis of iron-related biofouling in water wells and a flow-cell apparatus for field and laboratory investigations. *Ground Water.* 31(6): 982-988 (1993).
- van Paassen, J.A.M., Kruithof, J.C., Bakker, S.M., Schoonenberg Kegel F. Integrated multi-objective membrane systems for surface water treatment: pre-treatment of nanofiltration by riverbank filtration and conventional ground water treatment. *Desalination.* 118(1-3): 239-248 (1998).
- van Paassen, J.A.M., van der Meer, W.G.J., Post, J. Optiflux®: from innovation to realisation. *Desalination.* 178(1-3): 325-331 (2005).
- van de Lisdonk, C.A.C., Rietman, B.M., Heijman, S.G.J., Sterk, G.R., Schippers, J.C. Prediction of supersaturation and monitoring of scaling in reverse osmosis and nanofiltration membrane systems. *Desalination.* 138(1-3): 259-270 (2001).
- van den Broek, W.B.P., Boorsma, M.J., Huiting, H., Dusamos, M.G., van Agtmaal S. Prevention of biofouling in industrial RO systems: experiences with Peracetic Acid, *Water Sci. Technol.* 5(2): 1-11 (2010).
- van der Meer, W.G.J., van Winkelen, J.C. European Patent No. 1034139. Method for purifying water, in particular groundwater, under anaerobic conditions, using a membrane filtration unit, a device for purifying water, as well as drinking water obtained by such a method. European patent office (2001).
- van der Meer, W.G.J., van Paassen, J.A.M., Riemersma, M.C., van Ekkendonk, F.H.J. Optiflux®: from innovation to realisation, *Desalination* 157(1-3): 159-165 (2003).
- Vrouwenvelder, J.S. and van der Kooij D. Diagnosis of fouling problems of NF and RO membrane installations by a quick scan, *Desalination* 153(1-3): 121-124 (2003).
- Vrouwenvelder, J.S., Manolarakis, S.A., van der Hoek, J.P., van Paassen, J.A.M., van der Meer, W.G.J., van Agtmaal J.M.C., Prummel, H.D.M., Kruithof, J.C., van van der Bruggen, B., Mänttari, M., Nyström, M. Drawbacks of applying nanofiltration and how to avoid them: A review. *Sep. Purif. Technol.* 63(2): 251-263 (2008).
- Vrouwenvelder, J.S., Manolarakis, S.A., van der Hoek, J.P., van Passen, J.A.M., van der Meer, W.G.J., van Aagtmaal, J.M.C., Prummel, H.D.M., Kruithof, J.C., van Loosdrecht, M.C.M. Quantitative biofouling diagnosis in full scale nanofiltration and reverse osmosis installations. *Water Res.* 42(19): 4856-4868 (2008).
- Vrouwenvelder, J.S., Beyer, F., Dahmani, K., Hasan, N., Galjaard, G., Kruithof, J.C., van Loosdrecht, M.C.M. Phosphate limitation to control biofouling. *Water Res.* 44(11): 3454-3466 (2010).





The background of the cover is a grayscale scanning electron micrograph (SEM) showing a complex, porous structure of a membrane. The structure consists of interconnected, elongated, and somewhat irregular fibers or filaments that form a dense, interconnected network. The surface of these fibers appears textured and granular, with many small, rounded protrusions and indentations, suggesting a high surface area and a complex morphology typical of a biofouled or fouling-resistant membrane. The overall appearance is that of a highly porous, three-dimensional material.

# Chapter 3

## **Bacterial communities in nanofiltration membranes used for drinking water production from anoxic groundwater**

Florian Beyer, Monika Jarzembowska,  
Alfons J.M. Stams, Caroline M. Plugge

## Abstract

Next-generation sequencing of 16S rRNA genes was used to study bacterial diversity of two nanofiltration installations treating anoxic groundwater and that do not suffer from rapid biofouling commonly occurring in membrane-assisted treatment of oxic water. The relative abundance of bacterial phyla, after extended periods (> 300 days) of operation without chemical cleaning, was: Firmicutes (2.9 - 46.2 %), Nitrospinae (0 - 65 %), Actinobacteria (0.7 - 55 %), Proteobacteria (7.8 -16.9 %), Nitrospirae (7.3 - 11.3 %), Chloroflexi (3 - 13.3 %), TM7 (0.5 - 12.5 %), Bacteroidetes (0.7 - 14 %), Planctomycetes (0.1 - 4.3 %) and Acidobacteria (0.2-3.5 %). The majority of the bacteria affiliated with uncultured lineages of environmental sequences. Microbial communities differed greatly between locations, and were significantly distinct from those detected during oxic filtration that are typically dominated by  $\alpha$ -,  $\beta$ -, and  $\gamma$ -Proteobacteria. The absence of biofouling in studied plants could be linked to the reducing conditions of the feed water, selecting for anaerobes with slow metabolism.

## 3.1. Introduction

During the last decades, membrane technology has become increasingly important for water treatment. At present, high pressure membrane filtration processes such as nanofiltration (NF) and reverse osmosis (RO) are widely applied for drinking water production, partial or full desalination, water reuse and waste water treatment.

A main problem and challenge of NF and RO membrane technology is reduced membrane performance caused by biofouling (*Paul 1991; Flemming et al., 1997; Peña et al., 2012*). Membrane biofouling is the unwanted development of microbial biofilms on membrane and spacer surfaces, typically causing reduced membrane permeability and increased feed-concentrate channel pressure drop (*Nederlof et al., 2000; Huiting et al., 2001*). Further negative side effects of membrane biofouling include: reduced rejection of solutes, facilitation of inorganic precipitation, and microbial deterioration of the polymeric filtration membrane (by e.g. the production of organic acids). Biofouling prevention traditionally involves three key strategies: i) the reduction of easily degradable organic carbon (*Griebe and Flemming, 1998*;

*Schneider et al., 2005*), ii) the reduction of the microbial load (by e.g. reducing total microbial counts) and iii) the inactivation of microorganisms (*van den Broek et al., 2010*). Membrane biofouling is the most common type of fouling in NF and RO membrane filtration systems and besides other types of fouling (e.g. scaling or organic fouling), it is also the hardest to control (*Paul 1991; Flemming et al., 1997; Peña et al., 2012*).

Previous studies that investigated the microbial community composition of biofilms on fouled membranes have focused on the bacterial biodiversity of oxic feed water systems (e.g. surface and seawater). Those studies found a strong predominance of the bacterial phylum Proteobacteria (especially the  $\alpha$ -,  $\beta$ -, and  $\gamma$ -Proteobacteria) in 'biofouling biofilms' (*Chen et al., 2004, Pang and Liu 2007, Bereschenko et al., 2011, Ayache et al., 2013; Al-Ashhab et al., 2014, Lee and Kim, 2011*). Other abundant phyla detected included Bacteroidetes, Planctomycetes, Firmicutes, Acidobacteria and Actinobacteria. In previous work (*Beyer et al., 2014*) the long-term performance and fouling behavior of four anoxic groundwater treating NF installations were investigated. Although pretreatment was limited to 10  $\mu\text{m}$  pore size filtration and antiscalant dosage, the installations did not suffer from severe biofouling problems (*Beyer et al., 2014*). It was hypothesized that the absence of high-energy yielding electron acceptors such as oxygen or nitrate in the anoxic groundwater, successfully prevented fast biofilm formation in the installations. Groundwater ecosystems typically are oligotrophic (*Danielopol et al., 2000*). In subsurface environments, the microbial activities are several orders of magnitude lower, when compared to surface environments (*Kieft and Phelps, 1997, Hoehler and Jørgensen, 2013*). The current understanding of the microbial diversity in oligotrophic subsurface systems is scarce (*Griebler and Lueders, 2009, Hoehler and Jørgensen, 2013*).

To understand the very slow biofilm development during anoxic NF, even without pretreatment, the bacterial biofilm-associated communities were studied using next-generation sequencing of the 16S rRNA gene.

## 3.2. Material and Methods

### 3.2.1.1. NF operation, fouling and feed water qualities

The two installations investigated in this study, Diepenveen (DV) and Weerseloseweg (WW) have been described previously (Beyer *et al.*, 2014). Briefly, the two installations use direct nanofiltration for drinking water production from anoxic groundwater (Table 3.1). Pretreatment is limited to 10 µm pore size cartridge filtration and the addition of a phosphonate based antiscalant (2 - 2.5 mg L<sup>-1</sup>).

Table 3.1. Feed water qualities of the two installations (adapted from Beyer *et al.*, 2014)

Measurement	Units	DV (Diepenveen) n ≥ 3	WW (Weerseloseweg) n ≥ 3
temp <sub>min,max</sub>	°C	9.5 - 13.1	9.5 - 14.2
pH	pH	7.22 ± 0.03	7.22 ± 0.05
TOC	mg L <sup>-1</sup>	7.3 ± 0.3	3.1 ± 0.3
DOC	mg L <sup>-1</sup>	6.6 ± 0.3	2.9 ± 0.2
ATP	ng L <sup>-1</sup>	2.4 ± 1.8	1.9 ± 1.4
oxygen	mg L <sup>-1</sup>	< 0.01	< 0.01
sulfate	mg SO <sub>4</sub> <sup>2-</sup> L <sup>-1</sup>	65.3 ± 1.2	123.8 ± 4.1
sulfide	mg S <sup>2-</sup> L <sup>-1</sup>	n.d.	< 2
nitrate	mg NO <sub>3</sub> <sup>-</sup> L <sup>-1</sup>	< 1	< 1
ammonium	mg NH <sub>4</sub> <sup>+</sup> L <sup>-1</sup>	1.1 ± 0.0	0.3 ± 0.0
ortho-phosphate	mg PO <sub>4</sub> <sup>3-</sup> L <sup>-1</sup>	0.5 ± 0.0	0.5 ± 0.3
hydrogen carbonate	mg HCO <sub>3</sub> <sup>-</sup> L <sup>-1</sup>	319 ± 2	286 ± 3
methane <sub>(headspace)</sub>	µg L <sup>-1</sup>	313 ± 8	145 ± 20
conductivity	mS m <sup>-1</sup>	63 ± 1	67 ± 1
total hardness (tH)	mmol (Ca <sup>2+</sup> + Mg <sup>2+</sup> ) L <sup>-1</sup>	3.25 ± 0.1	3.48 ± 0.1
calcium	mg L <sup>-1</sup>	116 ± 3	121 ± 4
chloride	mg L <sup>-1</sup>	37.3 ± 0.9	30.8 ± 1.1
sodium	mg L <sup>-1</sup>	22.1 ± 0.8	22.6 ± 0.8
magnesium	mg L <sup>-1</sup>	8.5 ± 0.2	11.3 ± 0.6
iron	mg L <sup>-1</sup>	4.2 ± 0.0	2.0 ± 1.2
potassium	mg L <sup>-1</sup>	3.7 ± 0.1	3.3 ± 0.1
manganese	mg L <sup>-1</sup>	0.3 ± 0.0	0.2 ± 0.1
silicon	mg L <sup>-1</sup>	6.7 ± 0.2	11.6 ± 0.2
strontium	µg L <sup>-1</sup>	409 ± 11	772 ± 35
barium	µg L <sup>-1</sup>	197 ± 6	101 ± 5
aluminum	µg L <sup>-1</sup>	4.1 ± 2.1	< 2

n.d. = not determined

The installations investigated are built in a two stage design, housing 6 membrane elements per pressure vessel and are operated at 78 % (DV) and 80 % (WW) recovery. Feed pressure range was 6.5 - 7.8 bar for DV and 6.8 - 9.8 bar for WW. Both installations use Trisep8040-TS82 (Trisep Corporation, CA, USA) NF membrane elements. The main difference between the two installations can be found in the feed water composition (*Table 3.1.*), although there are also slight operational differences (e.g. recovery or feed pressure) (*Beyer et al., 2014*). Based on extensive fouling characterization of the installations, including membrane autopsies and fouling layer analysis, fouling in the studied locations can be described as very slow and controllable (*Beyer et al., 2014*).

### 3.2.2. Sampling

From both installations (DV and WW) a lead membrane element from the first stage and a tail membrane element from the second stage were taken out of operation for membrane fouling analysis as described in *Beyer et al., 2014*. The accumulated biofilms were collected by carefully scraping off the membrane surfaces (approximately 1m<sup>2</sup> surface area per membrane element). The collected biomass was then stored at -80°C until DNA extraction.

### 3.2.3. DNA extraction

Biofilm samples were thawed and homogenized by vortexing. Total genomic DNA was extracted from approx. 500 mg of biofilm by using the Power Biofilm™ DNA Isolation Kit (Mo Bio Laboratories, Carlsbad, CA, US), according to the manufacturer's instructions. DNA quality and quantity was spectrophotometrically determined using a NanoDrop™ 1000 (Thermo Scientific, Waltham, MA, USA).

From the lead DV element two separate DNA extractions were performed (DV-lead S1 and DV-lead S2). Both DNA samples were then subjected in triplicate to PCR amplification and Illumina MiSeq sequencing (DV-lead S1-(1-3) and DV-lead S2-(1-3)). From the other membranes (DV-tail, WW-lead and WW-tail) only one DNA sample was used for sequencing. The DV-tail sample was sequenced in duplicate, while the WW samples were sequenced once only.

### 3.2.4. Bacterial Next Generation Sequencing

#### 16S rRNA gene amplification

Illumina 16S rRNA gene amplicon libraries were generated and sequenced at BaseClear BV (Leiden, The Netherlands). In short, genomic DNA was checked for integrity and lack of degradation by agarose gel electrophoresis, and the concentration was measured using the Quant-iT™ dsDNA Broad-Range Assay Kit (Invitrogen, Carlsbad, CA). Barcoded 16S rRNA amplicons from the V4 region were generated using the 515F primer (5'-GTGCCAGCMGCCGCGGTAA-3') appended with the forward Illumina adaptor (5'-AATGATACGGCGACCACCGAGATCTACAC TCTTTCCCTACACGACGCTCTTCCGATCT-GT-3') and the 806R primer (5'-GGACTACHVGGGTWTCTAAT-3') appended with the reverse Illumina adaptor (5'-CAAGCAGAAGACGGCATAACGAGAT-NNNNNN-GTACTGGAGTTCAGACGTGTG CTCTTCCGATCT-CC-3'). The 'GT' and 'CC' extensions of the adaptors did not match with the 16S rRNA gene. NNNNNN is a sequence of six nucleotides that was unique for each sample. PCR was performed in a total volume of 50 µl containing 50 ng DNA, 800 nM of the forward and reverse primer. PCR conditions were: 98°C for 30 s followed by 30 cycles of 98°C for 10 s, 50°C for 30s, and 72°C for 30s. The approximately 420 bp PCR amplicons were purified and mixed in equimolar amounts and sequenced on the Illumina MiSeq platform using the 150 cycles protocol.

#### Next generation sequencing analysis

Sequence analysis was performed at BaseClear BV (Leiden, The Netherlands). In short, FASTQ sequence reads were generated using the Illumina Casava pipeline version 1.8.3. Number of raw reads was then normalized to the sample with the least amount of reads (296275 reads). The data was initially checked for base quality and filtered for data passing the Illumina Chastity default parameters. Subsequently, reads containing adapters and/or PhiX control signal were removed using an in-house filtering protocol. FastQC v. 0.10.0 was used for further quality assessment and to check that the average Phred values were above 33. All reads generated for this study are deposited in the European Nucleotide Archive (ENA) within the study PRJEB21781. Initial quality assessment was based on data passing the Illumina

Chastity filtering. The second quality assessment was based on the remaining reads using the FASTQC quality control tool version 0.10.0. The quality of the FASTQ paired-sequences was enhanced by trimming off low-quality bases using the 'Trim sequences' option of the CLC Genomics Workbench version 6.5.1. The quality-filtered sequence reads were subsequently aligned against the Silva 115 SSU rRNA Database Database using the 'Map reads to reference' option of the CLC Genomics Workbench version 6.5.1. Dependent on the alignment of the paired-reads against the Silva database, taxonomic analysis was performed with MEGAN version 4.70.4 (Huson *et al.*, 2011). In order to reduce false positives, the min-support filter was set to 0.01 % of the total number of aligned reads as a threshold for the minimum number of sequences that must be assigned to a taxonomic profile. For the preparation of figures and tables in this manuscript, the taxonomic classification was manually adjusted to NCBI taxonomy.

### 3.3. Results and Discussion

#### Bacterial diversity

The two biological replicates of the DV-lead sample, which were both sequenced in triplicate, showed high similarity in the taxonomic assignment at phylum level (*Supplementary Figure S3.1*). High similarity was also observed at the order level (data not shown) and class level (*Table 3.2*). The replicates clearly group together (*Supplementary Figure S3.1*), while distinct differences could be observed for the four different membrane elements autopsied (*Table 3.2*). Taken together, the data shows high reproducibility of the taxonomic assignment across the technical and biological replicates.

Substantial differences between the bacterial membrane biofilm communities of the two installations investigated were observed (*Table 3.2*). Differences were also found within the same installation, when comparing the lead and the tail elements (*Table 3.2*). While the lead membrane element of DV was dominated by Firmicutes ( $46.2 \pm 7.1$  %), the tail membrane element of the same installation (DV-tail) was largely dominated by Nitrospinae ( $65 \pm 6.2$  %). For the installation WW, the lead element was dominated by the Actinobacteria phylum (55 %), while the tail element showed high relative abundance of Firmicutes (25.5 %).

*Figure 3.1.* Relative abundance of bacterial at phylum (bold) and class level (regular) of the four membrane elements autopsied. Major bacterial phyla (bold) of the taxonomically classified sequences detected with average relative sequence abundances in one of the samples > 1 % are displayed. Class-level (regular) is presented as class relative abundance within the respective phylum. Column “Other phyla” indicates combined relative sequence abundances of all the rare phyla and unfiltered archaeal reads.

	DV lead % (n=6)	DV tail % (n=2)	WW lead % (n=1)	WW tail % (n=1)
<b>Firmicutes</b>	<b>46.16 ± 7.1</b>	<b>8.27 ± 1.9</b>	<b>2.85</b>	<b>25.46</b>
Clostridia	99.14 ± 0.4	96.68 ± 0.01	92.28	98.66
Bacilli	0.76 ± 0.4	2.89 ± 0.1	7.72	0.82
Erysipelotrichia	0.09 ± 0.02	0.43 ± 0.04	0	0.51
<b>Nitrospinae</b>	<b>0.34 ± 0.1</b>	<b>64.99 ± 6.2</b>	<b>0</b>	<b>11.2</b>
Nitrospina	100	100	100	100
<b>Actinobacteria</b>	<b>9.23 ± 3</b>	<b>0.69 ± 0.3</b>	<b>54.99</b>	<b>4.96</b>
not assigned to class	100	100	100	100
<b>Proteobacteria</b>	<b>7.78 ± 1.2</b>	<b>8.02 ± 1.1</b>	<b>16.9</b>	<b>9.32</b>
Delta-, and Epsilonproteobacteria	64.07 ± 4.7	75.59 ± 1.5	74.97	71.35
Gammaproteobacteria	17.04 ± 1.9	12.68 ± 0.6	14.26	6.76
Betaproteobacteria	8.8 ± 1.1	6.82 ± 1.1	4.85	16.42
Alphaproteobacteria	10.1 ± 2.5	4.71 ± 0.2	5.92	5.47
<b>Nitrospirae</b>	<b>11.3 ± 2</b>	<b>7.96 ± 1.1</b>	<b>7.27</b>	<b>9.38</b>
Nitrospira	100	100	100	100
<b>Chloroflexi</b>	<b>3.61 ± 0.4</b>	<b>2.97 ± 0.7</b>	<b>6.72</b>	<b>13.25</b>
not assigned to class	100	100	100	100
<b>candidate division TM7</b>	<b>12.53 ± 4.6</b>	<b>0.48 ± 0.2</b>	<b>0.77</b>	<b>5.7</b>
not assigned to class	100	100	100	100
<b>Bacteroidetes</b>	<b>0.74 ± 0.2</b>	<b>2.68 ± 0.4</b>	<b>0.94</b>	<b>14</b>
Bacteroidia	7.63 ± 1.3	16.12 ± 0.2	20.75	73.26
Cytophagia	1.82 ± 0.5	6.67 ± 0.2	0	0.26
Flavobacteriia	29.74 ± 1.3	27.23 ± 1.8	36.9	23.86
Sphingobacteriia	59.07 ± 3.1	29.64 ± 1.6	42.35	0.21
not assigned to class	1.74 ± 0.9	20.33 ± 0.1	0	2.42
<b>Planctomycetes</b>	<b>0.12 ± 0.03</b>	<b>0.09 ± 0.03</b>	<b>4.25</b>	<b>3.58</b>
Planctomycetia	100	91.67 ± 8.3	100	99.16
Phycisphaerae	0	8.33 ± 8.3	0	0.84
<b>Acidobacteria</b>	<b>0.29 ± 0.04</b>	<b>0.17 ± 0.03</b>	<b>3.45</b>	<b>1.11</b>
Holophagae	72.54 ± 5.1	65.72 ± 5.8	3.97	44.61
Acidobacteriia	20.62 ± 3	24.1 ± 4.4	96.03	48.98
not assigned to class	6.83 ± 2.4	10.18 ± 1.4	0	6.41
<b>Other phyla</b>	<b>7.91 ± 1.1</b>	<b>3.71 ± 0.5</b>	<b>1.86</b>	<b>2.04</b>



Overall, 10 phyla (> 1 % sequence abundance) were detected on all membranes (sorted by average relative abundance): Firmicutes (2.9 - 46.2 %), Nitrospinae (0 - 65 %), Actinobacteria (0.7 - 55 %), Proteobacteria (7.8 - 16.9 %), Nitrospirae (7.3 - 11.3 %), Chloroflexi (3 - 13.3 %), TM7 (0.5 - 12.5 %), Bacteroidetes (0.7 - 14 %), Planctomycetes (0.1 - 4.3 %) and Acidobacteria (0.2 - 3.5 %).

Amongst the abundant phyla, the Nitrospirae were the most evenly distributed over the four membrane elements (indicated by the lowest relative deviation = deviation/average), followed by Proteobacteria and Chloroflexi (Table 3.2.). Nitrospinae were most unevenly distributed, with a high relative abundance in the DV-tail element (65 %) and very low relative abundance or absence in the lead elements. A strong predominance was observed for the Actinobacteria in WW-lead (55 %). Actinobacteria were more abundant in the lead elements when compared to the tail elements from the same installation, while Bacteroidetes appeared more abundant in the tail elements. Planctomycetes and Acidobacteria had a high relative abundance only in the WW installation.

### Firmicutes

Despite the fact that the relative abundance of the Firmicutes phylum fluctuated in the membrane elements analyzed (DV-lead  $46.2 \pm 7.1$  %, DV-tail  $8.3 \pm 1.9$  %, WW-lead 2.9 % and WW-tail 25.5 %), their class distribution was similar, with the Clostridia predominating in all membrane element samples (92.3 - 99.1% Firmicutes relative abundance). In the DV-lead sample, which was dominated by Firmicutes ( $46.2 \pm 7.1$  % relative abundance), an uncultured *Desulfosporosinus* species from the *Peptococcaceae* family represented  $81.3 \pm 2.4$  % of the Clostridial sequences. The *Desulfosporosinus* genus harbors endospore forming, Gram-positive sulfate-reducing bacteria (SRB). Previously, we speculated that the black iron(II)sulfide precipitates that were detected and identified on the membrane elements, were due to the activity of SRBs, that reduced sulfate to sulfide, readily forming insoluble iron(II)sulfide deposits (Beyer *et al.*, 2014). The sulfate reducing activity of the *Desulfosporosinus sp.* can cause metal-sulfide precipitation and corrosion (Labrenz and Banfield, 2004). In the other membrane element samples (DV-tail, WW-lead and WW-tail), the majority of the Clostridial sequences were related to uncultured

*Desulfosporosinus* species (DV-tail 49.6 %  $\pm$  4.6, WW-lead 25.9 % and WW-tail 36.7 %).

### **Nitrospinae**

All Nitrospinae-affiliating reads were further classified to the *Nitrospina* genus. Interestingly, *Nitrospina* were only abundant in the tail membrane elements (Table 3.2.). The DV-tail sample was dominated by the *Nitrospina* (65  $\pm$  6.2 % relative abundance). In the other membrane element samples, the relative abundance of the *Nitrospina* genus was much lower (DV-lead 0.3  $\pm$  0.1 %, WW-lead 0 %, and WW-tail 11.2 %). *Nitrospina* species are thought to be marine obligate aerobic chemolitho-autotrophic nitrite-oxidizing bacteria (NOB) (Lücker *et al.*, 2013). Nitrospinae are abundant in the mesopelagic zone, oxygen minimum zones, deep-sea waters and sediments (Daims *et al.*, 2016). Their proliferation in the tail elements, is likely linked to the concentration of solutes from the feed water during the NF process. This results in an increased salinity specifically in the tail membrane elements. The Trisep TS80 membrane elements have an average monovalent ion rejection of about 90 % and divalent ion rejection of about 99 %, leading to a concentration factor of 4.5 - 5 (at 80 % recovery), between lead and tail membrane elements (or feed and concentrate streams).

### **Actinobacteria**

The Actinobacteria is one of the largest bacterial phyla, including Gram-positive microorganisms that are widely abundant in soil, water and air (Barka *et al.*, 2016). The lead membrane element from WW was dominated by the Actinobacteria phylum (55 % relative abundance), and 99.5 % of those sequences could be assigned further to an uncultured *Mycobacterium* species (data not shown). Mycobacteria are facultative anaerobes and widespread and abundant in nature, typically sharing a saprophytic lifestyle (Barka *et al.*, 2016). However, some of the members seem to exhibit an obligate parasitic lifestyle and therefore cannot be found in their free-living form. Mycobacteria are typically found in water distribution system biofilms (Gomez-Smith *et al.*, 2015). Their competitive advantage may be attributed to factors such as increased resistance to disinfectants, the ability to form biofilms, and their ability to survive in nutrient-poor conditions under oxygen limitation (Gomez-Smith

*et al.*, 2015). In the remaining membrane elements, the relative abundance of Actinobacteria was moderate to low (DV-lead  $9.2 \pm 3$  %, DV-tail  $0.7 \pm 0.3$  % and WW-tail 5 %).

### **Proteobacteria**

The Proteobacteria were most abundant in the WW-lead sample (16.9 %) and moderately abundant in the other membrane element samples (DV-lead  $7.8 \pm 1.2$  %, DV-tail  $8 \pm 1.1$  %, and WW-tail 9.3 %). The distribution of the Proteobacteria classes revealed predominance of the Delta/Epsilon subdivision in all samples (64.1 - 75.6 % of Proteobacteria sequences, 5 - 12.7 % of all assigned sequences). The Deltaproteobacteria sequences, detected in all samples, affiliated with groups of known sulfate-reducing bacteria such as members of the *Desulfobulbaceae*, *Desulfobacteraceae* and *Syntrophaceae*. The presence of sulfate in the feed water provides an electron acceptor for respiration leading to the reducing conditions, and explaining the observed deposition of iron(II)sulfide in the membrane elements.

The other Proteobacteria classes  $\alpha$ ,  $\beta$  and  $\gamma$  were low in relative abundance (DV-lead  $2.8 \pm 0.2$  %, DV-tail  $1.9 \pm 0.1$  %, WW-lead 4.2 % and WW-tail 2.7 % relative abundance  $\Sigma$   $\alpha$ -,  $\beta$ - and  $\gamma$ -Proteobacteria). The  $\alpha$ -,  $\beta$ -, and  $\gamma$ -Proteobacteria classes have been frequently reported to dominate biofouled membrane elements, irrespective of feed water quality. However, all these reports studied feed waters that were oxic (*Chen et al.*, 2004, *Pang and Liu* 2007, *Bereschenko et al.*, 2011, *Ayache et al.*, 2013, *Al-Ashhab et al.*, 2014). The  $\alpha$ -,  $\beta$ -, and  $\gamma$ -Proteobacteria harbor a large and diverse group of fast growing heterotrophic biofilm formers. Their low relative abundances observed during anoxic NF, may be one of the reasons for the very low biofouling tendencies of the studied systems (*Beyer et al.*, 2014).

### **Nitrospirae**

The Nitrospirae phylum is the most abundant and diverse group of nitrite-oxidizing bacteria (NOB). They are autotrophs that conserve energy by oxidizing nitrite to nitrate. Recently, 'Comammox bacteria', members of the *Nitrospira* genus which perform complete nitrification, were discovered (*van Kessel et al.*, 2015). Nitrospirae are widely distributed in natural habitats such as soils, sediments, oceans and groundwater (*Lücker et al.*, 2010, *Daims et al.*, 2016). Members of the Nitrospirae

were abundant in groundwater treatment processes (Roeselers *et al.*, 2015 and Gülay *et al.*, 2016). Nitrospirae were identified as core taxa in anoxic groundwater-fed rapid gravity filters (Gülay *et al.*, 2016). This phylum showed similar and moderate relative abundance in all membrane samples analysed (DV-lead  $11.3 \pm 2$  %, DV-tail  $8 \pm 1.1$  %, WW-lead 7.3 % and WW-tail 9.4 %). All Nitrospirae sequences obtained affiliated with the *Nitrospira* genus. However, the majority of *Nitrospira* are uncultured, and the few available cultures are difficult to maintain (Off *et al.*, 2010, Daims *et al.*, 2016). The ecophysiology of the Nitrospirae phylum and, as well as other NOB, remains to be uncovered (Daims *et al.*, 2016).

### **Chloroflexi**

$3.6 \pm 0.4$  % (DV-lead),  $3 \pm 0.7$  % (DV-tail), 6.7 % (WW-lead) and 13.3 % (WW-tail) of all reads affiliated with the Chloroflexi phylum. None of those reads could be assigned further than to the phylum level. The deep-branching Chloroflexi phylum is ubiquitous and abundant in nature and man-made systems (Hugenholtz *et al.*, 1998). Due to the limited number of cultivated species exhibiting divergent physiologies it is difficult to predict the features of Chloroflexi related microorganisms detected in environmental samples such as in this study (Rappé and Giovannoni, 2003).

### **Candidate division TM7**

Candidate divisions/clusters represent microbial monophyletic groups that have not yet been isolated, cultured and described. The TM7 candidate phylum was moderately abundant in the DV-lead sample ( $12.5 \pm 4.6$  % relative abundance) and less abundant in the other membrane element samples (DV-tail  $0.5 \pm 0.2$  %, WW-lead 0.77 %, and WW-tail 5.7 %, respectively). TM7 representatives are widely distributed in terrestrial environments (e.g. soil, peat bog and rhizosphere), aquatic environments (e.g. hot springs, groundwater, freshwater, seawater and wastewater) and animals and humans (e.g. human oral cavity, termite guts and mammalian faeces) (Hugenholtz *et al.*, 2001; Dinis *et al.*, 2011), and they also have been detected in biofouled membranes (Pang and Liu, 2007, Ayache *et al.*, 2013). A first successful cultivation approach of an axenic TM7 culture was reported (Soro *et al.*, 2014). However, a detailed physiological description of any of the TM7 representatives is

still missing and the phylum remains a candidate phylum 'Candidatus Saccharibacteria'. Some information about this candidate phylum was obtained by culture independent approaches. Candidate division TM7 members have been associated with biofilm formation in the presence of high concentrations of silica and metal ions (Winsley *et al.*, 2014), similar to the conditions found in the membrane elements during operation (Table 3.1.) and the membrane surface as shown by membrane autopsies for fouling analyses (Beyer *et al.*, 2014).

### **Bacteroidetes**

Besides the Proteobacteria, the Bacteroidetes phylum was reported to be abundant in membrane biofilms from oxic feed water treating RO installations (Pang and Liu, 2007, Ayache *et al.* 2013, Al-Ashhab *et al.*, 2014). In the membrane elements analysed, the relative abundance of Bacteroidetes was generally very low (DV-lead  $0.7 \pm 0.2$  %, DV-tail  $2.7 \pm 0.4$  % and WW-lead 0.94 %), while moderate relative abundance was only observed for the WW-tail membrane element sample (14 %). In the WW-tail sample, the majority of the Bacteroidetes sequences grouped with the classes Bacteroidia (73.3% Bacteroidetes) and Flavobacteriia (23.9 %). The Bacteroidia were furthermore composed of the three families *Rikenellaceae*, *Marinilabiaceae* and *Porphyromonadaceae* (63.5 %, 23.8 % and 12.7 % Bacteroidia relative abundance, respectively). From those families, only the sequences of the *Porphyromonadaceae* could be further assigned to the *Paludibacter* genus (data not shown).

### **Planctomycetes**

The Planctomycetes phylum is ubiquitous in soil, sediments, fresh water and the oceans (Rappé and Giovannoni, 2003, Fuerst and Sagulenko, 2011) and are also found in biofouled membranes (Chen *et al.*, 2004, Pang and Liu, 2007, Bereschenko *et al.*, 2011, Lee and Kim, 2011). Members of the Planctomycetes phylum possess atypical bacterial features such as intracellular compartmentalization and a lack of peptidoglycan in their cell walls. Planctomycetes show a wide range of phenotypes and physiologies and remain largely unexplored (Rappé and Giovannoni, 2003, Fuerst and Sagulenko, 2011). The Planctomycetes showed a higher relative abundance in the WW installation (WW-lead 4.25 % and WW-tail 3.58 %) when compared to the DV installation (DV-lead 0.1 % and DV-tail 0.1 %). In all samples

the majority of Planctomycetes sequences were related to the Planctomycetia class (Table 3.2.). The vast majority of the Planctomycetia class reads was assigned to the *Planctomycetaceae* family (DV-lead  $73.6 \pm 13$  %, DV-tail  $50.3 \pm 8.7$  %, WW-lead 100 % and WW-tail 98.9 %). The remaining *Planctomycetaceae* sequences were assigned to the 'Candidate Brocadia' genus, with members that are known as chemoautotrophic anaerobic ammonium oxidizers 'Anammox' (Rappé and Giovannoni, 2003, Fuerst and Sagulenko, 2011).

### **Acidobacteria**

Members of this phylum are ubiquitous and abundant in nature (Barns *et al.*, 1999, Hugenholtz *et al.*, 1998) and have also been found on biofouled RO membranes treating oxic freshwater, seawater and wastewater (Chen *et al.*, 2004, Bereschenko *et al.*, 2011, Lee and Kim, 2011, Al-Ashab *et al.*, 2014). However, there are only a small number of cultured representatives, which show a diverse range of phenotypes and physiologies (Barns *et al.*, 1999). In the membrane elements analysed, the relative abundance of Acidobacteria was generally low (DV-lead 0.3 %, DV-tail 0.2 %, WW-lead 3.5 % and WW-tail 1.1 %).

### **Archaea**

Only from the DV-lead sample, archaeal diversity was determined in addition to the bacterial diversity (Supplementary Data S3.1., Supplementary Table S3.1.). The Archaea population was dominated by the Chrenarchaeota phylum (DV-lead: 65.3 % relative abundance), which was entirely composed of the Thermoprotei class. Only 6 % of those reads could be further assigned to the order of Desulfurococcales. Many Crenarchaeota are heterotrophic, anaerobic, sulfur-reducing hyperthermophiles (Anderson *et al.*, 2009) and therefore, their presence in the anoxic membrane elements is not surprising. The vast majority of the Euryarchaeota reads could not be further assigned than phylum level, and the rest of the reads (2.4 %) affiliated with the Methanomicrobia class. The Methanomicrobia class is known to embrace methanogenic Archaea. Methanogenesis spreads through seven orders of the phylum Euryarchaeota: Methanomassiliicoccales, Methanobacteriales, Methanococcales, Methanopyrales, Methanocellales, Methanomicrobiales, and Methanosarcinales, of which the latter two were detected in the sample analyzed.

### Dedicated anaerobes in anoxic membrane elements

Microbial communities differed substantially between installations or the position of the membrane elements within the installation and therefore an 'endemic' microbiome for anoxic groundwater treating nanofiltration membranes could not be determined. The differences in the microbial composition between lead and tail membrane elements can be explained by the change of the feed water qualities along a membrane filtration installation, where: i) nutrients and electron acceptors are consumed along the length of the installations, and ii) feed water is approximately five times more concentrated between lead and tail membrane elements, due to permeate production. It is likely that a shift from heterotrophs to lithotrophs (such as *Nitrospina*) occurs towards the tail membrane elements, where inorganic compounds are concentrated and easily biodegradable organic carbon is already consumed. The differences between the two installations cannot be explained by the plant design or operation, as both installations are similar in design (e.g. pretreatment, staging, membranes used) and operation (e.g. velocity, recovery, chemical addition, chemical cleaning) (Beyer *et al.*, 2014). Ayache *et al* (2013) observed that the microbial community that developed on the membranes was mainly determined by the feed water, not by the operating conditions. The main differences in the feed water source and quality are well depth, TOC and sulfate concentration. While DV is fed with water from a transitional aquifer (transitional zone between shallow and deep aquifer, well depth 33-35 m) with around 7 mg L<sup>-1</sup> TOC, the WW installation is fed with water from a deep aquifer (well depth 80-150m) with only 3 mg L<sup>-1</sup> TOC and up to 123 mg L<sup>-1</sup> sulfate (Table 3.1.).

Sequences affiliating with sulfate-reducing bacteria were abundant (Firmicutes genus *Desulfosporosinus*, Delta-Proteobacteria families Desulfobulbaceae, Desulfobacteraceae, Syntrophaceae), reflecting the strongly reducing conditions in the aquifers and membrane elements. Although the archaeal community appeared to consist of unknown biodiversity, methanogens have been detected (Supplementary Data S3.1.). The hypothesis made previously that the microbial community is composed of strict anaerobes (Beyer *et al.*, 2014), could be confirmed by our microbial community data.

Sequences affiliating with groups of nitrite-oxidizing bacteria (*Nitrospina* genus within the Nitrospinae phylum and the Nitrospirae phylum) as well as ammonia-oxidizing bacteria ('*Candidatus Brocadia*' genus within the Planctomycetes phylum) were abundant. This visualizes the importance of nitrogen cycling in the aquifers, but also on the membrane elements. Although considered an oxygen requiring process, there is some evidence that nitrite oxidation also occurs under anoxic conditions (Casciotti and Buchwald, 2012). It is thermodynamically feasible to use alternative electron acceptors such as Fe(III) or Mn(IV) for nitrite oxidation under oxygen-limiting conditions (Casciotti and Buchwald, 2012). However, it was questioned, whether nitrite oxidation indeed was the primary lifestyle of NOB (Daims et al., 2016). NOB remain a "big unknown" in the biogeochemical nitrogen cycle, which are understudied and difficult to cultivate in laboratory environments (Daims et al., 2016). The NOB community detected was complex (abundance of Nitrospirae and Nitrospinae in same membrane elements), indicating some metabolic flexibility that may result in niche specialization of NOB. Recent studies revealed a surprising ecophysiological versatility of NOB (Daims et al., 2016), possibly explaining the observed co-occurrence in the systems studied.

The majority of the bacterial and archaeal sequences detected grouped with environmental sequences and yet uncultured lineages. Accordingly, the physiological properties of those groups hardly can be predicted. Besides, the physiological properties cannot be determined from 16S rRNA gene analysis alone. Consequently, the prediction of the biofouling potential of a microbial community based on 16S rRNA comparative gene analysis remains difficult. Our data clearly show that the microbial communities developed in the NF membranes during anoxic groundwater filtration are very distinct from those generally found during the filtration of oxic waters. For example, the  $\alpha$ -,  $\beta$ -, and  $\gamma$ -Proteobacteria classes that typically dominate 'biofouling layers' were only detected in low relative abundance in our samples. The genus *Sphingomonas* that is a key inhabitant of 'biofouling layers', was not detected at all in this study. This likely is due to the anoxic nature of the feed waters, which are characterized by low concentrations of easily



biodegradable compounds and the absence of high energy yielding electron acceptors.

### 3.3.2. Conclusion and outlook

Here, NGS was used for the first time to investigate the microbial composition of biofilms that developed in NF installations that treat anoxic groundwater and do not suffer from extensive biofouling. We have shown that anoxic NF systems harbor distinct microbial communities that are different from the ones that are usually found in aerobic systems. Ecophysiological interpretations can only be speculated, as the majority of the biodiversity present affiliated with unknown and not yet cultivated taxonomic lineages, an observation on groundwater diversity also made by other authors (*Roeselers et al., 2015*). Culture based research approaches are needed to understand the physiology of the observed dominant phyla, and their contribution to the biofouling process.

### Acknowledgments

This work was performed at Wetsus, European Centre of Excellence for Sustainable Water Technology ([www.wetsus.nl](http://www.wetsus.nl)). Wetsus is funded by the Dutch Ministry of Economic Affairs, the European Union European Regional Development Fund, the Province of Fryslân, the city of Leeuwarden and by the EZ-KOMPAS Program of the 'Samenwerkingsverband Noord-Nederland'. The authors would like to thank the participants of the research theme 'Biofouling' for the fruitful discussions and their financial support, and in particular the water company 'Vitens', for the supply of the membrane elements and the possibility to perform the research presented in this manuscript. Research of AJMS is financed by ERC grant project 323009, and by Gravitation grant project 024.002.002 from the Netherlands Ministry of Education, Culture and Science.

## Supplementary data Chapter 3

### Supplementary data S3.1. - *Archaeal sequence analysis DV-lead*

In addition to the bacterial community analysis, the DV-lead sample was subjected to archaeal community analysis (n=1).

#### Archaeal diversity composition

For 16S rRNA gene based Archaea composition profiling, a method adapted from *Jaeggi, et al.* (2015) was employed. In short, barcoded amplicons of 16S rRNA genes were generated by PCR using the 340F (5'-CCCTAYGGGGYGCASCAG-3'; (*Gantner et al., 2011*)) that were 5'- extended with the titanium adaptor A and a 6 nt sample specific barcode extended, and 1000R (5'-GGCCATGCACYWCYTCTC-3'; (*Gantner et al., 2011*)) that was appended with the titanium adaptor B at the 5'-end.

PCRs were performed in a total volume of 50 µl containing 1 µl DNA, 200 nM of the forward and reverse primer, 1 U KOD Hot Start DNA Polymerase (Novagen, Madison, WI, USA), 5 µl KOD-buffer (10×), 3 µl MgSO<sub>4</sub> (25 mM), 5 µl dNTP mix (2 mM each), and 33 µl sterile water.

PCR conditions were: 95°C for 2 minutes followed by 35 cycles of 95°C for 20 s, 5°C for 10 s, and 70°C for 15 s. The approximately 660 bp PCR amplicon was subsequently purified using the MSB Spin PCRapace kit (Invitex) and the concentration was checked with a Nanodrop 1000 spectrophotometer (Thermo Scientific). Purified PCR products were mixed in equimolar amount by pooling 200 ng of the purified PCR products of each sample. The pooled sample was purified using the Purelink PCR Purification kit (Invitrogen), with high-cut-off binding buffer B3, and submitted for pyrosequencing on the 454 Life Sciences GS-FLX platform using Titanium sequencing chemistry (GATC-Biotech, Germany).

#### Pyrosequencing analysis

The pyrosequencing data was analysed with a workflow based on Quantitative Insights Into Microbial Ecology (QIIME) v1.2 (*Caporaso et al., 2010*), and reads were filtered for chimeric sequences using Chimera Slayer (*Haas et al., 2011*). OTU clustering was performed with settings as recommended in the QIIME newsletter of December 17th 2010 (<http://qiime.wordpress.com/2010/12/17/new-default->

parameters-for-uclost-otu-pickers/) using an identity threshold of 97b%. Diversity metrics were calculated as implemented in QIIME 1.2. Hierarchical clustering of samples was performed using UPGMA with weighted UniFrac as a distance measure as implemented in QIIME 1.2 (Caporaso *et al.*, 2010). The Ribosomal Database Project (RDP) classifier version 2.2 was performed for taxonomic classification (Cole *et al.*, 2009).

### Supplementary data – Figure S3.1.

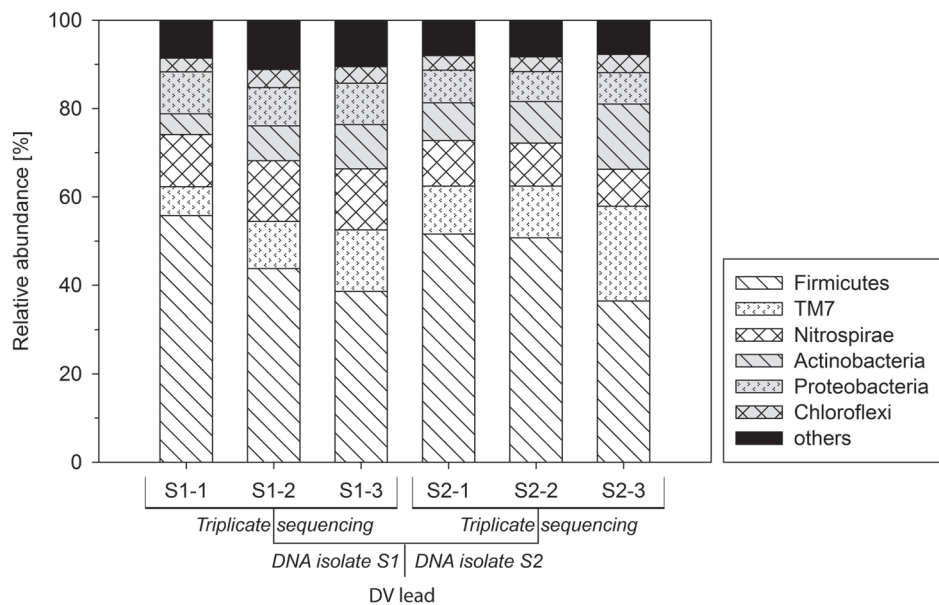


Figure S3.1. Reproducibility of sequence analysis using biological duplicates (S1 and S2) sequenced in triplicate. Relative abundance of the main bacterial phyla in DV-lead biofilm sample as revealed by 16S rRNA MiSeq sequence analysis.

## Supplementary data – Table S3.1.

Table S3.1. Archaea taxonomic assignment of the DV-lead sample

Phylum	Class	Order	Family	Genus	% Abundance
Crenarchaeota	Thermoprotei	unspec. class Thermoprotei	-	-	59.4
Crenarchaeota	Thermoprotei	Desulfurococcales	unspec. order Desulfurococcales	-	5.9
Euryarchaeota	unspec. phylum Euryarchaeota	-	-	-	16.3
Euryarchaeota	Methanomicrobia	unspec. class Methanomicrobia	-	-	1.7
Euryarchaeota	Methanomicrobia	Methanomicrobiales	unspec. order Methanomicrobiales	-	0.3
Euryarchaeota	Methanomicrobia	Methanosarcinales	unspec. order Methanosarcinales	-	0.2
Euryarchaeota	Methanomicrobia	Methanosarcinales	Methanosarcinaceae	<i>Methanosarcina</i>	0.2
unspec. domain Archaea	-	-	-	-	15.9

unspec. = unspecified

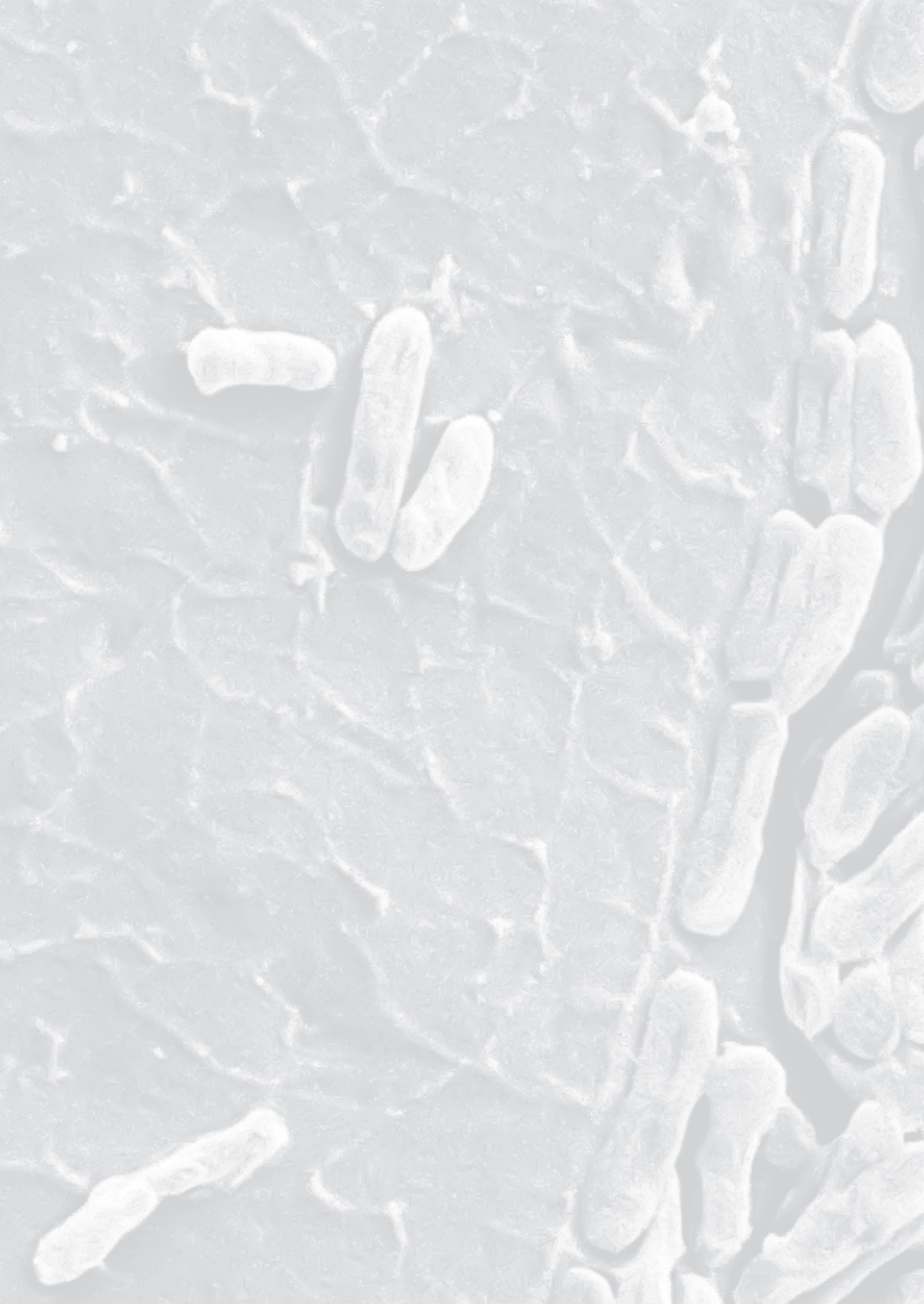
## References

- Anderson, I.J., Dharmarajan, L., Rodriguez, J., Hooper, S., Porat, I., Ulrich, L.E., Elkins, J.G., Mavromatis, K., Sun, H., Land, M. The complete genome sequence of *Staphylothermus marinus* reveals differences in sulfur metabolism among heterotrophic Crenarchaeota. *BMC Genomics*. 10:145 (2009).
- Al-Ashhab, A., Herzberg, M., Gillor, O. Biofouling of reverse-osmosis membranes during tertiary wastewater desalination: Microbial community composition. *Water Res.* 50: 341-349 (2014).
- Ayache, C., Manes, C., Pidou, M., Croué, J.P., Gernjak, W. 2013. Microbial community analysis of fouled reverse osmosis membranes used in water recycling. *Water Res.* 47: 3291-3299.
- Barka, E.A., Vatsa, P., Sanchez, L., Gaveau-Vaillant, N., Jacquard, C., Klenk, H.-P., Clément, C., Ouhdouch, Y., van Wezel, G.P. Taxonomy, physiology, and natural products of Actinobacteria. *Microbiol. Mol. Biol. Rev.* 80: 1-43 (2016).
- Barns, S.M., Takala, S.L., Kuske, C.R. Wide distribution and diversity of members of the bacterial kingdom acidobacterium in the environment. *Appl. Environ. Microbiol.* 65: 1731-1737 (1999).
- Bereschenko, L.A., Prummel, H., Euverink, G.-J.W., Stams, A.J.M., van Loosdrecht, M.C.M. Effect of conventional chemical treatment on the microbial population in a biofouling layer of reverse osmosis systems. *Water Res.* 45: 405-416 (2011).
- Beyer, F., Rietman, B.M., Zwijnenburg, A., van den Brink, P., Vrouwenvelder, J.S., Jarzembowska, M., Laurinoyte, J., Stams, A.J.M., Plugge, C.M. Long-term performance and fouling analysis of full-scale direct nanofiltration (NF) installations treating anoxic groundwater. *J. Membr. Sci.* 468: 339-348 (2014).
- Caporaso, J.G., Kuczynski, J., Stombaugh, J., Bittinger, K., Bushman, F.D., Costello, E.K., Fierer, N., Pena, A.G., Goodrich, J.K., Gordon, J.I., et al. QIIME allows analysis of high-throughput community sequencing data. *Nat. Methods*. 7: 335-336 (2010).
- Casciotti, K.L., Buchwald, C. Insights on the marine microbial nitrogen cycle from isotopic approaches to nitrification. *Front Microbiol.* 3:356 (2012).
- Chen, C.L., Liu, W.-T., Chong, M.L., Wong, M.T., Ong, S.L., Seah, H., Ng, W.J. Community structure of microbial biofilms associated with membrane-based water purification processes as revealed using a polyphasic approach. *Appl. Microbiol. Biotechnol.* 63: 466-473 (2004).
- Cole, J.R., Wang, Q., Cardenas, E., Fish, J., Chai, B., Farris, R.J., Kulam-Syed-Mohideen, A.S., McGarrell, D.M., Marsh, T., Garrity, G.M., Tiedje, J.M. The Ribosomal Database Project: improved alignments and new tools for rRNA analysis. *Nucleic Acids Res.* 37: 141-145 (2009).
- Daims, H., Lückner, S., Wagner, M. A new perspective on microbes formerly known as nitrite-oxidizing bacteria. *Trends Microbiol.* 24: 699-712 (2016).
- Danielopol, D.L., Pospisil, P., Rouch, R. Biodiversity in groundwater: A large-scale view. *Trends Ecol. Evol.* 15: 223-224 (2000).
- Dinis, J.M., Barton, D.E., Ghadiri, J., Surendar, D., Reddy, K., Velasquez, F., Chaffee, C.L., Lee, M.C., Gavrilova, H., Ozuna, H., Smits, S.A., Ouverney, C.C. In search of an uncultured human-associated TM7 bacterium in the environment. *PLoS ONE*. 6:e21280 (2011).
- Flemming, H.-C., Schaule, G., Griebe, T., Schmitt, J., Tamachkiarowa, A. Biofouling - The achilles heel of membrane processes. *Desalination*. 113: 215-225 (1997).

- Fuerst, J.A., Sagulenko, E. Beyond the bacterium: planctomycetes challenge our concepts of microbial structure and function. *Nat. Rev. Microbiol.* 9: 403-413 (2011).
- Gantner, S., Andersson, A.F., Alonso-Saez, L., Bertilsson, S. Novel primers for 16S rRNA-based archaeal community analyses in environmental samples. *J. Microbiol. Methods* 84: 12-18 (2011).
- Gomez-Smith, C.K., LaPara, T.M., Raymond, M. Hozalski, R.M. Sulfate reducing bacteria and Mycobacteria dominate the biofilm communities in a chloraminated drinking water distribution system. *Environ. Sci. Technol.* 49: 8432-8440 (2015).
- Griebe, T., Flemming, H.-C. Biocide-free antifouling strategy to protect RO membranes from biofouling. *Desalination.* 118: 53-156 (1998).
- Griebler, C., Lueders, T. Microbial biodiversity in groundwater ecosystems. *Freshwater Biol.* 54: 649-677 (2009).
- Gülay, A., Musovic, S., Albrechtsen, H.-J., Al-Soud, W.A., Sørensen, S.J., Smets, B.F. Ecological patterns, diversity and core taxa of microbial communities in groundwater-fed rapid gravity filters. *ISME J.* 10: 2209-2222 (2016).
- Haas, B.J., Gevers, D., Earl, A.M., Feldgarden, M., Ward, D.V., Giannoukos, G., Ciulla, D., Tabbaa, D., Highlander, S.K., Sodergren, E., et al. Chimeric 16S rRNA sequence formation and detection in Sanger and 454-pyrosequenced PCR amplicons. *Genome Res.* 21: 494-504 (2011).
- Hoehler, T.M., Jørgensen, B.B. Microbial life under extreme energy limitation. *Nat. Rev. Microbiol.* 11: 83-94 (2013).
- Hugenholtz, P., Goebel, B.M., Pace, N.R. Impact of culture-independent studies on the emerging phylogenetic view of bacterial diversity. *J. Bacteriol.* 180: 4765-4774 (1998).
- Hugenholtz, P., Tyson, G.W., Webb, R.I., Wagner, A.M., Blackall, L.L. Investigation of candidate division TM7, a recently recognized major lineage of the domain bacteria with no known pure-culture representatives. *Appl. Environ. Microbiol.* 67: 411-419 (2001).
- Huiting, H., Kappelhof, J.W.N.M., Bosklopper, T.G.J. Operation of NF/RO plants: from reactive to proactive. *Desalination.* 139: 183-189 (2001).
- Huson, D.H., Mitra, S., Weber, N., Ruscheweyh, H.-J., Schuster, S.C. Integrative analysis of environmental sequences using MEGAN 4. *Genome Res.* 21: 1552-1560 (2011).
- Jaeggi, T., Kortman, G.A., Moretti, D., Chassard, C., Holding, P., Dostal, A., Boekhorst, J., Timmerman, H.M., Swinkels, D.W., Tjalsma, H., et al. Iron fortification adversely affects the gut microbiome, increases pathogen abundance and induces intestinal inflammation in Kenyan infants. *Gut.* 64: 731-42 (2015).
- Kieft, T.L., Phelps, T.J. *The microbiology of the terrestrial deep subsurface.* Lewis Publishers: Boca Raton, FL. Chapter 9, *Life in the slow lane: activities of microorganisms in the subsurface.* 137-163 (1997).
- Labrenz, M., Banfield, J.F. Sulfate-reducing bacteria-dominated biofilms that precipitate ZnS in a subsurface circumneutral-pH mine drainage system. *Microbial Ecol.* 47: 205-217 (2004).
- Lee, J., Kim, I.S. Microbial community in seawater reverse osmosis and rapid diagnosis of membrane biofouling. *Desalination.* 273: 118-126 (2011).
- Lücker, S., Wagner, M., Maixner, F., Pelletier, E., Koch, H., Vacherie, B., Rattei, T., Damste, J.S.S., Spieck, E., le Paslier, D., Daims, H. A Nitrospira metagenome illuminates the physiology and

- evolution of globally important nitrite-oxidizing bacteria. *Proc. Natl. Acad. Sci. USA.* 107: 13479-13484 (2010).
- Lücker, S., Nowka, B., Rattei, T., Spieck, E., Daims, H. The genome of *Nitrospina gracilis* illuminates the metabolism and evolution of the major marine nitrite oxidizer. *Front. Microbiol.* 4:27 (2013).
- Nederlof, M.M., Kruithof, J.C., Taylor, J.S., van der Kooij, D., Schippers, J.C. Comparison of NF/RO membrane performance in integrated membrane systems. *Desalination.* 131: 257-269 (2000).
- Off, S., Alawi, M., Spieck, E. Enrichment and physiological characterization of a novel *Nitrospira*-like bacterium obtained from a marine sponge. *Appl. Environ. Microbiol.* 76: 4640-4646 (2010).
- Pang, C.M., Liu, W.-T. Community structure analysis of reverse osmosis membrane biofilms and the significance of Rhizobiales bacteria in biofouling. *Environ. Sci. Technol.* 41: 4728-4734 (2007).
- Paul D.H. Reverse osmosis: scaling, fouling & chemical attack. *Desal. Water Reuse.* 1: 8-II (1991).
- Peña, N., Gallego, S., del Vigo, F., Chesters, S.P. Evaluating impact of fouling on reverse osmosis membranes performance. *Desalin. Water Treat.* 51: 958-968 (2012).
- Rappé, M.S., Giovannoni, S.J. The uncultured microbial majority. *Ann. Rev. Microbiol.* 57: 369-394 (2003).
- Roeselers, G., Coolen, J., van der Wielen, P.W.J.J., Jaspers, M.C., Atsma, A., de Graaf, B., Schuren, F. Microbial biogeography of drinking water: patterns in phylogenetic diversity across space and time. *Environ. Microbiol.* 17: 2505-2514 (2017).
- Schneider, R.P., Ferreira, L.M., Binder, P., Bejarano, E.M., Góes, K.P., Slongo, E., Machado, C.R., Rosa, G.M.Z. Dynamics of organic carbon and of bacterial populations in a conventional pretreatment train of a reverse osmosis unit experiencing severe biofouling. *J. Membr. Sci.* 266: 18-29 (2005).
- Soro, V., Dutton, L.C., Sprague, S.V., Nobbs, A.H., Ireland, A.J., Sandy, J.R., Jepson, M.A., Micaroni, M., Splatt, P.R., Dymock, D., Jenkinson, H.F. Axenic culture of a candidate division TM7 bacterium from the human oral cavity and biofilm interactions with other oral bacteria. *Appl. Environ. Microbiol.* 80: 6480-6489 (2014).
- van Kessel, M.A.H.J., Speth, D.R., Albertsen, M., Nielsen, P.H., op den Camp, H.J.M., Kartal, B., Jetten, M.S.M., Lücker, S. Complete nitrification by a single microorganism. *Nature.* 528: 555-559 (2015).
- van den Broek, W.B.P., Boorsma, M.J., Huiting, H., Dusamos, M.G., van Agtmaal S. Prevention of Biofouling in Industrial RO Systems: Experiences with Peracetic Acid, *Water Sci. Technol.* 5(2): I-II (2010).
- Winsley, T.J., Snape, I., McKinlay, J., Stark, J., van Dorst, J.M., Ji, M., Ferrari, B.C., Siciliano, S.D. The ecological controls on the prevalence of candidate division TM7 in polar regions. *Front. Microbiol.* 5: 345 (2014).







# Chapter 4

## **Membrane fouling and chemical cleaning in three full-scale reverse osmosis plants producing demineralized water**

Florian Beyer, Judita Laurinonyte, Arie Zwijnenburg, Alfons J. M. Stams, Caroline M. Plugge

This chapter is adapted from:  
Beyer, F., Laurinonyte, J., Zwijnenburg, A., Stams, A.J.M., Plugge, C.M.  
Membrane fouling and chemical cleaning in three full-scale reverse osmosis plants producing demineralized water.  
J. Eng. 2017: 1-14 (2017).

## Abstract

Membrane fouling and cleaning were studied in three reverse osmosis (RO) plants. Feed water was secondary wastewater effluent, river water, and surface water. Membrane autopsies were used for fouling characterization. Fouling layer measurements included total organic carbon (TOC), adenosine triphosphate, polysaccharides, proteins, and heterotrophic plate counts. In all locations, membrane and spacer fouling was (bio)organic. Plant chemical cleaning efficiencies were evaluated from full-scale operational data and cleaning trials in a laboratory setup. Standard cleaning procedures were compared to two cleaning procedures specifically adapted to treat (bio)organic fouling using commercial blend cleaners (mixtures of active substances). The three RO plants were impacted by irreversible foulants causing permanently decreased performance in normalized pressure drop and water permeability even after thorough chemical cleaning. The standard plant and adapted cleaning procedures reduced the TOC by 45 % on average, 80 %. In general, around 20 % higher biomass removal could be achieved with adapted procedure I compared to adapted procedure II. TOC measurements and SEM showed that none of cleaning procedures applied could remove foulants completely from the membrane elements. This study underlines the need for novel cleaning approaches targeting resistant foulants, as none of the procedures applied resulted in highly effective membrane regeneration.

## 4.1. Introduction

High-pressure driven reverse osmosis (RO) membrane filtration is capable of generating large amounts of ultrapure water for industrial applications. The excellent removal capacity of contaminants, decreasing prices for membranes, and enhanced membrane lifetimes led to widespread acceptance and popularity of RO.

One of the major concerns in the operation of RO plants is reduced membrane performance by fouling. Biofouling, the most common form of membrane fouling, is the type of fouling that is the hardest to control (*Paul 1991, Flemming et al., 1997, Peña et al., 2012*). An increase of the normalized feed channel pressure drop (NPD) over the feed spacer channel, a decrease in the normalized specific water permeability ( $K_w$ ), and/or changes in salt retention are common operational key

performance indicators that show fouling development in full-scale applications (Nederlof *et al.*, 2000, Huiting *et al.*, 2001, Peña *et al.*, 2012). Rapid biofouling typically manifests in the lead modules of the first stage, causing a strong increase in NPD and moderate decrease in  $K_w$  (Nederlof *et al.*, 2000, Huiting *et al.*, 2001, Peña *et al.*, 2012), while slow biofouling may manifest throughout the whole installation (Huiting *et al.*, 2001). Rarely, biofouling manifests in other parts of the installation, such as the tail elements of the last stage (Vrouwenvelder *et al.*, 2010).

To overcome the fouling problems, chemical cleaning in place (CIP) is applied to restore the original RO performance in terms of NPD,  $K_w$ , and normalized salt rejection capacity. Generally applied acid-base CIPs often fail to fully restore RO performance and to remove all deposits from the membrane elements (Vrouwenvelder *et al.*, 1998, Huiting *et al.*, 2001, Beyer *et al.*, 2014). If the membrane performance cannot be restored up to a specifically defined level (e.g. permanently increased NPD by > 15 % after CIP), the RO plant will continuously operate with fouling problems.

CIP efficiencies strongly depend on chemical reactions between foulants and membrane surface, as well as the reactions between foulants and chemicals, which include hydrolysis, peptization, saponification, solubilization, dispersion, and chelation (Chen *et al.*, 2003, Ang *et al.*, 2006, Garcia-Fayos *et al.*, 2015). There are several categories of cleaning agents such as alkaline solutions, acids, metal chelating agents, surfactants, enzymes, and oxidizing agents. Additionally, commercial blends of chemical active substances are available, but manufacturers often do not reveal the precise composition (Ang *et al.*, 2006). Chemical cleaning agents act specifically and the choice of the CIP procedure should depend on the fouling composition of the individual RO plant. Alkaline solutions, for instance, remove organic foulants on membranes through hydrolysis and consecutive solubilization. Metal chelating agents specifically remove divalent cations from complex molecules (e.g. extracellular polymeric substances (EPS)) and as such weaken the structural integrity of the fouling layer matrix. Surfactants solubilize macromolecules by forming micelles around them, thereby facilitating the removal of foulants from the membrane surface (Ang *et al.*, 2006). Acid cleaning dissolves

scaling (Mo *et al.*, 2010) and destroys the cell wall integrity of microorganisms and also precipitates proteins. Oxidizing agents, such as hydrogen peroxide, are able to oxidize natural organic matter (NOM), act as biocide (Linley *et al.*, 2012), and can increase hydrophilicity by increasing the amount of oxygen-containing functional groups such as carboxyl and phenolic groups (Liu *et al.*, 2001).

Operational parameters such as duration, temperature, shear stress, and pressure also have a significant influence on cleaning efficiency (Ang *et al.*, 2006, zum Kolk *et al.*, 2013, Garcia-Fayos *et al.*, 2015). Short filtration cycles (i.e. more frequent but shorter cleaning procedures) are beneficial, as the fouling layers become more compact with time and become more difficult to remove (Chen *et al.*, 2003, Goode *et al.*, 2013). In general, cleaning efficiency increases with temperature, but the heat tolerance of membranes must be considered (Liikanen *et al.*, 2002).

In this study, fouling and membrane cleaning was investigated at three full-scale plants producing demineralized water by RO from extensively pretreated feed water. Membrane fouling layers from the three locations were studied and extensively characterized. Efficiencies of full-scale CIP of persistent and harsh fouling layers were evaluated from membrane performance data and during laboratory membrane cleaning experiments. Two (bio)organic fouling specific adapted cleaning procedures (AP I and II), using commercial blend cleaners, were tested and compared with the respective standard plant cleaning procedures (PP) in a laboratory cleaning setup.

The aim of this study was to determine the limitations of conventional chemical cleaning with persistent and harsh bio(organic) fouling layers developed during long-term operation.

## **4.2. Materials and methods**

### **4.2.1. RO plants characteristics and membrane elements used**

Membrane and spacer materials for this study (Table 4.1.) were taken from fouled spiral-wound membrane elements from three different RO filtration plants producing demineralized water from secondary wastewater effluent, river water, and surface water (RO location I (Sas van Gent, Netherlands), location II (Dordrecht,

Netherlands), and location III (Veendam, Netherlands), resp.). A description and schematic representation of the plant designs and pretreatment can be found in *Supplementary data S4.1*. The operational history and specifications of the membrane elements are summarized in *Table 4.1*.

*Table 4.1.* Specification and operational history of the membrane elements used in this study

	Location I	Location II	Location III
Location	Sas van Gent, The Netherlands	Dordrecht, The Netherlands	Veendam, The Netherlands
Feed water	Secondary waste water effluent	River water	Surface water
Membrane element	DOW Filmtec BW30XFR-400/34i	DOW Filmtec LE-440i	DOW Filmtec LE-440i
Membrane configuration & type	Spiral wound thin-film composite	Spiral wound thin-film composite	Spiral wound thin-film composite
Spacer thickness [mil / $\mu\text{m}$ ]	34 / 864	28 / 711	28 / 711
Active membrane area [ $\text{m}^2$ ]	37	41	41
CIP frequency	~ 17 year <sup>1</sup>	~ 17 year <sup>1</sup>	~ 7 year <sup>1</sup>
Days of operation [elements]	644 / 652 <sup>a</sup>	1056	1057
Days since last CIP	33 / 2 <sup>a</sup>	15	20

1 mil = 0.001 inch = 25.4  $\mu\text{m}$

<sup>a</sup>) From this installation two membrane elements were autopsied, one before last full-scale CIP and one after last full-scale CIP

#### 4.2.2. Membrane cleaning and performance in full-scale

Full-scale operational performance data, normalized pressure drop (NPD), normalized specific water permeability ( $K_w$ ), and normalized salt rejection, were calculated as described by (Huiting *et al.*, 1999, Beyer *et al.*, 2014).

The CIPs applied in all three installations (*Table 4.2*) are essentially a high pH cleaning step followed by a low pH cleaning step. However, there are differences in the circulation and soaking times. The total duration of the CIPs varies from 6.5 to 24 hours between locations (*Table 4.2*). At locations II and III, the low pH cleaning is performed with a commercial mixed acid detergent, intended to improve foulant solubility. At location III, which has been extensively studied for its biofouling problems (Bereschenko *et al.*, 2007, Bereschenko *et al.*, 2008, Bereschenko *et al.*, 2010, Bereschenko *et al.*, 2011), sodium bisulfite is used during the high pH cleaning in order to achieve anoxic conditions and improved microbial inactivation. The volumetric flow rate during cleaning at all locations is 9  $\text{m}^3 \text{h}^{-1}$  for each membrane vessel in the first stage. However, as location I uses membrane elements with a thicker feed spacer (34 mil / 864  $\mu\text{m}$ ) than locations II and III (28 mil / 711  $\mu\text{m}$ ) (*Table 4.1*), linear flow velocity in the lead membrane element during CIP is lower at location I (0.184  $\text{m s}^{-1}$  for location I and 0.202  $\text{m s}^{-1}$  for locations II and III) (*Table 4.2*).

Table 4.2. Chemical cleaning in place (CIP) procedures applied at the three locations studied

	Location I	Location II	Location III
Location	Sas van Gent, The Netherlands	Dordrecht, The Netherlands	Veendam, The Netherlands
Linear flow velocity	0.184 m s <sup>-1</sup>	0.202 m s <sup>-1</sup>	0.202 m s <sup>-1</sup>
Feed pressure	1 bar	1 bar	1 bar
Total duration	8 hours	24 hours	6.5 hours
Step 1	Circulation with NaOH 60 min; T=35°C; pH = 12	Circulation with NaOH; 120min; T=35°C; pH = 12	Pre-rinsing with demi water
Step 2	Soaking with NaOH 30 min; T=35°C; pH = 12	Soaking (overnight) with NaOH T=20°C; pH = 12	Soaking with demi water 30min
Step 3	Circulation with NaOH 60 min; T=35°C; pH = 12	Rinsing with demi water	NaHSO <sub>3</sub> ; pH=10.5 (adjust pH with NaOH); 60min; T=35°C; C=1-1.5% v/v
Step 4	Soaking with NaOH 30 min; T=35°C; pH = 12	Circulation with Divos 2 90min; T=35°C; pH = 1.6	Soaking with NaHSO <sub>3</sub> 120min; T=20°C; pH = 10.5
Step 5	Circulation with NaOH 60 min; T=35°C; pH = 12	Final rinsing with demi water	Rinsing with demi water
Step 6	Soaking with NaOH 30 min; T=35°C; pH = 12		Divos 2 30min; T=35°C; pH = 2.5
Step 7	Rinsing with demi water		Soaking with Divos 2 60min; T=20°C; pH = 2.5
Step 8	Circulation with HCl 60 min; T=35°C; pH = 2.1		Final rinsing with demi water
Step 9	Soaking with HCl 30 min; T=35°C; pH = 2.1		
Step 10	Circulation with HCl 60 min; T=35°C; pH = 2.1		
Step 11	Soaking with HCl 30 min; T=35°C; pH = 2.1		
Step 12	Final rinsing with demi water		

demi water = demineralised water (RO permeate); Divos 2 = mixed acid detergent descaler (JohnsonDiversey, UK)

#### 4.2.3. Protocol for chemical cleaning at laboratory-scale

Two short (3 and 4.5 hours) adapted cleaning procedures (AP I and AP II) with commercial blend cleaners (Table 4.3.) were benchmarked against the individual plant CIP procedures (PP) (Table 4.2.). AP I and AP II protocols are shown in Table 4.3.. AP I (Table 4.3.) was carried out with low pH acid, surfactant-based, liquid detergent cleaner ((P3-Ultrasil 73), containing citric acid (10 – < 20 %), L-(+)-lactic acid (5 – < 10 %), and alkyl-aryl-sulfonic acid (3 – < 5 %)), enzymatic cleaner ((P3-Ultrasil 53) containing unspecified proteases, tetrasodium-EDTA (~35 – < 50 %), and phosphates (20 – < 30 %)), and sanitizing cleaner ((P3-oxonia active) containing acetic acid (8 %), peroxyacetic acid (5.8 %), and hydrogen peroxide (27.5 %)). AP II (Table 4.3.) was performed with alkaline cleaner ((P3-Ultrasil I10) containing NaOH



(7 %), tetrasodium-EDTA (5 – 20 %), and benzenesulfonic acid (2 – 10 %) and the same acid, surfactant-based, liquid detergent (P3-Ultrasil 73) as in AP I. All information about cleaner compositions was deduced from their respective MSDS datasheets.

Table 4.3. CIP procedures for (bio)organic fouling removal at laboratory scale.

	Adapted procedure (AP) I	Adapted procedure (AP) II
Feed pressure	1 bar	1 bar
Total duration	4.5 hours	3 hours
Step 1	Pre-rinsing with demi water	Pre-rinsing with demi water
Step 2	Acid - P3-ultrasil 73 45 min; T=45°C; C=1.5% v/v; pH = 2.5	Alkaline - P3-ultrasil 110 30 min; T=30°C; C=1.5% v/v; pH = 12.1-12.3
Step 3	Rinsing with demi water	Rinsing with demi water
Step 4	Neutral - P3-ultrasil 53 90 min; T=37°C; C=1.5% w/v; pH = 9.6-10	Acid-P3-ultrasil 73 30 min; T=45°C; C=1% v/v; pH = 2.5
Step 4	Neutral - P3-ultrasil 53 30 min; T=30-45°C; C=4% w/v; pH = 8-10	Rinsing with demi water
Step 5	Rinsing with demi water	Alkaline-P3-ultrasil 110 30 min; T=35°C; C=0.8% v/v; pH = 11.6-11.8
Step 6	Sanitizing - P3-oxonia active 60 min; T <sub>max</sub> =25°C; C=1% v/v	Final rinsing with demi water
Step 7	Final rinsing with demi water	

demi water = demineralised water

#### 4.2.4. High-pressure test cell

A flat sheet high-pressure crossflow cell (University of Twente, Netherlands), consisting of two stainless steel metal plates, was used for the laboratory experiments. Flow chamber spatial dimensions were  $w \cdot l \cdot h = 12.7 \text{ cm} \cdot 19.8 \text{ cm} \cdot 0.3 \text{ cm}$ . Flow channel height was adjusted to the respective spacer thickness (Table 4.1) with solid plastic spacers. Permeate is collected through a porous aluminum sintered plate. Feed water is distributed by a cylindrical flow distribution channel and concentrate is collected in similar manner. Separate channels at feed and concentrate side are used to measure the feed-concentrate pressure drop. The flow

cell was successfully employed in previous biofouling studies (*Bereschenko et al., 2010, Bereschenko et al., 2011*).

#### **4.2.5. High-pressure filtration setup**

A high-pressure laboratory filtration setup (*Supplementary Figure S4.1*) was used to determine key performance indicators, water permeability ( $K_w$ ), feed-concentrate channel pressure drop (FCP), and salt rejection capacity.

The setup is operated at constant pressure and flow; thus permeability decrease is detected by reduced permeate flow. The setup is fed with cartridge filtered (Borso-Spun PP 10  $\mu\text{m}$ , Van Borselen Filters B.V., Zoetermeer, Netherlands) drinking water from a buffer tank. A frequency controlled high-pressure pump (Hydra-Cellpump, Wanner Engineering Inc., Minneapolis, USA) is used to pressurize the feed water to 6 bar. Constant pressure is achieved using a pressure controller (EL-PRESS, P-702C-AGB-020A, digital pressure meter/controller, Bronkhorst High-Tech, Ruurlo, Netherlands), located in a bypass over the high-pressure feed pump. Stable flow is maintained using a flow controller (CORI-FLOW, M55C4-AGD-44-K-C, digital mass flow meter/controller, Bronkhorst High-Tech, Ruurlo, Netherlands). Feed-concentrate channel pressure drop is assessed with an accurate differential pressure meter Cerabar T, 0 – 500 mbar (+/- 0.1 mbar) (Endress+Hauser, Reinach, Switzerland). Permeate production is measured using a flow meter (LIQUI-FLOW, L23-AGB-33-0, digital mass flow meter, Bronkhorst High-Tech, Ruurlo, Netherlands). All data is registered and stored using a data logger (RSG30, Endress+Hauser, Reinach, Switzerland).

#### **4.2.6. Data normalization from laboratory-scale cleaning experiments**

FCP was directly measured. Water permeability ( $K_w$ ) and water flux ( $J_w$ ) were derived as described in (*Dreszer et al., 2013*). During the experiments, temperature was maintained at 20 °C.  $K_w$ , FCP, and salt rejection cleaning efficiencies are presented as % improvement.

#### **4.2.7. Membrane cleaning setup**

A low-pressure setup (*Supplementary Figure S4.2*) was used to perform the chemical cleaning experiments on laboratory scale. The cleaning setup consists of a thermo-



controlled vessel (JULABO P 1000W and JULABO VC 1050W, Juchheim Labortechnik KG, Seelbach/West Germany) containing 8 L of cleaning agent. The cleaning agent is pumped into the test cell using a high velocity peristaltic pump (Masterflex L/S pumps, Cole- Palmer Instrument Company, Vernon Hills, Illinois, USA). A manometer is placed between the pump and the test cell. During chemical cleaning, permeate production is prevented by blocking the permeate channel outlet. Cleaning agent is filtered using a 10  $\mu\text{m}$  pore size cartridge filter (Borso-Spun PP 10  $\mu\text{m}$ , Van Borselen Filters BV, Zoetermeer, Netherlands) to reject removed foulants, before being recycled to the cleaning vessel. Flow is adjusted using a manual flow controller (Brooks 8805, Brooks Instrument, Hatfield, USA). Temperature is measured using a PT 100 temperature sensor (S + S Regeltechnik GmbH, Nürnberg, Germany).

#### 4.2.8. Cleaning procedures and assessment of cleaning effectiveness

Chemical cleaning studies were performed in the laboratory membrane cleaning setup (*Supplementary Figure S4.2.*) with fouled sheets of membrane and spacer material from full-scale operation. The fouled membrane elements were autopsied as described by Beyer *et al.* (2014) and sheets of fouled membrane and spacer material were cut and stored in tap water at 4 °C for cleaning experiments.

Cleaning efficiencies of the fouled membrane and spacer sheets were assessed using the key performance indicators FCP,  $K_w$ , and salt rejection and deposit measurements such as total organic carbon (TOC), adenosine triphosphate (ATP), colony-forming units (CFU), scanning electron microscopy (SEM), and energy dispersive X-ray spectroscopy (EDS) measurements.

For fouling characterization of the full-scale membrane elements, protein and polysaccharide quantification was applied in addition to TOC, ATP, CFU, SEM, and EDS measurements.

Key performance indicators FCP,  $K_w$ , and salt rejection were assessed using the high-pressure filtration setup.

### 4.2.9. Analytical methods

TOC, ATP, SEM, and EDS measurements were performed as described by Beyer *et al.* (2014). For protein and polysaccharide quantification, biofilms were harvested and homogenized as described in (Dreszer *et al.*, 2013). Homogenates were subsequently centrifuged at  $3,000 \times g$  for 10 min, at room temperature, to remove debris. Protein concentration and polysaccharide concentrations in the supernatant were then determined as described by (Dreszer *et al.*, 2013).

Bacterial cell counts were performed using a CFU measurement. Biomass was scraped off the membrane ( $\sim 15 - 20 \text{ cm}^2$  surface area) and dissolved in 1 – 1.5 mL of PBS. The sample was then homogenized using vortex mixing, before serial dilutions ( $10^{-1}$  to  $10^{-7}$ ) were prepared. Dilutions  $10^{-4}$  to  $10^{-7}$  were plated in duplicate on R2A agar plates (Difco). Plates were standing upright for 30 min and then were incubated upside down at  $25 \text{ }^\circ\text{C}$  for 7 days. Colonies were counted according to ISO 8199. CFU per  $\text{cm}^2$  membrane area was then calculated.

## 4.3. Results and discussion

### 4.3.1. Full-scale operation: effect of fouling on performance (NPD and $K_w$ ) and CIP efficiencies

#### Location I (Sas van Gent, Netherlands)

Fouling causes increased NPD and decreased  $K_w$  in both stages of the installation (Figure 4.1.). Starting in summer, NPD increases rapidly in both stages, and while  $K_w$  can be kept stable with CIPs applied, it is permanently reduced ( $\sim -10 \%$ , first stage;  $\sim -15 \%$ , second stage). The rapid increase in NPD and decrease in  $K_w$  in the summer and autumn months (Figure 4.1.) are likely due to the increased temperature of the effluent during this period. The cleaning frequency was 17 times in one year (Figure 4.1. and Table 4.1.). In summer months, the conventional CIPs applied do not restore the NPD and, after several CIPs, NPD increases to about 30 – 40 % (Figure 4.1.) of day zero values.

Two lead elements from the first stage, one before last full-scale CIP and one after the last full-scale CIP, were autopsied for fouling analyses and to evaluate representativeness of the laboratory cleaning setup. At the time of membrane autopsies for cleaning studies (before last CIP applied in Figure 4.1.), NPD was

increased in both stages ( $\sim + 10\%$ , first stage, and  $\sim + 25\%$ , second stage) and  $K_w$  was reduced in both stages ( $\sim - 15\%$ , first stage, and  $\sim - 20\%$ , second stage). The last CIP applied resulted in some reduction in NPD in the first stage, while NPD in the second stage and  $K_w$  in both stages were not affected much (Figure 4.1).

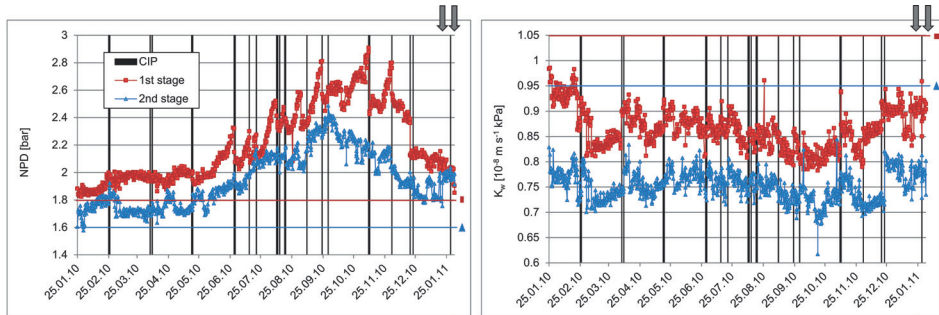


Figure 4.1. Performance parameters NPD (left panel) and  $K_w$  (right panel) of plant location I (Sas van Gent, The Netherlands). The vertical lines indicate chemical cleanings in place (CIP). Horizontal lines indicate performance with new membranes [day zero]. From this installation a lead element from the first stage was taken before (25.01.2011) and directly after the last CIP indicated (02.02.2011).

### Location II (Dordrecht, Netherlands)

Fouling causes a strong increase in NPD in the first stage and  $K_w$  reductions in the plant during the summer months (Figure 4.2.) and cleaning frequency was 17 times in one year (Figure 4.2. and Table 4.1.). At this location,  $K_w$  is not determined separately for the first and second stages but only as overall plant  $K_w$ .

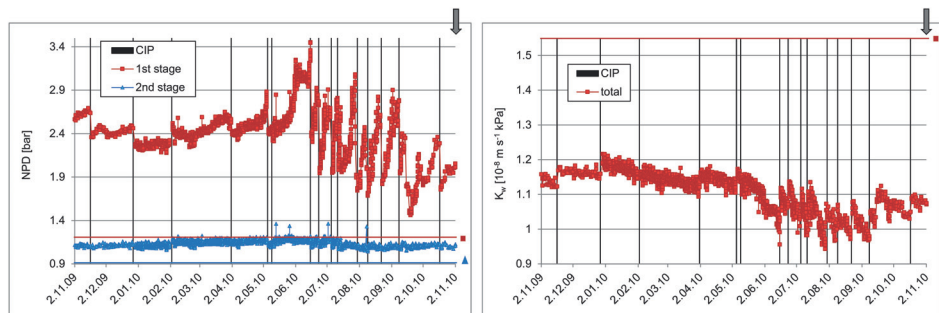


Figure 4.2. Performance parameters NPD (left panel) and  $K_w$  (right panel) of plant location II (Dordrecht, The Netherlands). The vertical lines indicate chemical cleanings in place (CIP). Horizontal lines indicate performance with fresh membrane [day zero]. Directly after the last data point (02.11.2010) a lead membrane element from the first stage was autopsied, analyzed and used for laboratory membrane cleaning studies.

Looking at the NPD and  $K_w$  efficiencies from both stages (*Figure 4.2.*), the overall plant  $K_w$  reduction is expected to originate mainly from the NPD increase in the first stage. NPD in the first stage and  $K_w$  are affected by rapid fouling especially in the summer and autumn months, requiring more frequent cleaning. In the winter and spring months, NPD increase and  $K_w$  decrease are slower and can be kept relatively stable with the CIPs applied (*Figure 4.2.*). In general, the CIPs applied were only partly effective, causing the installation to operate constantly with reduced  $K_w$  and increased NPD in the first stage.

A lead element from the first stage was autopsied for fouling analyses and laboratory cleaning experiments. At the moment of the membrane autopsies, NPD was strongly increased ( $\sim + 50 \%$ ) in the first stage and the overall plant  $K_w$  was reduced substantially ( $\sim - 30 \%$ ).

### **Location III (Veendam, Netherlands)**

Fouling is characterized by strong NPD increase in the second stage and a temporary  $K_w$  decrease, which is stronger in the second stage (*Figure 4.3.*). NPD and  $K_w$  are affected by rapid fouling especially in the summer and autumn months, requiring more frequent cleaning. In the winter and spring months, NPD increase and  $K_w$  decrease are less rapid and can be kept relatively stable with the CIPs applied (*Figure 4.3.*). Increased NPD in the second stage is main reason for CIPs applied, leading to a cleaning frequency of seven times in one year (*Figure 4.3.* and *Table 4.1.*). CIPs applied (*Table 4.2.*) are only partly effective, causing the installation to operate constantly with reduced  $K_w$  and increased NPD in the second stage of the installation.

A lead element from the first stage was autopsied for fouling analyses and laboratory cleaning experiments. At the moment of the membrane autopsies, NPD ( $\sim + 20 \%$ ) and  $K_w$  ( $\sim - 15 \%$ ) values in the first stage were only moderately affected (*Figure 4.3.*).

The conventional CIPs applied (*Table 4.2.*) were not successful under all circumstances, especially during summer months (*Figures 4.1. - 4.3.*). The efficiency of CIPs applied differed from case to case (*Figures 4.1. - 4.3.*), indicating that cleaning efficiency cannot always be predicted from previous experience. This could likely be

due to, for example, seasonal changes in the fouling layers and changes in feed water quality when processing, for example, industrial wastewater. All installations permanently operate suboptimally (Figures 4.1 – 4.3.). Foulants that could not be removed by previous conventional CIPs (day zero performance is indicated by horizontal lines in Figures 4.1 – 4.3.) had been built up after extended periods of operation (644, 1056, and 1057 days (Table 4.1.) in locations I, II, and III, resp.).

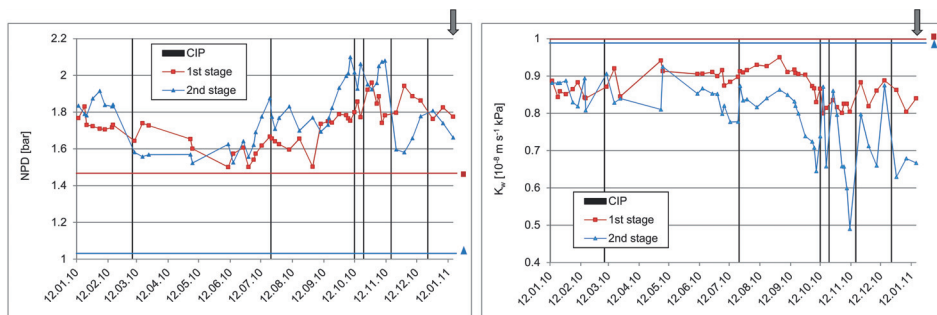


Figure 4.3. Performance parameters NPD (left panel) and  $K_w$  (right panel) of plant location II (Veendam, The Netherlands). The vertical lines indicate chemical cleanings in place (CIP). Horizontal lines indicate performance with fresh membrane [day zero]. Directly after the last data point (12.01.2011) a lead membrane element from the first stage was autopsied, analyzed and used for laboratory membrane cleaning studies.

#### 4.3.2. Full-scale operation: effect of CIP on membrane integrity (salt rejection)

The chemical resistance of the membranes (illustrated by the free chlorine resistance  $< 0.1$  ppm, *Supplementary Table S4.1.*) limits some of the cleaning parameters (e.g. choice of the cleaning agent, concentration, and temperature). Oxidative damage by single or repetitive harsh CIPs will lead to decreased salt rejection of the membranes. Oxidative damage was diagnosed in  $\sim 15$  % (severe damage) to  $\sim 50$  % (slight damage) of all membranes analyzed in a big study of 500 autopsied membrane elements (Peña *et al.*, 2012). All three plants produce demineralized water and therefore membrane integrity as indicated by stable and high salt rejection is a key performance parameter. The effects of the CIP on overall normalized salt rejection of the three locations are illustrated in Figures 4.4. A - C.

At location I, normalized salt rejection is relatively stable at about 99.5 %. Some of the CIPs have a slightly negative effect on normalized salt rejection, but this effect

does not seem to be permanent (*Figure 4.4. A*). At location I, the CIPs applied do not have a negative effect on membrane integrity.

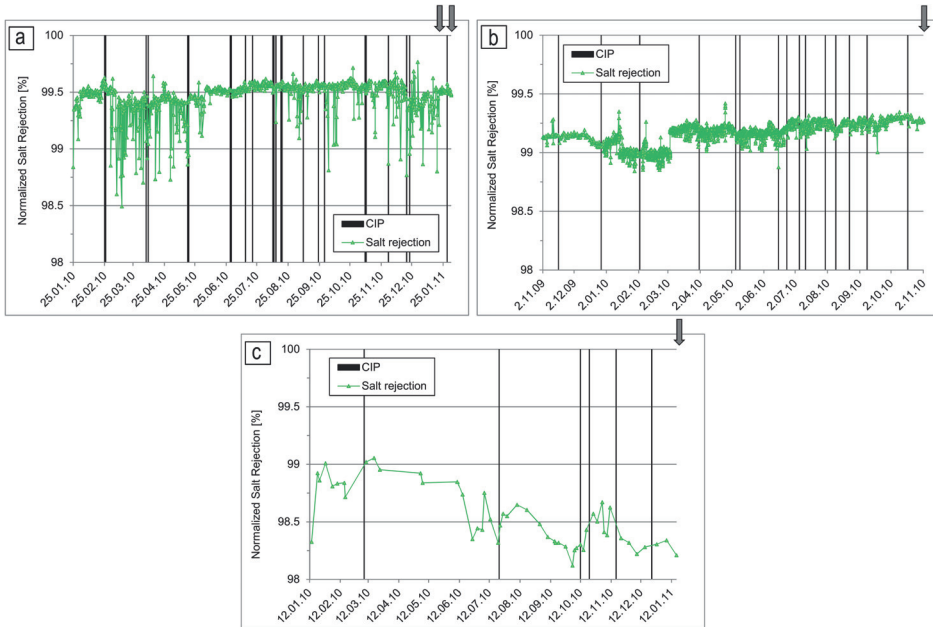


*Figure 4.4.* Membrane integrity as indicated by % salt rejection (= 100 – salt passage) for a) plant location I, b) plant location II and c) plant location III. Vertical lines indicate CIP. Time points of membrane autopsies are indicated with dark grey arrows.

At plant location II, normalized salt rejection was largely unaffected by fouling or CIP in the last 8 months before membrane autopsies (*Figure 4.4. B*). Only in January and February (before sampling), salt rejection was about 0.25 % lower which was restored in March. The effect could not be deduced from the  $K_w$  measurements and remains unexplained.

At location III, normalized salt rejection is unstable and decreases throughout the year by about 0.7 %. It is not clear from *Figure 4.4. C* whether the decreased normalized salt rejection is due to the CIPs applied or other factors such as ageing of the membranes. However, membrane age is similar to location II (*Table 4.1.*) and if normalized salt rejection drops below 98 %, membrane replacement may be unavoidable at location III.

### 4.3.3. Membrane fouling characterization by membrane autopsies of full-scale membrane elements

(Bio)organic material was the major foulant found during the fouling layer analyses by EDS in all installations studied. Inorganic compounds were typically below 0.6 at% in all samples analyzed. A representative EDS spectrum with related elemental analyses of locations I, II, and III can be found in *Supplementary data S4.3*. The (bio)organic origin of the fouling layers could already be deduced from the observations made during autopsies, when fouling layers could be removed by soft mechanical force leaving a smooth membrane surface. An inorganic precipitation or scaling layer in contrast would reveal a sandpaper-like structure on the membrane surface. Furthermore, at location III, biofouling was reported in earlier studies and several biofouling key studies were performed at this location (*Bereschenko et al., 2007, Bereschenko et al., 2008, Bereschenko et al., 2010, Bereschenko et al., 2011*). To differentiate between organic fouling and biological fouling, TOC, polysaccharides, proteins, and CFU measurements (*Figure 4.5.*) and SEM were performed.

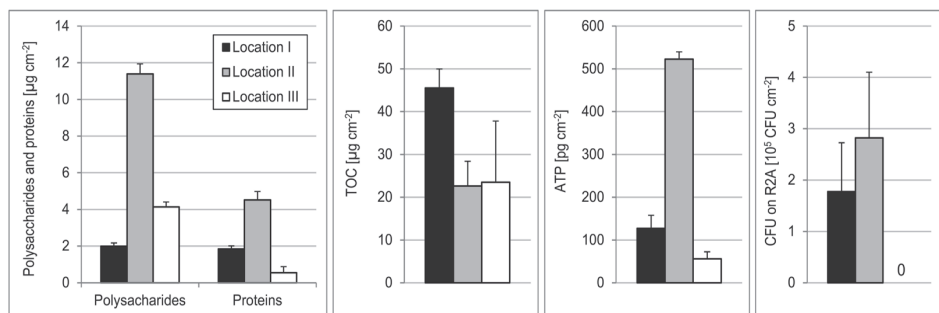


*Figure 4.5.* Fouling characterization from membrane and spacer samples from three RO locations studied. From left to right: Polysaccharides and proteins, Total organic carbon, Adenosine triphosphate, Colony forming units on R2A agar.

TOC values in this study (45.5, 22.6, and 23.5  $\mu\text{g cm}^{-2}$  for locations I, II, and III, resp.) are in the low - to - medium range when compared to literature values (5 - 150  $\mu\text{g cm}^{-2}$  (*Beyer et al., 2014*)). Compared to ATP literature values (4 - 102,000  $\mu\text{g cm}^{-2}$ ) (*Vrouwenvelder and van der Kooij 2003, Vrouwenvelder et al., 2008, Beyer et al., 2014, Filloux et al., 2015*), all values measured in this study were low. Location II, which had the highest ATP in this study, also had the highest measured polysaccharides concentration and CFU plate counts (*Figure 4.5.*). Biofouling is a

major type of fouling at this location, which was confirmed by SEM observations (data not shown) showing microorganisms embedded in a polymeric matrix. Location III, very frequently associated with biofouling problems (Bereschenko *et al.*, 2007, Bereschenko *et al.*, 2008, Bereschenko *et al.*, 2010, Bereschenko *et al.*, 2011), showed no CFU plate counts and ATP concentrations were very low (Figure 4.5). However, 20 days prior to membrane autopsy, an emergency CIP (Table 4.1 and Figure 4.3.) with oxalic acid had to be performed due to a leak in the UF system (Supplementary Figure S4.3.), which possibly explains the very low biomass parameters. At location I with the highest TOC values measured, ATP, protein, and polysaccharide concentrations were low (Figure 4.5). SEM observations showed microorganisms embedded in an organic matrix (data not shown), which was supported by the CFU counts (Figure 4.5). For location I, fouling consisted of organic and biological deposits. Based on ATP, protein, and polysaccharide concentrations, fouling in all autopsied membrane elements can be characterized as mild to moderate (Filloux *et al.*, 2015).

#### **4.3.4. Validation of laboratory-scale cleaning setup**

To validate the representativeness of the laboratory cleaning setup and high-pressure setup, bio(organic) fouling reduction (TOC, ATP, and CFU) during full-scale CIP was compared to cleaning efficiencies achieved during laboratory cleaning for location I, using the standard plant procedure (Table 4.2.). Full-scale cleaning efficiency (Figure 4.6.) was determined by membrane autopsy of a lead element before CIP and autopsy of a lead membrane element after CIP (Figure 4.1.). Sheets of the lead element before CIP were then cleaned in the laboratory membrane cleaning setup to evaluate laboratory-scale cleaning efficiency (Supplementary Figure S4.2.).

During full-scale CIP, TOC reduction was  $67 \pm 19\%$  as opposed to  $33 \pm 19\%$  in the laboratory setup. ATP reduction was  $70 \pm 10\%$  for full-scale CIP and  $93 \pm 5\%$  for laboratory-scale cleaning (Figure 4.6.). CFU counts were reduced to zero in both full-scale and laboratory-scale CIPs.

Cleaning efficiencies in terms of TOC and ATP reduction were somewhat dissimilar (Figure 4.6.), but deviation must also be taken into account. The membrane elements from full-scale cleaning before and after CIP originated from two different



pressure vessels, while laboratory-scale cleaning was performed on a single sheet, causing some deviation of the results.

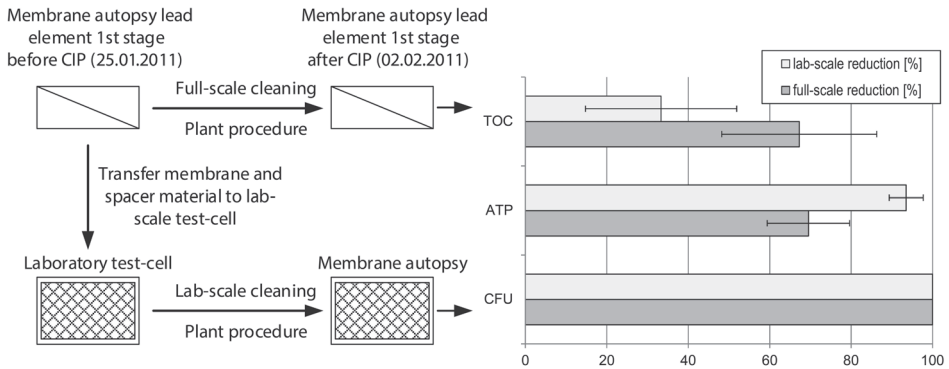


Figure 4.6. Laboratory cleaning setup and TOC, ATP and CFU reduction after standard plant cleaning procedure in full-scale and laboratory-scale test cell at Location I.

Moreover, the membrane elements from full-scale cleaning were sampled over the whole length (1 m), while for cleaning experiments in the laboratory, only membrane and spacer samples from the first 30 cm of the full-scale membrane elements were used. Fouling is not distributed evenly over membrane elements or single membrane envelopes, causing deviation when comparing samples from different membrane envelopes of the same membrane element. However, the trends were consistent. SEM-EDS observations (*Supplementary data S4.3., SEM not shown*) and visual observations after full-scale and laboratory-scale CIPs were also more consistent.

It was concluded that cross-flow filtration test cells offer good representation of the complex physical interactions, when, for example, compared to simple static cleaning tests using model foulants. Although not 1 : 1 translatable into full-scale operation, the laboratory cleaning setup using cross-flow cells can be a useful tool for comparative testing of cleaning chemicals and CIP procedures of full-scale membrane elements.

### 4.3.5. Comparative CIPs with alternative procedures on laboratory-scale

#### 4.3.5.1. Effect of cleaning on membrane integrity (salt rejection)

Salt rejection is a key performance parameter during the production of ultrapure water by RO. For the respective plant procedures and alternative procedure AP II, no significant changes in salt rejection could be observed for all three locations (Figure 4.7.). For AP I, salt rejection increased in all three locations (0.25 to 0.6 %).

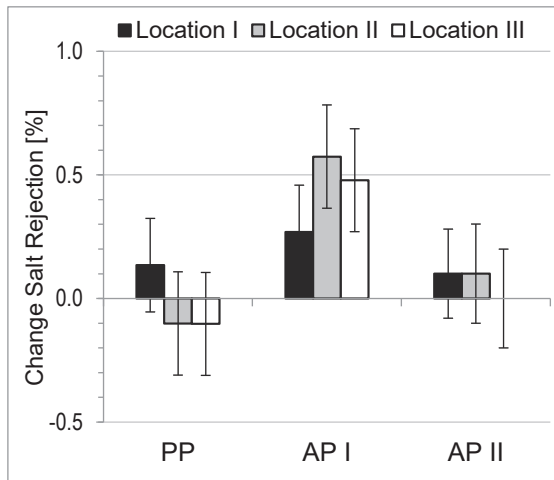


Figure 4.7. Change in salt rejection after standard plant cleaning procedure (PP) and two adapted cleaning procedures (AP I and AP II) for membrane and spacer samples from location I, II and III. Chemical cleaning of full-scale fouled membrane elements was performed in laboratory test cell; error bars represent standard deviation (n=2).

There are temporal or permanent interactions of cleaners with the fouling layers and membrane properties. The missing NaOH cleaning step in AP I may explain the observed increase in salt rejection for this procedure (membrane shrinking by low pH cannot be restored by a high pH cleaning step).

The comparative cleaning experiments performed under laboratory-scale conditions showed no negative effect on membrane integrity as indicated by stable salt rejection (Figures 4.7. and 4.10.). After all, oxidative damage after repetitive CIPs with the alternative procedures (Table 4.3.) cannot be excluded but seems unlikely.

#### 4.3.5.2. (Bio)organic fouling parameters (ATP and TOC) before and after laboratory-scale cleaning

Figure 4.8. shows TOC and ATP removal after laboratory cleaning, with the respective standard plant cleaning procedures (Table 4.2.) and the two adapted cleaning procedures (Table 4.3.) for location I, location II, and location III ( $n \geq 2$ ). None of the CIPs applied (standard plant procedures and AP I and AP II) (Tables 4.2. and 4.3.) was able to remove all TOC from the membrane and spacer samples (Figure 4.8.). Average TOC reduction was approximately 45 % (~ 20 – 80 %) (Figure 4.8.).

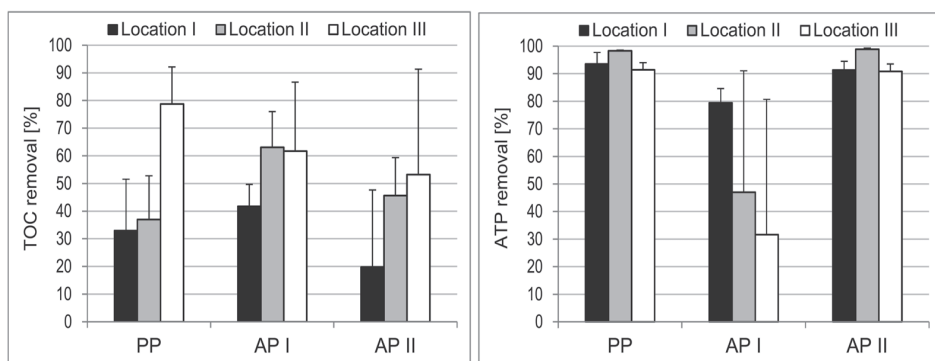


Figure 4.8. TOC and ATP removal after standard plant cleaning procedure (PP) and two adapted cleaning procedures (AP I and AP II) for membrane and spacer samples from location I, II and III. Chemical cleaning of full-scale fouled membrane elements was performed in laboratory test cell; error bars represent standard deviation ( $n=2$ ).

It is worth noting that AP I (Table 4.3.), which ends with a sanitizing step using a biocidal cleaner (acetic acid (8 %), peroxyacetic acid (5.8 %), and hydrogen peroxide (27.5 %) as active ingredients), showed the lowest efficiencies in ATP removal (79 %, 47 %, and 32 % for locations I, II, and III, resp. (Figure 4.8.)). In general, ATP removal was high (about 90 – 99 %) for plant procedures and AP II, which is in accordance with CFU counts, which were zero after all CIPs applied (*data not shown*). As only a very small portion of the microbial diversity can be recovered on agar plates, CFU counts are only a rough estimation of biological activity. Location II showed the highest ATP concentrations before cleaning ( $523 \text{ pg cm}^{-2}$ ) and the highest CFU count  $2.8 \times 10^5 \text{ cm}^{-2}$  (Figure 4.5.), while ATP removal using AP I was 79 %. The plant procedures and AP II were more effective in reducing the ATP levels (91 – 99 %) when compared to alternative procedure AP I (Figure 4.8.). Location I

showed the highest TOC values during autopsies ( $45.5 \mu\text{g cm}^{-2}$ ), which were approximately double of locations II ( $22.6 \mu\text{g cm}^{-2}$ ) and III ( $22 \mu\text{g cm}^{-2}$ ) (Figure 4.5.). The highest TOC removal in location I was achieved with AP I ( $\sim 40\%$ ) (Figure 4.8.), which reduced already low ATP concentrations ( $127 \text{ pg cm}^{-2}$ ).

The data suggests that the NaOH cleaning step, which is included in all cleaning procedures except AP I, leads to high removal of ATP in the plant procedures and AP II. The lower ATP removal efficiencies may be further related to the production of catalases in the biofilms, rendering peroxide based treatments ineffective.

In general, around 20 % (Figure 4.8.) higher TOC removal could be achieved with AP I when compared to AP II. CIP procedure AP I includes EDTA in the enzymatic blend cleaner. EDTA is a chelating agent that destabilizes EPS like structures, such as alginate, by a ligand-exchange reaction between EDTA and complexed divalent cations in EPS-like structures (Ang *et al.*, 2006). The usage of EDTA and proteases in AP I may explain the better (bio)organic fouling removal when compared to AP II. Overall, best cleaning results in terms of TOC removal were achieved for location III, followed by location II and location I, irrespective of the cleaning procedures applied (Figure 4.8.). This indicates that fouling was most resistant to cleaning efforts in location I, which also had the highest initial TOC concentrations measured (Figure 4.5.).

#### **4.3.5.3. Performance parameters ( $K_w$ and FCP) before and after laboratory-scale cleaning.**

Figure 4.9. shows  $K_w$  and FCP improvements after laboratory cleaning with all cleaning procedures applied. Performance improvements after chemical cleaning of the aged and persistent fouling layers were generally very low, with the highest permeability increase of 5 % for AP II at location III and the highest FCP reduction of  $\sim 17\%$  for AP I at location I (Figure 4.9.).

The observations do not seem to match with the (bio)organic foulant removal reported in Figure 4.8.. With an average TOC removal of approximately 45 %, some improvement in membrane performance ( $K_w$  and FCP) for all three locations was expected. At location II, the procedures AP I and AP II caused FCP increase in combination with  $K_w$  decrease, which could be a sign of compaction of bio(organic)

fouling layers. A similar effect was observed for location I and AP I (Figure 4.9.). However, the low performance improvements of the plant procedures (Figure 4.9.) match with the general low CIP efficiencies observed at the respective locations during the winter months, when the autopsies were performed (Figures 4.1. – 4.3.). The aged and persistent remainders of unsuccessful CIPs (Figures 4.1. – 4.3.) were also not effectively removed using the two alternative cleaning procedures (AP I and II).

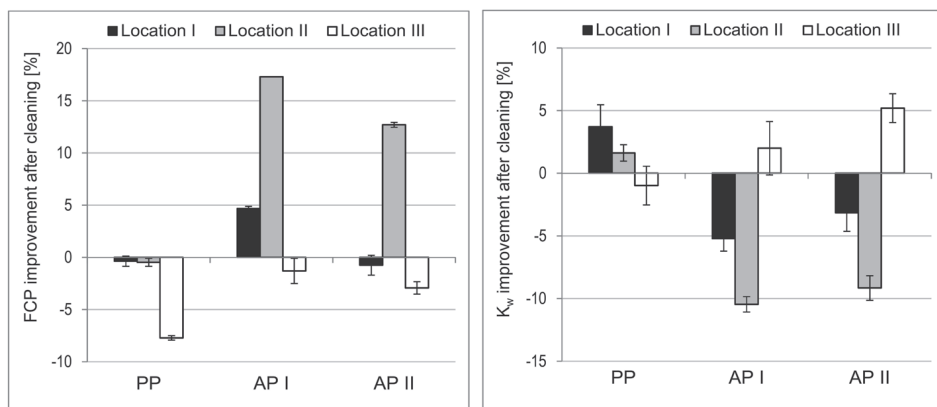


Figure 4.9. Normalized permeability ( $K_w$ ) and FCP improvements after laboratory cleaning with standard plant cleaning procedure and the two adapted cleaning procedures for membrane and spacer samples from location I, II and III; error bars represent standard deviation (n=2).

There are temporal or permanent interactions of cleaners with the fouling layers and membrane material itself. Contact with chemical cleaners influences membrane properties such as surface charge, porosity, or hydrophobicity and thereby may also influence operational parameters such as  $K_w$  and salt rejection. In general, chemical cleaning at high pH may cause membrane swelling, while cleaning at low pH may cause membrane shrinking (Simon *et al.*, 2013).

Therefore,  $J_w$  or  $K_w$  measurements taken shortly after chemical cleaning must be evaluated with care. Furthermore, the test cell used in this study has very small spatial dimensions compared to full-scale 8-inch spiral-wound membrane elements, giving some limitation in accuracy and representativeness. Biomass removal (Figure 4.8.), in contrast to performance increase, therefore might be the more suitable parameter for laboratory-scale cleaning efficiency comparison tests.

#### 4.3.5.4. Effect of hydraulic forces on CIP efficiency at laboratory-scale

Shear stress (hydraulic forces) is an important factor in CIP. Typically, CIP is performed at high velocity to facilitate foulant removal by high shear forces and at low pressure to prevent fouling layer compaction. For the shortest of the alternative cleaning procedures (AP II), cleaning efficiencies were compared between standard velocity ( $0.184 \text{ m s}^{-1}$ ), 50 % decreased velocity ( $0.092 \text{ m s}^{-1}$ ), and 50 % increased velocity ( $0.267 \text{ m s}^{-1}$ ) for location I (Figure 4.10.).

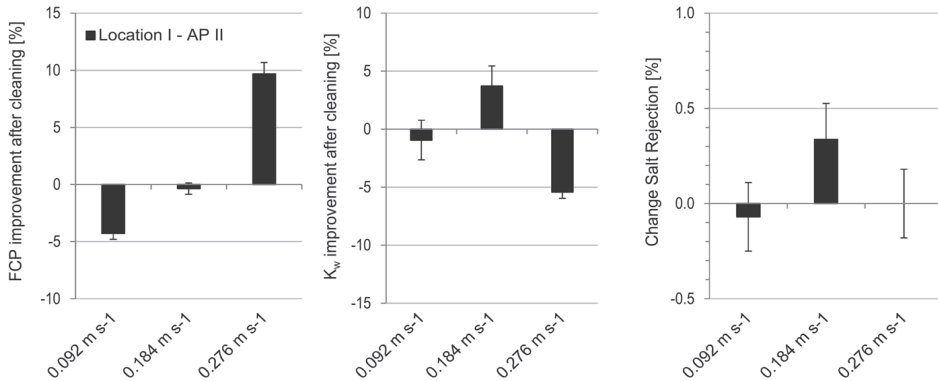


Figure 4.10. Normalized permeability, FCP and salt rejection improvements after laboratory cleaning with AP II cleaning procedure for membrane and spacer samples from location I; error bars represent standard deviation ( $n=2$ ).

Lowest cleaning efficiency (FCP increased 4 %;  $K_w$  decreased 1 %) was observed for the lowest velocity (Figure 4.10.). For the standard velocity ( $0.184 \text{ m s}^{-1}$ ), a slight improvement in permeability (4 %) and salt rejection (0.3 %) could be observed, while FCP remained unchanged. For the highest velocity ( $0.276 \text{ m s}^{-1}$ ), FCP improved by 10 %, but this comes together with a  $K_w$  decrease (5 %) at unchanged salt rejection, indicating compaction of the fouling layer. After all, none of the conditions applied was able to overcome the fouling of aged and persistent (bio)organic remainders from earlier unsuccessful CIPs (Figures 4.8. – 4.10.). Higher velocities are generally believed to give better cleaning results, but maximum allowable cleaning solution velocity is limited by the maximum permitted NPD, especially at locations with strong NPD problems. To prevent spacer displacement within the membrane elements (telescoping), the maximum permitted NPD is 1 bar for a single element or 3.4 bar for one pressure vessel (typically containing 6 - 7 membrane elements) (Supplementary Table S4.1.).

#### 4.4. Outlook

CIP is inevitable for membrane industry, as all membranes will eventually foul. Costs for membrane element cleaning can add up to 50 % of all RO operational costs (Ridgway 2003). Although some of the factors affecting cleaning efficiency (e.g. pH or temperature) were not directly investigated in this study, the adapted cleaning procedures developed (Table 4.3.), as well as the standard cleaning procedures (Table 4.2.), were already performed at optimized conditions (based on literature data such as Ang *et al.*, 2006, zum Kolk *et al.*, 2013, Garcia-Fayos *et al.*, 2015). The CIPs were performed tightly at the permitted limits of the membrane manufacturer in terms of cleaning solution type, concentration, temperature, pH, and velocity (Tables 4.2. and 4.3. and Supplementary Table S4.1.). A laboratory cleaning trial with increased shear did not lead to overall performance improvements (Figure 4.10.). It seems that the feed spacer material in spiral-wound membranes limits the efficiency of foulant removal (Bereschenko *et al.*, 2011). After all, optimizing the cleaning conditions such as temperature, pH, cleaning duration, and velocity can only lead to increased CIP efficiencies, if there is a favorable chemical reaction between the foulant and the cleaner.

CIP remains one of the major bottlenecks in the stable operation of full-scale RO plants. Therefore, the avoidance of biofouling is a very important factor in an effective fouling prevention and control approach. Biofouling prevention may be achieved by application of excessive pretreatment or usage of biocides. However, the only biocidal active substances that are formally approved by the majority of RO manufacturers are limited to 2,2-dibromo-3-nitrilopropionamide (DBNPA) and chloromethylisothiazolone/methylisothiazolone (CMIT/MIT). Biocides, as well as cleaning chemicals, must be fully compatible with all materials of an RO element. When applied as slug dosage, the biocides must also be fast acting. Broadband biocides with biofilm dispersing properties (e.g. chlorine dioxide) may be promising alternatives but have no formal approval from the membrane manufacturers. Research on membrane fouling and chemical cleaning should strongly address harsh, aged, and persistent (composite) fouling layers, as typically found in full-scale installations. Alternative approaches to classical CIP, such as two-phase cleaning

(Wibisono *et al.*, 2015), should be deeper investigated and approved by the membrane manufacturers, as it is believed that the combination of chemical cleaning and mechanical cleaning improves CIP efficiencies. Research and development should furthermore concentrate on improvements in membrane element construction (e.g. allowing better fouling removal and lowering the impact of fouling on key performance parameters) and RO membranes with improved chemical resistance to (non-)oxidizing biocides and other chemical active substances used for fouling prevention and control.

#### **4.5. Conclusions**

Although different in feed water quality, design, operation, and chemical treatment, the three RO plants investigated had similar operational problems caused by aged and persistent (bio)organic fouling layers.

Traditional acid-base CIPs failed to fully restore RO performance and to remove all deposits from the membrane elements.

Comparative cleaning experiments performed in a laboratory setup showed that, even with the use of specialized bio(organic) fouling specific CIP procedures, the aged and persistent (bio)organic fouling layers were not fully removed from the membrane and spacer surfaces.

Cross-flow cells can be a useful tool for comparative testing of cleaning chemicals and CIP procedures, as they offer a good representation of the complex physical interactions during CIP. The laboratory setup can be used to access important CIP benchmark parameters such as foulant removal or membrane integrity.

Some limitations in transferring laboratory-scale data into full-scale data were unveiled and, therefore, a critical evaluation of the setup employed should be part of every study presented in literature.

The relatively low cleaning efficiencies achieved in this study were attributed to the membrane fouling history. The persistency of the aged fouling layers towards CIP in this study matches with the findings of other authors (*zum Kolk et al.*, 2013, *Goode et al.*, 2013, *Beyer et al.*, 2014).



## Acknowledgments

This work was performed at Wetsus, European Centre of Excellence for Sustainable Water Technology ([www.wetsus.nl](http://www.wetsus.nl)). Wetsus is funded by the Dutch Ministry of Economic Affairs, the European Union European Regional Development Fund, the Province of Fryslân, the city of Leeuwarden and by the EZ-KOMPAS Program of the “Samenwerkingsverband Noord-Nederland”. The authors like to thank the participants of the research theme “Biofouling” for the fruitful discussions and their financial support. In particular we like to thank the water companies Evides and Waterlaboratorium Noord for the possibility to perform the research presented in this manuscript at their RO locations. We are grateful to Wilbert van den Broek (Evides), Martin Pot (Evides) and Reinder de Valk (Waterlaboratorium Noord) for supplying the full-scale operational performance data and the fouled membrane elements used in this study. The authors furthermore like to thank Dolf van der Berg (Ecolab) for helping with the development of the adapted cleaning procedures and for supplying the chemicals cleaners used in this study.

## Supplementary data Chapter 4

### Supplementary data S4.1. - RO plant design and pre-treatment

#### Location I (Sas van Gent, The Netherlands)

The plant (Figure S4.1.) produces demineralized water, with conductivity less than  $10 \mu\text{S cm}^{-1}$ , from secondary wastewater effluent from the food industry. First, the secondary wastewater effluent is pre-treated with coagulation, flocculation, sedimentation process with ferric chloride ( $\text{FeCl}_3$ ) ( $2.5 \text{ mg L}^{-1}$ ), prior to ultrafiltration (UF). Hydrochloric acid (HCl) (pH 7.2) and antiscalant (Genesys LF) ( $1.78 \text{ mg L}^{-1} - 3.68 \text{ mg L}^{-1}$ ) are dosed to the UF permeate to prevent scaling in the RO membrane elements. Between the first and second stage of the RO membrane system, the water is degassed.

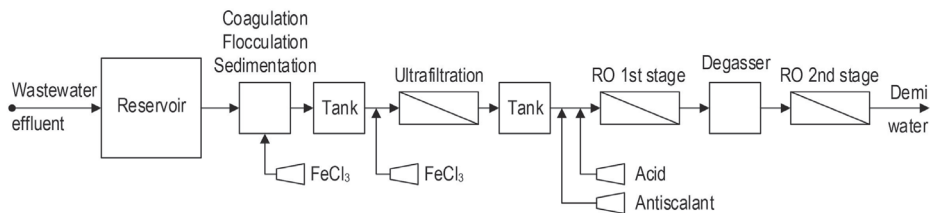


Figure S4.1. Schematic representation of RO plant location I (Sas van Gent, The Netherlands).

#### Location II (Dordrecht, The Netherlands)

The plant (Figure S4.2.) produces demineralized water, with conductivity less than  $0.2 \mu\text{S cm}^{-1}$ , from river water. First, river water is pumped through a 100 micron strainer, then ferric chloride ( $\text{FeCl}_3$ ) ( $1 \text{ mg L}^{-1}$ ) coagulant is dosed before UF. Antiscalant (PermaTreat® PC-19IT) ( $1.5 \text{ mg L}^{-1}$ ) and sulfuric acid ( $\text{H}_2\text{SO}_4$ ) (pH 7.5) is dosed to the UF permeate in order to prevent scaling in the RO membrane elements. RO permeate is then degassed and fed to a mixed-bed ion exchanger.

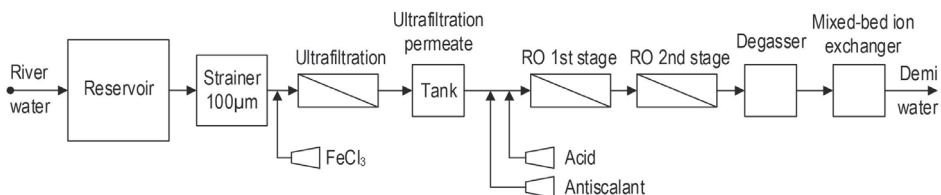


Figure S4.2. Schematic representation of RO plant location II (Dordrecht, The Netherlands).

**Location III (Veendam, The Netherlands)**

The plant (Figure S4.3.) produces demineralized water from surface water (channel water). First river water is pumped through a coarse screen, and is then pre-treated with coagulation, flocculation, sedimentation process with ferric chloride ( $\text{FeCl}_3$ ) (18 - 28  $\text{mg L}^{-1}$ ), prior to UF. The UF permeate then passes the two stage RO system before degasification.

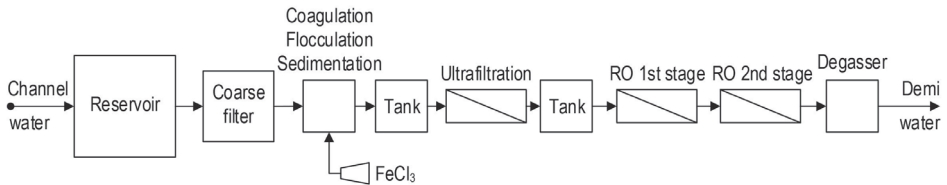


Figure S4.3. Schematic representation of RO plant location III (Veendam, The Netherlands).

**Supplementary data S4.2. - Schematic representation of high-pressure set-up for cleaning studies and cleaning set-up**

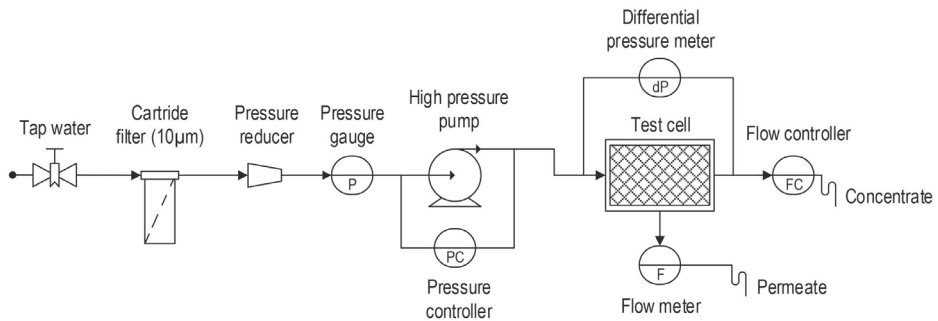


Figure S4.4. Schematic representation of high-pressure set-up for cleaning studies.

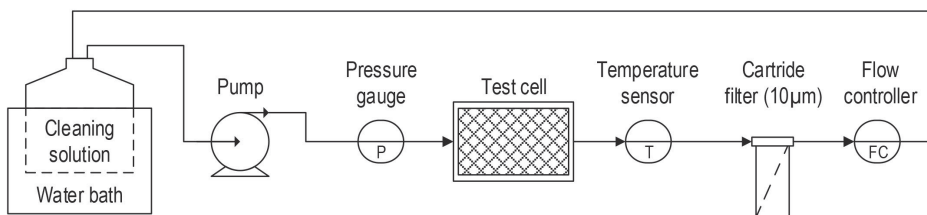
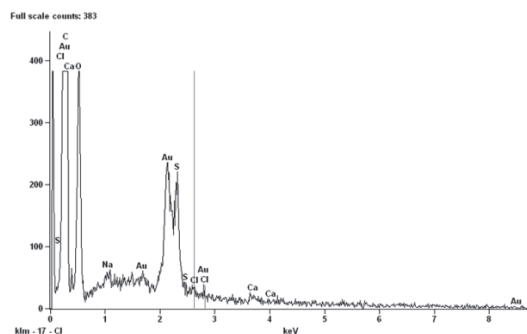


Figure S4.5. Schematic representation of chemical cleaning set-up for cleaning studies.

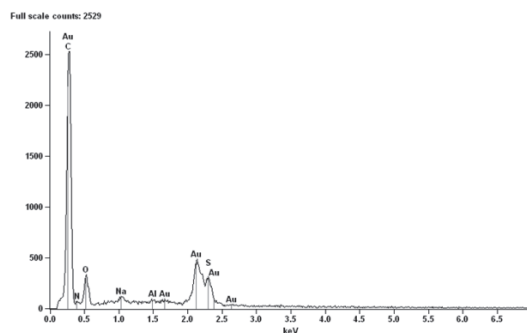
### Supplementary data S4.3. - Energy dispersive X-Ray spectroscopy (EDS) spectra and related elemental analysis

#### Location I (Sas van Gent, The Netherlands)



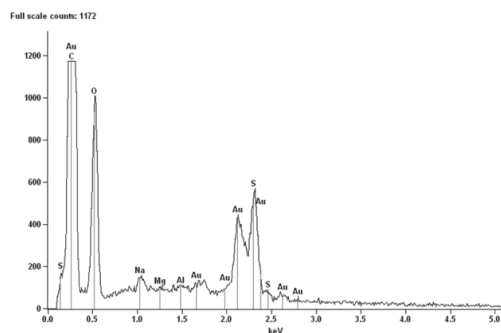
Element	Net	Weight %	Atom %
Line	Counts		
CK	10,531	51.3	70.17
OK	2,323	24	24.65
Na K	130	0.37	0.27
SK	1,827	5.79	2.97
SL	0	---	---
Cl K	126	0.51	0.24
Cl L	0	---	---
Ca K	100	0.66	0.27
Ca L	0	---	---
Au L	6	---	---
Au M	3,022	17.36	1.45
Total		100	100

#### Location II (Dordrecht, The Netherlands)



Element	Net	Weight %	Atom %
Line	Counts		
CK	14,989	53.84	78.89
NK	0	0	0
OK	1,719	13.28	14.61
Na K	381	0.75	0.58
Al K	185	0.3	0.19
SK	2,780	6.27	3.44
SL	775	---	---
Au L	4	---	---
Au M	6,443	25.55	2.28
Total		100	100

#### Location III (Veendam, The Netherlands)



Element	Net	Weight %	Atom %
Line	Counts		
CK	19,856	55.38	71.69
OK	3,980	24.26	23.58
Na K	323	0.54	0.37
Mg K	0	0	0
Al K	169	0.23	0.13
SK	3,602	6.61	3.21
SL	771	---	---
Au L	1	---	---
Au M	3,838	12.98	1.02
Total		100	100

Figure S4.6. Selected EDS spectra and elemental analysis of the location I (Sas van Gent, The Netherlands), location II (Dordrecht, The Netherlands) and location III (Veendam, The Netherlands) during autopsies of the full-scale membrane elements (before chemical cleaning in the laboratory cleaning set-up). The spectra presented were selected from multiple spectra per element ( $\geq 5$ ). The trends observed during multiple measurements are discussed in the manuscript.

### Supplementary data S4.4. - *Operational and cleaning limitations of the membranes used in this study*

Table S4.1. Operational and cleaning limitations of the membrane elements used in the three RO locations investigated in this study. FCP = feed-channel pressure drop.

DOW FILMTEC™ LE-440i and BW30XFR-400/34i	
<b>Operational limits</b>	
Max temperature	45 °C <sup>a</sup>
Max. working pressure	41 bar
Max. FCP (single element) Max.	1 bar
FCP (multi-element vessel)	3.4 bar
pH-range (continuous)	2 - 11
pH-range (CIP, max. 30 min)	1 - 13
Free chlorine tolerance	< 0.1 ppm

<sup>a</sup>) Max. temperature above pH 10 is 35°C for continuous operation

## References

- Ang, W.S., Lee, S., Elimelech, M. Chemical and physical aspects of cleaning of organic-fouled reverse osmosis membranes. *J. Membr. Sci.* 272: 198-210 (2006).
- Ang, W.S., Tiraferri, A., Chen, K.L., Elimelech, M. Fouling and cleaning of RO membranes fouled by mixtures of organic foulants simulating wastewater effluent. *J. Membr. Sci.* 376: 196-206 (2011).
- Bereschenko, L.A., Stams, A.J.M., Heilig, G.H., Euverink, G.-J.W., Nederlof, M.M., van Loosdrecht, M.C.M. Investigation of microbial communities on reverse osmosis membranes used for process water production. *Water Sci. Technol.* 55(8-9): 181-190 (2007).
- Bereschenko, L.A., Heilig, G.H., Nederlof, M.M., van Loosdrecht, M.C.M., Stams, A.J.M., Euverink, G.-J.W. Molecular characterization of the bacterial communities in the different compartments of a full-scale reverse-osmosis water purification plant, " *Appl. Environ. Microbiol.* 74(17): 5297-5304 (2008).
- Bereschenko, L.A., Stams, A.J.M., Euverink G.-J.W., van Loosdrecht, M.C.M. Biofilm formation on reverse osmosis membranes is initiated and dominated by *Sphingomonas* spp. *Appl. Environ. Microbiol.* 76(8): 2623-2632 (2010).
- Bereschenko, L.A., Prummel, H., Euverink, G.-J.W., Stams, A.J.M., van Loosdrecht, M.C.M. Effect of conventional chemical treatment on the microbial population in a biofouling layer of reverse osmosis systems. *Water Res.* 45(2): 405-416 (2011).
- Beyer, F., Rietman, B.M., Zwijnenburg, A., van den Brink, P., Vrouwenvelder, J.S., Jarzembowska, M., Laurinonyte, J., Stams, A.J.M., Plugge, C.M. Long-term performance and fouling analysis of full-scale direct nanofiltration (NF) installations treating anoxic groundwater. *J. Membr. Sci.* 468: 339-348 (2014).
- Chen, J.P., Kim, S.L., Ting, Y.P. Optimization of membrane physical and chemical cleaning by a statistically designed approach. *J. Membr. Sci.* 219: 27-45 (2003).
- Dreszer, C., Vrouwenvelder, J.S., Paulitsch-Fuchs, A.H., Zwijnenburg, A., Kruithof, J.C., Flemming, H.-C. Hydraulic resistance of biofilms. *J. Membr. Sci.* 429: 436-447 (2013).
- Filloux, E., Wang, J., Pidou, M., Gernjak, W., Yuan, Z. Biofouling and scaling control of reverse osmosis membrane using one-step cleaning-potential of acidified nitrite solution as an agent. *J. Membr. Sci.* 495: 276-283 (2015).
- Flemming, H.-C., Schaule, G., Griebe, T., Schmitt, J., Tamachkiarowa, A. Biofouling - The achilles heel of membrane processes. *Desalination.* 131(2): 215-225 (1997).
- Garcia-Fayos, B., Arnal, J.M., Gimenez, A., Alvarez-Blanco, S., Sancho, M. Static cleaning tests as the first step to optimize RO membranes cleaning procedure. *Desal. Water Treat.* 55(12): 1-11 (2015).
- Goode, K.R., Asteriadou, K., Robbins, P.T., Fryer, P.J. Fouling and cleaning studies in the food and beverage industry classified by cleaning type. *Compr. Rev. Food Sci. F.* 12(2): 121-143 (2013).
- Huiting, H., de Koning, M., Beerendonk, E.F. Normalisatie van gegevens bij nanofiltratie en omgekeerde osmose. Kiwa-VEWIN, SWI 99.166, 1999.
- Huiting, H., Kappelhof, J.W.N.M., Bosklopper, T.G.J. Operation of NF/RO plants: from reactive to proactive. *Desalination.* 139(1): 183-189 (2001).
- Liikanen, R., Yli-Kuivila, J., Laukkanen, R. Efficiency of various chemical cleanings for nanofiltration membrane fouled by conventionally-treated surface water. *J. Membr. Sci.* 195: 265-276 (2002).
- Linley, E., Denyer, S.P., McDonnell, G., Simons, C., Maillard, J.-Y. Use of hydrogen peroxide as a biocide: new consideration of its mechanisms of biocidal action. *J. Antimicrob. Chemother.* 67(7): 1589-1596 (2012).

- Liu, C., Caothien, S., Hayes, J., Caohuy, T., Otoyoy, T. *Membrane cleaning: from art to science. Proceedings AWWA Membrane Technology Conference, San Antonio TX, March 4 - 7, (2001).*
- Mo, Y., Chen, J., Xue, W., Huang, X. *Chemical cleaning of nanofiltration membrane filtering the effluent from a membrane bioreactor. Sep. Purif. Technol. 75(3): 407-414 (2010).*
- Nederlof, M.M., Kruithof, J.C., Taylor, J.S., van der Kooij, D., Schippers, J.C. *Comparison of NF/RO membrane performance in integrated membrane systems. Desalination. 131(1): 257-269 (2000).*
- Paul, D.H. *Reverse osmosis: scaling, fouling & chemical attack. Desalination Water Reuse. 1: 8-11 (1991).*
- Peña, N., Gallego, S., del Vigo F., Chesters, S.P. *Evaluating impact of fouling on reverse osmosis membranes performance. Desalin. Water Treat. 51(4-6): 958-968 (2012).*
- Ridgway, H.F. *Biological fouling of separation membranes used in water treatment applications. AWWA Research Foundation, Denver, CO, (2003).*
- Simon, A., Price, W.E., Nghiem, L.D. *Impact of chemical cleaning on the nanofiltration of pharmaceutically active compounds (PhACs): The role of cleaning temperature. J. Taiwan Inst. Chem. Eng. 44(5): 713-723 (2013).*
- Vrouwenvelder, J.S., van Paassen, J.A.M., Folmer, H.C., Hofman, J. A. M. H., Nederlof, M.M., van der Kooij, D. *Biofouling of membranes for drinking water production. Desalination. 118(1): 157-166 (1998).*
- Vrouwenvelder, J.S. and van der Kooij D. *Diagnosis of fouling problems of NF and RO membrane installations by a quick scan Desalination. 153(1-3): 121-124 (2003).*
- Vrouwenvelder, J.S., Manolarakis, S.A., van der Hoek, J.P., van Paassen, J.A.M., van der Meer, W.G.J., van Agtmaal J.M.C., Prummel, H.D.M., Kruithof, J.C., van van der Bruggen, B., Mänttari, M., Nyström, M. *Drawbacks of applying nanofiltration and how to avoid them: A review. Sep. Purif. Technol. 63(2): 251-263 (2008).*
- Vrouwenvelder, J.S., Beyer, F., Dahmani, K., Hasan, N., Galjaard, G., Kruithof, J.C., van Loosdrecht, M.C.M. *Phosphate limitation to control biofouling. Water Res. 44(11): 3454-3466 (2010).*
- Wibisono, Y., El Obied, K.E., Cornelissen, E.R., Kemperman, A.J.B., Nijmeijer, K. *Biofouling removal in spiral-wound nanofiltration elements using two-phase flow cleaning. J. Membr. Sci. 475: 131-146 (2015).*
- zum Kolk, C., Hater, W., Kempken, N. *Cleaning of reverse osmosis membranes. Desal. Water Treat. 51(1-3): 343-351 (2013).*







# Chapter 5

## Isolation and characterization of *Sphingomonadaceae* from fouled membranes

Hendrik J. de Vries\*, Florian Beyer\*, Monika Jarzembowska,  
Joanna Lipińska, Paula van den Brink, Arie Zwijnenburg,  
Peer H.A. Timmers, Alfons J.M. Stams, Caroline M. Plugge

\* Hendrik J. de Vries and Florian Beyer contributed equally to this work

This chapter is adapted from:

de Vries, H.J.\*, Beyer, F.\*, Jarzembowska, M., Lipińska, J., van den Brink, P.,  
Zwijnenburg, A., Timmers, P.H.A., Stams, A.J.M., Plugge, C.M.  
Isolation and characterization of *Sphingomonadaceae* from fouled membranes.  
Nature Biofilms Microbiomes. 5: 6 (2019).

**ABSTRACT**

Membrane filtration systems are widely applied for the production of clean drinking water. However, the accumulation of particles on synthetic membranes leads to fouling. Biological fouling (i.e. biofouling) of reverse osmosis and nanofiltration membranes is difficult to control by existing cleaning procedures. Improved strategies are therefore needed. The bacterial diversity on fouled membranes has been studied, especially to identify bacteria with specialized functions and to develop targeted approaches against these microbes. Previous studies have shown that *Sphingomonadaceae* are initial membrane colonizers that remain dominant while the biofilm develops. Here, we characterized 21 *Sphingomonadaceae* isolates, obtained from six different fouled membranes, to determine which physiological traits could contribute to colonization of membrane surfaces. Their growth conditions ranged from temperatures between 8 and 42 °C, salinity between 0.0 and 5.0 % w/v NaCl, pH from 4 and 10, and all isolates were able to metabolize a wide range of substrates. The results presented here show that *Sphingomonadaceae* membrane isolates share many features that are uncommon for other members of the *Sphingomonadaceae* family: all membrane isolates are motile and their tolerance for different temperatures, salt concentrations and pH is high. Although relative abundance is an indicator of fitness for a whole group, for the *Sphingomonadaceae* it does not reveal the specific physiological traits that are required for membrane colonization. This study therefore adds to more fundamental insights in membrane biofouling.

## 5.1. Introduction

The demand for high-quality water has increased in recent years and will rise even more in the future (Barnett *et al.*, 2005, Shannon *et al.*, 2008). Membrane filtration systems are attractive technologies to purify water: their high efficiency to separate water from its solutes delivers the option to remove most contaminants, including pharmaceutical remnants, within a single purification step in a relatively cost effective manner (Shannon *et al.*, 2008). Different membrane types have different separation properties and membranes can therefore be used in many applications (Werber *et al.*, 2016). Low pressure membranes (i.e. microfiltration and ultrafiltration) separate via pore-separation, while in high-pressure membranes (i.e. nanofiltration (NF) and reverse osmosis (RO)) separation occurs via solvent and diffusion processes (e.g. solution-diffusion model) (Wijmans and Baker 1995). Membrane filtration has one major disadvantage: fouling (Wijmans and Baker 1995, van den Broek *et al.*, 2010). Pretreatment of the influent and periodical chemical cleaning of the membrane are therefore needed to control membrane fouling (Vrouwenvelder *et al.* 2001, Bae *et al.*, 2011). Pretreatment for high-pressure membranes is conventionally performed using a combination of processes such as coagulation and flocculation, followed by granular media filtration (e.g. anthracite coal, silica sand, or garnet) and cartridge filtration (Voutchkov 2010). Low-pressure membranes (microfiltration and ultrafiltration) filtration systems provide better removal efficiency compared to conventional pretreatment systems, but high capital and operation costs have hampered their implementation in the past (Voutchkov 2010). Chemical cleaning leads to a reduction in membrane lifetime and does not restore membrane performance completely under most circumstances (depending on the fouling type) (Wijmans and Baker 1995, van den Broek *et al.*, 2010). The lack of alternatives makes chemical cleaning inevitable yet more effective and economically feasible antifouling strategies are needed.

Biofilm formation on the membrane surface leads to biological fouling (biofouling) (Flemming *et al.*, 1997, Calderón *et al.*, 2012). Compared to other fouling types (colloidal matter, scaling and organic fouling) biofouling is difficult to prevent or control because micro-organisms multiply and secrete extra-cellular polymeric

substances (EPS) that protect a part of the microbial community against the chemical cleaning agents (Flemming 1997, Vrouwenvelder and van der Kooij 2001). Natural biofilms commonly consist of many different microbial species (Costerton *et al.*, 1987). In membrane biofilms the microbial community composition is complex as well and is influenced by a variety of different parameters including the influent quality, pretreatment steps of the feed water, local conditions such as temperature and seasonal change, the oxygen concentration in the influent, the organization of cascading membrane elements into vessels and stages and membrane cleaning (Pang *et al.*, 2007, Bereschenko *et al.*, 2011, Bae *et al.*, 2011, Calderón *et al.*, 2012, Beyer *et al.*, 2014, Yu *et al.*, 2017). However, the significant change in microbial community diversity between free-floating bacteria present in the feed stream and membrane biofilms indicates that membrane filtration provides a selective force (Kim *et al.*, 2014). Bacteria belonging to the phylum of *Proteobacteria*, particular those belonging to  $\alpha$ -,  $\beta$ -, and  $\gamma$ -lineage, have been shown to frequently dominate membrane biofilms (Bereschenko *et al.*, 2010, Bereschenko *et al.*, 2011, Bae *et al.*, 2011, Calderón *et al.*, 2012, Kim *et al.*, 2014, Nagaraj *et al.*, 2017, Yu *et al.*, 2017).

Yabuuchi *et al.* (1990) discovered an  $\alpha$ -proteobacterium that contained glycosphingolipids (GSL) in its cell envelope and proposed the genus *Sphingomonas* to accommodate this species (Yabuuchi *et al.*, 1990). Takeuchi *et al.* (2001) classified the *Sphingomonas* species in four genera: *Sphingomonas sensu stricto*, *Sphingobium*, *Novosphingobium* and *Sphingopyxis* (Takeuchi *et al.*, 2001). These genera, together with other newly discovered genera, now constitute the *Sphingomonadaceae*, a family that belongs to the class of  $\alpha$ -*Proteobacteria* (Glaeser and Kämpfer 2014). It was found that *Sphingomonadaceae* initiate the formation of membrane biofilms and remain dominant during the biofilm maturation steps, both in spiral wound membranes and in membrane bioreactors, regardless of the surface properties of the membranes (Choi *et al.*, 2006, Huang *et al.*, 2008, Bereschenko *et al.*, 2010). Here we describe the properties of 21 *Sphingomonadaceae* isolates, isolated from membrane surfaces used in full-scale operation and laboratory simulation experiments. We aimed to get insight into the physiological traits that determine their effective colonization of membrane surfaces.

## 5.2. Material and methods

### 5.2.1. Enrichment and isolation

A total of 60 pure cultures were obtained from fouled membranes (Table 5.1. and Table S5.1.). Four membranes were acquired from four different full-scale water purification systems, and two membranes were obtained from laboratory experiments. The *Sphingomonadaceae* strains isolated in this study are listed in Table 5.1.

*Pseudomonas aeruginosa* PAO1 (DSM 1707) was obtained from the Deutsche Sammlung von Mikroorganismen und Zellkulturen (DSMZ; Braunschweig, Germany). This bacterium was selected in this study because of its ability to swim, swarm and twitch and could therefore be used as positive control. *P. aeruginosa* PAO1 is a Gram-negative model strain for biofilm research in general and has been thoroughly used to investigate membrane biofouling (Herzberg and Elimelech 2007, López *et al.*, 2010). Unless stated otherwise, *P. aeruginosa* PAO1 and the *Sphingomonadaceae* isolates were grown in R2 broth (Teknova, York, UK) at 30°C while shaken at 200 rpm.

For the enrichment of *Sphingomonadaceae*, biomass scraped from membranes was three times sonicated (40 kHz for 5 min) and vortexed (2 min), and plated on L9 minimal salt medium supplemented with streptomycin and piperacillin to select for *Sphingomonas* strains, as described previously (Yim *et al.*, 2010). Plates were incubated for three days at 31 °C, and selected colonies were re-streaked three times on R2 agar (Merck Millipore, Darmstadt, Germany) to obtain pure cultures. All isolates were stored at -80 °C using the Viabank™ (Medical Wire & Equipment, Corsham, Wiltshire, UK) cryoprotection system.

### 5.2.2. Bacterial identification

Bacterial identification was performed using 16S rRNA gene sequencing. Genomic DNA was extracted from single colonies grown on R2 agar plates using the FastDNA® SPIN Kit for soil (Bio 101 Corp., Vista, CA) according to manufacturer's instructions. The 16S rRNA gene was amplified using primers 7f (5'-GACGGATCCAGAGTTTGGATYWTGGCTCAG-3') (Dewhirst *et al.*, 1999) and 1541r (5'-

AAGGAGGTCATCCANCCRCA-3') (Lane 1991). For isolates Sph4, Sph11 and Sph19 the primer set 7f/154lr was unsuccessful in delivering an amplicon, and instead the primer set 27f (5'-GTTTGATCCTGGCTCAG-3') and 1492r (5'-CGGCTACCTTGTTACGAC-3') was used (Weisburg *et al.*, 1991). DNA amplification was carried out using a mixture (total volume, 50 µl) containing 2 µl of DNA extract, 1 U of *Taq* polymerase (Amersham Biosciences, Roosendaal, The Netherlands), 0.25 mM of deoxynucleoside triphosphates, 0.1 µM of each primer (Eurofins MWG Operon, Ebersberg, Germany), and 1 × PCR buffer under the following conditions: initial denaturation for 5 min at 94 °C, followed by 30 cycles of 30 seconds denaturation at 94 °C, 45 seconds annealing at 54 °C and 1.5 minute elongation at 72 °C. Post-elongation was performed for 5 min at 72 °C. Amplicons were sequenced using the Sanger method using the same primers at (BaseClear BV, Leiden, The Netherlands).

### 5.2.3. Phylogenetic analysis

For all the membrane isolates, the 16S rRNA gene was sequenced as described above. The forward and reverse sequences were assembled into contiguous reads and corrected with ChromasPro software (Technelysium Pty Ltd., Brisbane, Australia). After assembly, DECIPHER was used to check for chimeras (Wright *et al.*, 2012). Sequences were aligned using SINA Alignment Service (V1.2.11) (Pruesse *et al.*, 2012). The aligned almost full-length 16S rRNA sequences were merged with the SSU Ref NR 99 128 database (SSU Ref NR 128, September 2016) and a phylogenetic tree was constructed using the ARB software package (version arb-6.0.1) (Quast *et al.*, 2012). The phylogenetic tree was calculated using the ARB neighbor-joining algorithm from 1000 bootstraps samples with Jukes–Cantor correction and terminal filtering.

### 5.2.4. Biochemical tests

Biochemical properties of 21 selected isolates were determined using API 20NE strips according to manufacturer's instruction (BioMerieux, La Balme-les- Grottes, France). All tests were performed in duplicate and the results were interpreted following the manufacturer's instruction.



### 5.2.5. Motility assays

Swimming, swarming and twitching motility of the Sph isolates was assayed macroscopically and microscopically, in duplicate (*Filloux and Ramos 2014*). To assay swimming and swarming motility macroscopically, an overnight grown R2 broth culture was inoculated to an OD<sub>600</sub> of 0.1 in fresh R2 medium, grown to mid-exponential phase and centrally inoculated on M8 medium (adjusted to a final pH of 7.0 using NaOH) containing per litre 12.8 g Na<sub>2</sub>HPO<sub>4</sub> × 7 H<sub>2</sub>O, supplemented with 3.0 g agar or 3.0 g gellan gum (Wako pure chemical industries, Neuss, Germany), 10 mL of 20 % (w/v) glucose, 25 mL of 20 % (w/v) casamino acids, and 1 mL of 1M MgSO<sub>4</sub>, and grown for five days, as described previously (*Filloux and Ramos 2014*). To assay swimming microscopically, a mid-exponential culture was observed using phase contrast microscopy (Leica DM 750, Heerbrugg, Switzerland). To assay twitching macroscopically, colonies that were grown overnight on 1.5 % LBA (containing per litre 4.0 g Tryptone, BD Difco, Breda, The Netherlands), 2.0 g yeast extract (Merck Millipore, Darmstadt, Germany), and 2.0 g NaCl were picked and point inoculated to the bottom of LBA plates containing 1.0 % agar, and incubated at 30 °C for three days. To assay twitching microscopically, overnight grown colonies on twitching motility gellan gum plates (TMGG) (containing per 100 mL: 0.8 g gellan gum, 0.4 g tryptone, 0.2 g yeast extract, 0.2 g NaCl, 0.1 g MgSO<sub>4</sub> × 7H<sub>2</sub>O), were picked using a sterile plastic inoculation loop and streaked on a thin layer of a TMGG coated microscopic slide, covered by a glass coverslip and incubated at 30 °C. Microscopic images were recorded every 24 hours for 3 days using phase contrast microscopy equipped with a camera (Leica MC 120 HD) and connected to the LAS 4.5 software.

### 5.2.6. Growth parameters

To test growth at different pH values, NaCl concentrations, and temperatures, an overnight grown culture was used to inoculate R2 broth to an OD<sub>600</sub> of 0.1, and grown with the parameters specified below. To test growth at different pH values, the pH of R2 broth was set to 3.5, 4.0, 4.5, 5.0, 5.5 and 6.0 using a citric acid (0.5 M) – disodium hydrogen phosphate (0.5 M) buffered solution, and to pH 8.0, 8.5, 9.0, 9.5, 10.0, and 10.5 using a sodium carbonate (0.5 M) – sodium bicarbonate (0.5 M)

solution. To test growth at different NaCl concentrations, NaCl was added to R2 broth to 0, 3.5 and 5.0 % (w/v). Growth was tested at temperatures of 8, 15, 30, 37, 40, 42 and 45 °C. Determination of growth parameters was performed in duplicate and growth was monitored after two weeks by eye.

### **5.2.7. Electron microscopy**

For scanning electron microscopy (SEM) imaging, cells were grown in R2 broth at 30 °C and shaking at 200 rpm, and harvested in the mid-exponential phase. Bacterial cells were mounted on coverslips coated with Poly-L-Lysine (Fisher Scientific, Landsmeer, The Netherlands) and fixed with 3 % (v/v) glutaraldehyde and 1 % (v/v) OsO<sub>4</sub>, respectively. The sample was fixed for 1 hour at room temperature, dehydrated in graded ethanol solutions in water (30, 50, 70, 80, 90, 96, and 100 %) for 15 min each, and critical point dried using liquid carbon dioxide as transition fluid. The coverslips were coated with tungsten and examined with a scanning electron microscope (FEI Magellan 400, Eindhoven, The Netherlands).

### **5.2.8. Biofilm formation under static conditions**

Biofilm formation of the Sph isolates was assayed under static conditions using a microtiter plate assay as described previously, with some modifications (*Filloux and Ramos 2014*). The strains were grown overnight, diluted in fresh R2 broth medium to an OD<sub>600</sub> of 0.1 and grown to mid-exponential phase. Three wells of a polystyrene 96-wells flat-bottomed, hydrophobic polystyrene microtiter-plate (Corning incorporated, New York) were inoculated with 100 µL of the mid-exponential phase culture (OD<sub>600</sub> of 0.1) and statically incubated at 30 °C. Wells containing 100 µL R2 broth were taken as negative control. After 16 hours, the liquid was removed and wells were washed twice with sterile milliQ water. The plates were air-dried and the attached biomass was stained for 10 min with 125 µL 0.1 % (w/v) crystal violet. The unbound crystal violet was removed by rinsing the plates two times with milliQ water, after which the plates were air-dried. Attached biomass was subsequently solubilized in 150 µL 70 % ethanol. The optical density of this solution was measured at 570 nm using a microtiter plate reader (Victor 3 - 1420 Multilabel Counter, Perkin-Elmer, Waltham, MA, USA). The assay was performed in triplicate and the results were averaged.



### 5.2.9. Auto-aggregation

The ability to form cell aggregates was assayed quantitatively using OD<sub>600</sub> measurements as follows (Karched *et al.* 2015). The cell suspensions (grown for 24h in R2 medium) were centrifuged at 5000 *g* for 15 min at 4 °C and washed twice using buffered KCl (pH 6.0; 50 mM KCl, 1 mM CaCl<sub>2</sub>, 1 mM KH<sub>2</sub>PO<sub>4</sub>, 0.1 mM MgCl<sub>2</sub>). The turbidity of this culture was adjusted to OD<sub>600</sub> of 1.0 and an aliquot of 1 mL of this solution was pipetted into a micro-cuvette (VWR, Leuven, Belgium). The OD<sub>600</sub> was measured immediately (OD(0)) and after 24h (OD(24)). The percentage of auto-aggregation after 24h was calculated by eq. (1):

$$\% \text{ of aggregation} = \frac{OD(0) - OD(24)}{OD(0)} \cdot 100 \quad (1)$$

## 5.3. Results

### 5.3.1. Isolation and identification

To study the behavior of bacteria relevant in membrane-biofouling, we isolated 60 bacterial strains from twelve different membranes: ten used in full-scale operation and two in laboratory fouling simulation experiments. Because of the relevance of *Sphingomonadaceae* in membrane biofouling, the biomass obtained from the membranes was cultivated under conditions that select for *Sphingomonas* (Yim *et al.*, 2010). Nearly full-length 16S rRNA gene sequences were obtained from the sixty isolates (sequences varying in length from 1245 – 1431 bp, except for Sph43 and Sph56, which had a sequence length of 791 bp and 796 bp, respectively). The strains were assigned using BLAST searches against the nucleotide database to find the closest relative of named sequences in the GenBank. 39 of the 60 isolates did not belong to the *Sphingomonadaceae* family but belonged to groups that are commonly found on fouled membranes, including Actinobacteria and Bacteroidetes (Table S5.1.) (Ivnitsky *et al.*, 2007). The 21 *Sphingomonadaceae* (Sph) isolates that were selected for further characterization were isolated from six different membranes (Table 5.1., supplementary data S5.1.). In order to reveal the phylogenetic relationship between the Sph isolates, a phylogenetic tree was constructed based on the 16S rRNA gene sequences. This showed that the 21 Sph isolates clustered into 12 clades (a group of organisms considered as having evolved from a common ancestor) in the

genera *Sphingomonas*, *Sphingopyxis* and *Sphingobium* (Figure 5.1.). The members of each clade were isolated from the same membrane and therefore appeared to be paraphyletic (i.e. having a common evolutionary origin; Table 5.1.). As identical 16S rRNA gene sequences can be found in bacteria with divergent genomes, the 21 Sph isolates were assessed for biochemical (API) and physiological characteristics (swimming and twitching) to uncover their phylogenetic coherency (Hahn and Pöckl 2005, Filloux and Ramos 2014).

Table 5.1. Phylogenetic affiliation and origin of the Sph isolates.

Strain (clade)	Accession number*	Closest relative (%identity)	Closest cultivated relative (% identity)	Membrane type**	Feed water
Sph1 (A)	KP866793	<i>Sphingomonas</i> sp. GW5 (100%)	<i>Sphingomonas parapaucimobilis</i> strain NBRC 15100 (99%)	RO	Surface water (A.G. Wildervanckkanaal)
Sph2 (B)	KP866794	<i>Sphingomonas pseudosanguinis</i> strain HPLM-2 (100%)	<i>Sphingomonas sanguinis</i> strain NBRC 13937 (99%)	RO	Industrial wastewater (Starch production)
Sph3 (B)	KP866795	<i>Sphingomonas pseudosanguinis</i> strain HPLM-2 (99%)	<i>Sphingomonas sanguinis</i> strain NBRC 13937 (99%)	RO	Industrial wastewater (Starch production)
Sph4 (C)	KP866796	<i>Sphingobium</i> sp. EMB 221 (99%)	<i>Sphingobium yanoikuyae</i> strain NBRC 15102 (99%)	NF	Municipal wastewater
Sph5 (D)	KP866797	<i>Sphingomonas sanguinis</i> strain BAB-7166 (99%)	<i>Sphingomonas sanguinis</i> strain NBRC 13937 (99%)	MF	Tap water
Sph6 (E)	KP866798	<i>Sphingomonas echinoides</i> strain NRRL B-3127 (100%)	<i>Sphingomonas echinoides</i> strain NBRC 15742 (99%)	RO ***	Tap water
Sph7 (E)	KP866799	<i>Sphingomonas echinoides</i> strain NRRL B-3127 (100%)	<i>Sphingomonas echinoides</i> strain NBRC 15742 (99%)	RO***	Tap water
Sph10 (F)	KP866800	<i>Sphingomonas</i> sp. ZJ116 (100%)	<i>Sphingomonas melonis</i> strain DAPP-PG 224 (100%)	RO	Industrial wastewater (Starch production)
Sph11 (G)	KP866801	<i>Sphingomonas</i> sp. V1-2 (99%)	<i>Sphingomonas hankookensis</i> strain ODN7 (99%)	RO	Industrial wastewater (Starch production)
Sph16 (H)	KP866802	Uncultured bacterium clone HK34-1-11-4 (100%)	<i>Sphingomonas aquatilis</i> strain NBRC 16722 (98%)	RO	Surface water (A.G. Wildervanckkanaal)
Sph19 (A)	KP866803	<i>Sphingomonas</i> sp. GW5 (99%)	<i>Sphingomonas parapaucimobilis</i> strain NBRC 15100 (99%)	RO	Surface water (A.G. Wildervanckkanaal)
Sph22 (I)	KP866804	Uncultured bacterium HOCICI53 (100%)	<i>Sphingomonas hankookensis</i> strain ODN7 (99%)	RO	Surface water (A.G. Wildervanckkanaal)
Sph25 (A)	KP866805	<i>Sphingomonas</i> sp. GW5 (100%)	<i>Sphingomonas parapaucimobilis</i> strain NBRC 15100 (99%)	RO	Surface water (A.G. Wildervanckkanaal)
Sph27 (J)	KP866806	<i>Sphingomonas</i> sp. 2R-2 (99%)	<i>Sphingomonas hankookensis</i> strain ODN7 (99%)	RO	Industrial wastewater (Starch production)

Strain (clade)	Accession number*	Closest relative (%identity)	Closest cultivated relative (% identity)	Membrane type**	Feed water
Sph29 (A)	KP866807	<i>Sphingomonas</i> sp. GW5 (99%)	<i>Sphingomonas parapaucimobilis</i> strain NBRC 15100 (99%)	RO	Industrial wastewater (Starch production)
Sph30 (A)	KP866808	<i>Sphingomonas</i> sp. GW5 (99%)	<i>Sphingomonas parapaucimobilis</i> strain NBRC 15100 (99%)	RO	Industrial wastewater (Starch production)
Sph31 (A)	KP866809	<i>Sphingomonas</i> sp. GW5 (100%)	<i>Sphingomonas parapaucimobilis</i> strain NBRC 15100 (99%)	RO	Industrial wastewater (Starch production)
Sph32 (A)	KP866810	<i>Sphingomonas</i> sp. GW5 (100%)	<i>Sphingomonas parapaucimobilis</i> strain NBRC 15100 (99%)	RO	Industrial wastewater (Starch production)
Sph33 (K)	KP866811	<i>Sphingopyxis macrogoltabida</i> strain BSN54 (100%)	<i>Sphingopyxis soli</i> strain BL03 (99%)	RO	Industrial wastewater (Starch production)
Sph46 (L)	KP866812	<i>Sphingomonas</i> sp. HX-H01 (99%)	<i>Sphingobium xenophagum</i> strain BN6 (99%)	NF	Anoxic groundwater
Sph57 (L)	KP866813	<i>Sphingomonas</i> sp. HX-H01 (99%)	<i>Sphingobium xenophagum</i> strain BN6 (99%)	NF	Anoxic groundwater

\*) The 16S rRNA sequences of the Sph strains have been deposited in GenBank under accession numbers KP866793 - KP866813.

\*\*) RO = reverse osmosis, NF = nanofiltration, MF = microfiltration

\*\*\*) Bacteria isolated from membranes used in laboratory experiments.

### 5.3.2. Physiological and biochemical characteristics

The ability of the Sph isolates to proliferate at different temperatures, salinities and pH values was assessed. Growth was assessed for two weeks on a daily basis and qualitatively via macroscopic observation. All isolates grew at a temperature range of 8 to 37 °C (Table 5.2.). Sph16 and Sph57 grew between 8 and 42 °C, albeit at much lower growth rates compared to their optimum temperature. All Sph isolates grew at NaCl concentrations between 0 % and 3.5 %, and almost half (10/21) grew at 5.0 % NaCl. All isolates grew between pH values of 5 to 9, and many were either able to grow at pH 4 or at pH 10 (Table 5.2.). To compare the physiological features of the Sph isolates to closely related strains, we made an inventory of *Sphingomonas* type strains (Table S5.2. inclusion was based on alphabetical order). The biochemical properties of the 21 Sph isolates were profiled using API 20NE strips (Table S5.3.). To compare the characteristics of our Sph isolates with closely related strains, we made an inventory of *Sphingomonas* type strains (Table S5.3. inclusion was based on alphabetical order). All Sph isolates were able to assimilate glucose, maltose,

mannose and arabinose, except Sph6, which was unable to assimilate mannose. In addition, most Sph isolates tested positive for N-acetylglucosamine and malate assimilation, and for  $\beta$ -galactosidase activity.

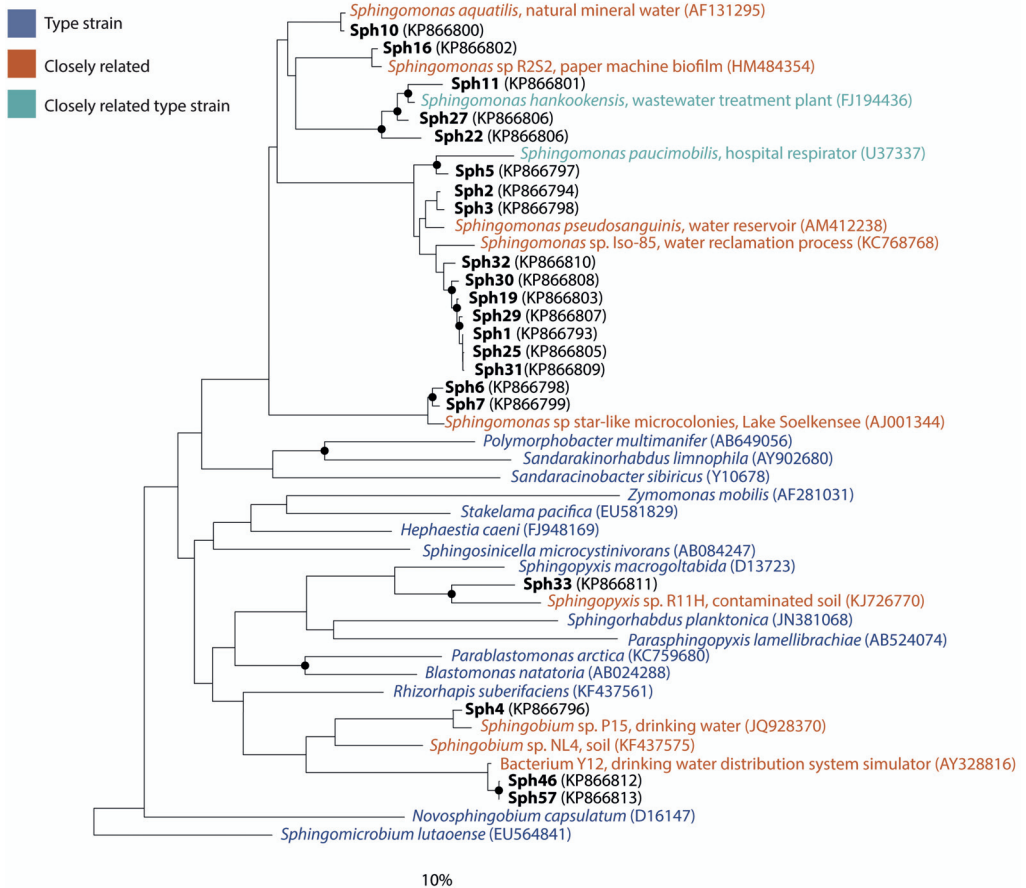


Figure 5.1. Phylogenetic tree inferred by the neighbour joining method using almost complete 16S rRNA gene sequences derived from the SILVA SSU Ref database and from the Sph isolates (this study). The tree was constructed using the ARB neighbour-joining method with terminal filtering and Jukes-Cantor correction. Closed circles represent bootstrap value > 50 % (1000 replicates). The scale bar represents the percentage of changes per nucleotide position. Color coding represents type species and closely related strains. Sequences found in this study are depicted in black and bold.

Table 5.2. Physiological characteristics of the Sph isolates.

Strain (Clade)	Swimming		Swarming	Twitching		Growth ranges		
	Micro*	Macro**		Micro***	Macro****	pH	Temp (°C)	Salt (NaCl% w/v)
Sph1 (A)	+	-	-	+	+	5.0–10.0	8–37	0–5.0
Sph2 (B)	+	+	-	+	+	5.0–10.0	8–37	0–5.0
Sph3 (B)	+	-	-	+	+	5.0–10.0	8–37	0–5.0
Sph4 (C)	+	+	-	+	-	5.0–10.0	8–37	0–3.5
Sph5 (D)	+	-	+	+	+	5.0–10.0	8–37	0–5.0
Sph6 (E)	+	+	+	+	+	5.0–10.0	8–37	0–5.0
Sph7 (E)	+	+	-	+	-	4.0–9.0	8–37	0–3.5
Sph10 (F)	-	+	-	+	-	5.0–10.0	8–37	0–3.5
Sph11 (G)	+	+	+	+	+	6.0–10.0	8–37	0–3.5
Sph16 (H)	-	-	-	+	+	4.0–10.0	8–42	0–3.5
Sph19 (A)	+	+	+	+	+	5.0–9.0	8–37	0–5.0
Sph22 (I)	+	+	-	+	+	5.0–10.0	8–37	0–3.5
Sph25 (A)	+	-	+	+	-	5.0–9.0	8–37	0–5.0
Sph27 (J)	+	+	-	+	+	5.0–9.0	8–37	0–3.5
Sph29 (A)	+	+	-	+	+	5.0–9.0	8–37	0–5.0
Sph30 (A)	+	+	+	+	+	5.0–10.0	8–37	0–5.0
Sph31 (A)	+	+	+	+	+	5.0–9.0	8–37	0–5.0
Sph32 (A)	+	+	+	+	+	5.0–10.0	8–37	0–5.0
Sph33 (K)	-	-	-	+	-	4.0–10.0	8–37	0–3.5
Sph46 (L)	+	-	-	+	+	5.0–10.0	8–37	0–3.5
Sph57 (L)	+	-	-	+	+	5.0–10.0	8–42	0–3.5

\*Swimming was assayed microscopically by phase contrast microscopy. \*\* Swimming and swarming was assayed macroscopically by plate assays. \*\*\*Twitching was assayed microscopically by growing the strains on TMGG medium amidst of a microscopic slide and a glass coverslip. \*\*\*\* Twitching was assayed macroscopically by growing the cells on twitching plates.

### 5.3.3. Twitching motility and pili

Twitching was assayed macroscopically using plate-based assays in which twitching is observed as the radial growth between the semisolid medium and the Petri dish. 17 of the 21 isolates (81 %) twitched on the twitching plates, indicating that these *Sph* isolates possess active pili (Table 5.2). Twitching motility was also visualized microscopically by growing the *Sph* isolates on TMGG medium amidst of a microscopic slide and a glass coverslip (Figure S5.1.), which confirmed the macroscopic observations (Filloux and Ramos 2014). All *Sph* isolates resembled the twitching phenotype of *Pseudomonas aeruginosa* strain PAK, which was observed using the same method (Filloux and Ramos 2014). In line with these observations, pili-like structures were observed for *Sph1* using SEM imaging (Figure 5.2.).

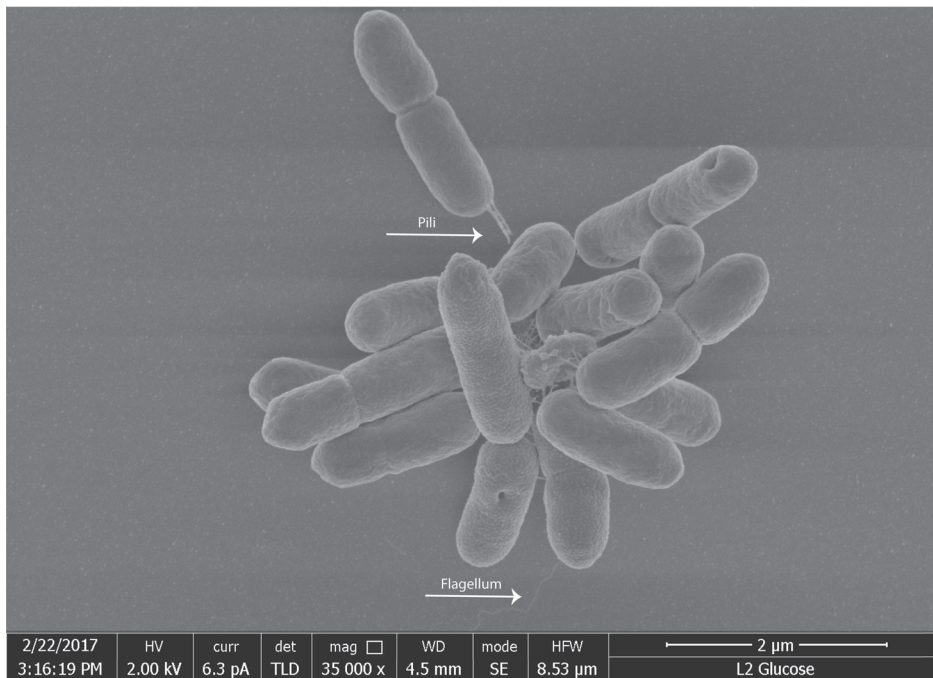
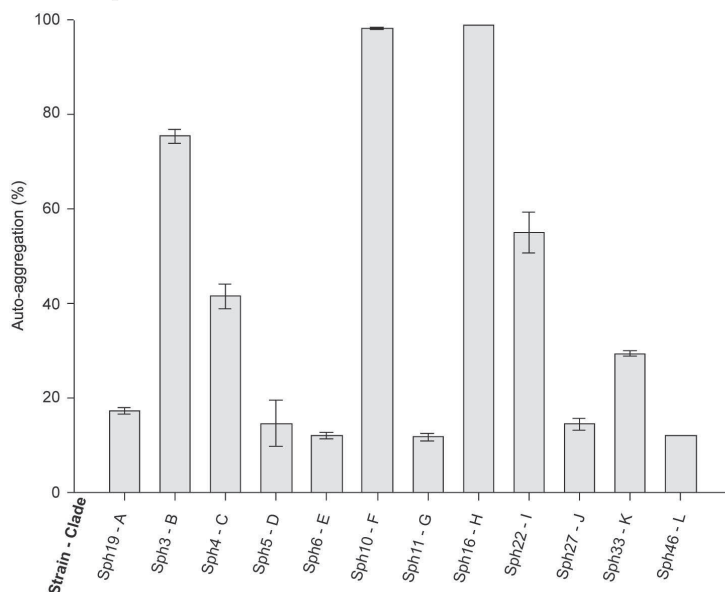


Figure 5.2. Scanning electron micrograph of membrane isolate *Sph1* mounted on Poly-L-Lysine coated coverslip. The cells were grown in R2medium and critical-point dried before being tungsten-coated. Scale bar is 2 μm.

### 5.3.4. Auto-aggregation and biofilm formation of 12 representative strains

Auto-aggregation was investigated by making repeated absorbance measurements for twelve unique strains (one strain was randomly selected per clade; *Figure 5.3.*). All 12 strains exhibited auto-aggregation. This observation was confirmed by microscopic observations (*data not shown*).



*Figure 5.3.* Auto-aggregation of the selected Sph isolates after 24h of incubation. Error bars indicate standard deviation from three replicates

The ability to form a biofilm under static conditions was assessed using the microtiter plate assay for the 12 representative strains. All representative strains formed biofilms, although the amount of attached biomass differed between strains (*Figure 5.4.*). We were unable to determine whether the Sph isolates formed co-aggregates, because the Sph isolates cannot be differentiated by microscopic observation and the spectrophotometric method lacked resolution to differentiate between auto-aggregation and co-aggregation.

### 5.3.5. Swimming motility and flagella

The ability of the Sph isolates to swim and swarm was investigated on plates solidified with agar using *P. aeruginosa* PAOI as positive control. Although *P. aeruginosa* PAOI tested positive, none of the Sph isolates was able to swim under these conditions. However, microscopic observations by phase contrast microscopy

indicated that 18 *Sph* isolates (86 %) are able to swim (Table 5.2). When agar was replaced with gellan gum, 14 *Sph* isolates (66 %) tested positive for either swimming or swarming. SEM imaging revealed that *Sph1* indeed produced a monotrichous polar flagellum (Figure 5.2.) and confirmed that besides clade A (*Sph1*), members of 8 of the other 10 clades produced a polar flagellum or monotrichous flagella (Figure 5.2.).

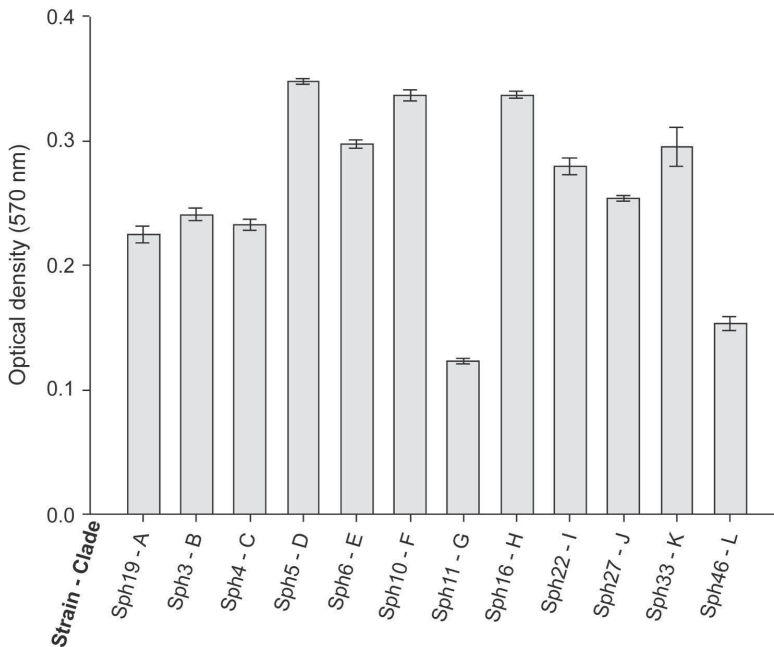


Figure 5.4. Biofilm formation of the selected *Sph* isolates: OD570 values of the crystal violet as measure of the amount of attached biomass after 16 h of incubation. Error bars represent standard deviation from three replicates.

## 5.4. Discussion

### 5.4.1. Comparison of the *Sph* isolates to closely related species: specific traits of the *Sph* membrane isolates

This study characterizes the physiology of *Sphingomonadaceae* membrane isolates, members of a family that previous studies have shown to be dominant on fouled membranes (Choi *et al.*, 2006, Huang *et al.*, 2008, Bereschenko *et al.*, 2010). Other studies investigating the microbial diversity and function of bacteria on high-pressure membranes used molecular identification technologies or investigated a small number of bacterial species for which the relative abundancy was unknown



(Pang et al., 2005, Ivnitsky et al., 2007, Bereschenko et al., 2010, Bae et al., 2011, Calderón et al., 2012, Kim et al., 2014, Nagarai et al., 2017, Yu et al., 2017). Comparison of the physiological features of the Sph isolates (Table 5.2.) to those of *Sphingomonas* type strains (Table S5.2.) shows that the tolerance for different temperatures, salt concentrations and pH values is high for the Sph isolates (Huang et al., 2008). Particularly their ability to tolerate multiple stressors is not often found among *Sphingomonadaceae*. For instance, *S. dokdonensis* and *S. aestuarii* are able to tolerate 5.0 % NaCl, but their growth range for different temperatures and pH values is more restricted compared to the Sph isolates (Table 5.2 and Table S5.2). The results presented here therefore highlight that physiological traits that were hitherto not affiliated to biofouling do contribute to the effective colonization of membrane surfaces by *Sphingomonadaceae*.

The versatile physiology of the Sph isolates explains why they maintain themselves on membrane surfaces and in the membrane installations. During membrane filtration, salts and carbohydrates accumulate on the membrane (Zhao et al., 2015). While the accumulated carbohydrates function as nutrient supply, the salt concentrations may become a stressor for microbial growth. Moreover, the pH is frequently and swiftly changed by the cleaning procedures that rely on acidic and alkaline cleaning agents to remove fouling (Beyer et al., 2017). These observations, as suggested before, support the hypothesis that the conditions on the membrane surface are highly selective (Nagaraj et al., 2017). This is also in line with the phylogenetic affiliation of the Sph isolates, which are most closely related to other *Sphingomonadaceae* isolated from water treatment systems or biofilms (Figure 5.1.).

However, the results presented here also clearly indicate that relative abundance, although used as an indicator of fitness of a whole group, would not have revealed the specific traits of the *Sphingomonadaceae* presented here. Conditions at the membrane surface are different from other habitats from which *Sphingomonadaceae* have been isolated. It is well-known that bacteria genetically and phenotypically adapt to changing environmental conditions, but this does not necessarily lead to sequence differences in the ribosomal operon (16S rRNA gene) (Hahn and Pöckl 2005). This implies that although molecular identification technologies, such as

next generation sequencing and FISH, accurately identify microbial communities, comparative analysis is limited by the reference database. Hence, culture-dependent approaches are key to discover the physiological and biochemical traits of representative bacteria. Some physiological features of the dominant bacteria on fouled membranes may have, for this reason, remained unknown. To determine which physiologies are required for membrane colonization, and to gain a better understanding of membrane biofouling, community studies should preferably be combined with culture-dependent or whole-genome analysis to uncover strain specific traits.

The number of different *Sphingomonadaceae* strains characterized in this study was limited to 21 strains because 39 of the membrane isolated strains did not belong to the *Sphingomonadaceae* family (Table 5.1. and Table S5.1.). These strains resisted the combination of streptomycin and piperacillin, although they do not belong to the *Sphingomonadaceae* family. However, this is not unpredictable based on the resistance of other bacteria to these antibiotics (Li *et al.*, 2017). Molecular identification is therefore essential in selecting *Sphingomonas* strains when using this selective isolation method. Some of the strains that were isolated from the same membrane share identical 16S rRNA sequences and appear not be unique but are rather paraphyletic because their physiological and biochemical traits are very similar. The strains Sph6 and Sph7 formed one clade, but differentiated in their biochemical and physiological behavior.

#### **5.4.2. *Sphingomonadaceae* have physiological advantages during membrane filtration**

There are several hypotheses for the dominance of *Sphingomonadaceae* in membrane biofilm formation. These include: (I) oligotrophic growth, (II) the arrangement of their cell wall, which is hydrophobic due to the presence of glycosphingolipids rather than lipopolysaccharides, (III) the EPS composition which facilitates membrane adhesion and also provides strong rigidity, and (IV) surface motility by twitching and swimming (Pang *et al.*, 2005, Gutman *et al.*, 2014, Haas *et al.*, 2015). Only one study has investigated the behavior of bacteria isolated from the influent of high-pressure membranes and this study illustrates that most of the

culturable bacteria present in the feed, including those belonging to the *Sphingomonadaceae* family, are nonmotile (Belgini *et al.*, 2014). Members of the *Sphingomonas* genus are known to be nonmotile or contain a single polar flagellum (Glaeser and Kämpfer, 2014) (Table S5.2.). All Sph isolates were motile, either by swimming, swarming or by twitching (Table 5.2.). These observations support the notion that flagella or pili might provide an advantage for membrane attached *Sphingomonadaceae*. Accordingly, Pang and coworkers, who showed that a *Sphingomonas* membrane isolate possessed both twitching and swarming motility, suggested that surface motility might be important in mediating (membrane) surface colonization (Pang *et al.*, 2005).

Flagella and type IV pili have multiple functions during biofilm formation. In membrane filtration, two flow directions affect membrane adhesion and biofilm formation: the flow parallel to the membrane (i.e. cross-flow) and the flow perpendicular to the membrane (i.e. permeate drag force) (Eshed *et al.*, 2008). Appendages like type IV pili and flagella are commonly used by bacteria to mediate surface attachment, but permeate drag forces make these appendages redundant for membrane adhesion (Eshed *et al.*, 2008). However, long-term biofouling experiments have shown that biofilm formation does not occur on the entire membrane, but strictly occurs close to the feed spacer where the cross-flow is quasi-stagnant (Picioreanu *et al.*, 2009, Vrouwenvelder *et al.*, 2009). Collectively, these observations imply that bacterial adhesion must occur on the entire membrane, but that biofilm formation is impeded on most locations due to the high cross-flow. *Sphingomonas leidyi* (previously *Caulobacter leidyi*) produces, in a process in which both flagella and pili play a key role, a holdfast that acts as a strong surface-adhesin for *Caulobacter* species (Chen *et al.*, 2012, Li *et al.*, 2013). Due to the high cross-flow velocities, this holdfast can be very favorable for the Sph isolates to establish a stable membrane interaction. Type IV pili (twitching) are important to form microcolonies via cell-aggregation (Klausen *et al.*, 2003, Min and Rickard 2009, Shen *et al.*, 2012, Ni *et al.*, 2016). For *Sphingomonas natatoria*, pili-mediated cell-aggregation has been proven essential for the dominance of *S. natatoria* in dual-species biofilms with *Micrococcus luteus* (Min and Rickard, 2009).

Like pili, flagella also have many important functions during the early and late biofilm formation stages. In the earliest biofilm stage, flagella provide a manner to sense the surface when flagellar rotation is interrupted. This mechano-sensing mechanism provides a signal to initiate biofilm formation (Belas 2014). *Sphingomonadaceae* and other closely related bacteria profit particularly from a flagellum because their cell wall is hydrophobic due to the presence of glycosphingolipids (Gutman *et al.*, 2012). Because of the hydrophilicity of the flagellum and the hydrophobicity of the cell wall, the interaction between the surface and *Sphingomonadaceae* is elastic, which stimulates surface exploration (Gutman *et al.*, 2012). Flagella are produced in mature biofilms, particularly at the outer edge of the biofilm, which indicates that flagella can be used for biofilm expansion (Serra *et al.*, 2013).

EPS plays a pivotal role in membrane biofouling because it provides embedded bacteria protection against cleaning agents (Flemming *et al.* 1997, Yu *et al.*, 2017). All Sph isolates formed biofilms, but the amount of attached biomass after 16h was different for most of the Sph isolates (Figure 5.4.). This is remarkable because EPS production is considered as an important feature for membrane colonization and survival (Flemming *et al.* 1997, Kim *et al.*, 2014). *Sphingomonadaceae* produce EPS with high mechanical and heat resistance; those produced by *S. paucimobilis* are even able to withstand autoclaving (Ashtaputre and Shah 1995). Therefore EPS quality might be a more important feature than EPS quantity. We have also shown that the Sph isolates have a flexible metabolism, which is beneficial for survival under conditions of changing nutrient supplies (Table S5.3.).

### **5.5. *Sphingomonadaceae* versatility: implications**

Biofouling remains the most frequent observed membrane fouling type, for reasons described above. Improved strategies to prevent biofouling are highly demanded because the current strategies to prevent (pretreatment of the influent) or control (membrane cleaning) biofouling are inadequate, relatively expensive, can damage the top layer of the membrane, lead to membrane downtime and add to the CO<sub>2</sub> footprint (Beyer *et al.*, 2017). Different types of cleaning agents can be used for biofouling removal. Alkaline and acidic cleaning removes organic foulants on

membranes and destroys the cell wall of microbes, respectively. Metal chelating agents and surfactants can be used to disintegrate EPS layers by removal of divalent cations and solubilisation of macromolecules, respectively (Beyer *et al.*, 2017). In many cases, membrane cleaning loses its efficiency over time, and this coincides with changes in the microbial community (Al Ashhab *et al.*, 2017). We show that the *Sph* isolates are, as free-floating bacteria, capable to grow under pH values that approach those used to remove membrane biofouling. This is in line with the work of Bereschenko *et al.*, who showed that members of the *Sphingomonadaceae* family are able to persist membrane cleaning, but this is uncommon for the *Sphingomonadaceae* family as a whole (Bereschenko *et al.*, 2011, Glaeser and Kämpfer 2014). The results of this study therefore indicate that the conditions on the membrane surface are selective for microbial populations that withstand these conditions. As a consequence, the biofilm embedded cells, and the EPS layer, become more difficult to remove over time.

Knowledge on the efficiency of membrane cleaning agents and their effect on bacteria is limited, possibly because the manufacturers in most cases are not very willing to share details. However, the results shown here indicate that biofilm ageing is an important factor that should be taken into account when investigating the proficiency of membrane cleaning agents under representative conditions. Another implication would be to frequently change the cleaning strategy to prevent microbial adaptation. However, similar approaches have been studied before and with low efficiency (Beyer *et al.*, 2017). This might indicate that aged biofilms in general are difficult to remove. The aim of more effective strategies should therefore be two-fold: (I) prevent biofilm formation on the membrane surface, and (II) prevent biofilms from adapting to the conditions during membrane cleaning.

## **Acknowledgments**

This work was performed in the cooperation framework of Wetsus, European Centre of Excellence for Sustainable Water Technology ([www.wetsus.nl](http://www.wetsus.nl)). Wetsus is cofounded by the Dutch Ministry of Economic Affairs and Ministry of Infrastructure and Environment, the European Union Regional Development Fund, the Province of Fryslân and the Northern Netherlands Provinces. Research of Alfons J.M. Stams is supported by the SIAM Gravitation grant (project 024.002.002) of the Netherlands Ministry of Education, Culture and Science and the Netherlands Science Foundation (NWO) and by the advanced ERC grant (project 323009). Research of Peer H.A. Timmers is supported by the SIAM Gravitation grant (project 024.002.002) of the Netherlands Ministry of Education, Culture and Science and the Netherlands Science Foundation (NWO).

## Supplementary data Chapter 5

### **Supplementary data S5.1. - Description of the isolation sources**

**Isolation source A** - Kisuma II: The isolates Sph16 and Sph22 were isolated from a reverse osmosis (RO) installation extensively reported in literature for its biofouling problems (Bereschenko *et al.*, 2008). The installation treats surface water for process water production. The feed water is first pre-treated by coagulation, flocculation and sand filtration and ultrafiltration, before entering the two-stage RO system (Bereschenko *et al.*, 2008). In this installation biofouling causes strong normalized pressure drop increase leading to a high cleaning frequency of about once per week.

**Isolation source B** - DWP Sas van Gent: The isolates Sph2, Sph3, Sph10, Sph11, Sph27 and Sph33 were retrieved from two lead RO membrane elements from an installation producing demineralized water from industrial wastewater effluent from a starch producing plant (van den Broek, *et al.*, 2010). The isolates Sph2 and Sph3 were recovered from a membrane element that was taken out shortly after chemical cleaning of the RO system, while the isolates Sph10, Sph12, Sph27 and Sph33 were recovered from a membrane element that was not cleaned for several weeks prior to membrane autopsies (Beyer *et al.*, 2017). The RO feed water is characterized by high temperatures (25 - 35 °C) and high concentration of total organic carbon (TOC; 15 - 25 mg TOC L<sup>-1</sup>). The treatment consists of an inline flocculation with iron, dual media filtration, ultrafiltration, antiscalant dosing, first stage RO system, degasifiers and a second stage RO system (van den Broek, *et al.*, 2010). When the effluent water quality is out of specifications, the RO is operated on drinking water to maintain demineralized water production. The RO stages are cleaned preventive once every 6 weeks.

**Isolation source C** - Engelse werk WTP: The isolates Sph46 and Sph57 were retrieved from a lead nanofiltration (NF) membrane element from an installation producing drinking water from anoxic groundwater, similar to the anoxic groundwater treating NF installations described in detail in (van der Meer *et al.*, 2004, Beyer *et al.*, 2014). The treatment main objectives is the removal of hardness, taste and organic micropollutants. The operation and performance of such anoxic

groundwater treating NF plants is typically very stable and unproblematic, resulting in a cleaning frequency of once per year or less (Beyer *et al.*, 2014).

**Isolation source D** – Laboratory cleaning experiments of full-scale membrane samples: The isolates Sph1, Sph19, Sph25, Sph29, Sph30, Sph31 and Sph32 were retrieved from full-scale membrane samples after cleaning in a laboratory flow-cell setup (Beyer *et al.*, 2017). Sph1, Sph19 and Sph25 membrane were retrieved from the membrane from isolation source A after laboratory cleaning, while Sph29, Sph30, Sph31 and Sph32 were retrieved from the laboratory cleaned membrane from isolation source B. For the cleaning experiments, smaller sheets of and spacer material from the full-scale 8” SWRO membrane elements (Isolation source A & B) were transferred to a membrane flow-cell (Beyer *et al.*, 2017). The membranes were then cleaned using procedures similar to full-scale. A typical cleaning protocol included a) Pre-Rinse with demineralized water, b) Acid cleaning circulation with P3-ultrasil 73 (45 min; T = 45°C), c) Rinse with demineralized water, d) Alkaline cleaning circulation with P3-ultrasil 53 (90 min; T=37°C; %1.5; pH=9,6-10,0), e) Alkaline cleaning soaking with P3-ultrasil 53 Alkaline - P3-ultrasil 53 (30min; T=30-45°C), f) Rinse with demineralized water g) Sanitizing circulation with P3-oxonia active (60 min; T=max 25°C; %1.0), h) Final rinse with demineralized water (Beyer *et al.*, 2017). The cleanings were performed at low pressure (~1bar) and high velocity (>0.2m s<sup>-1</sup>), similar to typical full-scale cleaning procedures. To evaluate cleaning efficiencies in terms of operation (e.g. differential pressure drop and flux), the membrane and spacer sheets were operated in a high pressure laboratory setup before and after cleaning (~1h of operation). Only after the performance evaluation the flow-cells were opened for membrane autopsies and the *Sphingomonadaceae* were isolated. It is possible that the isolated *Sphingomonadaceae* isolates from these samples survived the cleaning. However, it is more likely that the *Sphingomonadaceae* isolates originate from the Wetsus feed water used for membrane performance evaluation after cleaning.

**Isolation source E** - MBR-NF: Isolate Sph4 was recovered from a 2.5” DOW NF270 membrane element operated on MBR effluent from an integrated MBR NF system for municipal wastewater treatment with 100% NF concentrate recirculation back

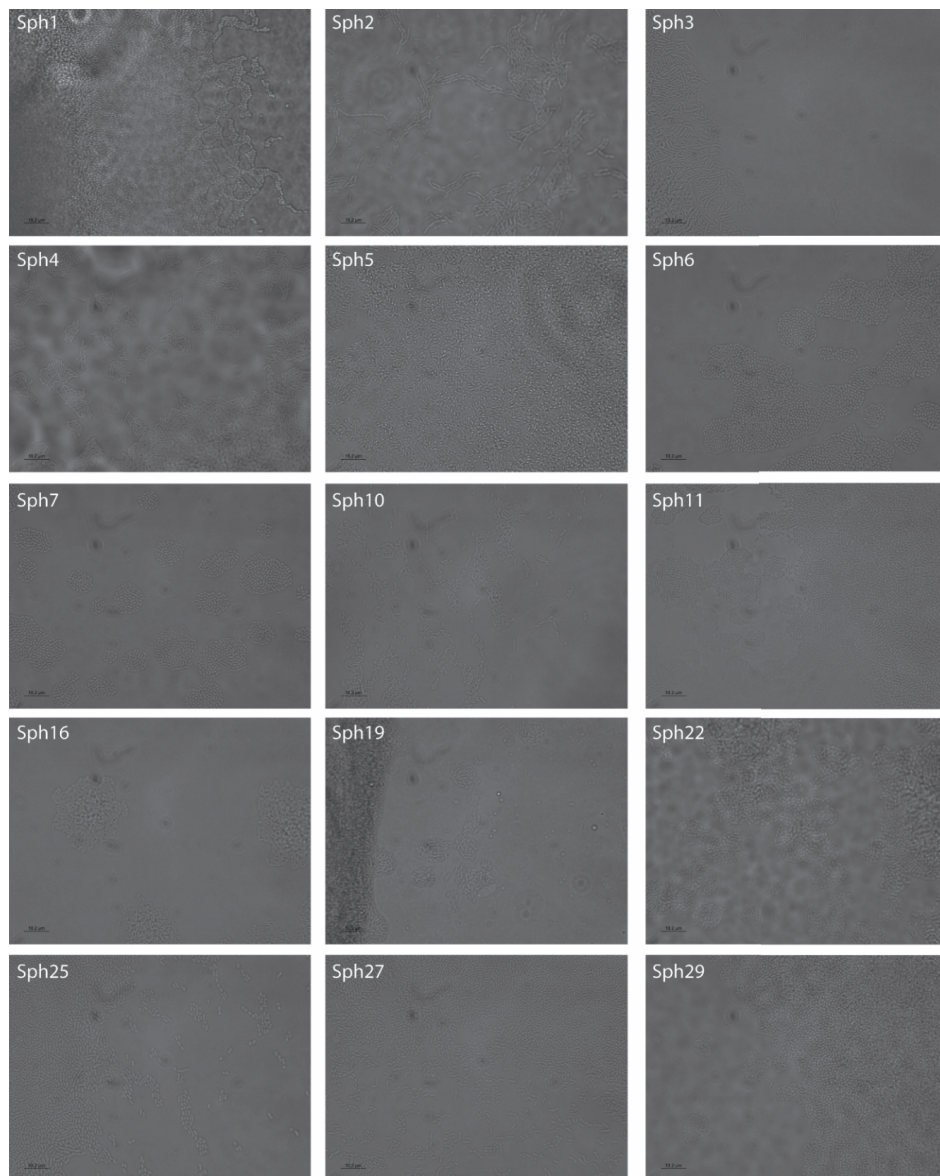


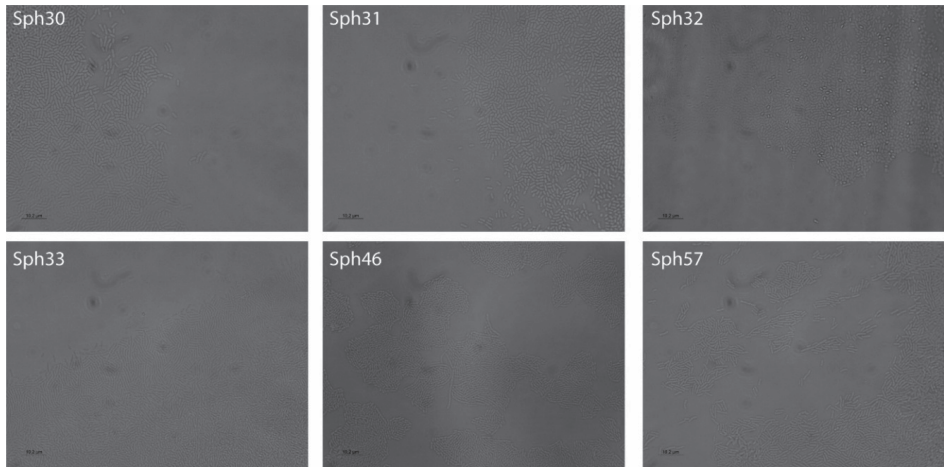
to the MBR (Kappel *et al.*, 2014). The NF feed was characterized by high concentration of total organic carbon ( $17\pm 4$  mg TOC L<sup>-1</sup>), phosphorus ( $18\pm 4$  mg PO<sub>4</sub><sup>3-</sup> L<sup>-1</sup>) and sulfate ( $43\pm 25$  mg SO<sub>4</sub><sup>2-</sup> L<sup>-1</sup>) (Kappel *et al.*, 2014).

**Isolation source F - NADIR MF:** The isolate Sph5 was recovered from a Nadir MP005 microfiltration flat sheet membrane used for laboratory flow-cell biofouling studies. The flow-cells are operated on drinking water with additional dosage of easily biodegradable nutrients (Dreszer *et al.*, 2014).

**Isolation source G – ESPA2 RO:** The isolates Sph6 and Sph7 were recovered from an accelerated laboratory flow-cell biofouling experiment and the flow-cell used was identical to the flow-cell used by Bereschenko *et al.* (2010).

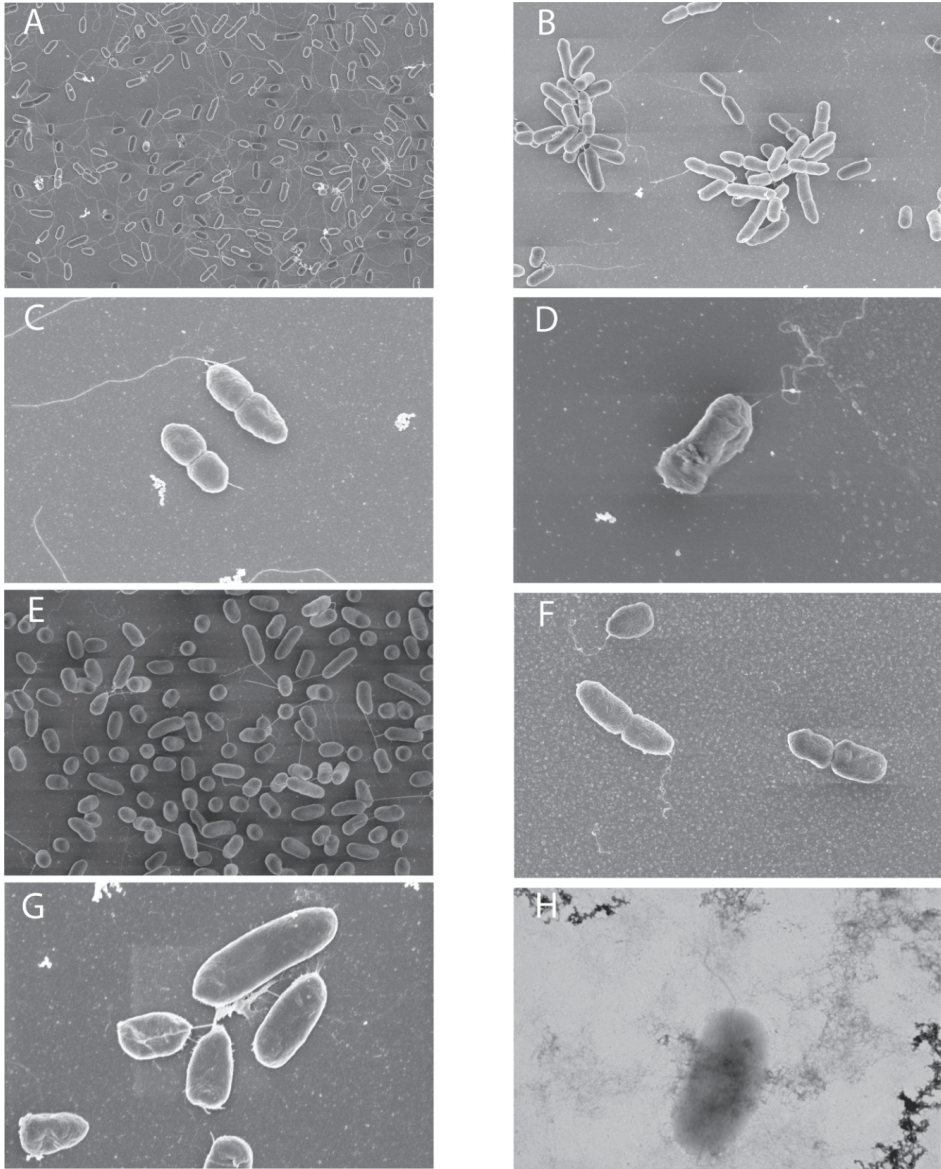
**Supplementary data – Figure S5.1.**





*Figure S5.1.* Phase contrast microscope micrographs of all Sph isolates twitching on the TMGG medium amidst of a microscopic slide after 24h of incubation. Under these conditions, twitching motility mediates active expansion of the colony and this results in the typical network of cells located at the leading edge of the colony. Twitching was considered positive in case the leading edge of the colony featured a lattice network of cells.

Supplementary data – Figure S5.2.



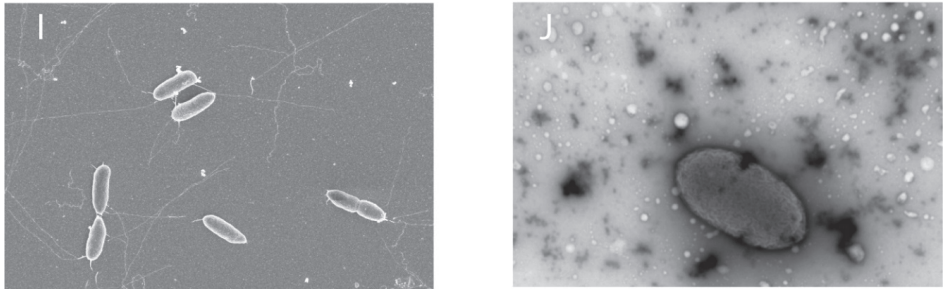


*Figure S5.2.* Scanning and transmission electron microscope micrographs of the Sph isolate clades B, C, D, E, F, G, H, I, J and K. Scanning electron microscopy was used to image Sph2, Sph4, Sph5, Sph6, Sph10, Sph11, Sph16 and Sph27. Transmission electron microscopy was used to image Sph22 and Sph33. A) at 10,000 times magnification: Sph2 (Clade B), B) at 20,000 times magnification: Sph4 (Clade C), C) at 50,000 times magnification: Sph5 (Clade D), D) at 80,000 times magnification: Sph6 (Clade E), E) at 25,000 times magnification: Sph10 (Clade F), F) at 20,000 times magnification: Sph11 (Clade G), G) at 50,000 times magnification: Sph16 (Clade H), H) at 100,000 times magnification: Sph22 (Clade I), I) at 25,000 times magnification: Sph27 (Clade J), J) at 100,000 times magnification: Sph33 (Clade K).

**Supplementary data – Table S5.1.**Table S5.1. Overview of the non-*Sphingomonadaceae* strains and their most closely related species.

Strain	Membrane	Feed water	Closest relative	Phylum
Sph8	RO	Tap water	<i>Pedobacter nutrimenti</i>	Bacteroidetes
Sph9	RO	Surface water	<i>Staphylococcus petrasii</i>	Firmicutes
Sph12	RO	Surface water	<i>Microbacterium hominis</i>	Actinobacteria
Sph13	RO	Surface water	<i>Pedobacter koreensis</i>	Bacteroidetes
Sph14	RO	Surface water	<i>Pedobacter koreensis</i>	Bacteroidetes
Sph15	RO	Surface water	<i>Pedobacter koreensis</i>	Bacteroidetes
Sph17	RO	Surface water	<i>Brevundimonas vesicularis</i>	Proteobacteria
Sph18	RO	Surface water	<i>Brevundimonas vesicularis</i>	Proteobacteria
Sph20	RO	Surface water	<i>Brevundimonas vesicularis</i>	Proteobacteria
Sph21	RO	Surface water	<i>Brevundimonas vesicularis</i>	Proteobacteria
Sph23	RO	Surface water	<i>Pedobacter koreensis</i>	Bacteroidetes
Sph24	RO	Surface water	<i>Pedobacter koreensis</i>	Bacteroidetes
Sph26	RO	Surface water	<i>Massilia aurea</i>	Proteobacteria
Sph28	RO	Surface water	<i>Brevundimonas vesicularis</i>	Proteobacteria
Sph34	RO	Surface water	<i>Pedobacter koreensis</i>	Proteobacteria
Sph35	RO	Surface water	<i>Microbacterium saccharophilum</i>	Actinobacteria
Sph36	RO	Surface water	<i>Pedobacter steynii</i>	Bacteroidetes
Sph37	RO	Surface water	<i>Pedobacter koreensis</i>	Bacteroidetes
Sph38	RO	Surface water	<i>Micrococcus antarcticus</i>	Actinobacteria
Sph39	RO	Surface water	<i>Chryseobacterium taeanense</i>	Bacteroidetes
Sph40	NF	Anoxic Groundwater	<i>Microbacterium oxydans</i>	Actinobacteria
Sph41	NF	Anoxic Groundwater	<i>Microbacterium oxydans</i>	Actinobacteria
Sph42	NF	Anoxic Groundwater	<i>Rhodococcus cerastii</i>	Actinobacteria
Sph43	NF	Anoxic Groundwater	<i>Rhodococcus cerastii</i>	Actinobacteria
Sph44	NF	Anoxic Groundwater	<i>Rhodococcus cerastii</i>	Actinobacteria
Sph45	NF	Anoxic Groundwater	<i>Dyella ginsengisoli</i>	Proteobacteria



Strain	Membrane	Feed water	Closest relative	Phylum
Sph47	NF	Anoxic Groundwater	<i>Dietzia cercidiphylli</i>	Actinobacteria
Sph48	NF	Anoxic Groundwater	<i>Dyella ginsengisoli</i>	Proteobacteria
Sph49	NF	Anoxic Groundwater	<i>Dyella ginsengisoli</i>	Proteobacteria
Sph50	NF	Anoxic Groundwater	<i>Mitsuaria chitosanitabida</i>	Proteobacteria
Sph51	NF	Anoxic Groundwater	<i>Microbacterium oxydans</i>	Actinobacteria
Sph52	NF	Anoxic Groundwater	<i>Rhodococcus cerastii</i>	Actinobacteria
Sph53	NF	Anoxic Groundwater	<i>Microbacterium phyllosphaerae</i>	Actinobacteria
Sph54	NF	Anoxic Groundwater	<i>Rhodococcus cerastii</i>	Actinobacteria
Sph55	NF	Anoxic Groundwater	<i>Mitsuaria chitosanitabida</i>	Proteobacteria
Sph56	RO	Surface water	<i>Rhodococcus cerastii</i>	Actinobacteria
Sph58	NF	Anoxic Groundwater	<i>Microbacterium oxydans</i>	Actinobacteria
Sph59	NF	Anoxic Groundwater	<i>Microbacterium oxydans</i>	Actinobacteria
Sph60	RO	Surface water	<i>Terrabacter terrae</i>	Actinobacteria

**Supplementary data – Table S5.2.**Table S5.2. Physiological characteristics of *Spingomonas* type strains.

Strain	Source	Motile by flagella	Growth tolerance			Reference
			pH	Temp (°C)	Salt (NaCl % w/v)	
<i>S. alpina</i>	Soil	Yes	6.0–10.0	1–30	0–1.0	1
<i>S. arantia</i>		No	6.0–9.0	4–35	0–0.5	2
<i>S. changbaiensis</i>		Yes	5.0–8.0	20–33	0–0.1	3
<i>S. desiccabilis</i>		No	N.D.	15–37	0–4.0	4
<i>S. dokdonensis</i>		Yes	5.0–9.5	10–34	0–5.0	5
<i>S. flava</i>		No	6.5–8.5	18–30	0–2.5	6
<i>S. formosensis</i>		Yes	5.0–9.0	25–37	0–3.0	7
<i>S. alaskensis</i>	Freshwater	Yes	N.D.	4–48	0–3.0	8
<i>S. astaxanthinifaciens</i>		Yes	5.5–11.0	20–45	>0.25	9
<i>S. daechungensis</i>		No	5.0–9.0	15–37	0.5–3.0	10
<i>S. fonticola</i>		Yes	5.0–8.0	15–37	0–1.0	11
<i>S. hankookensis</i>		No	4.0–10.0	4–37	0–1.0	12
<i>S. hengshuiensis</i>		Yes	5.0–10.0	20–35	0–1.0	13
<i>S. jaspsi</i>		Yes	6.0–9.0	20.0–40.0	>0.25	14
<i>S. abaci</i>	Hospital table	No	N.D.	15–37	0–1.0	15
<i>S. aerophila</i>	Air	Yes	6.0–9.0	4–37	0–1.0	16
<i>S. aestuarii</i>	Sediment	No	N.D.	20–35	0–5.0	17
<i>S. endophytica</i>	Plant	Yes	N.D.	12–45	0–1.0	18
<i>S. gei</i>	Plant	Yes	6.0–9.0	4–33	0–2.0	19
<i>S. gimensis</i>	Mine	Yes	6.0–8.0	15–32	0–4.0	20
<i>S. ginsengisoli</i>	Ginseng field	No	N.D.	15–37	0–1.0	21

N.D.: not determined.

**References to Table S5.2.**

1 (Margesin et al., 2012), 2 (Jia et al., 2015), 3 (Zhang et al., 2010), 4 (Reddy and Garcia-Pichel 2007), 5 (Yoon et al., 2006), 6 (Du et al., 2015), 7 (Lin et al., 2012), 8 (Vancanneyt et al., 2001), 9 (Asker et al., 2007a), 10 (Huy et al., 2014), 11 (Sheu et al., 2015), 12 (Yoon et al., 2009), 13 (Wei et al., 2015), 14 (Asker et al 2007b), 15 (Busse et al., 2005), 16 (Kim et al., 2014), 17 (Roh et al., 2009), 18 (Huang et al., 2012), 19 (Zhu et al., 2015), 20 (Feng et al., 2014), 21 (An et al., 2013)









## References

- Al Ashhab, A., Sweity, A., Bayramoglu, B., Herzberg, M. & Gillor, O. Biofouling of reverse osmosis membranes: effects of cleaning on biofilm microbial communities, membrane performance, and adherence of extracellular polymeric substances. *Biofouling*. 33(5): 397-409 (2017).
- An, D.-S. Liu, Q.M., Lee, H.G., Jung, M.S., Kim, S.C., Lee, S.T., Im, W.T. *Sphingomonas ginsengisoli* sp. nov. and *Sphingomonas sediminicola* sp. nov. *J. Syst. Evol. Microbiol.* 63: 496-501 (2013).
- Ashtaputre, A.A., Shah, A. K. Studies on a viscous, gel-forming exopolysaccharide from *Sphingomonas paucimobilis* GSI. *Appl. Environ. Microbiol.* 61(3): 1159-1162 (1995).
- Asker, D., Beppu, T., Ueda, K. *Sphingomonas astaxanthinifaciens* sp. nov., a novel astaxanthin-producing bacterium of the family Sphingomonadaceae isolated from Misasa, Tottori, Japan. *FEMS Microbiol Lett.* 273: 140-148 (2007a).
- Asker, D., Beppu, T., Ueda, K. *Sphingomonas jaspsi* sp. nov., a novel carotenoid-producing bacterium isolated from Misasa, Tottori, Japan. *J. Syst. Evol. Microbiol.* 57: 1435-1441 (2007b).
- Bae, H., Kim, H., Jeong, S., Lee, S. Changes in the relative abundance of biofilm-forming bacteria by conventional sand-filtration and microfiltration as pretreatments for seawater reverse osmosis desalination. *Desalination*. 273(2-3): 258-266 (2011).
- Barnett, T.P., Adam, J.C., Lettenmaier, D.P. Potential impacts of a warming climate on water availability in snow-dominated regions. *Nature*. 438: 303-309 (2005).
- Belas, R. Biofilms, flagella, and mechanosensing of surfaces by bacteria, *Trends Microbiol.* 22(9): 517-527 (2014).
- Belgini, D.R.B., Dias, R.S., Siqueira, V.M., Valadares, L.A., Albanese, J.M., Souza, R.S., Torres, A.P., Sousa, M.P., Silva, C.C., De Paula, S.O., Oliveira, V.M. Culturable bacterial diversity from a feed water of a reverse osmosis system, evaluation of biofilm formation and biocontrol using phages. *World J. Microbiol. Biotechnol.* 30(10): 2689-2700 (2014).
- Bereschenko, L., Heilig, G.H.J., Nederlof, M.M., van Loosdrecht, M.C.M., Stams, A.J.M., Euverink, G.-J.W. Molecular characterization of the bacterial communities in the different compartments of a full-scale reverse-osmosis water purification plant. *Appl. Environ. Microbiol.* 74(17): 5297-5304 (2008).
- Bereschenko, L.A., Stams, A.J.M., Euverink, G.J.W., van Loosdrecht, M.C.M. Biofilm formation on reverse osmosis membranes is initiated and dominated by *Sphingomonas* spp. *Appl. Environ. Microbiol.* 76(8): 2623-2632 (2010).
- Bereschenko, L.A., Prummel, H., Euverink, G.J.W., Stams, A.J.M., van Loosdrecht, M.C.M. Effect of conventional chemical treatment on the microbial population in a biofouling layer of reverse osmosis systems. *Water Res.* 45(2): 405-416 (2011).
- Beyer, F., Rietman, B.M., Zwijnenburg, A., van den Brink, P., Vrouwenvelder, J.S., Jarzembowska, M., Laurinonyte, J., Stams, A.J.M., Plugge, C.M. Long-term performance and fouling analysis of full-scale direct nanofiltration (NF) installations treating anoxic groundwater. *J. Membr. Sci.* 468: 339-348 (2014).
- Beyer, F., Laurinonyte, J., Zwijnenburg, A., Stams, A.J.M., Plugge, C.M. Membrane fouling and chemical cleaning in three full-scale reverse osmosis plants producing demineralized water. *J. Eng.* 2017: 1-14 (2017).

- Busse, H.-J., Hauser, E., Kämpfer, P. Description of two novel species, *Sphingomonas abaci* sp. nov. and *Sphingomonas panni* sp. nov. *J. Syst. Evol. Microbiol.* 55: 2565-2569 (2005).
- Calderón, K., González-Martínez, A., Montero-Puentea, C., Reboleiro-Rivas, P., Poyatos, J.M., Juárez-Jiménez, B., Martínez-Toledo, M.V., Rodelas, B. Bacterial community structure and enzyme activities in a membrane bioreactor (MBR) using pure oxygen as an aeration source. *Bioresour. Technol.* 103(1): 87-94 (2012).
- Chen, H., Jogler, M., Rohde, M., Klenk, H.P., Busse, H.J., Tindall, B.J., Spröer, C., Overmann, J. Reclassification and emended description of *Caulobacter leidyi* as *Sphingomonas leidyi* comb. nov., and emendation of the genus *Sphingomonas*, *Int. J. Syst. Evol. Microbiol.* 62(P112): 2835-2843 (2012).
- Choi, H., Zhang, K., Dionysiou, D.D., Oerther, D.B., Sorial, G.A. Effect of activated sludge properties and membrane operation conditions on fouling characteristics in membrane bioreactors. *Chemosphere.* 63: 1699-1708 (2006).
- Costerton, J.W., Cheng, K.J., Geesey, G.G., Ladd, T.I., Nickel, J.C., Dasgupta, M., Marrie, T.J. Bacterial biofilms in nature and disease. *Annu. Rev. Microbiol.* 41: 435-464 (1987).
- Dewhirst, F.E., Chien, C.C., Paster, B.J., Ericson, R.L., Orcutt, R.P., Schauer, D.B., Fox, J.G. Phylogeny of the defined murine microbiota: altered Schaedler flora. *Appl. Environ. Microbiol.* 65(8): 3287-3292 (1999).
- Dreszner, C., Wexler, A.D., Drusová, S., Overdijk, T., Zwijnenburg, A., Flemming, H.C., Kruithof, J.C., Vrouwenvelder, J.S. In-situ biofilm characterization in membrane systems using optical coherence tomography: Formation, structure, detachment and impact of flux change. *Water Res.* 67: 243-254 (2014).
- Du, J., Singh, H., Won, K.H., Yang, J.E., Akter, S., Jin, F.-X., Yi, T.H. *Sphingomonas flavus* sp. nov. isolated from road soil. *Arch. Microbiol.* 197(7): 883-888 (2015).
- Eshed, L., Yaron, S., Dosoretz, G.C. Effect of permeate drag force on the development of a biofouling layer in a pressure-driven membrane separation system. *Appl. Environ. Microbiol.* 74(23): 7338-7347 (2008).
- Feng, G.-D., Yang, S.Z., Wang, Y.H., Zhao, G.Z., Deng, M.R., Zhu, H.H. *Sphingomonas gimensis* sp. nov., a novel Gram-negative bacterium isolated from abandoned lead-zinc ore mine. *Antonie van Leeuwenhoek.* 105: 1091-1097 (2014).
- Filloux, A. and Ramos, J.-L. *Pseudomonas Methods and Protocols.* (Springer, 2014).
- Flemming, H.C., Schaule, G., Griebe, T., Schmitt, J., Tamachkiarowa, A. Biofouling—the Achilles heel of membrane processes. *Desalination* 113(2-3): 215-225 (1997).
- Glaeser, S. P. and Kämpfer, P. in *The Prokaryotes* 641-707 (Springer, 2014).
- Gutman, J., Walker, S.L., Freger, V., Herzberg, M. Bacterial attachment and viscoelasticity: physicochemical and motility effects analyzed using quartz crystal microbalance with dissipation (QCM-D). *Environ. Sci. Technol.* 47(1): 398-404 (2012).
- Gutman, J., Herzberg, M., Walker, S. L. Biofouling of reverse osmosis membranes: Positively contributing factors of *Sphingomonas*. *Environ. Sci. Technol.* 48(23): 13941-13950 (2014).
- Haas, R., Gutman, J., Wardrip, N.C., Kawahara, K., Uhl, W., Herzberg, M., Arnusch, C.J. Glycosphingolipids enhance bacterial attachment and fouling of nanofiltration membranes. *Environ. Sci. Tech. Let.* 2(2): 43-47 (2015).

- Hahn, M.W., Pöckl, M. Ecotypes of planktonic Actinobacteria with identical 16S rRNA genes adapted to thermal niches in temperate, subtropical, and tropical freshwater habitats. *Appl. Environ. Microbiol.* 71(2): 766-773 (2005).
- Herzberg, M., Elimelech, M. Physiology and genetic traits of reverse osmosis membrane biofilms: a case study with *Pseudomonas aeruginosa*. *ISME J.* 2(2): 180-194 (2007).
- Huang, L.-N., de Wever, H., Diels, L. Diverse and distinct bacterial communities induced biofilm fouling in membrane bioreactors operated under different conditions. *Environ. Sci. Technol.* 42(22): 8360-8366 (2008).
- Huang, H.-Y., Zhao, G.Z., Zhu, W.Y., Yang, L.L., Tang, H.Y., Xu, L.H., Li, W.J. *Sphingomonas endophytica* sp. nov., isolated from *Artemisia annua* L. *J. Syst. Evol. Microbiol.* 62: 1576-1580 (2012).
- Huy, H., Jin, L., Lee, K.C., Kim, S.G., Lee, J.S., Ahn, C.Y., Oh, H.M. *Sphingomonas daechungensis* sp. nov., isolated from sediment of a eutrophic reservoir. *J. Syst. Evol. Microbiol.* 64: 1412-1418 (2014).
- Ivnitsky, H., Katz, I., Minz, D., Volvovic, G., Shimoni, E., Kesselman, E., Semiat, R., Dosoretz, C.G. Bacterial community composition and structure of biofilms developing on nanofiltration membranes applied to wastewater treatment. *Water Res.* 41(17): 3924-3935 (2007).
- Jia, L., Zheng, Z., Feng, X., Nogi, Y., Yang, A., Zhang, Y., Han, L., Lu, Z., Lv, J. *Sphingomonas arantia* sp. nov., isolated from Hoh Xil basin, China. *Antonie van Leeuwenhoek.* 108: 1341-1347 (2015).
- Kappel, C., Kemperman, A.J.B., Temmink, H., Zwijnenburg, A., Rijnaarts, H.H.M., Nijmeijer, K. Impacts of NF concentrate recirculation on membrane performance in an integrated MBR and NF membrane process for wastewater treatment, *J. Membr. Sci.* 453: 359-368 (2014).
- Karched, M., Bhardwaj, R.G., Asikainen, S.E. Coaggregation and biofilm growth of *Granulicatella* spp. with *Fusobacterium nucleatum* and *Aggregatibacter actinomycetemcomitans*, *BMC Microbiology.* 15: 114 (2015).
- Kim, I.S., Lee, J., Kim, S.-J., Yu, H.-W., Jang, A. Comparative pyrosequencing analysis of bacterial community change in biofilm formed on seawater reverse osmosis membrane. *Environ. Technol.* 35(1-4): 125-136 (2014).
- Kim, S.-J., Moon J.Y., Lim, J.M., Ahn, J.H., Weon, H.Y., Ahn, T.Y., Kwon, S.W. *Sphingomonas aerophila* sp. nov. and *Sphingomonas naasensis* sp. nov., isolated from air and soil, respectively. *J. Syst. Evol. Microbiol.* 64: 926-932 (2014).
- Klausen, M., Aaes-Jørgensen, A., Molin, S., Tolker-Nielsen, T. Involvement of bacterial migration in the development of complex multicellular structures in *Pseudomonas aeruginosa* biofilms. *Mol. Microbiol.* 50(1): 61-68 (2003).
- Lane, D. J. 16S/23S rRNA sequencing. *Nucleic acid techniques in bacterial systematics.* 125-175 (1991).
- Li, G., Brun, Y.V., Tang, J.X. Holdfast spreading and thickening during *Caulobacter crescentus* attachment to surfaces, *BMC Microbiol.* 13: 139 (2013).
- Li, J., Cao, J., Wang, X., Liu, N., Wang, W., Luo, Y. *Acinetobacter pittii*, an emerging new multi-drug resistant fish pathogen isolated from diseased blunt snout bream (*Megalobrama amblycephala* Yih) in China, *Appl. Microbiol. Biotechnol.* 101(16): 6459-6471 (2017).
- Lin, S.-Y., Shen, F.T., Lai, W.A., Zhu, Z.L., Chen, W.M., Chou, J.H., Lin, Z.Y., Young, C.C. *Sphingomonas formosensis* sp. nov., a polycyclic aromatic hydrocarbon-degrading bacterium isolated from agricultural soil. *J. Syst. Evol. Microbiol.* 62(7): 1581-1586 (2012).

- López, D., Vlamakis, H., Kolter, R. Biofilms. *Cold Spring Harb. Perspect. Biol.* 2(7): a000398 (2010).
- Margesin, R., Zhang, D.-C., Busse, H.-J. *Sphingomonas alpina* sp. nov., a psychrophilic bacterium isolated from alpine soil. *J. Syst. Evol. Microbiol.* 62: 1558-1563 (2012).
- Min, K.R., Rickard, A. H. Coaggregation by the freshwater bacterium *Sphingomonas natatoria* alters dual-species biofilm formation. *Appl. Environ. Microbiol.* 75(12): 3987-3997 (2009).
- Nagaraj, V., Skillman, L., Ho, G., Li, D., Gofton, A. Characterisation and comparison of bacterial communities on reverse osmosis membranes of a full-scale desalination plant by bacterial 16S rRNA gene metabarcoding. *npj Biofilms and Microbiomes.* 3(13): 1-14 (2017).
- Ni, L., Yang, S., Zhang, R., Jin, Z., Chen, H., Conrad, J.C., Jin, F. Bacteria differently deploy type-IV pili on surfaces to adapt to nutrient availability. *npj Biofilms and Microbiomes.* 2: 15029 (2016).
- Pang, C.M., Hong, P., Guo, H., Liu, W.-T. Biofilm formation characteristics of bacterial isolates retrieved from a reverse osmosis membrane. *Environ. Sci. Technol.* 39(19): 7541-7550 (2005).
- Pang, C.M., Liu, W.T. Community structure analysis of reverse osmosis membrane biofilms and the significance of Rhizobiales bacteria in biofouling. *Environ. Sci. Technol.* 41(13): 4728-4734 (2007).
- Picioreanu, C., Vrouwenvelder, J.C., van Loosdrecht, M.C.M. Three-dimensional modeling of biofouling and fluid dynamics in feed spacer channels of membrane devices. *J. Membr. Sci.* 345(1-2): 340-354 (2009).
- Pruesse, E., Peplies, J., Glöckner, F. O. SINA: accurate high-throughput multiple sequence alignment of ribosomal RNA genes. *Bioinformatics.* 28(14): 1823-1829 (2012).
- Quast, C., Pruesse, E., Yilmaz, P., Gerken, J., Schweer, T., Yarza, P., Peplies, J., Glöckner, F.O. The SILVA ribosomal RNA gene database project: improved data processing and web-based tools. *Nucleic Acids Res.* 41: D590-6 (2012).
- Reddy, G., Garcia-Pichel, F. *Sphingomonas mucosissima* sp. nov. and *Sphingomonas desiccabilis* sp. nov., from biological soil crusts in the Colorado Plateau, USA. *J. Syst. Evol. Microbiol.* 57: 1028-1034 (2007).
- Roh, S.W., Kim, K.H., Nam, Y.D., Chang, H.W., Kim, M.S., Oh, H.M., Bae, J.W. *Sphingomonas aestuarii* sp. nov., isolated from tidal flat sediment. *J. Syst. Evol. Microbiol.* 59: 1359-1363 (2009).
- Serra, D.O., Richter, A.M., Klauck, G., Mika, F., Hengge, R. Microanatomy at cellular resolution and spatial order of physiological differentiation in a bacterial biofilm. *mBio.* 4: e00103-00113 (2013).
- Shannon, M.A., Bohn, P.W., Elimelech, M., Georgiadis, J.G., Mariñas, B.J., Mayes, A.M. Science and technology for water purification in the coming decades. *Nature.* 452: 301-310 (2008).
- Shen, Y., Siryaporn, A., Lecuyer, S., Gitai, Z., Stone, H.A. Flow directs surface-attached bacteria to twitch upstream. *Biophys. J.* 103(1): 146-151 (2012).
- Sheu, S.-Y., Chen, Y.-L., Chen, W.-M. *Sphingomonas fonticola* sp. nov., isolated from spring water. *J. Syst. Evol. Microbiol.* 65: 4495-4502 (2015).
- Takeuchi, M., Hamana, K., Hiraishi, A. Proposal of the genus *Sphingomonas* sensu stricto and three new genera, *Sphingobium*, *Novosphingobium* and *Sphingopyxis*, on the basis of phylogenetic and chemotaxonomic analyses. *Int. J. Syst. Evol. Microbiol.* 51(PT4): 1405-1417 (2001).
- van den Broek, W., Boorsma, M.J., Huiting, H., Dusamos, M.G., van Agtmaal, S. Prevention of biofouling in industrial RO systems: Experiences with peracetic acid. *Water Pract. Technol.* 5(2): 1-11 (2010).

- van der Meer, W.G., van Paassen, J.A.M., Riemersma, M.C., van Ekkendonk, F.H.J. *Optiflux®: from innovation to realisation, Desalination* 157(1-3): 159-165 (2003).
- Vancanneyt, M., Schut, F., Snauwaert, C., Goris, J., Swings, J., Gottschal, J.C. *Sphingomonas alaskensis* sp. nov., a dominant bacterium from a marine oligotrophic environment. *J. Syst. Evol. Microbiol.* 51: 73-79 (2001).
- Voutchkov, N. Considerations for selection of seawater filtration pretreatment system. *Desalination.* 261(3): 354-364 (2010).
- Vrouwenvelder, J.S., van der Kooij, D. Diagnosis, prediction and prevention of biofouling of NF and RO membranes. *Desalination.* 139(1-3): 65-71 (2001).
- Vrouwenvelder, J.S., von der Schulenburg, D.A.G., Kruihof, J.C., Johns, M.L., van Loosdrecht, M.C.M. Biofouling of spiral-wound nanofiltration and reverse osmosis membranes: a feed spacer problem. *Water Res.* 43(3): 583-594 (2009).
- Wei, S., Wang, T., Liu, H., Zhang, C., Guo, J., Wang, Q., Liang, K., Zhang, Z. *Sphingomonas hengshuiensis* sp. nov., isolated from lake wetland. *J. Syst. Evol. Microbiol.* 65: 4644-4649 (2015).
- Weisburg, W.G., Barns, S.M., Pelletier, D.A., Lane, D.J. 16S ribosomal DNA amplification for phylogenetic study, *J. Bacteriol.* 173(2): 697-703 (1991).
- Werber, J.R., Osuji, C.O., Elimelech, M. Materials for next-generation desalination and water purification membranes. *Nat. Rev. Mater.* 1: 16018 (2016).
- Wijmans, J.G., Baker, R.W. The solution-diffusion model: a review. *J. Membr. Sci.* 107(1-2): 1-21 (1995).
- Wright, E.S., Yilmaz, L.S., Noguera, D.R. DECIPHER, a search-based approach to chimera identification for 16S rRNA sequences. *Appl. Environ. Microbiol.* 78: 717-725 (2012).
- Yabuuchi, E., Yano, I., Oyaizu, H., Hashimoto, Y., Ezaki, T., Yamamoto, H. Proposals of *Sphingomonas paucimobilis* gen. nov. and comb. nov., *Sphingomonas parapaucimobilis* sp. nov., *Sphingomonas yanoikuyae* sp. nov., *Sphingomonas adhaesiva* sp. nov., *Sphingomonas capsulata* comb. nov., and two new species of the genus *Sphingomonas*, *Microbiol. Immunol.* 34(2): 99-119 (1990).
- Yim, M.-S., Yau, Y.C., Matlow, A., So, J.S., Zou, J., Flemming, C.A., Schraft, H., Leung, K.T. A novel selective growth medium-PCR assay to isolate and detect *Sphingomonas* in environmental samples. *J. Microbiol. Methods.* 82(1): 19-27 (2010).
- Yoon, J.-H., Lee, M.-H., Kang, S.-J., Lee, S.-Y., Oh, T.-K. *Sphingomonas dokdonensis* sp. nov., isolated from soil. *J. Syst. Evol. Microbiol.* 56, 2165-2169 (2006).
- Yoon, J.-H., Park, S., Kang, S.-J., Kim, W., Oh, T.-K. *Sphingomonas hankookensis* sp. nov., isolated from wastewater. *J. Syst. Evol. Microbiol.* 59: 2788-2793 (2009).
- Yu, T., Meng, L., Zhao, Q.B., Shi, Y., Hu, H.Y., Lu, Y. Effects of chemical cleaning on RO membrane inorganic, organic and microbial foulant removal in a full-scale plant for municipal wastewater reclamation. *Water Res.* 113: 1-10 (2017).
- Zhang, J.-Y., Liu, X.-Y., Liu, S.-J. *Sphingomonas changbaiensis* sp. nov., isolated from forest soil. *J. Syst. Evol. Microbiol.* 60: 790-795 (2010).
- Zhao, F., Xu, K., Ren, H., Ding, L., Geng, J., Zhang, Y. Combined effects of organic matter and calcium on biofouling of nanofiltration membranes. *J. Membr. Sci.* 486: 177-188 (2015).



Zhu, L., Si, M., Li, C., Xin, K., Chen, C., Shi, X., Huang, R., Zhao, L., Shen, X., Zhang, L. *Sphingomonas* *gei* sp. nov., isolated from roots of *Geum aleppicum*. *J. Syst. Evol. Microbiol.* 65: 1160-1166 (2015).



The background of the page is a grayscale, high-magnification micrograph of numerous rod-shaped bacteria, likely Bacillus or Clostridium species, scattered across the field of view. The bacteria are oriented in various directions, some appearing as single cells and others in small clusters or chains. The lighting creates a sense of depth, highlighting the three-dimensional structure of the cells.

# Chapter 6

## General discussion and outlook

## 6.1. Introduction

High pressure membrane filtration processes such as nanofiltration (NF) and reverse osmosis (RO) are capable of producing high quality water for industrial applications and human consumption. As a result of the increasing world population, expanding industries, climate change, desertification, drought, pollution of existing water resources, new emerging pollutants and more stringent water quality regulations, the global market for high pressure membrane filtration is expanding rapidly (Greenlee *et al.*, 2009, van der Bruggen *et al.*, 2008, Hilal and Wright 2018). The reverse osmosis market is expected to reach \$40 billion in 2020 (Hilal and Wright 2018). The major concern in the operation of RO plants is reduced performance by membrane fouling. Among other types of fouling, biofouling remains the most frequent and formidable type of membrane fouling (Flemming *et al.*, 1997, Nguyen *et al.*, 2012, Peña *et al.*, 2012, Bucs *et al.*, 2014, Jiang *et al.*, 2017, Maddah and Chogle 2017), despite almost four decades of research and excessive efforts spent on its prevention and control (Figure 6.1).

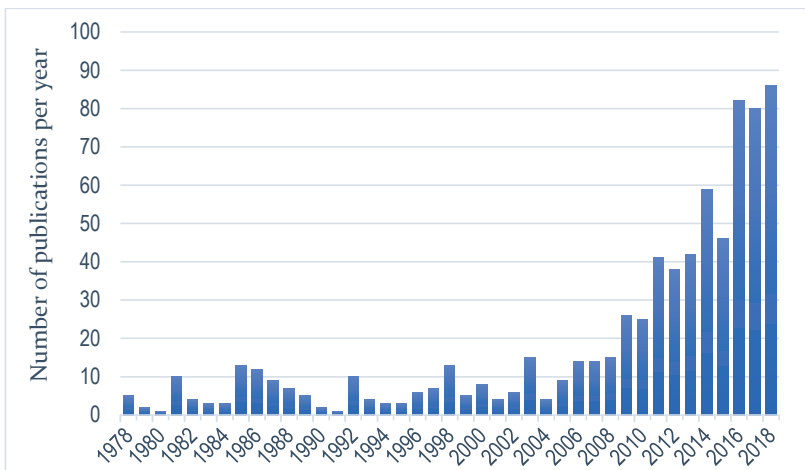


Figure 6.1. Annual publications (articles, reviews and conferences papers) on biofouling prevention and control (search on biofouling combined with other search terms such as prevent, inhibit, mitigate, reduce, eradicate, control, combat, fight, minimize, limit, avoid, delay, etc.) in the period of 1978 to 2018. The total number of publications is 778 (Scopus database: 25.10.2018).

## 6.2. Laboratory experiments to study biofouling

Biofouling is undeniably a biofilm problem. Biofilm properties and development are characterized by huge variations in space and time and are influenced by an almost uncontrollable set of variables, which complicates biofilm research (*Flemming 2008*). Traditional microbiological methods (e.g. growth on agar plates or in shake flasks) are often inadequate to mimic the environmental conditions of microorganisms in biofilms. Biofilms are therefore best studied in their natural environments (*Chapter 2, 3 and 4*) or in laboratory scale bioreactors (*Franklin et al., 2015*). The awareness of the high importance of hydrodynamic conditions during biofilm development has led to the development of a diverse range of bioreactors operated under continuous flow conditions such as the CDC biofilm reactor® (*Goeres et al., 2005*), the drip-flow biofilm reactor® (*Goeres et al., 2009*) or flow cells (*Vrouwenvelder et al., 2007, Vanysacker et al., 2013, Dreszer et al., 2014*).

The use of flow cells has become “best practice” in laboratory-scale membrane biofouling research, as they can best mimic the actual environmental conditions experienced during full-scale operation. Yet, many, if not all, of these flow cells are not representative for full-scale plants (*Dreszer et al., 2014*). As biofouling is an operational defined problem (*Chapter 2 and 3*), representative laboratory studies must include determination of the key performance indicators normalized membrane permeability ( $K_w$ ), normalized pressure drop (NPD) and salt rejection (*Chapter 2 and 4*). *Vrouwenvelder et al., 2007* proposed a set of tests to validate the representativeness of flow cells in membrane biofouling research. This methodology was later applied for the validation of other designs (*Dreszer et al., 2014*). In principle, most flow cell studies described are either performed under i) no recycling conditions (single-pass / once-through operation) with unspecific microbial communities (*Hijnen et al., 2009, Vrouwenvelder et al., 2010, Dreszer et al., 2013*) or ii) recycling conditions (partial or fully recycle) with specific microbial communities (*Chong et al., 2008, Baek et al., 2011, Suwarno et al., 2014*).



### 6.3. The choice of microorganisms for laboratory studies

The choice of micro-organisms, when studying the fundamentals of biofouling in RO/NF systems is crucial and therefore laboratory research should ideally use microorganisms isolated from membrane autopsies (*Habimana et al., 2014*). The choice of microorganisms, together with the experimental design is a key parameter determining the relevance and quality of scientific work on membrane biofouling in laboratory settings.

The two most frequently used microorganisms for research on membrane biofouling are *Escherichia coli* and *Pseudomonas aeruginosa* (*Barnes et al., 2014, Wibisono et al., 2015, Zhao et al., 2015, Faria et al., 2017, Ma et al., 2018, Wang et al., 2018*). Both bacteria are not or not frequently detected in studies on microbial diversity of fouled membranes (*Bereschenko et al., 2008, Al Ashab et al., 2014, Levi et al., 2016, Nagaraj et al., 2017*).

Presence, abundance, and physiological properties related to biofilm formation make the group of Sphingomonads, consisting of *Sphingomonas sp.*, *Sphingobium sp.*, *Sphingopyxis sp.*, and *Novosphingobium sp.* interesting candidates for membrane biofouling studies (*Chapter 5*). In a pioneering study on the biofouling behavior of Sphingomonads, *Sphingomonas wittichii* strain RW1 outperformed *E. coli* and *Pseudomonas aeruginosa* in terms of adhesion strength and membrane flux decline (*Gutman et al., 2014*). We examined the biofouling capabilities of *Sphingomonas* strain Sph1 in a proof of principle experiment under representative conditions using a modified laboratory setup (*Figure S6.1.*) that was operated under controlled and axenic conditions.

After 5.5 days of operation, biofouling was evident by both NPD increase (~15%) and  $K_w$  decrease (~18%) in the flow cell inoculated with Sph1, while absent in the blank flow cell and visualized by SEM. The membrane and spacer surfaces of the blank cell did not show anything, but clean surfaces (*Figure 6.2. A and B*). To prevent microbial contamination of the blank flow cell and operational setup during the experimental runs, a tight protocol was developed from experience of failed experimental runs (*Supplementary data S6.1*).

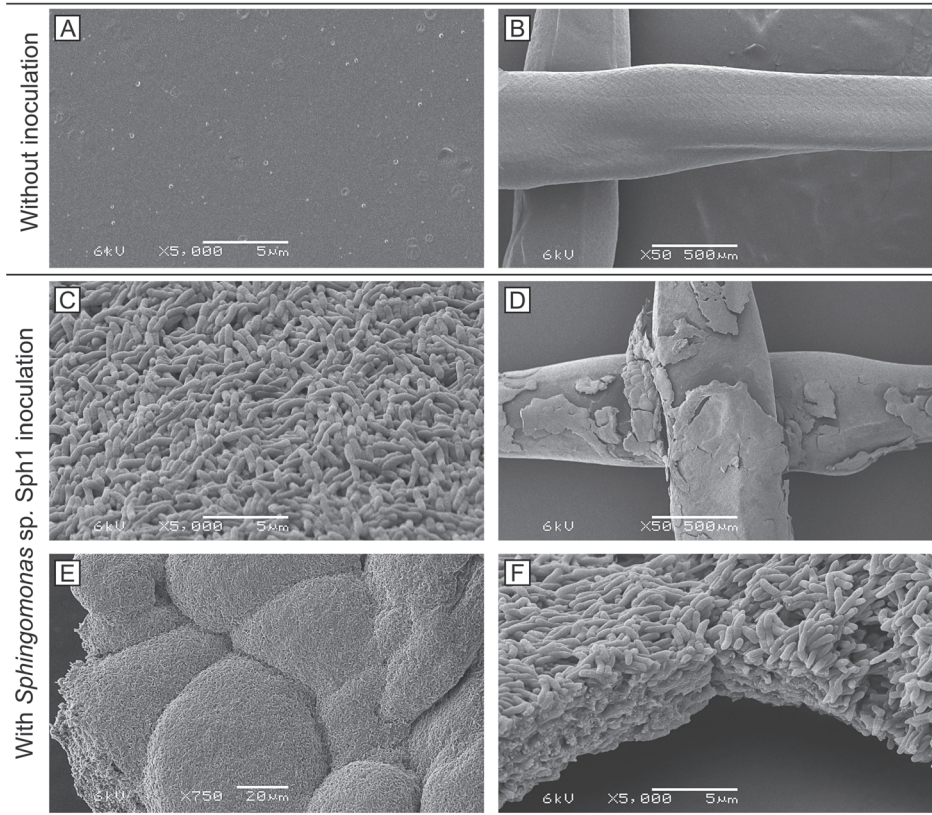


**Figure 6.2.** SEM pictures of the membrane-, (A, C, E) and spacer (B, D, F) surfaces of the flow cell with nutrients and no inoculation (A, B), and the flow cell with nutrients and strain Sph1 (C, D, E, F). The images show clean membrane- (A) and spacer (B) surfaces in the flow cell with nutrients, but and no inoculation. In contrast, the membrane- (C) and spacer (D) surfaces of the flow cell with nutrients and Sph1 inoculation showed biofouling by rod shaped microorganisms. In particular: dense layers of Sph1 on the membrane surface (C) patches of Sph1 biofilm on the spacer surface (D) colonies of Sph1 biofilm on the membrane surface (E) and multiple cell layers of dehydrated *Sphingomonas* sp. Sph1 biofilm on the spacer surface (F).

The flow cell inoculated with Sph1 showed a rather uniform and dense growth on both the membrane and spacer surfaces (Figure 6.2. C – F). In particular, dense layers of Sph1 were observed on the membrane surface (Figure 6.2. C), and patches of Sph1 were observed on the spacer surface (Figure 6.2. D). Growth appeared to originate from microcolony development (Figure 6.2. E) that are multiple cell layers thick (Figure 6.2. F).

The pilot experiment demonstrated that:

1. Aseptic conditions could be maintained for the experimental duration of 7 days in the flow cell without *Sphingomonas sp.* SphI inoculation despite dosage of nutrients and absence of antimicrobials
2. *Sphingomonas sp.* SphI could attach to the membrane and spacer surface
3. *Sphingomonas sp.* SphI caused biofouling on the NF membrane)

The recent focus on the role of *Sphingomonas* in the biofouling process should be extended from initial colonization to all stages of biofilm formation, as we have shown in controlled laboratory studies that *Sphingomonas* can cause biofouling on its own. In *Chapter 5* we have shown that Sphingomonads isolated from industrial membrane plants have a wide range of physiological properties that are required for successful colonization and subsequent biofilm formation. As Sphingomonads are also frequently associated with biofouling in other industries, their study is of particular interest. For example, *Sphingomonads* were shown to belong to the core microbiome of cooling systems where they seem to play an important role in primary colonization (*Di Gregorio et al. 2017*).

## **6.4. Lessons learned from biofouling prevention**

In the context of this thesis, biofouling prevention describes the measures taken to inhibit biofilm development. Fouling control on the other hand describes the measures taken to remove biofilms once they have developed.

The techniques used to prevent biofilm formation and subsequent biofouling on membrane include (*Nguyen et al., 2012*):

- removal of nutrients from the feed (induced nutrient limitation)
- (dis)continuous dosage of antimicrobials
- physical methods to remove, inactivate or kill microorganisms
- usage of fouling resistant surfaces

### **6.4.1. Nutrient limitation**

The concept of nutrient limitation originates from the field of agriculture and Liebig's law of the minimum. The concept basically describes that maximum growth rate of plants is dictated by the scarcest essential nutrient available (*Liebig 1840*). The concept has been broadened to include microorganisms and biofilms.



Furthermore, the concept has also been extended to other growth conditions such as sunlight or the availability of high energy yielding electron acceptors (*Chapter 2 and 3*).

It was proposed that organic carbon is typically the most important growth determining parameter in membrane systems (*Hijnen et al., 2009*). Assimilable organic carbon (AOC), a sum parameter describing the easily biodegradable fraction of organic carbon that is determined via a biological growth assay with *Spirillum* strain NOX and *Pseudomonas fluorescens* strain PI7 (*Rice et al., 2017*), has been quantitatively related to microbial growth and biofouling in reverse osmosis membranes (*Hijnen et al., 2009*). The threshold AOC concentration to prevent biofouling in membrane systems has been estimated at about 1 – 30 µg per liter (*Hijnen et al., 2009, Weinrich et al., 2015*). A wide range of biological pretreatments, such as aerated submerged media reactors, fluidized bed filters, slow sand filters, rapid sand filters and granular activated carbon filters have proven to reduce the organic carbon load of waters, and for some technologies TOC removal efficiencies exceeding 90% have been reported (*LeChevallier 1991*). In order to achieve highly efficient AOC removal, two-stage filtration (e.g. rapid sand filtration followed by granular activated carbon filtration) or single-stage biological filtration have been proposed (*Volk and LeChevallier 2002*). In pilot studies presented by *van der Hoek et al. (2000)*, AOC concentrations of about 4 – 6 µg per liter (achieved by slow sand filtration) strongly slowed down biofouling development, so that only one CIP per year was needed to maintain stable operation.

In the studies presented in *Chapter 2* we show that similar or lower cleaning frequencies (once per year or less) could be achieved in anoxic groundwater treating NF installations that do not have any pretreatment besides cartridge filtration (10 µm pore size) and antiscalant dosage. The process has been shown to be feasible during long-term operation (6-10 years) of four full-scale installations, as anoxic conditions could be maintained throughout the installation (*Chapter 2*). An additional advantage of anoxic groundwater treatment by NF marks the insensitivity to iron fouling. While iron concentrations  $\geq 0.3 \text{ mg L}^{-1}$  in the feed water of oxic membrane installations may lead to rapid iron fouling, high concentrations of

reduced metal ions ( $\leq 8.4 \text{ mg L}^{-1}$ ) did not cause membrane fouling under anoxic conditions (*Chapter 2*).

To develop “induced oxygen limitation” to a general biofouling prevention strategy, two open questions remain. How can this approach be applied to industrial plants where the feed water is oxic by nature? How does this approach perform with feed waters rich in AOC and alternative high energy yielding electron acceptors such as nitrate?

Technologies available to deoxygenate water are either based on physical treatment or chemical treatment (*Durdevic et al., 2018*). Physical deoxygenation includes methods such as gas purging ( $\text{N}_2$ ), stripping, boiling or membrane exchange. Chemical deoxygenation includes methods to scavenge oxygen in reactions with e.g. sulfite, certain organics and the use of hydrogen sulfide (*Patrick and Wagner 1949, Butler et al., 1994, Shao et al., 2008, Durdevic et al., 2018*). The majority of single physical methods is believed to be incapable of removing all oxygen at reasonable investment-, and operational costs (*Patrick and Wagner 1949*). Chemical methods in contrast often show full removal of oxygen, but the chemicals added (or the products of the chemical reaction) may lead to the contamination of the water and must therefore be carefully chosen (*Patrick and Wagner 1949*).

The oxygen scavenger sodium bisulfite is used as “reducing biocide” in membrane filtration and is applied as shock dosage during online operation, or during CIP (*Chapter 2*), or for the preservation of the membrane elements during storage and transport (*Applegate and Erkenbrecher 1987, Dow FILMTEC™ technical manual*).

In membrane filtration installations suffering from rapid biofouling, daily 30 min shock dosages of  $500 - 1000 \text{ mg L}^{-1}$  food-grade sodium metabisulfite (catalyzed with cobalt) are proposed to mitigate biofouling (*Applegate and Erkenbrecher 1987, Dow FILMTEC™ technical manual*). Such shock dosages may help to mitigate biofouling in plants suffering from severe biofouling, but do not deliver the added benefits of continuous anoxic membrane filtration (e.g. high solubility of iron and manganese) (*Chapter 2*).

Large-scale deoxygenation is used in other water intensive industries for the pretreatment of e.g. boiler water or injection water with the aim to reduce corrosion rather than biofouling (Shao *et al.*, 2008, Durdevic *et al.*, 2018).

Another alternative membrane biofouling control strategy is phosphate limitation (Vrouwenvelder *et al.*, 2010, Kim *et al.*, 2014). Phosphate concentrations of about 0.25 µg phosphorus per liter were shown to prevent rapid biofilm formation on reverse osmosis membranes, despite high concentrations of easily biodegradable nutrient supplied in the form of acetate (Vrouwenvelder *et al.*, 2010).

Phosphate removal can be achieved by diverse methods such as precipitation, crystallization, ion exchange, adsorption or electrochemical coagulation (Jacobs *et al.*, 2010, Nguyen *et al.*, 2012). Depending on the technology chosen, removal efficiencies can be very low with costs of treatment being very high (Nguyen *et al.*, 2012). A combination of several traditional methods may be required in order to achieve high removal efficiencies (Bunce *et al.*, 2018). Some of those methods have been able to reach the desired phosphate levels of about 10 µg per liter, but have not found large-scale applications for ecological sensitive waters (Jacobs *et al.*, 2010).

### **Outlook - Nutrient limitation**

Induced or natural “nutrient limitation” has been shown effective to drastically slow down biofouling development (Vrouwenvelder *et al.*, 2010, van der Hoek *et al.*, 2000, Chapter 2 and 3). Additional pretreatment steps are usually a prerequisite to achieve the removal efficiencies required to prevent biofilm growth and subsequent biofouling development.

Although induced carbon limitation has shown to mitigate biofouling (van der Hoek *et al.*, 2000), the added investment-, operational and maintenance costs of an additional pretreatment step may not be justified by the costs of biofouling without an additional pretreatment step. In a similar fashion, induced phosphate limitation or oxygen limitation will have to prove themselves. In addition, the concept of induced oxygen limitation must still be proven for feed waters vast amounts of AOC and nitrate (which may serve as an alternative high-energy yielding electron acceptor in anaerobic respiration).

With an ever increasing concerns and pressure on the use of antimicrobials, environmental friendly biofouling prevention approaches are expected to gain importance. Furthermore, in order meet increasingly stringent environmental regulations and policies, higher costs of treatment are to be expected. This could potentially lead to a revival of existing technologies that are not cost competitive yet.

#### **6.4.2. Dosage of antimicrobials**

Many industries that are affected by biofouling are relying on the usage of oxidizing and/or non-oxidizing biocides to ensure reliable operation. Biocides may be dosed intermittently, as shock or continuous, dependent on the treatment strategy, local legislations or history of the biofouling problem. Thin film composite membranes, which are the industry standard in NF and RO filtration, are unfortunately very sensitive to free chlorine (continuous free chlorine tolerance of  $< 0.1 \text{ mg L}^{-1}$ ) and some other oxidizing agents and therefore the use of biocides in NF and RO is limited (*Dow FILMTEC™ technical manual*). Chemical attack by oxidation of the polyamide top layer of the thin film composite membranes may quickly result in a loss of salt rejection, leading to a rapid decrease in permeate quality (lower retention to salt, pesticides and other contaminants).

Moreover, in *Chapter 2* we have shown that even standard acid-base cleaning operations, which are believed to not harm membranes (*Dow FILMTEC™ technical manual*), can result in 1.8% loss of rejection for each cleaning applied. With the very low cleaning frequency of this particular installation (WH) (once every 1.5 years), the membranes still lasted about six years or four cleanings. With a cleaning frequency of an installation suffering from rapid biofouling (*Chapter 2*) those membranes would have lasted just a month.

In recent years, many tests have been performed with oxidizing and non-oxidizing biocides. Most of such treatments are not well established yet, as some open questions remain (e.g. compatibility with the membrane materials). An overview of NF and RO biocides that are frequently used, or currently researched, can be found in *Table 6.1*.

Table 6.1. Overview of biocides for NF and RO applications

Type	Acronym	Mode of action	Advantages	Disadvantages	compatible with membranes
non-oxidizing					
DBNPA		reacts with thiols in enzymes and proteins; DNA and the cell membrane	broad-spectrum efficiency; particular efficient on slime forming bacteria; kills microorganisms immediately upon addition; compatible with oxidizers; low environmental impact; deteriorates rapidly	bromine releasing; sensitive to ultraviolet light; nucleophiles and reducing agents; rapid deterioration at pH >8; formation of adsorbable organic halides	yes
CMIT/MIT		reacts with cellular nucleophiles such as amino, amide and thiol groups; inhibition of enzymes; quick inhibition of cellular activity; slow death via protein disruption	cost-effective; broad-spectrum microbicide; causes immediate inhibition of growth; compatible with most biocides and water additives; activity is retained in presence of organic matter; active over wide pH range	slow kill rate; sensitive to nucleophiles and reducing agents; formation of adsorbable organic halides	yes
oxidizing					
	Monochloramine	oxidation of thiols in enzymes and proteins, DNA and the cell membrane	active against broad spectrum of microorganisms; good penetration of biofilms; protection against regrowth of bacteria	formation of trihalomethanes, haloacetic acids and nitrogenous-by-products	unclear
	Peracetic acid (PAA) and hydrogen peroxide	oxidation of thiols in enzymes and proteins, DNA and the cell membrane; free radicals may oxidize protein backbones	active against broad spectrum of microorganisms; particular efficient on anaerobic and spore-forming bacteria; kills microorganisms immediately upon addition; removes biofilms; produces little to no toxic byproducts	limited efficiency of microorganisms with thick cell walls; relatively high costs	unclear
	chlorine dioxide	oxidation of thiols in enzymes and proteins, DNA and the cell membrane; disrupts the permeability of the cell membrane	active against broad spectrum of microorganisms; most effective biocide against biofilms; kills microorganisms immediately upon addition; effective at low concentrations over wide pH range	explosive gas that usually must be generated on site; relatively high costs; chlorite and chlorate are disinfection byproducts	unclear

References used to compile Table 6.1.: Adams 1990, Amy, 2000, Bott 2011, Christiani and Perboni 2014, da Silva et al., 2006, Dow FILMTEC™ technical manual, Farhat et al., 2018, Finnegan et al., 2010, Glaser 1983, Hydranautics technical application bulletin - TAB I15, Hydranautics technical service bulletin - TSB I10.12, Jacangelo et al., 1987, Kitis 2004, Koh and Jang 2017, Nguyen et al., 2012, Oh and Jang, 2016, Valentino et al., 2015

### **Outlook - Antimicrobials**

The usage of antimicrobials in NF and RO membrane filtration has various limitations. Many biocides, including their degradation by-products and impurities, have detrimental effects on the integrity of commonly applied thin film composite membranes (e.g. free chlorine (and biocides with combined chlorine such as chloramine, chloramine-T, and N-chloroisocyanurate), ozone, iodine, quaternary ammonium compounds and phenolic compounds), and are therefore not endorsed by the membrane manufacturers (*Dow FILMTEC™ technical manual*).

However, the use of certain oxidizing biocides (e.g. peracetic acid, hydrogen peroxide, chlorine dioxide and monochloramine) have been shown to deliver promising results in fouling prevention, but have tight guardrails (*van den Broek et al., 2010, Farhat et al., 2018*). The interactions between biocides, their impurities and degradation / disinfection by-products are still not fully understood and require further research at laboratory- and full-scale.

The production of toxic disinfection by-products (DPBs) (e.g. trihalomethanes (THMs), haloacetic acids (HAAs), bromate, chlorite and "emerging" DBPs such as halonitromethanes, haloacetonitriles, haloamides, halofuranones, iodo-acids such as iodoacetic acid, iodo-THMs (iodotrihalomethanes), nitrosamines, etc.) (*Richardson et al., 2017*) are of particular concern regarding permeate (product) quality and concentrate (discharge) quality, especially when the membranes are used for drinking water production or for the discharge of the concentrate.

The statement made by *Flemming in 1997* "Facing increasing difficulties in the application of biocides both in effectiveness and in environmental regulations, those in membrane technology might be well advised to develop biocide-free antifouling strategies" remains valid 20 years later.

#### **6.4.3. Membrane modifications**

In the quest of superior performance, fouling resistance and cleanability of RO membranes many efforts have been dedicated to membrane (surface) modifications or the development of novel membrane materials, a whole field of research on its own that has been extensively reviewed by others recently (*Kochkodan and Hilal,*

2015, Misdan et al., 2016, Jiang et al., 2017, Goh et al., 2018, Otitoju et al., 2018, Yang et al., 2018).

In short, novel membranes can be classified, based on their location within the membrane layers(s), into (Yang et al., 2018):

- Membranes using novel desalting materials (forming the primary rejection layer of the membrane)
- Thin film nanocomposite membranes (incorporating novel materials into the primary rejection layer)
- Surface located nanocomposite membranes (bonding of novel materials onto the primary rejection layer)
- Mixed matrix substrate membranes (embedding novel materials into the bottom layers of the membrane)

Examples of membranes using novel desalting materials are aquaporin membranes, carbon nanotubes, nanoporous graphene or graphene oxide (Yang et al., 2018). Membranes from those materials are very interesting as they exhibit superior permeability for water, but are still far from commercialization (Yang et al., 2018). Membranes from carbon nanotubes and graphene oxide may exhibit antimicrobial- and anti-adhesion properties (Yang et al., 2018) and are therefore also very interesting from biofouling prevention and control point of view.

### **Outlook - Membrane modifications**

In *Chapter 2* we have described that the choice of membrane had an influence on the development of fouling by natural organic matter, and therefore membrane choice is important. In terms of novel anti-(bio)fouling membranes, the following question must be asked: What remains after the membrane is covered with a conditioning or fouling layer (of dead biomass or other foulants)? Masking of the primary rejection layer by e.g. a conditioning layer or other foulants may quickly render surface modifications ineffective. Therefore, the positive long-term effect of surface modifications, by e.g. grafting or coating with anti-(bio)fouling polymers or antimicrobials has been questioned by multiple authors (Rana and Matsuura 2010, Miller et al., 2012, Bernstein et al., 2014, Semião et al., 2014).

It is crucial to look further than initial performance, as important membrane characteristics such as resistance to biofouling and cleanability are not determined

during the first few hours of operation, but over the course of a membrane lifetime (which can be 10 years or more as shown in *Chapter 2*). Consequently, research on anti-(bio)fouling materials and surface modification should strongly focus on long-term experiments and improved cleanability. After all, the field of membrane and spacer (surface) modifications and novel membrane and spacer materials may hold very promising developments, but as of now still is in its infancy.

### **6.5. Lessons learned from biofouling prevention**

As shown throughout this thesis (*Chapter 2,3,4 and 5*), all membranes will eventually foul. And, although fouling prevention can be very powerful to mitigate biofouling, it does not eradicate it. Consequently, all membranes eventually have to be cleaned.

During the course of this thesis research approximately 50 NF and RO have been autopsied (*unpublished data*) that all showed irreversible and aged foulants (*Chapter 4*). Microorganisms have been detected in all of those autopsies and biofilm formation was diagnosed as the major foulant in most of the membrane elements. Clearly, the measures taken to prevent and control biofouling have not been fully effective under all circumstances. The following paragraphs include a critical view on the lessons learned regarding biofouling prevention and control in full-scale membrane filtration plants.

Similar to the application of antimicrobials, chemical cleaning in place (CIP) is typically limited to offline operation, dependent on the intended quality and use of the permeate. Based on the severity and rate of biofilm formation, the CIPs required can lead to considerable downtime and costs for chemicals and manpower.

Even with very low cleaning frequencies of once per year or less, as shown for anoxic groundwater treating NF installations in *Chapter 2 and 3*, a CIP installation must typically still be an integral part of an NF and RO installation, which puts limitations to the savings that can be achieved by fouling prevention. The overall costs of CIP (added investment-, operational and maintenance costs) may not be much different for 1 or 4 CIPs per year. This limitation can be overcome, when a mobile CIP unit is used for a multitude of plants with very low cleaning frequencies.



As long as CIP is highly efficient and does not deteriorate the membranes, high cleaning frequency may still be accepted, as the cost for traditional chemical cleaning (when a CIP unit is available) is cheaper than an additional pretreatment step (to reduce the CIP frequency). Irreversible foulants that accumulate as remainders of inefficient previously applied CIP operations are a major concern, as they may ultimately define the membranes lifetime. Furthermore, the constantly reduced performance adds significantly to operational costs. In *Chapter 2 and 4* we have shown that irreversible foulants will build up, regardless of CIP frequency (up to 17 times a year) or pretreatment chosen. Depending on severity, the plants may operate with 20% reduced  $K_w$  and 100% increased NPD) (*Chapter 4*).

When irreversible foulants have built up, advanced CIP with more specific or harsh cleaners may be applied. In our studies (*Chapter 4*), the use of (bio)organic fouling specific CIP procedures employing e.g. PAA, hydrogen peroxide, enzymes or surfactants, cleaning success on aged (bio)organic fouling layers was very limited (*Chapter 4*). Those cleanings were performed at the permitted limits of the membrane manufacturer in terms of cleaning solution type, concentration, temperature, pH and velocity (shear) (*Chapter 4*). Therefore, only marginal improvements are to be expected in the development of novel chemical cleaners.

### Physical cleaning

Traditional and advanced chemical cleaning may be combined with physical cleaning strategies to improve foulant removal efficiencies. Physical methods (e.g. reverse flushing or air sparging) employ mechanical forces to remove foulants from the membrane- and spacer surfaces (*Qin et al., 2009*).

In many membrane systems such as MF and UF, backwashing is used to physically clean the membrane surface. In RO membrane systems the peculiarity lies in the fact that the permeate gauge pressure may never exceed the feed gauge pressure, as the membranes otherwise will rupture. This contradiction can be circumvented by introducing osmotic pressure higher than gauge pressure in the feed-concentrate channel of the membrane in an attempt to lift or sweep biofouling and to introduce a bio-osmotic- and salt dissolve shock (*Qin et al., 2009*). Direct osmosis can be induced by e.g. up to 17% NaCl solution (osmotic pressure of 170 bar) to the feed

stream of the membranes. This method is quick (less than one minute), environmental friendly, cost-effective (low chemical- and capital investment costs) (Lieberman 2018). This promising technology has been tested in a Dutch RO plant where other cleaning methods were not effective in restoring membrane permeability. The direct osmosis treatment had only limited effect in this case (personal communication Wilbert van den Broek).

### **Detachment, dispersion and desorption**

Research on novel biofouling control approaches based on biofilm detachment and dispersal is scarce. Although the literature provides some clues how dispersal in biofilms can be induced on laboratory scale (Petrova and Sauer 2016), not much of this work was followed up in the development of novel biofouling control strategies.

There are several possibilities for microorganisms to leave biofilms (Petrova and Sauer 2016).

1. **Desorption** – direct transfer of microorganisms from substratum to the bulk liquid (in many ways similar to reversal of attachment)
2. **Dispersion** – Release of single microorganisms from inside of biofilm microcolonies (a highly regulated and active process).
3. **Detachment** – Release of cells or clusters of cells (that are already in contact with the bulk liquid) from the biofilm

While detachment and desorption display passive release mechanisms, natural or induced dispersion usually relies on an active physiological response of the biofilm microorganisms and therefore, dispersion is a highly regulated and active process (Petrova and Sauer 2016). Currently available commercial biofilm cleaners that are aimed at biofilm detachment will typically be composed of a blend of antimicrobials and so called biodispersants, vigorously inhibiting active dispersal. The induced biofilm dispersal still holds many secrets that may be exploited in generating novel biofouling control strategies. Some of described dispersal triggering conditions are of particular interest, as realization in full scale operation seems feasible. Those triggers include, but are not limited to, i) rapid increase of carbon concentration (Sauer et al. 2004, Gjermansen et al. 2005), ii) gradual depletion of carbon or nitrogen concentration, iii) rapid decrease in oxygen tension (Thormann et al., 2005)

In a proof of principle experiment we grew biofilms under continuous conditions. The flow cells were supplied with a nutrient solution containing acetate. The biofilm was allowed to grow until strong biofouling could be noticed in terms of a ten-fold NPD increase. Then acetate dosing was discontinued for one flow-cell, while phosphate dosing was discontinued for the other flow cell. In the flow cell where acetate dosing was discontinued, a gradual and strong decrease in FCP was observed (80% of the NPD could be restored). On the other hand, the flow cell where phosphate dosage was discontinued, no decline in FCP could be noticed. Analysis of the biofilm at the end of the experiment confirmed that biomass developed less in the flow cell with discontinued acetate dosing, compared to the flow cell with discontinued phosphate dosing. In full-scale operation it is has been frequently observed that overnight soaking of the membrane elements in NF or RO permeate improves membrane performance (*personal observation of Dutch NF and RO plant operators*), which is another hint that induced active dispersal may hold some secrets that can be exploited for development of novel biofouling control approaches.

### **Outlook - Membrane cleaning**

The opportunities for traditional and advance chemical cleaning methods seem to be exhausted, and only marginal fouling removal efficiency improvements are to be expected by the development of new formulations. As the quest for more chemical resistant membranes that have excellent filtration characteristics is still ongoing, this could open new doors for e.g. the application of oxidizing biocides. While traditional chemical cleaning aims at inactivation and removal of biomass, induced dispersal relies on active microorganisms. The field of induced dispersal of biofouling layers is still understudied and may hold some secrets that could be exploited for novel cleaning and control strategies and should be further studied. A multi-approach of combining and alternating several individual cleaning approaches may help to increase overall efficiency by prevention of quick biofilm adaptation.

## 6.6. Concluding remarks

Currently, there are no biofouling prevention strategies that can work under all circumstances and at reasonable cost. Biofouling can be mitigated, controlled (to a certain extent), but not eradicated (*Chapter 2 and 4*). Successful biofouling mitigation requires a combination of biofouling prevention and control techniques. Still, biofouling prevention and control frequently fails despite huge efforts taken.

Biofilm adaptation seems to be a major driver in failing biofouling prevention and control approaches. A biofouling control approach that is working very efficiently today, may lose its effect tomorrow as biofilms quickly adapt to changing environments. Consequently, biofouling prevention and control approaches (e.g. CIP, biocide dosage, phosphate limitation, etc.) must not only be combined, but also alternated. Alternation of several approaches with different working mechanism may prevent quick adaptation.

Induced detachment and dispersal of biofilms is still an understudied field. Deeper exploration of this field may unravel new insights that can be exploited for the development of novel biofouling prevention and control strategies.

The development of highly efficient RO membranes that are resistant to a wide range of oxidizing biocides is surely an interesting challenge. However, as most biocides also have a negative impact on the environment, their use should be minimized and focus may be better laid on environmental friendly biofouling prevention and control approaches.

To date, nutrient limitation seems to remain the most promising biofouling prevention strategy. When such an approach is applied on full-scale, additives such as antiscalants or acids must be of highest quality, as they increase the TOC load of the feed water and their biodegradation may accelerate biofouling (*van der Hoek et al., 2000, Hijnen et al., 2009*).

Moreover, the choice of the experimental setup and model organisms in biofouling research is crucial to unravel the underlying mechanisms of biofouling in full scale installations in order to develop novel prevention and control approaches. Sphingomonads are relevant in industrial membrane biofouling and therefore

should be more frequently used in biofouling studies, especially when research concerns anti-biofouling material-, or surface modifications. Research on Sphingomonads should furthermore extend beyond their role as primary colonizers.

## Supplementary data Chapter 6

### Supplementary figure S6.1. – Feed water pretreatment

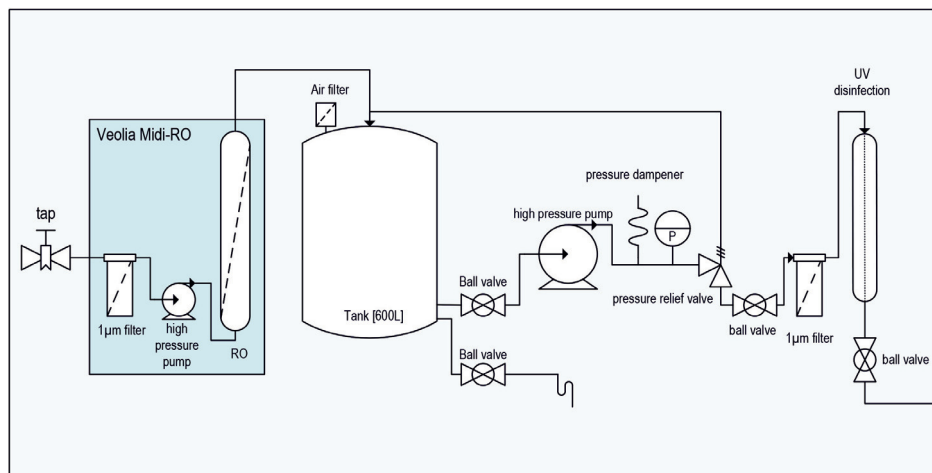


Figure S6.1. Schematic representation of the feed water pre-treatment. P = pressure

### Supplementary data S6.1. – Disinfection procedure

Before and after each experimental run, chemical cleaning of the setup (without flow cells) was performed according the following protocol; i) pre-flush with RO permeate at RT for 30min ii) alkaline cleaning with 2 – 2.5 % v/v (pH 12.5) Ultrasil P3-I10 (Ecolab Inc., St. Paul, MN) at RT for 2h continuous flow followed by overnight soaking and 2h of continuous flow and iv) flushing with RO permeate at RT for 30min.

The flow cells were manually cleaned it hot water with hand-soap and flushed with Milli-Q. The setup was then disinfected with a commercial blend cleaner P3-oxonia® active (Ecolab Inc., St. Paul, MN) containing a mixture of hydrogen peroxide, peroxyacetic acid and acetic acid. Disinfection and cleaning of the setup (without flow cells) was performed according the following protocol; i) pre-flush with RO permeate at 20°C for 30min ii) sanitation with 1.5 % v/v P3-oxonia® active (Ecolab Inc., St. Paul, MN) at RT for 2h continuous flow, followed by overnight soaking, followed by 2h of continuous flow and iv) flushing with RO permeate (UV switched on) at RT for 30min. The flow cells were carefully cleaned manually and then soaked in 1.5% P3-oxonia® active (Ecolab Inc., St. Paul, MN) for 2h at RT. Membranes and

spacers were first soaked in Milli-Q water overnight and then sanitized for 2h in 0.5% P3-oxonia® active (Ecolab Inc., St. Paul, MN) followed by 2h of 70% Ethanol before assembly of the flow cells in the laminar flow cabinet. Ready assembled flow cells were then connected to the fouling setup and sanitized with 0.5 % P3-oxonia® active (Ecolab Inc., St. Paul, Minnesota, MN) for another 2h before overnight membrane conditioning with RO permeate at RT and 3.2bar. Then, membranes were conditioned with feed water (RO permeate with nutrient solution) for 3h.

## References

- Adams, W.R. *The effects of chlorine dioxide on reverse osmosis membranes*. *Desalination*. 78(3): 439-453 (1990).
- Al Ashhab, A., Gillor, O., Herzberg, M. *Biofouling of reverse-osmosis membranes under different shear rates during tertiary wastewater desalination: Microbial community composition*. *Water Res.* 67: 86-95 (2014).
- Amy, G., Bull, R., Gunther, G.F., Pegram, R.A., Siddiqui, M., *Disinfectants and Disinfectant by-products*. World Health Organization, Geneva, Finland (2000).
- Applegate, L.E., Erkenbrecher, C.W. *Monitoring and control of biological activity in Permasep® seawater RO plants*. *Desalination*. 65: 331-359 (1987).
- Baek, Y., Yu, J. Kim, S.H., Lee, S., Yoon, J. *Effect of surface properties of reverse osmosis membranes on biofouling occurrence under filtration conditions*. *J. Membr. Sci.* 382(1): 91-99 (2011).
- Barnes, R.J., Bandi, R.R., Chua, F., Hui Low, J., Aung, T., Barraud, N., Fane, A.G., Kjelleberg, S., Rice, S.A. *The roles of Pseudomonas aeruginosa extracellular polysaccharides in biofouling of reverse osmosis membranes and nitric oxide induced dispersal*. *J. Membr. Sci.* 466: 161-172 (2014).
- Bereschenko, L.A., Heilig, G.H., Nederlof, M.M., van Loosdrecht, M.C.M., Stams, A.J.M., Euverink, G.-J.W. *Molecular characterization of the bacterial communities in the different compartments of a full-scale reverse-osmosis water purification plant*, *Appl. Environ. Microbiol.* 74(17): 5297-5304 (2008).
- Bernstein, R., Freger, V., Lee, J.-H., Kim, Y.-G., Lee, J., Herzberg, M. *'Should I stay or should I go?' Bacterial attachment vs biofilm formation on surface-modified membranes*. *Biofouling*. 30: 367-376 (2014).
- Bott, T.R. *Biofouling control*. In: Bott, T.R. (ed.) *Industrial Biofouling*. Elsevier, Amsterdam. 81-150 (2011).
- Bunce, J.T., Ndam, E., Ofiteru, I.D., Moore, A., Graham, D.W. *A review of phosphorus removal technologies and their applicability to small-scale domestic wastewater treatment systems*. *Front. Environ. Sci.* 6:(8) 1-15 (2018).
- Bucs, S.S., Valladares Linares, R., van Loosdrecht, M.C.M., Kruithof, J.C., Vrouwenvelder, J.S. *Impact of organic nutrient load on biomass accumulation, feed channel pressure drop increase and permeate flux decline in membrane systems*, *Water Res.*, 67: 227-242 (2014).
- Chong, T.H., Wong, F.S., Fane, A.G. *The effect of imposed flux on biofouling in reverse osmosis: Role of concentration polarisation and biofilm enhanced osmotic pressure phenomena*. *J. Membr. Sci.* 325(2): 840-850 (2008).
- Cristiani, P., Perboni, G. *Antifouling strategies and corrosion control in cooling circuits*. *Bioelectrochemistry*. 97: 120-126 (2014).
- da Silva, M.K., Tessaro, I.C., Wada, K. *Investigation of oxidative degradation of polyamide reverse osmosis membranes by monochloramine solutions*. *J. Membr. Sci.* 282: 375-382 (2006).
- Di Gregorio, L., Tandoi, V., Congestri, R., Rossetti, S., Di Pippo, F. *Unravelling the core microbiome of biofilms in cooling tower systems*. *Biofouling*. 14: 1-14 (2017).
- Dow Water & Process Solutions. *FILMTEC™ Reverse osmosis membranes technical manual*. Form no. 609-00071- 0416.



- Dreszer, C., Vrouwenvelder, J.S., Paulitsch-Fuchs, A.H., Zwijnenburg, A., Kruithof, J.C., Flemming, H.-C. Hydraulic resistance of biofilms. *J. Membr. Sci.* 429: 436-447 (2013).
- Dreszer, C., Flemming, H.-C., Wexler, A.D., Zwijnenburg, A., Kruithof, J.C., Vrouwenvelder, J.S. Development and testing of a transparent membrane biofouling monitor. *Desalin. Water Treat.* 52: 10-12 (2014).
- Durdevic, P., Raju, C.S., Yang, Z. Potential for Real-Time Monitoring and Control of Dissolved Oxygen in the Injection Water Treatment Process. *IFAC-PapersOnLine.* 51(8): 170-177 (2018).
- Farhat, N.M., Loubineaud, E., Prest, E.I.E.C., El-Chakhtoura, J., Salles, C., Bucs, S.S., Trampé, J., van den Broek, W.B.P., van Agtmaal, J.M.C., van Loosdrecht, M.C.M., Kruithof, J.C., Vrouwenvelder, J.S. Application of monochloramine for wastewater reuse: Effect on biostability during transport and biofouling in RO membranes. *J. Membr. Sci.* 551: 243-253 (2018).
- Faria, A.F., Liu, C., Xie, M., Perreault, F., Nghiem, L.D., Ma, J., Elimelech, M. Thin-film composite forward osmosis membranes functionalized with graphene oxide-silver nanocomposites for biofouling control. *J. Membr. Sci.* 525: 146-156 (2017).
- Finnegan, M., Linley, E., Denyer, S.P., McDonnell, G., Simons, C., Maillard, Y.-Y. Mode of action of hydrogen peroxide and other oxidizing agents: differences between liquid and gas forms. *J. Antimicrob. Chemother.* 65(10): 2108-2115 (2010). Flemming, H.-C., Schaule, G., Griebe, T., Schmitt, J., Tamachkiarowa, A. Biofouling - the Achilles heel of membrane processes. *Desalination.* 113: 215-225 (1997).
- Flemming, H.-C. Reverse osmosis membrane biofouling, *Exp. Thermal Fluid. Sci.*, 14: 382-391 (1997).
- Flemming, H.-C. Biofilms. In: *Encyclopedia of Life Sciences (ELS)*. John Wiley & Sons, Ltd, Chichester. 1-10 (2008).
- Franklin, M.J., Chang, C., Akiyama, T., Bothner, B. New technologies for studying biofilms. *Microbiol. Spectr.* 3(4): (2015).
- Gjermansen, M., Ragas, P., Sternberg, C., Molin, S., Tolker-Nielsen, T., 2005. Characterization of starvation-induced dispersion in *Pseudomonas putida* biofilms. *Environ. Microbiol.* 7, 894-906
- Glater, J., Zachariah, M.R., McCray, S.B., McCutchan, J.W. Reverse osmosis membrane sensitivity to ozone and halogen disinfectants. *Desalination*, 48: 1-16 (1983).
- Gutman, J., Herzberg, M., Walker, S.L. Biofouling of reverse osmosis membranes: positively contributing factors of *Sphingomonas*. *Environ. Sci. Technol.* 48(23):13941-13950 (2014).
- Goeres DM, Loetterle LR, Hamilton MA, Murga R, Kirby DW, Donlan RM. Statistical assessment of a laboratory method for growing biofilms. *Microbiology.* 151:757-762 (2005).
- Goeres DM, Hamilton MA, Beck NA, Buckingham-Meyer K, Hilyard JD, Loetterle LR, Lorenz LA, Walker DK, Stewart PS. A method for growing a biofilm under low shear at the air-liquid interface using the drip flow biofilm reactor. *Nat Protoc.* 4:783-788 (2009).
- Goh, P.S., Lau, W.J., Othman, M.H.D., Ismail, A.F. Membrane fouling in desalination and its mitigation strategies. *Desalination.* 425: 130-155 (2018).
- Greenlee, L.F., Lawler, D.F., Freeman, B.D., Marrot, B., Moulin, P. Reverse osmosis desalination: Water sources, technology, and today's challenges. *Water Res.* 43: 2317-2348 (2009).

- Habimana, O., Semião, A.J.C., Casey, E. The role of cell-surface interactions in bacterial initial adhesion and consequent biofilm formation on nanofiltration/reverse osmosis membranes. *J. Membr. Sci.* 454: 82-96 (2014).
- Hijnen, W.A.M.; Biraud, D.; Cornelissen, E.R.; van der Kooij, D. Threshold concentration of easily organic carbon in feedwater for biofouling of spiral-wound membranes. *Environ. Sci. Technol.* 43: 4890–4895 (2009).
- Hilal, N., Wright, C.J. Exploring the current state of play for cost-effective water treatment by membranes. *NPJ Clean Water.* 8: 1-4. (2018).
- Hydranautics technical service bulletin - TSB 110.12. Biocides for Disinfection and Storage of Hydranautics Membrane Elements. (2015).
- Hydranautics technical application bulletin - TAB 115. Potential use of ClO<sub>2</sub> as a disinfectant for polyamide RO/NF membranes. (2013).
- Jacangelo, J.G., Olivieri, V.P., Kawata, K. Oxidation of sulfhydryl groups by monochloramine. *Water Res.* 21: 1339-1344 (1987). Kochkodan, V., Hilal, N. A comprehensive review on surface modified polymer membranes for biofouling mitigation. *Desalination.* 356: 187-207 (2015).
- Jacobs, J.F., Hasan, M.N., Paik, K.H., Hagen, W.R., van Loosdrecht, M.C.M. Development of a bionanotechnological phosphate removal system with thermostable ferritin. *Biotechnol. Bioeng.* 105(5): 918e923 (2010)
- Jiang, S., Li, Y., Ladewig, B.P. A review of reverse osmosis membrane fouling and control strategies. *Sci. Total. Environ.* 595: 567-583 (2017).
- Kim, C.-M., Kim, S.-J., Kim, L.H., Shin, M.S., Yu, H.-W., Kim, I.S. Effects of phosphate limitation in feed water on biofouling in forward osmosis (FO) process. *Desalination,* 349: 51-59 (2014).
- Kitis, M. Disinfection of wastewater with peracetic acid: a review. *Environ. Int.* 30: 47-55 (2004).
- Kochkodan, V., Hilal, N. A comprehensive review on surface modified polymer membranes for biofouling mitigation. *Desalination.* 356: 187-207 (2015).
- Koh, J.H., Jang, A. Effect of chlorine dioxide (ClO<sub>2</sub>) on polyamide-based RO membrane for seawater desalination process: exposure to high concentration of ClO<sub>2</sub>. *Desalin. Water. Treat.* 80: 11–17 (2017).
- LeChevallier, M.V. Biocides and the current status of biofouling control in water systems. In: Flemming, H.-C., Geesey, G.G. (eds.) *Biofouling and biocorrosion in industrial water systems. Proceedings of the international workshop on industrial biofouling and biocorrosion, Stuttgart, Sept. 13 -14, 1990.* Springer, Berlin, Heidelberg. 113-132 (1991).
- Levi, A., Bar-Zeev, E., Elifantz, H., Berman, T., Berman-Frank, I. Characterization of microbial communities in water and biofilms along a large scale SWRO desalination facility: Site-specific prerequisite for biofouling treatments, *Desalination,* 378: 44-52 (2016).
- Liberman, B. Three methods of forward osmosis cleaning for RO membranes. *Desalination.* 431: 22-26 (2018).
- Liebig, J. *Die organische Chemie in ihrer Anwendung auf Agricultur und Physiologie (Organic chemistry in its applications to agriculture and physiology).* Friedrich Vieweg und Sohn Publ. Co., Braunschweig, Germany. (1840).

- Ma, W., Panecka, M., Tufenkji, N., Rahaman, M.S. Bacteriophage-based strategies for biofouling control in ultrafiltration: In situ biofouling mitigation, biocidal additives and biofilm cleanser. *J. Colloid Interface Sci.* 253: 254-265 (2018).
- Maddah, H. Chogle, A. Biofouling in reverse osmosis: phenomena, monitoring, controlling and remediation. *Appl. Water Sci.* 7: 2637-26517 (2017).
- Miller, D.J., Araújo, P.A., Correia, P.B., Ramsey, M.M., Kruihof, J.C., van Loosdrecht, M.C.M., Freeman, B.D., Paul, D.R., Whiteley, M., Vrouwenvelder, J.S. Short-term adhesion and long-term biofouling testing of polydopamine and poly(ethylene glycol) surface modifications of membranes and feed spacers for biofouling control. *Water Res.* 46: 3737-3753 (2012).
- Misdan, N., Ismail, A.F., Hilal, N. Recent advances in the development of (bio)fouling resistant thin film composite membranes for desalination. *Desalination.* 380: 105-III (2016).
- Nagaraj, V., Skillman, L., Li, D., Gofton, A. Characterisation and comparison of bacterial communities on reverse osmosis membranes of a full-scale desalination plant by bacterial 16S rRNA gene metabarcoding. *NPJ Biofilms Microb.* 3(13): 1-14 (2017).
- Nguyen, T., Roddick, F.A., Fan, L. Biofouling of water treatment membranes: a review of the underlying causes, monitoring techniques and control measures, *Membranes.* 2: 804-840 (2012).
- Oh, J.H., Jang, A. Application of chlorine dioxide (ClO<sub>2</sub>) to reverse osmosis (RO) membrane for seawater desalination. *J. Taiwan Inst. Chem. Eng.* 68: 281-288 (2016).
- Otitoju, T.A., Saari, R.A., Ahmad, A.L. Progress in the modification of reverse osmosis (RO) membranes for enhanced performance. *J. Ind. Eng. Chem.* 67: 52-71 (2018).
- Patrick, W.A., Wagner, H.B. Method for complete deoxygenation of water. *Anal. Chem.* 21(6): 752-753 (1949).
- Peña, N., Gallego, S., del Vigo, F., Chesters, S.P. Evaluating impact of fouling on reverse osmosis membranes performance. *Desalin. Water Treat.* 51(4-6): 958-968 (2012).
- Petrova, O.E., Sauer, K. Escaping the biofilm in more than one way: desorption, detachment or dispersion. *Curr. Opin. Microbiol.* 30: 67-78 (2016).
- Qin, J.J., Liberman, B., Kekre, K.A. Direct osmosis for reverse osmosis fouling control: principles, applications and recent developments. *Open Chem. Eng. J.* 3: 8-16 (2009).
- Rana, D., Matsuura, T. Surface modifications for antifouling membranes. *Chem. Rev.* 110(4): 2448-2471 (2010).
- Rice, E.W., Baird, R.B., Eaton, A.D., Clesceri, L.S. Standard methods for the examination of water and wastewater, 23rd Edition. American Public Health Association, American Water Works Association, Water Environment Federation. (2017).
- Richardson, S.D., Plewa, M.J., Wagner, E.D., Schoeny, R., De Marini, D.M. Occurrence, genotoxicity, and carcinogenicity of regulated and emerging disinfection by-products in drinking water: A review and roadmap for research. *Mutat. Res. Rev.* 636(1-3): 178-242 (2007)
- Sauer, K., Cullen, M.C., Rickard, A.H., Zeef, L.A., Davies, D.G., Gilbert, P. Characterization of nutrient-induced dispersion in *Pseudomonas aeruginosa* PAOI biofilm. *J. Bacteriol.* 186(21): 7312-7326 (2004).
- Semião, A.J.C., Habimana, O., Casey, E., Bacterial adhesion onto nanofiltration and reverse osmosis membranes: Effect of permeate flux. *Water Res.* 63: 296-305 (2014).

- Suwarno, S.R., Chen, X., Chong, T.H., McDougald, D., Cohen, Y., Rice, S.A., Fane, A.G. Biofouling in reverse osmosis processes: The roles of flux, crossflow velocity and concentration polarization in biofilm development. *J. Membr. Sci.* 467: 116-125 (2014).
- Thormann, K.M., Saville, R.M., Shukla, S., Spormann, A.M., 2005. Induction of rapid detachment in *Shewanella oneidensis* MR-1 biofilms. *J. Bacteriol.* 187:1014–1021.
- Valentino, L., Renkens, T., Maugin, T., Croue, J.P., Marinas, B.J. Changes in physicochemical and transport properties of a reverse osmosis membrane exposed to chloraminated seawater. *Environ. Sci. Technol.* 49: 2301-2309 (2015).
- van den Broek, W.B.P., Boorsma, M.J., Huiting, H., Dusamos, M.G., van Agtmaal S. Prevention of Biofouling in Industrial RO Systems: Experiences with Peracetic Acid, *Water Sci. Technol.* 5(2): 1-11 (2010).
- van der Bruggen, B., Mänttari, M., Nyström, M. Drawbacks of applying nanofiltration and how to avoid them: A review. *Sep. Purif. Technol.* 63(2): 251-263 (2008).
- van der Hoek, J.P., Hofman, J.A.M.H., Bonn e, P.A.C., Nederlof, M.M., Vrouwenvelder, J.S. RO treatment: selection of a pretreatment scheme based on fouling characteristics and operating conditions based on environmental impact. *Desalination.* 127(1): 89-101 (2000).
- Vanysacker, L., Declerck, P., Vankelecom, I. Development of a high throughput cross-flow filtration system for detailed investigation of fouling processes. *J. Membr. Sci.* 442: 168-176 (2013).
- Volk, C.J., LeChevallier, M.V. Effects of Conventional Treatment on AOC and BDOC Levels. *J. Am. Water Works Assoc.* 94(6): 112-123 (2002).
- Vrouwenvelder, J.S., Bakker, S.M., Cauchard, M., Le Grand, R., Apacandi e, M., Idrissi, M., Lagrave, S., Wessels, L.P., van Paassen, J.A.M., Kruithof, J.C., van Loosdrecht, M.C.M. The membrane fouling simulator: a suitable tool for prediction and characterization of membrane fouling. *Water Sci. Technol.* 55: 197-205 (2007).
- Vrouwenvelder, J.S., Beyer, F., Dahmani, K., Hasan, N., Galjaard, G., Kruithof, J.C., van Loosdrecht, M.C.M. Phosphate limitation to control biofouling. *Water Res.* 44(11): 3454-3466 (2010).
- Wang, Y., Wang, Z., Wang, J., Wang, S. Triple antifouling strategies for reverse osmosis membrane biofouling control. *J. Membr. Sci.* 549: 495-506 (2018).
- Weinrich, L., LeChevallier, M.V., Haas, C.N. Contribution of assimilable organic carbon to biological fouling in seawater reverse osmosis membrane treatment. *Water Res.* 101: 203-213 (2016).
- Wibisono, Y., Yandi, W., Golabi, M., Nugraha, R., Cornelissen, E.R., Kemperman, A.J.B., Ederth, T., Nijmeijer, K. Hydrogel-coated feed spacers in two-phase flow cleaning in spiral wound membrane elements: A novel platform for eco-friendly biofouling mitigation. *Water Res.* 71: 171-186 (2015).
- Yang, Z., Ma, X.-H., Tang, C.Y., Recent development of novel membranes for desalination. *Desalination.* 434: 37-59 (2018).
- Yin, J., Yang, Y., Hu, Z., Deng, B. Attachment of silver nanoparticles (AgNPs) onto thin-film composite (TFC) membranes through covalent bonding to reduce membrane biofouling. *J. Membr. Sci.* 441: 73-82 (2013).
- Zhao, F., Xu, K., Ren, H., Ding, L., Geng, J., Zhang, Y. Combined effects of organic matter and calcium on biofouling of nanofiltration membranes. *J. Membr. Sci.* 486: 177-188 (2015).







# Appendices

**Summary**

**Co-authors' affiliations**

**List of publications**

**Acknowledgments**

**About the author**

**Overview of completed training activities (SENSE certificate)**

## Summary

High pressure membrane filtration processes such as nanofiltration (NF) and reverse osmosis (RO) produce high quality water for industrial applications and human consumption. The global high pressure membrane filtration market is growing rapidly. Unfortunately, (bio)fouling contributes significantly to the operational costs and downtime of membrane filtration installations.

In this thesis, microbiological and process technological aspects of NF and RO membrane biofouling were examined. Biofilm formation and its negative effects on engineered systems (biofouling) of various industries were summarized, with a focus on NF and RO (*Chapter 1*). An operational definition of NF and RO biofouling is given and generally applied preventative and corrective measures to manage membrane biofouling are reviewed (*Chapter 1*).

In *Chapter 2*, the long-term performance and fouling behavior of four full-scale anoxic groundwater treating NF plants were characterized and compared with data reported for oxic NF plants. Pretreatment of water was limited to 10 µm pore size cartridge filtration and antiscalant dosage, but the anoxic groundwater treating NF plants did not suffer from substantial biofouling. Chemical cleaning of once per year or less was sufficient to maintain satisfying operation during direct NF of iron rich anoxic groundwater. Autopsies of eight NF membrane elements, which had been in service since the plant startup (6 - 10 years), revealed very thin “fouling” layers composed of organic, biological and inorganic materials. The high solubility of reduced metal ions and the slow biofilm development under anoxic conditions were probably the reasons for the good performance of the anoxic groundwater treating NF plants (*Chapter 2*).

To confirm that the very slow biofilm development observed in the NF installations described in *Chapter 2* was indeed related to slow growing anaerobic microorganisms, 16S rRNA gene amplicon sequencing was used to unravel the microbial community that developed on the membranes from two plants. The majority of the bacteria affiliated with environmental sequences of yet uncultured lineages. Microbial communities found at membranes of anoxic NF (*Chapter 3*) were representative for anoxic environments and markedly distinct from those of oxic NF.



As all membranes will eventually foul, the development of effective membrane cleaning processes is important. Foulants that cannot be removed by conventional chemical cleaning are of particular interest, as they might ultimately define a membranes lifetime. Membrane fouling and cleaning was studied in three reverse osmosis (RO) plants and in a laboratory scale cleaning setup. Standard chemical cleaning procedures were compared to two cleaning procedures that were specifically adapted to treat (bio)organic fouling in a laboratory setup. The study underlines the need for novel cleaning approaches, specifically targeting resistant foulants, as none of the procedures applied resulted in highly effective membrane regeneration (*Chapter 4*).

The survey presented in *Chapter 1* emphasized that glycosphingolipid producing bacteria in general and Sphingomonads in particular are microorganisms involved in membrane biofouling. Therefore, 21 Sphingomonads were isolated from six NF and RO membranes, and subsequently physiologically characterized. Various traits contributing to successful colonization of membrane surfaces, such as metabolic versatility, motility and high tolerance for different temperatures, salt concentrations and pH, were observed of the Sphingomonads isolated (*Chapter 5*).

In a pilot study, performed under representative conditions using flow cells, the biofouling development of a *Sphingomonas* strain described in *Chapter 5* was examined (*Chapter 6*). *Sphingomonas* strain Sph1 was able to initiate biofilm development which was followed by subsequent biofilm maturation leading to membrane biofouling. Consequently, we propose to extend the focus on Sphingomonads beyond their typically attributed role as initial colonizers (*Chapter 6*).

Furthermore, the results presented in this thesis, in conjunction with the lesson learned along the way, are discussed in *Chapter 6* where they are brought into perspective regarding full-scale membrane biofouling prevention and control. Finally, suggestions for future research are given.

## **Co-authors' affiliations**

**Alfons J.M. Stams, Caroline M. Plugge, Hendrik J. de Vries, Johannes S. Vrouwenvelder, Judita Laurinonyte, Monika Jarzembowska, Peer H.A. Timmers**

Laboratory of Microbiology, Wageningen University & Research, Stippeneng 4, 6708 WE Wageningen, The Netherlands

**Arie Zwijnenburg, Caroline M. Plugge, Hendrik J. de Vries, Joanna Lipińska, Peer H.A. Timmers, Paula van den Brink**

Wetsus, European Centre of Excellence for Sustainable Water Technology, Oostergoweg 9, 8911 MA Leeuwarden, The Netherlands

**Bas M. Rietman**

Vitens N.V., P.O. Box 1205, 8001 BE Zwolle, The Netherlands

**Johannes S. Vrouwenvelder**

Department of Biotechnology, Faculty of Applied Sciences, Delft University of Technology, Julianalaan 67, 2628 BC Delft, The Netherlands

King Abdullah University of Science and Technology, Water Desalination and Reuse Center, Thuwal, Saudi Arabia

**Judita Laurinonyte**

Department of Environmental Technology, Wageningen University, P.O. Box 8129, 6700 EV Wageningen, The Netherlands

---

## List of publications

Vrouwenvelder, J.S., **Beyer, F.**, Dahmani, K., Hasan, N., Galjaard, G., Kruithof, J.C., van Loosdrecht, M.C.M. Phosphate limitation to control biofouling. *Water Res.* 44(11): 3454-3466 (2010).

**Beyer, F.**, Rietman, B.M., Zwijnenburg, A., van den Brink, P., Vrouwenvelder, J.S., Jarzembowska, M., Laurinonyte, J., Stams, A.J.M., Plugge, C.M. Long-term performance and fouling analysis of full-scale direct nanofiltration (NF) installations treating anoxic groundwater. *J. Membr. Sci.* 468: 339-348 (2014).

Jarzembowska, M., Sousa, D.Z., **Beyer, F.**, Zwijnenburg, A., Plugge, C.M., Stams, A.J.M. *Lachnotalea glycerini* gen. nov., sp. nov., a novel anaerobe isolated from a nanofiltration unit treating anoxic groundwater. *Int. J. Syst. Evol. Microbiol.* 66: 774-779 (2016).

**Beyer, F.**, Laurinonyte, J., Zwijnenburg, A., Stams, A.J.M., Plugge, C.M. Membrane fouling and chemical cleaning in three full-scale reverse osmosis plants producing demineralized water. *J. Eng.* 2017: 1-14 (2017).

de Vries, H.J.\* **Beyer, F.\***, Jarzembowska, M., Lipińska, J., van den Brink, P., Zwijnenburg, A., Timmers, P.H.A., Stams, A.J.M., Plugge, C.M. Isolation and characterization of Sphingomonadaceae from fouled membranes. *Nature Biofilms Microbiomes* 5: 6 (2019).

\* de Vries, H.J. and Beyer, F. contributed equally to this work.

## Acknowledgments

Eventually, all (good) things come to an end, or as the Germans would say “Alles hat ein Ende, nur die Wurst hat zwei” (Everything has an end, only sausages have two)! I am sitting here on a rainy Saturday writing these acknowledgments, one of the final pieces of the puzzle to complete this thesis. Overall, it has been a long journey of eight and a half years. It is now time to express my utmost gratitude to everyone that supported me throughout this journey, contributed scientifically to this thesis or helped me to become the person I am today. Although these acknowledgements might be somewhat superficial, generic or abstract, you can be sure that my gratitude is way deeper than these words can reflect.

First of all, I would like to thank Prof. Dr Fons Stams for giving me the opportunity to start a PhD project in his workgroup. I am thankful for your patience and your acceptance of my deviation from the original research proposal. Your critical and analytical mind has strongly helped me to shape this thesis (and related manuscripts) to their final quality. I admire your incredible contribution to science, as well as your modesty about it.

My sincere gratitude and appreciation goes to my co-promotor Dr Caroline Plugge. You played a crucial role in the preparation and completion of this thesis. I cannot thank you enough for your motivation, endurance and enthusiasm. You always made sure that I stayed on track. Without your drive and persistence, this thesis would not be here (yet).

Dr. Arie Zwijnenburg, thank you for your great support and daily supervision. From you I have learned pretty much everything I know about membrane processes, membrane manufacturing, scanning electron microscopy, apple pie, whistling, cycling and ice skating. Your immense knowledge has greatly contributed to the development of this thesis. Your open attitude, modesty, warm personality, and happiness have been very inspiring. Unfortunately, we will not have the opportunity to celebrate this milestone together. You are greatly missed.

Thank you Cees and Johannes for your dedication and endurance to make your dream vision of “Wetsus” an undeniable truth. This “thank you” extends to everyone that helped Cees and Johannes with the realization of their dreams.

A huge thank you to the analytical-, technical-, IT-, administrative-, and finance department of Wetsus: Aga, Doekle, Foppe, Harm, Harrie, Helena, JJ, Jan T., Jan d.G., Janneke, Jelmer, Marianne, Mieke, Nynke, Pieter, Rien, Ton and Wim. Thank you for all the “fire-fighting” and straightforward solutions, especially in those moments that seemed hopeless. Your support, enthusiasm and creativity have strongly contributed to the foundation of this thesis!

Thank you to all my students: Dyan, Esther, Judita, Monika and Tamas. It remains a mystery how this thesis took me so long, despite all the hard work you have put into this. It was great working with you and I wish you all the best for your future careers.

I would like to thank all the colleagues and companies that have participated in the biofouling / biofilms theme. In addition, I would also like to thank all the professionals outside the biofouling theme that have shared their immense knowledge with me. Together, you contributed in many different ways to the development of this thesis, but also to the development of the professional person I am today. Thank you for sharing your experience, giving me access to your plants, sharing heaps of operational data, the constructive criticism and all the other things you did for me. In particular, I like to thank some of the real experts: Bas, Dolf, Hans, Joop, Marcel, Mark, Paul, Wilbert v.d.B and Wilbert v.d.V.

Dear co-authors, thank you for your clear contribution to this thesis. In particular I would like to thank Rik de Vries for his commitment to continue the work on the isolated *Sphingomonadaceae*. After all, it could not have been done better!

My fellow PhD students and friends of Wetsus and Wageningen University, thank you for the great working atmosphere, nice talks, open ears, guidance, help, explanations, parties and sport activities. You have, in many different ways, contributed to the development of this thesis.

Adam, Aga, Andrea, Anna, Astrid, Christina, Cristina, Claudia, Cláudia F, Cláudia S, Charu, Daniel, Derya, Elsemiek, Enver, João, Johannes, Joeri, Jordi, Judita, Kamuran, Martin, Nirajan, Lena, Lina, Loreen, Luewton, Mapi, Monir, Oane, Olivier, Paula, Pawel, Pedro, Petra, Ricardo, Rik, Samet, Sanne, Slawomir, Vicente, Vytautas and Zlatica, it has been a pleasure!

My dear friends Hannes, Heike, Jochen, Mate, Monika, Robin, Sanne, Samet and Tom, thank you for being especially successful at what you were supposed to do – being great friends! Without you, I would have probably not endured this journey. Thank you for the support and countless great memories. Agi, thank you for your colossal amounts of energy and the very good times we had. Eileen, thank you for your support during the final spurt towards the finishing line. Tom and Monika, you endured this journey from the beginning to the end. You have been always there when needed and I am beyond grateful for this!

To my dearest outdoor addicts Agi, Asti, Chandni, Cor, Daan, Jobber, Jonas, Lukas, Maik, Marcel, Marco, Mario, Max, Soraya, Tom, Slackline Leeuwarden, Slackline Wageningen and the MadNes gang. Thank you for all those crazy park and mountain adventures. Thank you for all the bouldering, climbing, coffee, slacklining, highlining, pommies and safety meetings. With you I experienced some of the most beautiful, yet most scary moments of my entire life. I have trusted my life to most of you and have not been disappointed! I can't wait for the upcoming months, when writing this thesis is not a valid excuse to stay behind the desk anymore!

I would like to thank Karina Möldner, Kerstin Voigt, Lysett Wagner, Magdalena Scheibler, Steffen Münch and the other “early” supporters and believers. Without your encouragement, selfless help and support, I would not have even been able to start this journey. Your contribution to my personal development and professional career is greatly appreciated and will never be forgotten!

I would like to thank my new colleagues at Solenis for their help, motivation and trust. During all the projects with you, I have met many great people and learned an incredible amount about industrial water treatment. Being introduced to the beauty and cuisine of your respective home countries was especially appreciated. Olaf P, Olaf R and Mick, a special thank you for the countless hours of teaching, coaching and support.

A bitter-sweet thank you to the people who did not believe in me, or that have discouraged me in my early days. From you, I actually took a lot of energy and motivation, especially in the days that felt like being lost in dead-end roads (both scientific and personal). Needless to say, also you have significantly contributed to my personal development and to the completion of this thesis.

Zuletzt möchte ich mich besonders bei meiner Familie für das Verständnis, die Unterstützung, die Motivation und die Geborgenheit bedanken. Liebe Mama, ich danke Dir von ganzem Herzen für Deine Unterstützung und dafür, dass Du immer an mich geglaubt hast. Mama, Papa, Oma, Anne, Bernd, Silke und Marleen, ohne Euch wäre es nicht gegangen. Lieber Joachim, Lieber Toni, schade, dass ihr diesen Tag nicht mehr miterleben könnt. Ich halte Euch in meiner Erinnerung wach, denn auch ohne Euch wäre es nicht gegangen.

Last but not least, thank you to everyone that I missed in these acknowledgments.

Florian Beyer

January 2019







## About the author

Florian Beyer was born on 23rd March, 1985 in Gera (Germany). In 2003, he obtained his gymnasium diploma. After one year of engineering intermezzo, he started his studies in biology at the Friedrich-Schiller-University Jena (Germany) in 2004.

After his pre-diploma, he specialized into microbiology. Due to his growing passion for applied research, he joined the biofouling workgroup of Wetsus, European centre of excellence for sustainable water technology (Leeuwarden, The Netherlands), with a Leonardo da Vinci scholarship of the European Union.



The results of his diploma thesis (phosphate limitation to control biofouling) were graded excellent and published in Journal of Membrane Science. In 2010, he finished his studies with specializing in microbiology, environmental biotechnology and water technology.

Half a year before finishing his diploma studies, in November 2009, he started his PhD research on “physiological properties of microorganisms involved in membrane biofouling” with the microbial physiology workgroup of Wageningen University (The Netherlands). The research has been performed externally at Wetsus. The results of this studies, though under a dissimilar title, have led to the preparation of this thesis.

In 2015, Florian worked as a researcher at Wetsus on the topic of “hydrodynamic optimization of membrane spacers to reduce biofouling”. In 2016, he has started to work as application specialist and platform launch manager at Solenis (formerly known as Ashland Water Technologies). His strong field of expertise is microbiological monitoring, prevention and control in industrial water treatment. Due to his outstanding achievements in the field of legionella prevention, as well as biofilm monitoring and control, he received the Solenis Pinnacle award in 2018.



*Netherlands Research School for the  
Socio-Economic and Natural Sciences of the Environment*

# D I P L O M A

*For specialised PhD training*

The Netherlands Research School for the  
Socio-Economic and Natural Sciences of the Environment  
(SENSE) declares that

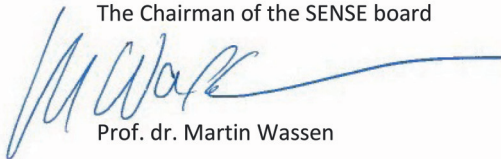
***Florian Beyer***

born on 23 March 1985 in Gera, Germany

has successfully fulfilled all requirements of the  
Educational Programme of SENSE.

Wageningen, 22 February 2019

The Chairman of the SENSE board



Prof. dr. Martin Wassen

the SENSE Director of Education



Dr. Ad van Dommelen

*The SENSE Research School has been accredited by the Royal Netherlands Academy of Arts and Sciences (KNAW)*



K O N I N K L I J K E N E D E R L A N D S E  
A K A D E M I E V A N W E T E N S C H A P P E N



The SENSE Research School declares that **Florian Beyer** has successfully fulfilled all requirements of the Educational PhD Programme of SENSE with a work load of 33.8 EC, including the following activities:

#### SENSE PhD Courses

- o Environmental research in context (2011)
- o Research in context activity: 'Co-organizing Wetsus Water Challenge, Leeuwarden' (2013)
- o New frontiers in microbial ecology (2013)
- o New frontiers in microbial ecology (2013)
- o SENSE writing week (2014)

#### Other PhD and Advanced MSc Courses

- o Advanced course environmental biotechnology, Biotechnological Sciences Delft Leiden - BSDL (2011)
- o Advance biofilm course, Delft University of Technology (2011)
- o Laser and optics in fluid research, Wetsus, Leeuwarden (2013)

#### Poster Presentations

- o *Fouling characterization in NF/RO membrane filtration installations for water production: A study at 12 plants.* International congress on membranes and membrane processes (ICOM), 25-29 July 2011, Amsterdam, The Netherlands.
- o *Long term performance and fouling analyses of full-scale nanofiltration installations treating anaerobic groundwater.* 5th congress of European Microbiologists (FEMS), 21-25 July 2013, Leipzig, Germany

#### Oral Presentations

- o *Long term performance, (bio)fouling analysis and microbial composition of direct nanofiltration installations treating anoxic groundwater.* Environmental Technology for Impact (ETEI), 29-30 April 2015, Wageningen, The Netherlands

SENSE Coordinator PhD Education

Dr. Peter Vermeulen

This work was performed in the cooperation framework of Wetsus, European Centre of Excellence for Sustainable Water Technology ([www.wetusus.nl](http://www.wetusus.nl)). Wetsus is co-founded by the Dutch Ministry of Economic Affairs and Climate Policy, the Northern Netherlands Provinces and the Province of Fryslân.

The authors like to thank the participants of the research theme “Biofilms” for the fruitful discussions and financial support.

Cover design: Lena Wolters

Thesis layout: Florian Beyer